AGARD-CP-576

AGARD-CP-576

AGARD

ADVISORY GROUP FOR AEROSPACE RESEARCH & DEVELOPMENT
7 RUE ANCELLE, 92200 NEUILLY-SUR-SEINE, FRANCE

AGARD CONFERENCE PROCEEDINGS 576

Technologies for Precision Air Strike Operations in Rapid-Reaction and Localised-Conflict Scenarios

(les Techniques pour les opérations air-sol dans les situations de conflits localisés et de réactions rapides)

Papers presented at the Mission Systems Panel 4th Symposium held in Seville, Spain from 16-19 October 1995.

DISTRIBUTION STATEMENT A
Approved for public release;
Distribution Unlimited

NORTH ATLANTIC TREATY ORGANIZATION

Published June 1996

Distribution and Availability on Back Cover

DTIC QUALITY INSPECTED 4

DISCLAIMER NOTICE

UNCLASSIFIED

Technical Report distributed by

DEFENSE TECHNICAL INFORMATION CENTER

UNCLASSIFIED

THIS DOCUMENT IS BEST QUALITY AVAILABLE. THE COPY FURNISHED TO DTIC CONTAINED A SIGNIFICANT NUMBER OF PAGES WHICH DO NOT REPRODUCE LEGIBLY.

AGARD-CP-576

AGARD

ADVISORY GROUP FOR AEROSPACE RESEARCH & DEVELOPMENT

7 RUE ANCELLE, 92200 NEUILLY-SUR-SEINE, FRANCE

AGARD CONFERENCE PROCEEDINGS 576

Technologies for Precision Air Strike Operations in Rapid-Reaction and Localised-Conflict Scenarios

(les Techniques pour les opérations air-sol dans les situations de conflits localisés et de réactions rapides)

Papers presented at the Mission Systems Panel 4th Symposium held in Seville, Spain from 16-19 October 1995.

19960805 105

North Atlantic Treaty Organization
Organisation du Traité de l'Atlantique Nord

The Mission of AGARD

According to its Charter, the mission of AGARD is to bring together the leading personalities of the NATO nations in the fields of science and technology relating to aerospace for the following purposes:

- Recommending effective ways for the member nations to use their research and development capabilities for the common benefit of the NATO community;
- Providing scientific and technical advice and assistance to the Military Committee in the field of aerospace research and development (with particular regard to its military application);
- Continuously stimulating advances in the aerospace sciences relevant to strengthening the common defence posture;
- Improving the co-operation among member nations in aerospace research and development;
- Exchange of scientific and technical information;
- Providing assistance to member nations for the purpose of increasing their scientific and technical potential;
- Rendering scientific and technical assistance, as requested, to other NATO bodies and to member nations in connection with research and development problems in the aerospace field.

The highest authority within AGARD is the National Delegates Board consisting of officially appointed senior representatives from each member nation. The mission of AGARD is carried out through the Panels which are composed of experts appointed by the National Delegates, the Consultant and Exchange Programme and the Aerospace Applications Studies Programme. The results of AGARD work are reported to the member nations and the NATO Authorities through the AGARD series of publications of which this is one.

Participation in AGARD activities is by invitation only and is normally limited to citizens of the NATO nations.

The content of this publication has been reproduced
directly from material supplied by AGARD or the authors.

Published June 1996

Copyright © AGARD 1996
All Rights Reserved

ISBN 92-836-0028-2

Printed by Canada Communication Group
45 Sacré-Cœur Blvd., Hull (Québec), Canada K1A 0S7

Technologies for Precision Air Strike Operations in Rapid-Reaction and Localised-Conflict Scenarios

(AGARD CP-576)

Executive Summary

Air Strike Operations are a highly important function of NATO forces.

NATO's most frequent deployments will, in future, be involved with limited and localised conflicts, rather than large-scale all-out confrontations. The operational constraints, and sometimes the nature of the necessary technologies, differ between these two types of scenario.

In recent conflicts, it has been perceived that NATO air strike operations have been carried out with great effectiveness, but those closely concerned are well aware that there is still a great divide between what is really needed, and what today's technology can provide.

The main purpose of this symposium was to provide mutual education within the NATO community: for the operational people to educate the industrial and research community as to what is needed, and for the industrialists and researchers to educate the operational community as to what technologies are emerging — to indicate what is possible, and what is not, in a reasonable time frame.

The call for papers produced a good response, enabling the relevant features of precision strike operations to be covered adequately, and structured into sessions as follows:

- Operational Aspects;
- Mission Planning;
- En-route Navigation;
- Reconnaissance and Target Identification;
- Weapon Delivery and Self-defence.

The papers presented generated a high level of interest, including some healthy controversy in some cases. The symposium was well-attended throughout, and the programme committee is confident that it has achieved its objectives. In addition to the opportunities for discussion (both formal and informal) between the two "communities", the proceedings should provide a useful reference to guide research priorities, in this important area of NATO activity.

A.D. King
Programme Committee Chairman

Les techniques pour les opérations air-sol dans les situations de conflits localisés et de réactions rapides

(AGARD CP-576)

Synthèse

Les Opérations Air-Sol représentent une fonction importante des forces militaires de l'OTAN.

La plupart des déploiements fréquents de l'OTAN seront, dans l'avenir, appliqués à des conflits limités et localisés, plutôt qu'à des confrontations nombreuses de grande envergure. Les contraintes opérationnelles, et quelquefois la nature des technologies nécessaires, diffèrent d'un type de scénario à l'autre.

Les derniers conflits ont mis en évidence que les opérations air-sol de l'OTAN ont été menées à bien avec une grande efficacité, mais les plus récents ont mis en exergue le fait qu'il demeure un fossé entre ce qui est réellement demandé et ce, qu'aujourd'hui, la technologie est en mesure de fournir.

L'objectif principal de ce symposium était d'apporter une information à double sens au sein de la communauté de l'OTAN: d'une part, la partie opérationnelle devait instruire les communautés de l'industrie et de la recherche de "ce qui est nécessaire", et, d'autre part, les industriels et les scientifiques devaient informer la communauté opérationnelle des technologies émergentes, en indiquant dans un calendrier raisonnable ce qui est possible ou pas de réaliser.

La demande de participation a reçu une bonne réponse, permettant de couvrir pleinement les thèmes essentiels du symposium sur "les Opérations Air-Sol" qui fut structuré en sessions selon:

- Les Aspects Opérationnels;
- La Planification des Missions;
- La Navigation sur Route;
- La Reconnaissance et l'Identification de l'Objectif;
- L'Autorisation de Tir et l'Auto Défense.

Les papiers présentés ont suscité un vif intérêt, sans exclure, pour certains, quelques débats passionnés. Du début à la fin, le symposium a connu une bonne audience, et le Comité de Programme est persuadé d'avoir atteint ses objectifs. En plus des ouvertures à la discussion (tant formelle qu'informelle) entre les deux "communautés", la publication devrait apporter une référence utile afin de définir les priorités en matière de recherche, dans ce domaine important des activités de l'OTAN.

Contents

Page

Executive Summary iii

Synthèse iv

Theme/Thème vii

Panel Officers and Programme Committee viii

Reference

Technical Evaluation Report TER
by Dr. R.W. MacPherson

SESSION I: OPERATIONAL ASPECTS
Chairman: Dr. S. Butler (US)

The Need for Precision-Guided Munitions in Limited Conflict — An Operational Viewpoint 1
by I. Hall

Development of a Reconnaissance, Surveillance and Target Acquisition (RSTA) Architecture to meet NATO's Reaction Forces Requirements 2*
by P. Becher

Helicopter Task Force: A Mission Effective Solution for Precision Air Strikes 3
by D. Mellies

Advanced Targeting Improvements for Joint STARS (U) 4*
by B. Queen, M. Liggins, M. Justice, D. Rodkey, D.L. Reade, L. Hostetler, J. Ellis, D. Burton and L. Devine

SESSION II: MISSION PLANNING/MISSION MANAGEMENT
Chairman: Dr. G. Reid (UK)

Precision Imaging Strike Technology Integration Laboratory (PISTIL) 5
by T.F. Reese and R.W. Going

Paper withdrawn 6

TORNADO Mission Planning System for Allied Mobile Forces (TMPS-AMF) 7*
by R. Vogel

SESSION III: NAVIGATION
Chairman: Dr.-Ing. U.K. Krogmann (GE)

Precision Strike Concepts Exploiting Relative GPS Techniques 8
by G.T. Schmidt and R.H. Setterlund

Carrier Phase GPS Time, Space, Position Information Demonstration (CAPTIDE) 9
by G.D. Costabile, J. Fowler, T. Elbert and D. Reiter III

Advanced Terrain Referenced Navigation Technologies for Rapid Reaction Stand Off Weapon Systems 10*
by P. Simpson, J. Abbott and R.J. Handley

Multifunction Millimetre Wave Radar for Future Military Navigation 11
by M. Pirkl, H.J. Roschmann and F.J. Tospann

SESSION IV: RECONNAISSANCE AND TARGET IDENTIFICATION — PART I
Chairman: Ing. C. Cestrone (IT)

Multispectral Image Correlation Technologies for Rapid Response to Short Dwell Time Targets 12*
by W.R. Ditzler, M.J. Boyd, T.J. Corcoran, J.E. McKnight and M.M. Wirtz

Friend Identification by IR Pictures on Helmet Mounted Displays 13
by G. Balzarotti, L. Fiori and B. Midollini

ASTRID: Autonomous Search and Track [with] Radar [and] Infra-Red 14*
by F. Nivelle, Ph. Martini, W. Rudolph and F. Winter

SESSION IV: RECONNAISSANCE AND TARGET IDENTIFICATION — PART II
Chairman: Mr. P.B. Homer (US)

Targeting for Future Weapon Systems 15
by P.R.C. Collins, P. Greenway, D.R. Edmondson and M.A. Green

Digital Video Compression for Weapons Control and Bomb Damage Indication 16
by C.D. Creusere and G. Hewer

Airborne Non-Cooperative Target Identification Program 17†
by C.N. Shen, L. Girata and A. Lovett

SESSION V: TARGETING AND WEAPON DELIVERY GUIDANCE
Co-Chairmen: Mr. T. Uring (FR) and Dr. P. Sanz-Aranguez (SP)

Exploitation of Differential GPS for Guidance Enhancement (EDGE) High Gear Program 18
by J.L. Dargan, G. Howell, T. Elbert and D. Gaskill

Navigation and GPS Lessons Learned from the EDGE Program 19†
by D.A. Kelly, J. Dargan, C. Eckert and P. Harms

Acquisition Automatique d'Objectif en Tous Temps 20*
by B.E. Dortomb and B. Chrétien

Localisation Automatique d'Objectifs à Partir d'une Carte Radar 21
by JP. Mestre and R. de Peufeilhoux

Low Cost, Adverse Weather Precision Weapon Guidance 22*
by E.L. Fleeman

Association de Capteurs Optroniques de Nouvelle Génération aux Systèmes de Navigation et d'Attaque 23
by J. Joffre, E. Jullien, JP. Bernoville, R. Goulette and Y. Le Guilloux

IR Seeker for A/S Missile: Field Results from a Live Demonstrator 24*
by E. Crovari, G. Battaini and G.L. Scazzola

Navigation sans Initialisation d'une Bombe Guidée Inertiellement 25
by Y. Paturel, E. Martin and J-T. Audren

HARM on GE IDS and ECR TORNADO 26*
by H. Schlatt and P. Angenoorth

Analysis of Differential Global Positioning System (DGPS) Techniques and GPS Jamming on Precision Guided Munition (PGM) Performance 27
by S. Mahmood, J. Solomon, R. James and D. Lawrence

Neural Network Techniques for Missile Guidance and Control 28
by U.K. Krogmann

DIRCM: An Effective Technology for Aircraft Self Protection against Optronic Missile Seekers 29
by M. Noll, B. Warm and P. Kassens

---

* Published in classified volume CP-576 (Supplement).

† Not available at time of printing.

Theme

Current and future conflicts involving NATO forces involve the need for rapid-reaction, precision air strike operations, often in a localised, limited intensity scenario. Developments in technologies have a major impact on the potential capabilities and tactics in these situations, which are often complicated by the involvement of multi-service or even multi-national forces. These technologies embrace all phases of such operations: reconnaissance for target identification and location, mission planning, en-route navigation, target designation, weapon delivery, defence suppression, and damage assessment.

Emerging technical developments have the potential to create major improvements in response flexibility and weapon delivery accuracy. However, the need for inter-operability and the need to bring all the elements together to form an effective overall system, makes it necessary for those involved in this field to understand the nature of the new developments in the different areas. The Symposium offered the opportunity for technologists to understand the operational needs, for operations specialists to understand the emerging technology capabilities, and to expose any 'gaps' so that future R&D can be prioritised.

The Symposium addressed the implications of developments in Technologies on Precision Air Strike Operations in rapid-reaction and localised-conflict scenarios, covering the following topics:

— Operational aspects of precision air strike operations;
— Advances in technologies (e.g. sensor technologies for target identification and location);
— Near-real-time mission planning — gathering all the relevant data, producing the plans, and transferring them to the aircraft or stand-off weapons and co-operating elements;
— En-route navigation: getting the weapons to the target area;
— Generation of GPS-referenced (WGS-84) target coordinates by on-board aircraft sensors;
— IFF for ensuring that only hostile targets are engaged;
— Weapon delivery guidance — designation technologies, seeker technologies, guidance and aiming algorithms;
— Self-defence for the strike force assets;
— Overall command and control — the systems approach.

Thème

Les conflits actuels et futurs engageant les forces de l'OTAN requièrent une réaction rapide se traduisant par des opérations de frappe aérienne de précision de réaction rapide, souvent dans le contexte d'un scénario localisé, d'intensité limitée. Les développements technologiques ont un impact majeur sur les capacités potentielles et les tactiques à employer dans ces situations: ces dernières sont souvent rendues plus complexes par la mise en œuvre de forces interarmées voire même multinationales. Ces technologies couvrent l'ensemble des différentes phases de telles opérations: la reconnaissance en vue de l'identification et de la localisation de la cible, la planification des missions, la navigation en route, la désignation de l'objectif, le largage des armes, la destruction des moyens défensifs et l'évaluation des dommages.

Les développements technologiques émergeants sont potentiellement capables de générer des améliorations majeures en ce qui concerne la flexibilité de la riposte et la précision du largage des armes. Cependant, la nécessité d'assurer l'interopérabilité et de rassembler tous ces éléments pour créer un système global efficace, impose à tous ceux qui travaillent dans ce domaine l'obligation de bien comprendre la nature des développements en cours dans les différentes spécialités. Ce symposium a fourni l'occasion, d'une part, aux spécialistes en technologie d'assimiler les besoins opérationnels, et d'autre part, aux spécialistes opérationnels de s'informer sur les capacités technologiques émergeantes. Il a mis, en outre, en évidence toute lacune en vue de la prioritorisation des futurs travaux de R&D.

Le symposium a examiné les implications des développements dans les technologies demandées pour les opérations de frappe aérienne de précision dans des scénarios de réaction rapide et de conflits localisés. Les sujets suivants étaient présentés:

— Les aspects opérationnels des opérations de frappe aérienne de précision;
— Les avancées technologiques (par exemple, les technologies de détection pour la localisation et l'identification de la cible);
— La planification de la mission en quasi-temps réel — la collecte de toutes les données significatives, la réalisation des plans et leur transfert aux aéronefs ou aux systèmes d'armes pour tirer à distance de sécurité (SOW) et aux éléments coopérants;
— La navigation en route — la livraison des armes sur la zone de la cible;
— L'élaboration de coordonnées cible avec références GPS (WGS-84) par les senseurs de bord;
— IFF pour assurer uniquement l'interception de cibles hostiles;
— Le guidage des armes larguées — les technologies de désignation, des autodirecteurs et les algorithmes de guidage et de visée;
— L'autoprotection des moyens de la force aérienne d'attaque au sol;
— Commandement et contrôle global — la philosophie de la gestion des systèmes.

Mission Systems Panel Officers

Chairman: Mr. J.K. RAMAGE
Chief, Flight Control Systems Branch
WL/FIGS Bldg 146
2210 Eighth St, Ste 11
Wright-Patterson AFB, OH 45433-7521
United States

Deputy Chairman: Prof. Dr. H. WINTER
Direktor, Institut für Flugfuhrung, DLR
Deutsche Forschungsanstalt für
Luft und Raumfahrt e.v. Flughafen
D-38022 Braunschweig
Germany

TECHNICAL PROGRAMME COMMITTEE

Chairman:	Mr. A.D. KING	(UK)
Members:	Mr. T. URING	(FR)
	Ing. C. CESTRONE	(IT)
	Dr.-Ing. U.K. KROGMANN	(GE)
	Dr. P. SANZ-ARANGUEZ	(SP)
	Mr. G. BUTLER	(UK)
	Dr. G.E. REID	(UK)
	Mr. D. DEWEY	(US)
	Mr. P. HOMER	(US)

PANEL EXECUTIVE

From Europe:
Lt.-Col. P. FORTABAT
Executive, MSP
AGARD-OTAN
7, rue Ancelle
F-92200 Neuilly-sur-Seine
France

For USA and Canada only:
AGARD-NATO
Attention: MSP Executive
PSC 116
APO AE 09777

Tel: 33 (1) 4738 5780/82
Telex: 610176F
Telefax: 33 (1) 4738 5799/6720

HOST NATION COORDINATOR

Miss C. GONZALEZ-HERNANDEZ
Subdireccion de Programas y Sistemas Aeroespaciales
INTA
Carretera Torrejón a Ajalvir, Km 4
28850 Torrejón de Ardoz (Madrid)
Spain

ACKNOWLEDGEMENTS/REMERCIEMENTS

The Panel wishes to express its thanks to the Spanish National Delegates to AGARD for the invitation to hold this meeting in Seville and for the facilities and personnel which made the meeting possible.

Le Panel tient à remercier les Délégués Nationaux de l'Espagne près l'AGARD de leur invitation à tenir cette réunion à Seville et de la mise à disposition de personnel et des installations nécessaires.

Technical Evaluation Report
on the
Mission Systems Panel Symposium
on
Technologies for Precision Air Strike Operations in Rapid-reaction and Localised-conflict Scenarios

R.W. MacPherson
Directorate of Scientific Policy
Research and Development Branch
Department of National Defence
Ottawa, Ontario K1A 0K2
Canada

1. SUMMARY

The 4th AGARD Mission Systems Panel (MSP) took place in Seville, Spain on 16-19 October 1995 on the topic, "Technologies for Precision Strike Air Operations in Rapid-reaction and Localised-conflict Scenarios."

The symposium covered topics in operational aspects of precision air strike operations, advances in sensor technologies for target identification and location, near-real time mission planning, *en route* navigation, generation of GPS-referenced target coordinates with on-board aircraft sensors, IFF, weapon delivery guidance, self defence for strike force assets and overall command and control systems.

Operational requirements for rapid-reaction and localised-conflict scenarios include avoidance of collateral damage and loss of aircraft in addition to being able to hit targets in varying conditions. Cost is a significant consideration responsible for "shooting down" weapon systems as much as enemy fire.

The rapid progress in computing power provides opportunities for realising affordable systems that had previously been only expensive laboratory concepts and demonstrations. The impact on wide area surveillance, C^3I systems and target localisation identification and tracking is now being felt.

The synergies of multi-mode, multi-function systems show promise of being affordable and more capable through optimizing trade-offs between the cost and performance of individual sub-systems.

The ability to integrate systems to exploit synergies among sub-systems may make it possible to improve overall capabilities and also reduce costs by allowing individual sub-system performance to be relaxed without compromising that of the overall system. Further exploration of this avenue is warranted.

Planners of future Panel activities might consider including Specialists' Meetings to address concerns expressed here, and at other symposia, that discussions tended to be too general in nature and not detailed enough in specifics.

2. INTRODUCTION

The AGARD Mission Systems Panel (MSP) held its 4th symposium in Seville, Spain 16-19 October 1995 on "Technologies for Precision Air Strike Operations in Rapid-reaction and Localised-conflict Scenarios." This Technical Evaluation Report is a summary and evaluation of the matters discussed at the symposium.

AGARD considers this to be a very important topic. Indeed, the former Avionics (AVP) and Guidance and Control (GCP) Panels have often re-examined the subject in symposia on similar themes over the past couple of decades (See the Bibliography). The Technical Evaluation Report (TER) for the 1982 GCP symposium concluded that technology and its applications could be expected to advance rapidly and that the subject should be revisited within three years. In 1988 the GCP symposium TER referred to NATO's serious interest in precision guided weapons, particularly for line-of-sight and beyond-line-of-sight use against armour, supporting helicopters and other platforms. In addition, the meeting noted the need to consider costs. A promising idea, recommended for vigourous pursuit at the time, was the extension of the man-in-the-loop into automatic, but not autonomous systems, using fibre optics. This would allow costly processing to be kept on the ground or in the aircraft launch platform. The hope of reduced costs, however, has yet to be realised. Precision guided weapons were revisited in 1992 because of the subsequent rapid advances in the related technologies and the experiences gained during the Persian Gulf crisis. While costs for individual sensors were in steady decline in 1992, the cost of multi-mode sensors for target and terminal guidance had not yet been resolved.

Symposia predating the end of the Cold War emphasised target destruction. With the lessening of tensions after the Cold War and the end of the Warsaw Pact, new roles and different threats evolved for NATO forces. As the theme of this 4th MSP symposium stated, the experience of the Gulf conflict and the recent events in the former country of Yugoslavia have presented challenges involving the need for rapid-reaction, precision air strike operations, often in localised, limited intensity scenarios. Now not only do targets have to be destroyed but, even more important, collateral damage and loss of aircraft and aircrew must be avoided.

The symposium theme recognised that developments in technologies can have a significant impact on the potential capabilities and tactics in these new situations, which are often complicated by the involvement of multi-service and frequently multi-national forces. These technologies embrace all phases of such operations: reconnaissance for target identification and locations, mission planning, en-route navigation, target designation, weapon delivery, defence suppression, and damage assessment. In addition, new economic realities and the reduced threat of a major conflict have made costs of military equipment a much more significant consideration for future acquisitions.

The theme further elaborates that emerging technical improvements have the potential to create major improvements in response, flexibility and weapon delivery accuracy. However, the need for interoperability and the need to bring all elements together to form an effective, complete system, makes it necessary for those involved in this field to understand the nature of the developments in different areas. The Symposium offered an opportunity for technologists to understand the operational needs, for operations specialists to understand the emerging technology capabilities, and for the identification of any 'gaps' so that future R&D priorities could be set.

3. KEYNOTE ADDRESS

Dr. Don McErlean's Keynote Address was almost a technical paper itself. In describing the vision of the U.S. Joint Advanced Strike Technology Program he captured the essence of the challenge before us, that of developing affordable, successful next generation strike systems. Although today's threat is considerably reduced, the variety is many times greater than it was in the past. Lethality, survivability, supportability and affordability are central to effectiveness of future systems. Dr. McErlean pointed out that the maximum benefit will be derived from integration of the several technologies dealing with weapons, avionics, signatures, subsystems, flight systems and propulsion. Software integration remains the key technical challenge to meet for success. Overriding all this, the most critical aspect of system performance is now affordability. Many technically successful solutions are finding themselves victims of the "budget battle." If costs continue to rise as they have in the past, technical inflation will ensure that no one will be able to afford solutions. Performance trade-offs will be needed. Only systems that are affordable will be available.

4. SESSION I: OPERATIONAL ASPECTS

This session provided valuable insights from the operational commander's point of view. Group Captain Hall's paper emphasized the much greater certainty required now of not missing the target. The political reaction to collateral damage may cause more harm than not attacking the target at all. As a pilot and commander he preferred precision guided munitions in all confrontations, and particularly in limited conflicts. The characteristics required are increased accuracy, smaller warheads, and reduced collateral damage. He felt that the current accuracies may not be enough to prevent collateral damage. In limited conflicts targets are fewer but of higher value. As national survival is not at stake, there are more constraints on cost and the need to reduce the 'logistic tail'. In addition, in his experience, there was often more time to plan missions against less capable defences. Therefore, all weather capability may not be as important as it once was. Fewer, smaller weapons are needed that are more suitable for stealth platforms. In his opinion, man-in-the-loop systems carried less risk than those using autonomous weapons technology, which has not yet matured enough to be reliable. His choice for now is the laser-guided bomb as a general purpose weapon for limited conflict scenarios.

The remaining three papers in this session emphasized the need for improving C^3I systems and suggested that affordable, effective solutions were in sight using recently available technologies, many of which have had their origins in the commercial sector.

Peter Becher summarized the results of the AGARD Aerospace Applications Study (AAS) 39 which concentrated on Reconnaissance, Surveillance and Target Acquisition (RSTA) operations for NATO. RSTA systems include sensors and the C^3I assets required to integrate, analyze and distribute information for exploitation. The problem with current systems is that they lack connectivity, bandwidth (especially for images), and long range capability. The study concluded that affordable, commercial off-the-shelf (COTS) technology for connecting current military and commercial high-band-width communications is available now and the integration could be accomplished by the year 2000.

In the third paper in this session, Mr. Daniel Mellies presented a different set of requirements for precision air strikes. Some scenarios require a rapid reaction capability where the need is to reduce mission planning time for maximum surprise effect. An effective real time C^3I system is needed to shorten the decision making process and all weather capability is needed to deliver the strike expeditiously. He argued that the helicopter appeared to provide the most effective solution because of its survivability in low level flying at night and its stand-off engagement capability. It also has secure C^3I systems available providing updated target intelligence and positive identification. The performance of its weapons systems at night maximizes hit probability and avoids collateral damage. He believes the helicopter is less limited than fixed wing aircraft in adverse conditions, such as bad weather, when the challenge is to achieve pinpoint destruction of targets, while reducing losses and avoiding collateral damage.

Col. Bruce Queen described the use of wide area surveillance to give commanders and national command authorities near-real time data to support crisis management while demonstrating resolve. Such a system should be designed to detect, process, display and distribute information and provide options for a tailored response. Sensor enhancements required include expanding existing systems capacity to exploit both moving and stationary targets. Technical challenges include a threefold increase in SAR resolution. Data processing for fusing database information in near-real time will need 100 gFLOP (10^9 floating point operations per second) capability, which should be available by the year 2000. He predicted that using wide area sensors with near-real time coverage and massive data base retrieval and fusion capabilities will revolutionize joint and combined operations. Insertion of near term technologies into combat systems is expected to demonstrate the viability of these concepts and validate improved effectiveness.

5. SESSION II: MISSION PLANNING/MISSION MANAGEMENT

In his introductory remarks session Chairman, Dr. George Reid, pointed out that mission planning is critical to mission success. It was unfortunate that one of the three papers scheduled for this session was withdrawn.

In the first paper, Mr. Thomas Reese described a situation in which the cost of precision-guided weapons and the mission planning systems required to ensure mission success is increasing. Therefore, it is important to know if mission plans perform effectively, that subsystems function satisfactorily and at the right time, and whether unexpected or marginal subsystem performance occurs. The simulator Mr. Reese described to verify these aspects was designed to test weapons in a comprehensive, total system environment to reduce the number of live firings and captive flights that contribute heavily to development and life cycle costs. During development, the facility revealed several undesirable features in weapons that were corrected before production. Insight rather than oversight is the benefit of this approach.

Simulation and modelling are beginning to prove themselves as valuable adjuncts providing alternatives to extensive, costly development and verification trials.

In the second paper Mr. Rheihard Vogel likewise emphasized the importance of supporting mission planning with semi-automated mission planning systems. In rapid reaction scenarios local conflicts may be outside the "home" area of NATO operations. Thus, mission planning systems need to be portable and capable of carrying out tasking independent of national C^3I systems. They also need to be capable of coordinating missions with allies. Much of this capability has been demonstrated in the Open Skies program with an adaptation of the DIPLAS Mission Planning

System, and in Bosnia using a transportable Tornado Mission Planning System for Allied Mobile Forces (TMPS-AMF).

6. SESSION III: NAVIGATION

There have been enormous gains in navigational accuracy in recent years. There is more confidence in knowing one's exact position. Positional accuracy is now discussed in terms of a few rather than several tens of metres. This session concentrated on Global Positioning System (GPS) modes, terrain referenced navigation and millimetre wave radar.

A number of techniques using relative GPS and inertial guidance systems (INS) have demonstrated high accuracies for low-cost weapons systems, that is, weapons that do not have terminal seekers on board. Differential GPS (DGPS) systems also exhibit accuracies of a few metres. Carrier phase or kinematic GPS has the potential of determining positions to accuracies of a few centimetres. The difficulty in verifying such systems is the need to know actual positions within millimetres. Indications are, however, that carrier phase data is sufficiently accurate to verify accuracies of INS/DGPS systems at a reasonable cost.

Terrain referenced navigation has potential in situations where GPS is not available. It can exploit raw satellite imagery directly, thus reducing time consuming and error prone coordinate transformation processes. Although INS/GPS technology will likely provide the basic stand-off missile system navigation it depends upon precise target co-ordinates. Coupling INS/GPS with terrain referenced systems can provide the necessary accuracy. The databases required to do this are expected to become more readily available as libraries of satellite imagery accumulate.

An enhanced vision system based on multi-function millimetre radar can provide an all weather means of navigation that is independent of ground based and satellite systems. A key feature of the system Mr. M. Pirkl *et al.* described is a frequency scanning antenna that avoids mechanical rotation of the antenna itself. The technique can be combined with frequency modulated continuous wave principles to produce a radar whose range for small targets exceeds that of radar detection schemes used in high performance ESM systems. The system bridges that gap between conventional radar and SAR and provides enhanced performance for terrain avoidance, terrain following and airborne obstacle avoidance in adverse weather conditions. The accuracy achieved is adequate for autonomous landing in CAT IIIb conditions.

7. SESSIONS IV & V: RECONNAISSANCE AND TARGET IDENTIFICATION

The importance of this topic is reflected in the number of papers presented in these two sessions. Session chairman, Paul Homer, introduced the topic with the comment that the critical function in precision strike operations has been and remains that of acquiring, identifying and localising targets. Accurate target discrimination is required not only to maximize warhead effectiveness but also, just as important, especially now, to avoid collateral damage or harm to friendly forces.

Present-day tactical aircraft have difficulty attacking short-dwell-time targets with success because of shortcomings in current acquisition systems. In the first paper in this session, Mr. M.J. Boyd *et al.* attributed these deficiencies to the limited resolution of sensor systems, operator workload and the lack of automated target detection and cuing systems. Failure to find the target is the main reason for lack of mission success even for preassigned, large, stationary targets. As a solution to this problem the authors proposed the use of multi-spectral image correlation technologies in which FLIR and low-resolution ground-map radar images were correlated with templates generated from SAR data. Their research program demonstrated the feasibility of automated targeting at near video framing rates. However, the limiting factor was the time required for the operator to confirm or reject the aimpoint. Operator confirmation is a requirement of the current rules of engagement, therefore, further research is needed on the best way to present sensor data to the operator so he can make decisions quickly and correctly.

Similarly, the paper by Dr. F. Nivelle *et al.* discussed an autonomous, stand-off seeker that uses dual mode IR and mmW active radar correlated with ground maps to acquire and track targets. The advantages of the multi-mode seeker are found in the complementary aspects of the various modes that result in improved efficiency, robustness and resistance to countermeasures or adverse weather conditions. Such a dual mode seeker can be constructed today but a few difficult points have yet to be overcome. In particular, the bi-spectral dome needs work to satisfy demands of stealth and supersonic flight.

The paper by Mr. G. Balzarotti *et al.* addressed the problem of identifying friendly forces in localised, but high density conflict areas. As they saw it high performance infrared imaging sensors were highly desirable for identification of friends but the man-machine-interface needs improvement. They proposed solving part of the operator interface problem by presenting IR images on helmet mounted displays. The authors were able to show that observers' performance in identifying friendly objects improved significantly after a learning phase in which targets were repeated. The idea needs further study as rules for identifying objects could not be developed from the current results.

Mr. P.R.C. Collins described a mechanism for matching a model of a previously prepared database of terrain features to images obtained from an electro-optical sensor on board the air vehicle. The method is based on an image database fusion concept. The approach, called Model-Matching, was previously well developed for image processing and relies on relating line based features in an image with a 3D computer aided design (CAD) model of the objects of interest. It is robust with respect to noise in poor imagery or partially obscured targets, is capable of finding many different types of object and is able to pick out targets approached from any altitude or bearing. In addition to not requiring detailed information about the target beyond its general location among visible landmarks, it is stealthy as it emits no radiation and it does not rely on systems such as GPS.

Recent advances in computational hardware and signal processing have made real time digital video possible for a number of applications. Through image compression the number of bits of information needed to represent a given image can be reduced to lower the demands on communication links. The image quality and hardware requirements for weapons control and damage indication differ from those of video broadcast for which the MPEG compression algorithm was developed. The former requires transmitters to be of low complexity because of weight, size and power considerations. Even more important are costs related to sensors and associated transmitters that are expendable. Video broadcast, on the other hand, needs simpler receivers since there are many of them. It would not be surprising then, that the optimum techniques for digital video compression would differ for the two applications. In their analysis of compression techniques, Dr. Creusere and Dr. Hewer discovered that block-based discrete cosine transform algorithms were superior for high bit rate, high quality video applications but that wavelet-based algorithms were the better choice for low bit rate, reduced-quality video. However, before systems can be adopted for military applications, more work is required to determine the level of video quality required and how the battlefield might affect the data link.

Mr. C.N. Shen *et al.* described a demonstration of a scheme to identify non-cooperative targets at long range using a ruggedized, compact airborne laser radar (LIDAR) sharing an aperture with a staring focal plane array infrared sensor. In addition to being capable of operating in several modes including passive IR imaging, range profiling and high resolution three dimensional LIDAR infrared imaging, the system demonstrated the feasibility of using μ-Doppler signatures for air and surface target identification. Techniques developed for Doppler radar target signatures and sonar signal analysis were adapted to show that the vibrational signature inherent to ships, aircraft and ground vehicles are unique. Since it appears that these signatures would be difficult to hide, the technique shows very good promise for positive target identification.

8. SESSION V: TARGETING AND WEAPON DELIVERY GUIDANCE

Differential GPS can be used for weapons guidance in addition to the normal navigation function discussed in Section 6. The first two papers in this session described a method of achieving of enhanced navigational accuracy by generating theatre-wide DGPS corrections via a network of GPS receivers 1000 miles away. This kept the costly assets of the system well outside of the area of conflict. The work showed promising stand-off weapons delivery accuracies of a few meters, not only in the horizontal plane, but also vertically. However, not all of the DGPS errors are well understood, particularly those due to noise and multipath effects. The latter appear to contribute more to miss distances than originally thought.

Modern air defence systems make it very risky for aircraft to approach within 10 km of their intended targets. Many of these air defence systems depend upon optronic sensors for short range detection and guidance. This favours attacking during conditions of poor visibility when optronic sensors perform inadequately and acquiring targets at ranges sufficiently great and quickly enough to avoid remaining too long within the firing range of radar guided surface to air systems. Two ways of doing this have been recognised for some time: stand-off at very long ranges to avoid air defences altogether and, secondly, approach at high speed and very low altitude. The problem is to find, identify and localise targets of interest under these conditions.

Mr. Bernard Dortomb presented a paper on an automatic, all weather, ground target acquisition system that depended upon the creation of "target pattern" from various reconnaissance data beforehand. Care was required to avoid any distortion so that they could be compared automatically with radar maps generated on board the aircraft without elaborate image processing.

SAR images can likewise be used to locate targets. In its simplest form, the operator views SAR generated maps and finds and designates the target himself. Mestre and De Peufeilhoux described three methods of automating the process. In the first it is assumed that the location of every point of the SAR image with respect to the aircraft is well known as well as the position of the target. In the second method the radar map and position of the target are modelled ahead of time. In this situation the location of the target is determined indirectly so it is not necessary for the target to have a very characteristic signature. Thirdly, if the geometry of the radar map is not well known, the target can be found, but not precisely located, so firing on it requires some form of terminal guidance. The authors demonstrated that the second technique, correlating line segments extracted from radar images with segments in a reference model of the terrain prepared before the mission, was robust, could be realised in a real time system, was easily adaptable to different mapping modes or the addition of other features (such as bright points) besides line segments, and could "filter" out residual distortions in the radar image. The main application of this technique is the acquisition of targets with known fixed coordinates. A second application is as an aid to acquiring movable targets as described in the ASTRID paper by Dr. F. Nivelle *et al.* (Paper 14).

Mr. E.L. Fleeman analyzed a number of autonomous, adverse weather precision guidance techniques from the point of view of cost. The performance requirements were driven by the need to reduce pilot workload, improve aircraft survivability and improve effectiveness in adverse weather. He believes that a synergistic application of emerging technical developments including near real-time targeting, high accuracy mid-course guidance, and aim-point selection with a strapdown seeker will provide low cost, adverse weather precision guidance. The advantages he envisaged to be gained include the need for only one weapon per target, smaller warhead requirements, higher load out, and less collateral damage. His advice was to use GPS for initial mid-course guidance, INS final mid-course guidance and strapdown, and an imaging seeker terminal guidance with short range acquisition. His recommendations for strapdown imaging seekers include imaging IR, low power imaging mmW and imaging dual mode (mmW/IR). In the latter case, synergistic fusion of IR and mmW signals should allow for relaxed requirements for the individual sensors, resulting in dual mode seekers that are lower in cost and weight.

Recent developments in infrared detectors have led to the creation of high performance systems occupying a small volume that can address both navigation and attack functions. The appearance of imaging IRCCD detectors, for example, is an important advance for air-to-ground attack. These devices can produce images of quality similar to that obtainable in visible light and allow pilots to navigate at night at low altitudes. The spatial and thermal resolution is good enough to use image processing techniques to identify landmarks in the image accurately with a high degree of probability, which could in turn be used to update navigation systems. The precision possible is comparable with that of GPS and could be used in conditions where GPS is not available. For ground attack at night, IRCCD cameras offer the pilot the same visual capabilities for attacking targets that he would have in daylight.

Similarly, Dr. E. Crovari *et al.* demonstrated the effectiveness of infrared imagery in a stabilized seeker for air-to-surface missile. The system had three operational modes: lock before launch, guided mode and lock after launch. The system provided high detection range, excellent tracking stability and reliability, and offered stand-off capability via an ECCM video/data link. The seeker availability in all-weather (including rain and fog) and EOCM scenarios was good.

The limited stand-off range of bombs suggests the need for propulsion to increase ranges and thereby improve the survivability of bombing aircraft. In order to maintain the required accuracy some form of guidance is needed. INS systems require initialisation, which can be expensive to retrofit on older aircraft not fitted with digital data links to the bomb racks. To avoid this expense, Parturel *et al.* proposed a scheme to launch propelled guided bombs without initialising the inertial guidance systems. The basic idea is to program the bomb to follow and launch it into a predetermined trajectory that leads to the target. In effect the guidance system eliminates the effects of wind and atmospheric braking. Initial conditions need only be estimated from the initial launch velocity and acceleration. In a simulation, the authors demonstrated bombing ranges in excess of 10 km with propelled bombs and improvements in accuracy of 30% to 40% over classical bombs.

Modern air defence systems pose a significant threat to attacking aircraft and call for anti-radar missiles to counter them. With the collapse of the Warsaw Pact, modern Soviet systems are available to nearly anyone. In addition, western systems may be used aggressively by countries with previous access to western technology. Possible adversaries have a wide range of choices and the potential capabilities to modify them. Consequently new demands are placed upon the anti-radar systems that NATO needs. Although currently available high speed anti-radar systems, such as those on the TORNADO, can fulfil present and future UN peacekeeping missions, further improvements can be made. These include a wider spectrum to classify electronic threats and an increase in the number of modes that can be handled. The ability to enter ELINT data on the fly will enable attacks on targets not contained in system libraries. This will make it possible to deal with threats using "war reserve modes" that are currently unknown to intelligence and reconnaissance forces.

One of the criticisms of GPS derived guidance for precision weapons is the perceived apparent vulnerability of GPS receivers to jamming. Dr. S. Mahmood *et al.* described an analysis of DGPS using adaptive filtering and anti-jam techniques to enhance the accuracy of weapons in adverse weather as well as reducing the susceptibility to electronic countermeasures. (jamming). Whereas conventional GPS receivers have jamming to signal thresholds of 30-50 dB the Tactical High Anti-jam GPS Guidance (THAGG) program has demonstrated, in simulation, acquisition thresholds of 75 dB and tracking thresholds of 125 dB.

Progress in the development of artificial neural networks has reached the point where it is possible to envisage adapting them for nonlinear autopilots for missile guidance and control. Adaptive control systems find only a limited number of points on the control function surface. The learning process in neural networks finds the whole surface. Dr. U.K. Krogmann was able to show by simulation that neural networks can solve the problem of stable flight control of a fully non-linear, time varying dynamic model of an existing missile airframe. The results were very promising. Addressing the real problem of getting to the target with maximum acceleration is the next step.

The final paper by Dipl.-Ing. V. Scherm *et al.* addressed the problem of self protection against optronic missile seekers using a soft kill mechanism based on directed infrared countermeasures (DIRCM). Older missiles can be defeated by the use of chaff, flares and jamming, but newer ones are able to distinguish between flares and aircraft and imaging seekers are jam resistant. Jamming, blinding/dazzling or destruction of the sensor by means of a high power laser beam or light source are three mechanisms proposed for defeating optronic systems. Control and tracking is within reach of current technology. Out of band lasers kill by destroying domes and lenses, but are still too big for practical use. Lasers operating in the band width of hostile seekers need not be very large and can be flown on larger aircraft and helicopters. Outputs of a few joules and repetition rates of around 10 Hz are sufficient. Within the band a wide tuning range is needed. The authors' analysis suggests that DIRCM systems provide a complementary addition or replacement for traditional defence systems and offer new capabilities for dealing with newer missiles that are not otherwise available.

9. SUMMARY DISCUSSION

During the open discussion participants expressed their belief that the symposium had been very useful and that considerable material had been covered. Indeed, all the topics listed in the symposium theme received some attention. The depth of coverage was not as great as some had wished. In a symposium of this nature it is difficult to provide too much detailed information in papers targeted to a general audience. Some areas may be amenable to more in depth treatment in a Specialists' Meeting and the Panel may wish to consider this in future activities.

The vulnerability of precision guided munition systems to jamming was not covered to the extent that some had hoped. For example, laser decoys for designation systems were missing. It was felt that countermeasures, in general, could have been dealt with more thoroughly. This was in spite of the papers on hardened GPS and defence against optronic seekers. Although the latter discussed concepts that have been known for two decades or more and described results from simulations, indications are that the technology is closer to being demonstrated in deployable systems.

Of the information on countermeasures that was presented, the surprise was the capability of hardened GPS systems to withstand giga Watt level jammers. Countermeasures against IR seekers for missiles were covered in the self defence paper on DIRCM.

In line with a major theme in the keynote address the question of cost was raised almost immediately. One participant indicated that some commanders have expressed a dislike for seekers in weapons because of the cost and weapon size requirements. This reiterated the keynote speaker's main point that future weapons must be cost effective. Wing Commander Herriot commented that while research is great, developers must keep costs down. This suggests that further systems analyses are needed along the line of Mr. Fleeman's work of trading off costs and performance among subsystems to achieve overall effectiveness in systems that are affordable. In answer to a question on relative costs, participants quoted figures of between $10K and $12K for laser based seekers and $30K to $50K for SAR based seekers.

The papers on navigation indicated that we will soon have the capacity to steer anywhere in the world to sub-meter accuracy. This invited the question of whether much further research would be needed for navigation. Mr. King felt that the countermeasure and counter-counter measure aspects will remain a challenge for a while.

In summarizing the overall symposium Dr. Graham Wallis characterised the main mission functions as mission planning, navigation, target acquisition and tracking. For each of these, the authors offered various technical solutions or methods of addressing them.

Table 1. Operational Functions and Technical Methods

Function Method	Mission Planning	Navigation	Acquisition	Tracking
Signature			✔	✔
Geometry		✔		
Scene Feature			✔	✔
Scene				✔
Man-in-loop	✔		✔	

From Dr. Wallis' summary in Table 1 it is apparent that the various technical approaches can be applied to more than one function and, in turn, a particular function can exploit or may need more than one technological solution. This was evident from the number of papers on GPS and imaging radars with pattern matching that appeared in different sessions where authors had found new and different ways of applying basically the same technology to different aspects of the precision guidance problem.

In turn, each of the methods or technical solutions relies on a variety of sensors which he summarized in Table 2. Here again more than one sensor type is applicable to a particular technical solution. More often than not the sensors are complementary in their contribution rather than alternatives. This suggests that multi-sensor systems still provide the most technically competent solutions but at potentially greater cost. the cost issue may be not so severe as Mr. Fleeman indicated in his study in which it appeared possible to relax individual sensor requirements, and hence costs, and regain the technical advantages of the synergistic effect of using multiple sensors in an overall system.

Finally, the various sensors discussed can provide support to more than one mission function as summarized in Table 3. The sensors tend to fall into one of three classes: those that support acquisition and tracking (Class 1) as would be found in precision guided munitions; those supporting mission planning and navigation (Class 2), as required , for example, by cruise missiles; and those that support all four functions (Class 3) of the overall guidance mission.

Table 2. Sensors Employed in Various Technical Solutions

Method Sensor	Signature	Geometry	Target Features	Scene Matching	Man-in-the-Loop
IRCCD			✓	✓	✓
SAR/DBS				✓	
Ground Mapping Radar				✓	
MTI	✓				
Passive mmW					
Semi-active Laser					✓
Anti-Radiation	✓				
Laser Radar	✓		✓		
GPS		✓			
Radio Altimeter		✓			

Table 3. Classification Sensors Applicable to Operational Functions

Function Sensor	Mission Planning	Navigation	Acquisition	Tracking	Class
IRCCD[■]	✓	✓	✓	✓	3
SAR/DBS[*]	✓	✓			2
Ground Mapping Radar		✓	✓		2
MTI[†]			✓	✓	(3)
Passive mmW	✓				1
Semi-active Laser				✓	1
Anti-Radiation			✓	✓	
Laser Radar			✓		
GPS		✓			2
Radio Altimeter		✓			2

[■] IRCCD Infrared Charge Coupled Device

[†] MTI - Moving Target Indicator

[*] SAR/DBS - Synthetic Aperture Radar/ Doppler Beam Sharping

10. FEEDBACK FROM PARTICIPANTS

Unfortunately, due to the lack of a reminder, only a few evaluation questionnaires were returned to the symposium organizers so no meaningful statistical significance can be attached to the results. Of those that were received, the distribution of responses on the degree of impact in the various areas was fairly uniform except for the lack of ratings at the highly significant level. It is perhaps worth noting, however, that the greatest impact identified was in providing valuable new perspectives to participants' work. Several felt there was little impact in spawning specific new initiatives or on filling gaps in the existing research base. Nevertheless, respondants deemed theoverall value of the symposium to be in the range from 'generally or potentially important' to 'significant,' with one respondent rating it as 'extremely valuable.' No one felt that it was not worth the effort. Comments indicated the papers were good on the concepts and general aspects of the problems, but that details were missing. The time allotted for discussion and opportunities at lunch and coffee breaks for establishing new contacts was seen as too short by some. Aside from the questionnaire results most verbal comments were positive. Attendance was good and was maintained throughout the symposium. Of the approximately 200 who enrolled 140 registered at the meeting.

11. SYMPOSIUM ORGANIZATION

The Technical Program Committee is to be congratulated on developing a well balanced program and obtaining papers that covered the topics outlined in the theme. It was remarkable that there was only one cancellation in the entire program. Unfortunately it occurred in a session that had only three papers to begin with, leaving the mission planning topic a little under represented. Representation from the major defence industrial member nations was even. It was somewhat disappointing not to find papers from the other members of the Alliance.

The program and session chairmen exercised very good control over the time of presentations and ensuing question periods. Although there did not seem to be any particular point where discussion had to be terminated because time had run out some participants felt inadequate time had been allotted. This point may have been more related to periods for available informal discussion, as at breaks, than for the formal question periods.

Questions and the ensuing discussions would be easier to record accurately in future symposia if question sheets were made available to those asking questions or making comments. A single sheet could be provided with places marked for the questioner's name, affiliation, the title of paper to which he is referring and a half page area for his question followed by a half page area for the author's response. Session chairmen would be responsible for seeing that questioners received and filled out a sheet and that the authors subsequently completed them after the session. In this way, participants asking questions would have an additional opportunity to clarify their questions and authors could give more complete responses. Questions and responses could be reproduced verbatum at the end of the papers in the Conference Proceedings. This would enhance the value of the Conference Proceedings by having a more accurate record of the discussions in addition to a mere reproduction of papers.

Several participants asked about attendance lists. Many wished to follow up with other participants after the meeting and wanted a list of names and addresses. At one time lists of participants were available at the meeting and/or published in the Conference Proceedings but the practice was dropped in part for security reasons, especially for classified meetings, during periods when there had been a number of hostage taking incidents throughout the world. A participants list would certainly be a useful addition to the Proceedings and had been requested at other symposia. For classified meetings, including the list in the classified supplement might allay fears with respect to identifying participants openly.

The question of classification frequently arises at Panel Business Meetings and those of the National Delegates' Board concerning the cost of holding classified meetings. The point was not raised at the Symposium, but I raise it here because only a few papers were classified, and then only at the NATO Confidential level. This was in spite of the meeting being classified at the NATO Secret level. I would argue that this does not necessarily support the case for holding only unclassified meetings. The oral presentations and the discussions that took place both in the formal question periods and informally in individual conversations, did contain classified information. Had the meeting been unclassified, participants would not have been free to carry out these discussions and indeed may not have attended if they had felt they would have been restricted in what they could discuss.

12. SYMPOSIUM ADMINISTRATION

Seville was a good choice for an Autumn meeting site. The weather was pleasant, warm and dry, but not too hot. The area of Seville around the site and hotels provided an interesting diversion after hours with its many tourist attractions and historic sights.

The Spanish hosts provided superb facilities at the World Trade Centre on the site of the 1992 World's Fair. These facilities were very comfortable, had a well equipped auditorium and were located within easy walking distance of the recommended hotels. MSP Coordinator for Spain, Dr. Pedro Sanz-Aranguez and Spanish AGARD Coordinator, Ms Carmen Gonzalez Hernandez organised excellent support for the symposium through the staff of the World Trade Centre. Projection and sound equipment were particularly noteworthy as was the work of the technicians whose performance was exemplary. Past symposia at other sites have sometimes experienced difficulties with video projection, but here, several authors were able to use video effectively.

Of particular note was the reception the Spanish National Delegates to AGARD, D. Luís Guitart Poch and D. Julián Simón Calero, hosted in the Real Cartuja (Isla de la Cartuja, Seville) on Monday evening. In addition to providing a very interesting tour of the historic site they offered superb refreshments and an opportunity to meet with them and the authors and other participants in an informal setting.

The Programme Chairman, Mr. King, thanked the interpreters for their excellent work. It is frequently particularly difficult to interpret technical material, especially when there are gaps in material provided, or speakers diverge far from prepared texts. No one reported any significant problems with the interpretation.

The Spanish security staff were vigilant and courteous. Registration and daily check-in were accomplished quickly and effectively.

The Technical Tour to the Experimentation Centre of the Instituto Nacional de Técnica Aeroespacial (INTA) in El Arenosilla, Province of Heulva, was well attended. The Centre provided a light lunch before taking the participants on a visit to the drone refurbishing facility, tracking and telemetry trailers and scientific and technical experiments in solar energy use. Several staff were at our disposal and were eager to answer questions on all aspects of their work. It was one of the better Technical Tours the writer has had the opportunity to attend over many years' association with AGARD.

13. CONCLUSIONS AND RECOMMENDATIONS

It is remarkable that in a symposium of this size and nature, only one paper was withdrawn and then only because the author was unavailable and not for any second thoughts regarding security.

The quality of the papers was generally high. Technical content was at a level appropriate for a mixed audience of operational personnel and technologists form various disciplines. There were no marketing pitches even though some systems described were obviously available for sale. Authors stuck to describing the underlying technology and operational needs the systems satisfied. One frequent comment heard was that some papers were too general in nature and did not discuss details sufficiently. This observation has been made in previous symposia and may be a result of authors addressing a general audience rather than specialists. As suggested before, one way to address this issue if it is deemed to be significant, is to consider convening Specialists' Meetings to address some of the finer technical details.

The technical content of the papers themselves tended to reflect evolutionary advances rather than significantly new approaches. This is not meant as a negative comment but an observation. The fact that technology has advanced sufficiently to allow early concepts to be tried out in new systems is an advance in itself. It is evident that progress in computing power and manufacturing processes for sensors have now made affordable many approaches that have been heretofore only realisable in laboratory settings. In particular, computational capabilities for C^3I, signal and image processing, and implementation of neural networks in hardware have reached the point where weight, power requirements and costs are no longer seen to be impassable barriers.

In terms of future directions, the authors pointed out a number of specific areas where further work is needed. Compression algorithms need exploring for video links, but first the actual video quality required for military operations needs to be characterised and determined. Head-up display (HUD) of IR and radar imagery needs more work to develop "rules"for identifying objects. Lidar μ-Doppler signatures exploited known sonar techniques and data with good success. Further work is needed to generate libraries of signatures and to optimize for μ-Doppler lidar the data processing techniques adapted from sonar and radar. Distributed, wide area C^3I systems that transparently link systems across land, sea and air environments as well as amongst allies and even civilian resources are becoming more realisable and more work in this area should provide significant rewards in the future.

The ability to integrate systems to exploit synergies among sub-systems may not only make it possible to achieve improvements in overall capability but may also reduce costs by allowing relaxation of individual sub-system performance without compromising that of the overall system. This avenue warrants further exploration.

Ideally, mission specific weapons provide the best technical solutions, but the cost of specialised systems can be prohibitive. Rather, systems capable of multi-mode operation, achieved perhaps more through software than hardware development, appear to be a more productive approach. For example, the basic data from sensors, be they navigation, optronic or radar, can be processed and used for many mission functions and, therefore, having individual systems for each function no longer makes much sense. The immediate problem, however, is that existing air platforms have separate systems in varying degree so that integration is not a simple, straightforward problem unless everything is replaced. The challenge is to find ways of inexpensively interfacing a disparate variety of existing systems and sub-systems to extend their service until next generation equipment is developed with total integration capabilities in mind.

As a final comment, planning for subsequent Panel activities should take into consideration future technological trends revealed in the 2020 Study AGARD is now undertaking.

14. BIBLIOGRAPHY

Conference Proceedings

1. "Impact of Advanced Avionics Technology on Ground Attack Weapon Systems", Aghios-Andreas, Greece, October 1981, AGARD CP 306, February 1982 and CP 306(S), February 1982
2. "Precision Guided Munitions: Technological Operational Aspects", Norway, May 1982, CP 320, September 1982 and CP 320(S), October 1982
3. "Advanced Computer Aids in the Planning and Execution of Air Warfare and Ground Strike Operations", Bølkejo, Norway, May 1986, AGARD CP 404, February 1987 and CP 404(S), March 1987
4. "Guidance and Control of Precision Guided Weapons", Geilo, Norway, May 1988, AGARD CP 435, November 1988 and CP 435(S), January 1989
5. "Advances in Guidance and Control of Precision Guided Weapons", Ottawa, Canada, May 1992, AGARD CP 524, November 1992 and CP 524(S), December 1992

Reports

6. AASC Study No. 11, "Suppression of Detection and Guidance Systems, Other than Radar, Associated with SAMs, ASMs and Guided Bombs", AGARD AR 121, August 1979
7. AASC Study No. 6, "Use of Precision Positioning Systems by NATO", AR 88, Vol. 1, July 1976; Vol. 2 January 1977; Vol.3 November 1977
8. AGARD Advisory Report No.259, "Technical Evaluation Report of the Guidance and Control Panel Symposium on Guidance and Control of Precision guided Weapons", AGARD AR 259, January 1989

The need for precision-guided munitions in limited conflict
An operational viewpoint

Group Captain Ian Hall
Ops Log division
HQ BFJ BFPO 633
B-7010 SHAPE, Belgium

1. SUMMARY

A missed air-to-ground attack is never welcomed by an operational commander; collateral damage and the increased possibility of attrition engendered by the necessary re-attack are but two of the likely, undesirable results. The effects may assume increased significance in a limited conflict, where political factors may bear relatively more heavily than in general war. Thus precision-guided munitions may be a highly desirable option. In the purely military sense, the conditions prevailing on the less-dense battlefield may tend to present particularly favourable conditions for the employment of precision weapons; however, there may be counter arguments, and occasions where PGMs are not the best option. The paper offers examples from recent conflicts to support the general case for PGMs, before going on to discuss advantages and disadvantages of generic types of weapon. Finally, while acknowledging that nations are unlikely ever to procure weapons specifically for limited conflict, it discusses the ideal stockpile for small-scale operations. In doing so, it flags up the point that characteristics of the target identification and designation system are likely to be at least as significant as those of the weapon itself.

2. INTRODUCTION

From an operational commander's viewpoint, a miss is undesirable in *any* air-to-ground attack. The failure to kill a target will have an impact to varying degree on the overall campaign and in the close-range area as it affects the local ground commander. The mission may have to be re-tasked, with several consequent effects: the expenditure of additional, possibly scarce, munitions; the increased chance of attrition; and the reduced availability for other tasks. A miss also brings with it the danger of fratricide in certain, close-contact scenarios, as well as the possibility of collateral damage.

All this may be acceptable and or unavoidable in a large-scale conflict, where an isolated failure to neutralize a target may be hidden in the fog of war, while the scale of involvement and the multiplicity of targets may leave no alternative to the use of many cheap, inaccurate weapons. Moreover, in a fully-developed confrontation, the density of enemy defences may necessitate a single, high speed, low-level pass, with its associated target identification difficulties and possibility of a missed attack.

It is unwise to generalize in descriptions of localized conflict, which may take forms as diverse as anti-guerilla or

Paper presented at the AGARD MSP Symposium on "Technologies for Precision Air Strike Operations in Rapid-Reaction and Localised-Conflict Scenarios", held in Seville, Spain, from 16-19 October 1995, and published in CP-576.

peace-support operations, but it is reasonable to identify the common thread that, for various reasons, the *balance in the decision making process moves in a limited operation towards a requirement for a greater certainty of not missing any given target.* Own forces are, perhaps, more likely to be at close quarters, while attrition may be less of a factor, with enemy defences likely to be both less dense and less sophisticated. Fratricide and collateral damage are likely, for several reasons, to become increasingly unacceptable: in a small-scale conflict, because forces tend to be less numerous, such incidents would be likely to be more visible; public support for involvement in the conflict would be less likely to be firm, both from participating nations and from the world community, with displeasure possibly being expressed through the UN; and "mishaps" of any sort would be likely to undermine further the resolve of participating parties. All this could be exacerbated by media presence, whose rapid widespread reporting could be relatively more widespread in a limited operation.

3. PGMs IN LIMITED CONFLICT

Precision-guided weapons are desirable in any conflict, but this reasoning suggests that they tend towards being essential in localized scenarios. They offer increased accuracy, which in turn permits smaller warheads to be fitted for any given probability of kill. The chance and scale of collateral damage is, therefore, minimized. The characteristics of targets in a small-scale conflict might also militate against the employment of unguided munitions; there would be fewer, therefore, almost by definition, a large proportion might be regarded as "high value", the traditional target for a PGM. Target hardening might also need to be considered in the general discussion of unguided or precision weapons; although it could be argued that the probability of hardening is lower in limited conflict, there are likely to be sufficient exceptions to make this a neutral factor. On the other hand, it would be reasonable to accept the generalization that, because limited numbers of munitions would be employed in a small-scale conflict, there would be less danger of exhausting expensive stockpiles, and this could be a factor which would encourage the use of precision munitions in this scenario. The fact that national survival is unlikely to be at stake when a major nation becomes involved in a limited conflict would add to the pressure to hold down costs. Moreover, the imperative to limit the scale of logistic support - which tends to account for a large proportion of the costs of a deployed operation - might also argue for a requirement for a few precision weapons rather than large quantities of dumb ordnance. Reducing the size and cost of the logistic tail can, in many cases, produce savings which far outweigh the higher unit cost of PGMs.

Military considerations might not be uppermost in the types of warfare under discussion; indeed, the military objective in a limited campaign may not be paramount. An example of this occurred during the brief bombing campaign in Southern Iraq during January 1993 when, following an Iraqi build up and repeated infringements of the no-fly zone, the coalition was forced into military retaliation. The military objectives were very limited; little more than a demonstration of resolve was required. Of prime importance were, however, that no coalition forces were lost and that there was no collateral damage to Iraqi civilian facilities, especially those of a humanitarian or sacred nature. Either eventuality would have resulted in propaganda gain for Iraq, with a parallel loss of public support amongst friendly nations. It was, therefore, absolutely essential to use precision weapons, to ensure positive target identification before weapon release, and to have fully serviceable and reliable airborne systems.

In peace support operations, the balance is likely to tip even further towards use of precision weapons, while political considerations are likely to impinge even further on military objectives. An example here was the May 1995 request by the UNPROFOR military commander for an air strike in Sarajevo following hostile action within the weapons exclusion zone. This request was not supported by the UN higher command, on the basis that the primary outcome of any punitive action was assessed to be wider in the sense that it would cause inflammation of the overall situation in Croatia and Bosnia-Herzogovina.

Turning away from the political argument now, a limited operation can offer some particularly favourable conditions for the employment of precision-guided munitions. Specifically, the time may be available to either the commander or the aircrew to permit more leisurely planning, force packaging, target acquisition, identification and lock-on. At the tactical level, less dense defences and or air superiority might offer the aircrew the opportunity to work at medium level rather than make a single, low-level pass. Of course air superiority is not guaranteed in limited conflict, but it is more likely that even dense defences could be neutralized, by Electronic Support Measures, for example, more easily in a small-scale operation; not least, the inventory of own-force ESM platforms is more likely to be adequate to cope with limited opposition than when thinly-spread in large-scale conflict. The nature of coalition operations against Iraq in 1991 reflected all these considerations, and discussion of this conflict also gives an opportunity to raise points specific to the relationship between precision weapons and stealth aircraft; for there were, in 1991, instances where it was necessary for the attack to be covert. Here, the reduced size of warhead and better accuracy inherent in a precision weapon has the added benefit of minimizing weapon size and numbers - which particularly suits the limited payload and small weapon bay of certain stealthy aircraft.

All this is not to say that *every* situation arising in limited conflict inevitably points to precision-guided weapons being the best option; indeed situations may arise which are particularly suitable for employment of certain non-precision munitions. The AC-130 type of gunship, for example, has a pedigree stretching as far back as the Vietnam War and is, if anything, finding more opportunities for effective application today in Former

Yugoslavia than ever before.

And there may be some positive *disadvantages* to precision weapons in limited scenarios, not least the difficulty of their employment against mobile targets at close quarters with own forces, possibly in difficult terrain. In Former Yugoslavia, many Close Air Support missions have been called for but have not been able to release weapons: failure to identify the target has been a major factor; and weather has affected weapons delivery. Both of these considerations would impinge on employment of unguided weapons also, to some extent - but the stand-off inherent in most precision ordnance tends to make weather a more significant factor.

In other cases, the time taken to gain approval to attack has been too great; the window of opportunity has been lost and targets have moved or become obscured. This last line of reasoning would, again, apply as well to dumb weapons but, because attacks with precision weapons may take longer to set up, to coordinate with a designator for example, the effects of delays on precision missions may be more apparent.

Discussion of time taken to gain approval returns us, once again, to the political side of the equation. It is self evident that military freedom in Operation Deny Flight has been strongly constrained by political factors. The rules of engagement have had to have been much tighter than would be the case in general conflict. These considerations lead to the conclusion that political constraints may tend to have a greater effect on precision operations than on those with unguided weapons. However, the overall balance points to precision ordnance offering numerous very useful advantages in limited operations.

4. TYPES OF PGMs

So what types of precision weapons would offer the military commander the greatest utility in a limited conflict? In the case of fire-and-forget weapons, the primary question to be asked is whether the probability is high enough of the weapon maintaining track throughout its time of flight. If it is not, the danger of collateral damage and fratricide remains. A commander would have to be very certain, therefore, of tracking and guidance reliability before authorizing employment of fire-and-forget weapons in some of the scenarios that have been illustrated.

What about the so-called "brilliant" weapons, those with built-in target recognition algorithms? Is this technology mature enough to use in sensitive situations where own and enemy forces are at close quarters? Certain factors, here, might tend to assume great importance in a limited operation: orders of battle are likely to be more confused than in general war; both sides might be equipped with similar armoured vehicles at the outset; and equipments might be captured with a view to operation by the opposition. In the light of such risks, could a commander afford to take the chance?

GPS-guided weapons are looking promising, but are still only giving circular error probabilities of 10-12 metres. This may not be accurate enough to preclude collateral damage and or fratricide. Then there are area precision-guided weapons, sensor fuzed anti-armour weapons and so on. These may give an excellent probability of kill in a target-rich environment where enemy identification can be virtually assured by virtue of his position, but they may not be so suitable in a localized, close-quarter scenario.

The characteristics of stand-off weapons may, similarly, not assume so great an importance in a limited scenario. If target defences are less capable or less dense, the imperative to keep the launch platform at a distance may not be so pressing. And, as previously touched upon, long range, launch-before-lock modes may be unacceptable in the light of political constraints and rules of engagement pertaining to the limited scenario. Following through the favourable aspects of this argument, a limited stand-off requirement implies an unpowered, and therefore smaller and cheaper, weapon.

Is all-weather capability a factor? It may be; it is certainly desirable but, as already argued, military expedience may be of lower importance in a limited scenario than in large-scale war. In other words, it may be more likely that military action could wait until conditions improve; witness the attack on Udbina Airfield, Croatia, which was eventually flown on 21st November 1994 only after earlier weather aborts. One might also generalize that all-weather weapons tend to be more suitable for use against large, fixed installations, and these are, perhaps, less significant in limited operation than in large-scale conflict. Overall, then, it may be that all-weather capability may tend to assume lesser importance in limited operations.

Having looked at some of the weapons characteristics that are required, the question of availability - and particularly cost-effective availability - cannot be ignored. Indeed it is a factor which continually disturbs operational planners, particularly those involved in procurement and financing. In short, one must question the timescale and achievability of "brilliant" weapons technology. Lest this argument not be accepted by the industrial and research community, it is worth citing the UKAF requirement for a fire and forget anti-armour weapon. This dates back at least to 1984, and has been actively pursued throughout the intervening years - but nothing has yet been ordered into production. To some extent, the delay has undoubtedly been due to indecision and political factors, but the failure of promised technologies to mature leads to a healthy scepticism amongst operators when they are offered "brilliant" products.

So weapons suitable for a single, high-speed, low-level pass against a pinpoint target may be achievable and even available in time - but will undoubtedly be expensive. There is no denying that cost is a major factor, to the extent that it is feasible that ultra-sophisticated weapons could even be judged too expensive to use in an operation with limited objectives; the politico/military value of employing the weapon in a given circumstance might simply not be high enough.

Now this certainly cannot be taken as a generalization - indeed the substantial use of precision munitions in limited operations has occurred several times in recent years when the circumstances were right. It does, however, lead on to the final strand of the argument - that nations are unlikely to procure weapons specifically for limited operations. And, notwithstanding the demonstrated success of precision weapons, it's still true that many nations continue to be unwilling to invest solely in precision; it is still comforting to maintain, in many cases, a good stock of iron bombs.

5. AN IDEAL STOCKPILE

So what would comprise the ideal stockpile? Is a compromise, indeed, to be found? A limited scenario may not demand the highest sophistication, so perhaps proven technology such as laser guidance is the safest option. It has disadvantages: the need for a designator which needs line of sight - and is, therefore, vulnerable; it's not an all-weather option, which may, in some cases, be significant. But it also has great advantages: it's reliable; and it's versatile. Laser-guided weapons are, in most cases, not optimized against particular types of target, and are therefore usable in many forms of conflict. They may be guided by the launch aircraft, or other air or ground sources - although here must be mentioned again the assurance required that the weapon guides onto the correct target. This assurance may be increased considerably by self-designating rather than using a buddy or ground spiker, and this characteristic might lead to the commander, in very low intensity ops, having the luxury of being able to select a platform primarily for its acquisition and designation system rather than for its weapon. Indeed, it has been possible to follow this principle in certain circumstances during the current conflict in Former Yugoslavia. On the other hand, a laser-guided weapon operated with a man on the ground in the loop can add to political reassurance and control in "dual key" situations - of which, again, the current Balkan conflict offers examples.

So, after suggesting that the acquisition and designation system might assume at least as great an importance as the weapon system in many low-intensity operations, we reach a conclusion - that there is a significant requirement for precision munitions in limited conflict. Also a tentative suggestion: that the ideal air-delivered weapon for limited conflict - if it's possible to postulate an ideal to cover so many and various situations - would be relatively affordable, with a range of the order that points to target identification before launch and the need to be externally guided throughout time of flight. The term "General Purpose Weapon" is, perhaps, a little passé, but might, in the limited conflict scenario, now begin to be appropriate to describe a laser-guided bomb.

HELICOPTER TASK FORCE :
A MISSION EFFECTIVE SOLUTION
FOR PRECISION AIR STRIKES

D. MELLIES
EUROCOPTER INTERNATIONAL
B.P. 107 93-LA COURNEUVE - FRANCE

SUMMARY

Applied to rapid reaction forces, new technologies provide today the required level of mobility, round the clock operation, and firepower :

- Air mobility with the introduction of rotary wing vehicle able to operate without airfield infrastructure over distances of 800 km at speeds of 280 km/h.
- Round the clock operation is possible with night vision sensors for flying and digital avionics for pinpoint navigation even in adverse weather.
- Fire power is the end result of the integration of aircraft and weapons with system architecture optimised for single shot kill.

All these achievements in technologies introduced into the military helicopter represent an outstanding rapid reaction potential. Once combined with heliborne C3I systems and supply assets, they can constitute an **air mobile task force** able to conduct **airstrikes**.

Though major NATO countries have set up rapid reaction forces based on Air Force, Navy and Army assets to deal with unconventional situations worldwide, recent localised conflicts have shown that for reasons explained later on, **precision air strikes** have become a cardinal point of the mission requirements. The helicopter task force appears to be the most effective solution to conduct these precision missions because of :

- helicopter survivability by accurate low level night flying and stand-off engagement of targets,
- C3I secure systems with updated target intelligence and positive identification,
- weapon systems performance with the use of night sensors and missiles to maximize the hit probability and avoid collateral damages.

In the following three parts of my presentation, I will :

- first introduce the principles and techniques of air mobile operations,
- then apply theses considerations to a realistic scenario,
- finally detail the technologies used to achieve the required precision.

1. PRINCIPLES AND TECHNIQUES OF AIR MOBILITY

1.1 Mission planning

To benefit from maximum **surprise effect**, time must be saved to be on target at the earliest to avoid enemy to take cover or reinforcements called in. To cut time consuming procedures a high state of **readiness** is maintained :

1.1.1 The helicopter units are basically organised in light squadron units to be tailored into **task forces**.

Mixed teams of 2-3 machines are then dedicated to specific roles : scout, escort, antitank, utility, search and rescue (SAR), casualty evacuation, aerial surveillance, command and control. No airfield is required : they blend outstandingly with co-operative elements deployed and take advantage of their defensive dispositions.

1.1.2 To shorten the decision making process during the operation, the task force commander and staff officers (operations, intelligence and logistics) are airborne aboard a command and control helicopter and ensure real time C3I near the operation area. Practically, ground briefing time is kept to a minimum and orders details are stored in data transfer cartridges handed over to air crews or passed via datalink when airborne.

1.1.3 Long range detection of the enemy forces is ensured by organic ground surveillance radar helicopters which track their movements, the threatening air defence radars and transmit their characteristics in real time to the commander or directly to the attack helicopters.

Hence to ensure readiness to treat time critical target and before the action, a time saving process is based on :

- light task force organisation,
- airborne C3I system,
- early warning.

1.2 Course of action

Mission flexibility is inherent to airmobility, specifically to adapt to changing weather conditions or new tactical situations.

1.2.1 Secure communication systems enable the commanders to take immediate actions and reposition airborne assets which, using navigation computers, can immediately re deploy for new mission objectives. Timing modifications are equally managed in line with remaining fuel endurance.

1.2.2 For aviators, the main problem is the weather. But today, weather radars permit to avoid enroute inadvertent instrument flying conditions and to use alternate itineraries. In addition helicopters can fly low level and land almost everywhere or continue their flight with very low ceiling and short horizontal visibility at slow speed, avoiding mission abortion.

1.2.3 When tactical situation alters the planned route, additional fuel endurance can be arranged by forward field refuelling. This logistical and tactical operation is carried out by utility helicopters transporting external or

Paper presented at the AGARD MSP Symposium on "Technologies for Precision Air Strike Operations in Rapid-Reaction and Localised-Conflict Scenarios", held in Seville, Spain, from 16-19 October 1995, and published in CP-576.

FIGURE 1

eurocopter

HORIZON HELICOPTER

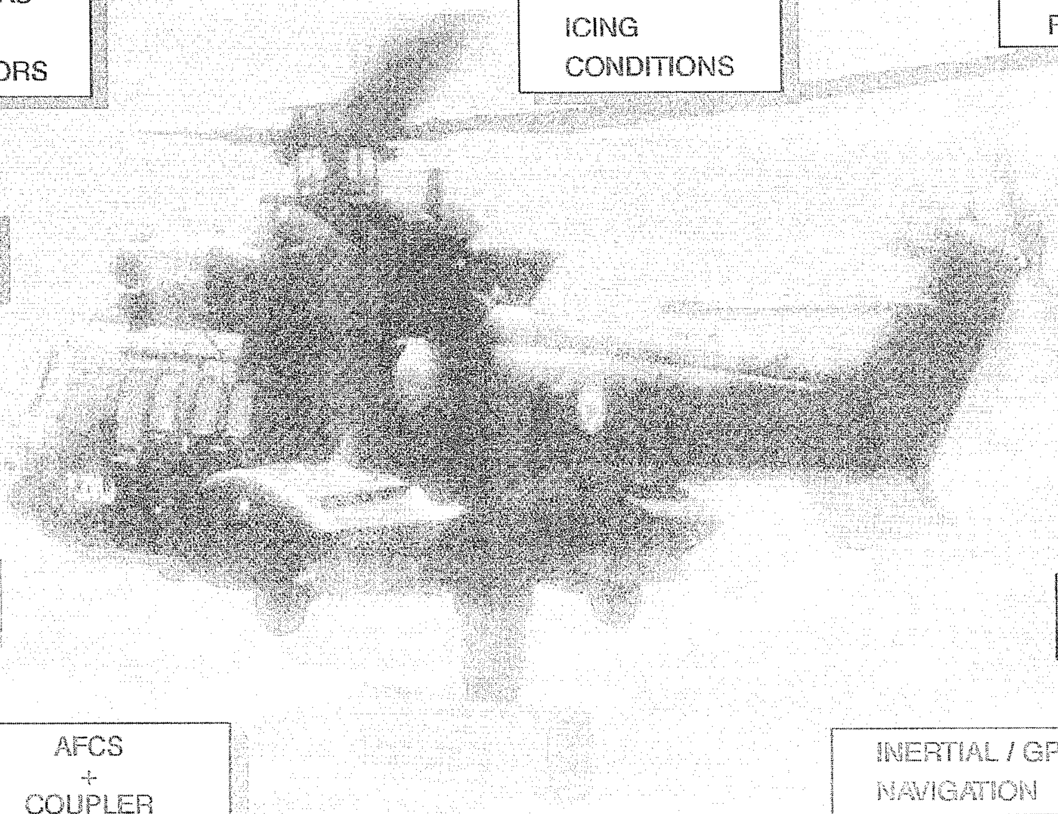

EXHAUST GAS INFRARED SUPPRESSORS

FLIGHT IN ICING CONDITIONS

PRESSURE REFUELING

CRASHWORTHINESS

NIGHT VISION CAPABILITY

COUNTER - MEASURES

ENCRYPTED RADIO COMMUNICATIONS

AFCS
+
COUPLER

INERTIAL / GPS NAVIGATION

EI-HZ-1003-SEP95

internal fuel tanks. Pressure refuelling of a helicopter takes around five minutes.

Hence, flexibility during the course of action is genuine to air mobility and enables to cope with any change thanks to :

- redundant radio communications and navigation systems,
- weather radar, and helicopter flying qualities,
- forward refuelling and rearming techniques.

1.3 Targets engagement

Effective fire power is a combination of **maximum lethal effect** obtained from a minimum of dedicated weapons to ensure the shortest helicopter exposure time.

1.3.1 Targeting is today the most delicate phase of the acquisition process. To **detect** targets at long range, radar and infrared sensors are used. The target detected has to be **recognised** to be a tank, a vehicle, an helicopter, before **positive identification** friend or foe.

Quick engagement time and high single shot kill probability are the characteristics of effective attack helicopters systems. In turn, they carry less ammunitions but more fuel for increased endurance.

1.3.2 In order to engage the right target with the appropriate projectile, a weapon mix is preferable : antitank, air to air missiles, gun against vehicles or personnel. For cost effectiveness, it makes sense not to use a 3rd generation antitank fire and forget missile to destroy an unarmed jeep or a bunker which has no chance to escape.

1.3.3 In case the helicopter formation is ammunition short, forward area rearming is possible using utility helicopters supplying additional ordnance.

Hence, air mobile firepower ensures lethality when it results from :

- integrated weapon system,
- a mix of dedicated ammunitions,
- a possibility to rearm during the action.

2. SCENARIO

Recent military operations in Central Europe have shown limitations to the use of force. Political decisions allow it, essentially air strikes, as deterrent actions. In turn, air power can be deterred by hostage taking for instance.

The following scenario will show that the helicopter task force could be the the most appropriate means either to deter or suppress adverse hostile actions with an acceptable level of political risk.

2.1 Situation

- Enemy forces

Around a besieged town, enemy units are on the attack to assault the suburbs using infiltrated tanks and armoured vehicles. Artillery shelling is extensively used to pound civilian areas.

- Friendly troops

Peace keeping force has requested jet air strikes but weather conditions are not suitable and the political decision is not yet made. Rapid reaction ground force is delayed by road blockings.

- Attachments to the rapid reaction force

One air mobile task force assembled at 50 km on STAND-BY.

. COMBAT ASSETS

- 1 squadron of 7 Scout/Escort **TIGER** armed helicopters
- 1 squadron of 7 Antitank **TIGER** armed helicopters
- 1 squadron of 7 Utility **COUGAR** helicopters for ammunitions, fuel, casualty evacuation, rescue

. C3I ASSETS

- 2 **HORIZON** heliborne Ground Surveillance radars **FIGURE 1**
- 1 Command and Control **COUGAR**

- Scope of the mission :

In order to avoid massive air strikes as repeatedly warned, the political decision has come out at night for a gradual response with the helicopter task force, to destroy ASAP **only** the involved heavy weapons in the exclusion zone since attacks are continuing.

Specific instructions :

- minimize human losses
- no collateral damage

The task force commander issues immediately the following order : "Operating at night, locate and destroy with missiles all the tanks, armoured vehicles and artillery howitzers in action.

- **specific instructions** : pinpoint accuracy and stand-off,
- **caution** : vicinity of friendly troops and civilian population".

2.2 Actions **FIGURE 2**

Phase 1 : Intelligence data gathering. **FIGURE 3, 4**

In daytime, on routine stand off missions, the 2 HORIZONS radars have spotted every enemy movement, specifically tanks in the suburbs, armoured vehicles in the mountains, gun towing vehicles in the valleys. In addition, they have performed electronic intelligence about enemy air defence radars. At night, the 2 HORIZONS, by joint operation continue their surveillance mission and transmit in real time.

The airborne command and control COUGAR starts coordination.

Phase 2 : Flight to contact

- Guided by HORIZONS, the Scout TIGER teams are sent to the targets areas to secure avenues of approach, spot air defence positions and recon stand-off firing positions.
- In turn, antitank TIGERS and escort TIGERS are sent to the firing positions.

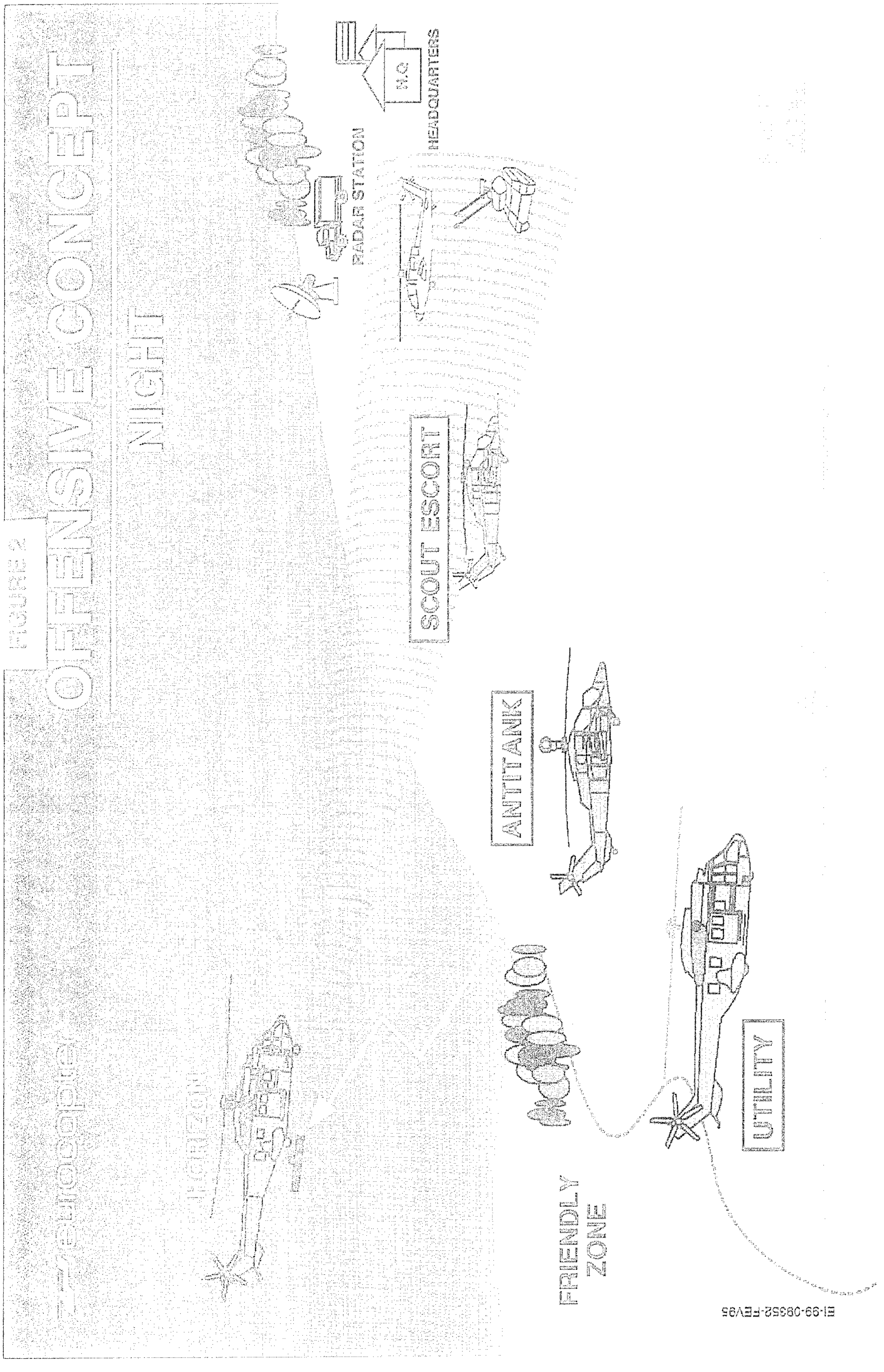

FIGURE 2

OFFENSIVE CONCEPT

NIGHT

Eurocopter
HORIZON
FRIENDLY ZONE
UTILITY
ANTITANK
SCOUT ESCORT
RADAR STATION
H.Q.
HEADQUARTERS
EI-99-09352-FEV95

FIGURE 3

eurocopter

HORIZON IN " A " CONFIGURATION : QUICK DEPLOYMENT, FLEXIBILITY, CONTROL BY USER

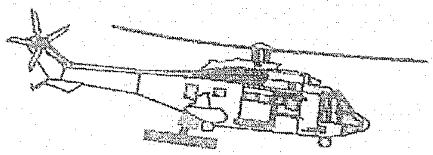

1000 KM WITH STANDARD TANKS

UP TO 4 HOURS
IN FLIGHT
OBSERVATION
WITH HF / VHF
DATA TRANSMISSION

MISSION PREPARATION
ON ON BOARD STATION

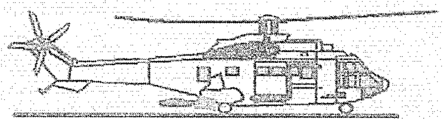

FURTHER ANALYSIS
WITH ON BOARD STATION
AFTER LANDING

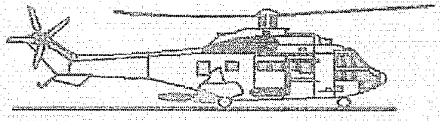

eurocopter

FIGURE 4

ZONE OBSERVED BY HORIZON

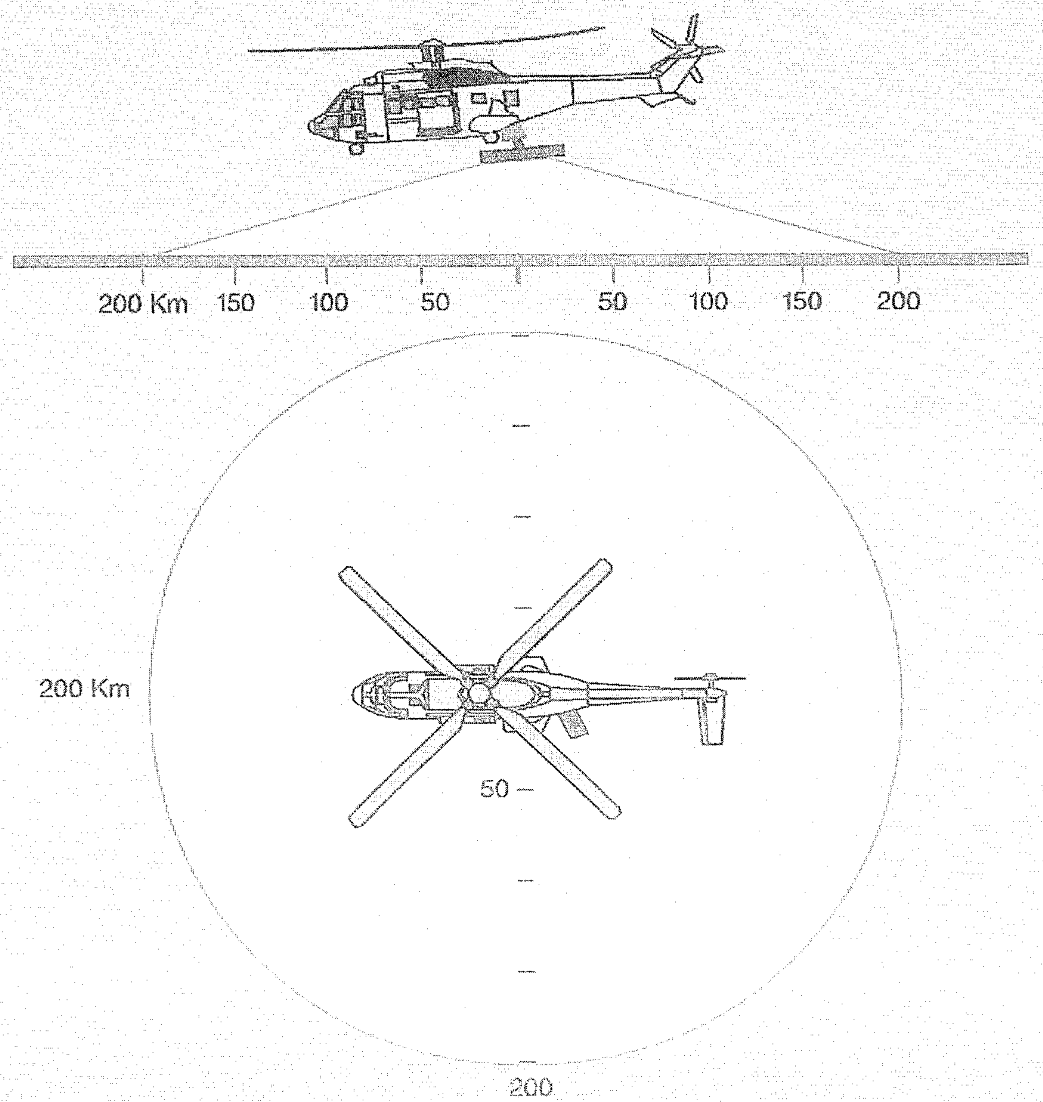
200 Km
150
100
50
50
100
150
200
200 Km
50
200

EI-HZ 1002-MAI84

FIGURE 5

eurocopter

LOCALIZATION ACCURACY

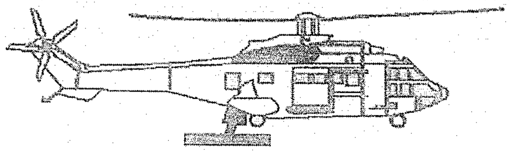

PERFORMANCE
WITH 1 HELICOPTER

150 Km

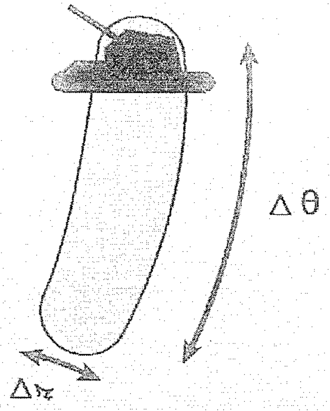

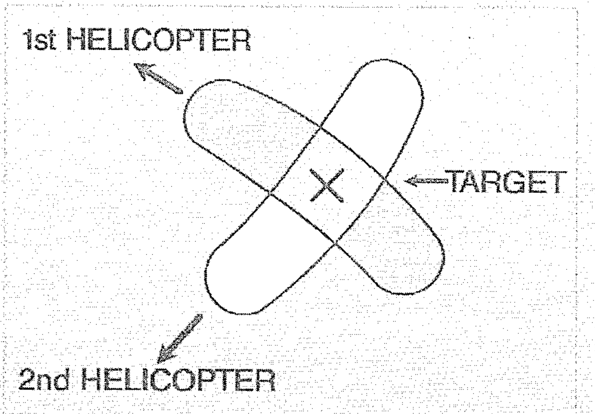
1st HELICOPTER
TARGET
2nd HELICOPTER

LOCALIZATION
PERFORMANCE
WITH 2 HELICOPTERS

- Utility COUGARS escorted by TIGERS are on stand-by to be prepared to rearm or refuel the combat formations.
- Search and Rescue and Casualty Evacuation COUGAR are on stand-by.

Phase 3 : Targets engagements

- Acquisition of each target is performed carefully at stand-off range using thermal imagery sensors. The high infrared (IR) signature of active weapons give a 100 % evidence of their involvement in the firings.
- Tanks and armoured vehicles are engaged with fire and forget missiles at 5 km range.
- Artillery howitzers with wire guided missiles at 4 km.

  All the helicopters movements are monitored from the HORIZON radars and conflicting trajectories avoided.
- The whole operation remains under the control and command of the Task Force Commander who watches the scenes via video transmission and ensures two way communications with his squadrons and the headquarters command. At any time, he is able to retask or withdraw his units according to the mission reports or political decision.

Phase 4 : Withdrawal and debriefing

After one hour of engagement, most of the assigned targets having been destroyed one by one at stand-off range, the Task Force commander reports the end of the mission and the return to the base.

All the firing sequences have been video recorded and debriefing confirms the success of the night mission :

- designated targets were destroyed (10 tanks, 10 guns),
- minimum human losses,
- no collateral damage,
- no fratricide.

3. TECHNOLOGIES FOR PRECISION

The success of precision airstrikes is based on :

- the attack helicopter survivability or its capacity to carry out an armed mission in a hostile environment,
- the heliborne C3I system which must provide updated intelligence data and the whole operation co-ordination (digital battlefield network),
- the weapon systems performance.

3.1 Survivability

The **modern attack helicopter is able to survive** in a localised conflict battlefield thanks to advanced technologies applied to :

3.1.1 reduce its detectability :

- **by** decreasing its signature:

. visual : silhouette, tandem cockpit, mast mounted sight,

. radar cross section : airframe design and composites structure, passive sensors,

. acoustic : main rotor and tail designs, engines,

. infrared : special paints, composites airframe.

- **by** enhancing its low level flying capabilities :

. agility and manoeuvrability to fly nap of the earth (below 50 m) with hingeless rotors and digital engine fuel control,

. night and adverse weather avionics with 4 axes digital automatic pilots to hover at night,

. stand-off operation : masked hovering several km from the target with mastmounted or roof sights,

- **by** accurate navigation and a "glass cockpit" to reduce crew workload in order for him to concentrate on the enemy localization (GPS, Doppler radar or inertial positioning with computer).

3.1.2 decrease its vulnerability :

- twin engine with crossfeed and titanium protection wall,
- extensive use of ballistic tolerant composites materials for rotors and fuselage (TIGER is 80 % made of composites),
- redundancy and segregation of hydraulics, fuel, lubricating, electrical systems, dual flight controls and self sealing fuel tanks with inerting gas against explosions,
- armoured crew seats in tandem cockpit,
- complete self protection suite :

. IR suppressors against surface to air missile seekers,
. missile launch detectors, approach warning,
. radar and laser warning receivers,
. chaff and flares dispensers,
. IR jammers.

3.2 Heliborne C3I systems :

The security and redundancy of communication systems are applied on modern helicopters to provide :

3.2.1 Intelligence

Precision, correlation, exchange of data are by far essential in the process. The collecting means cue each other.

- The radar information is cross checked and fused when two HORIZONS operate jointly giving more accuracy to the moving target co-ordinates in azimuth and distance (radar range 200 km). FIGURE 5
- The Scout TIGER equipped with IR and low level TV sighting systems, laser range finders and navigations computers provide exact coordinates of the target.
- Intelligence processing :

All targets characteristics are correlated by computer processing aboard the HORIZONS workstations.

The threats such as helicopters, tanks, vehicles and hostile radar transmissions are monitored with precision.

The availability of digital maps stored in cartridges and displayed on LCD colour screen enhance situational awareness thanks to tactical symbologies.

The pinpoint navigation provides reliable reports of friends and enemy layouts and IFF code identification **avoid air defence fratricides.**

FIGURE 6

eurocopter

EUROMEP ANTITANK SYSTEM

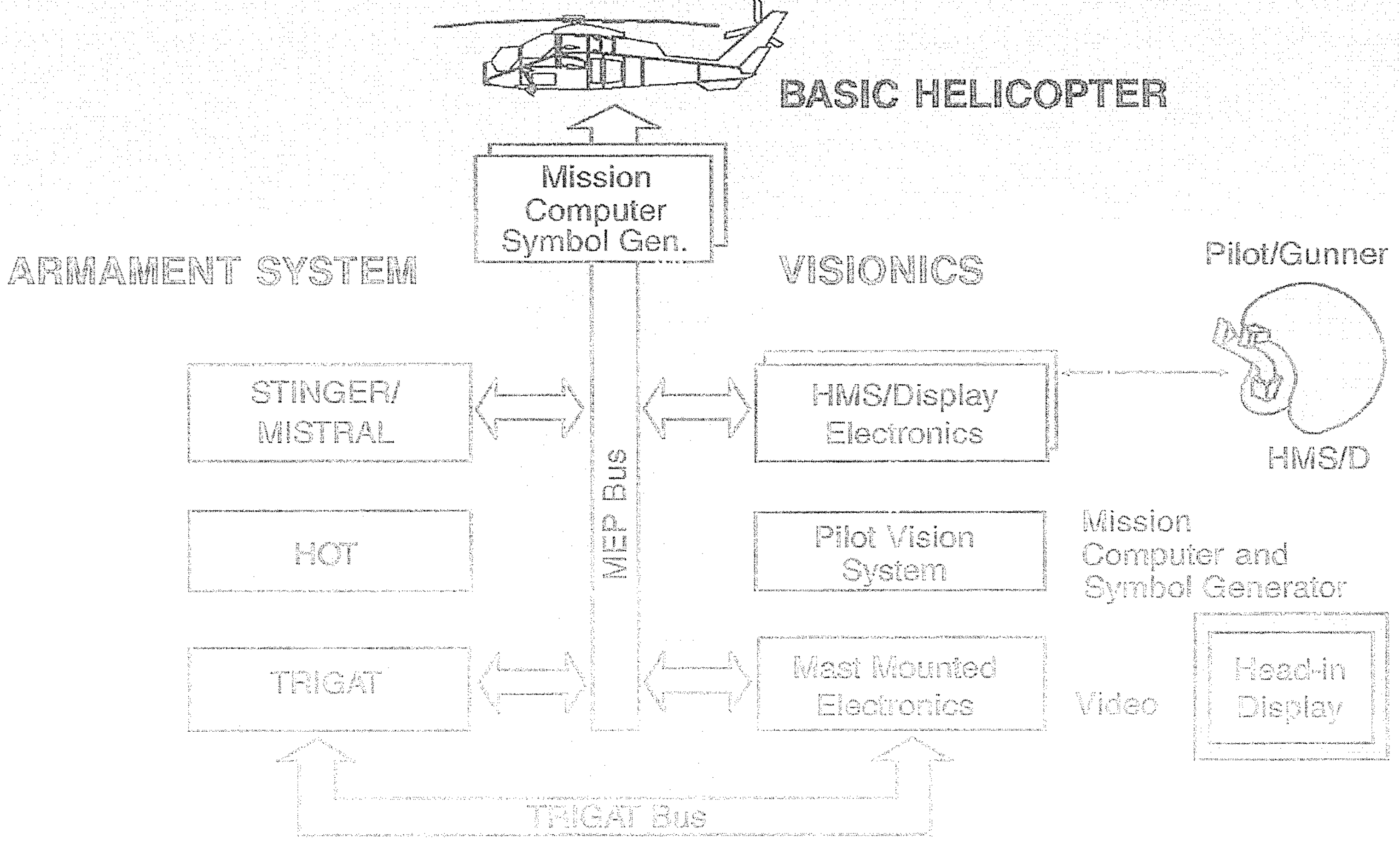

BASIC HELICOPTER
Mission Computer Symbol Gen.
ARMAMENT SYSTEM
VISIONICS
Pilot/Gunner
STINGER/ MISTRAL
MEP Bus
HMS/Display Electronics
HMS/D
HOT
Pilot Vision System
Mission Computer and Symbol Generator
TRIGAT
Mast Mounted Electronics
Video
Head-in Display
TRIGAT Bus

FIGURE 7

eurocopter

PEAN ISSION QUIPMENT ACKAGE

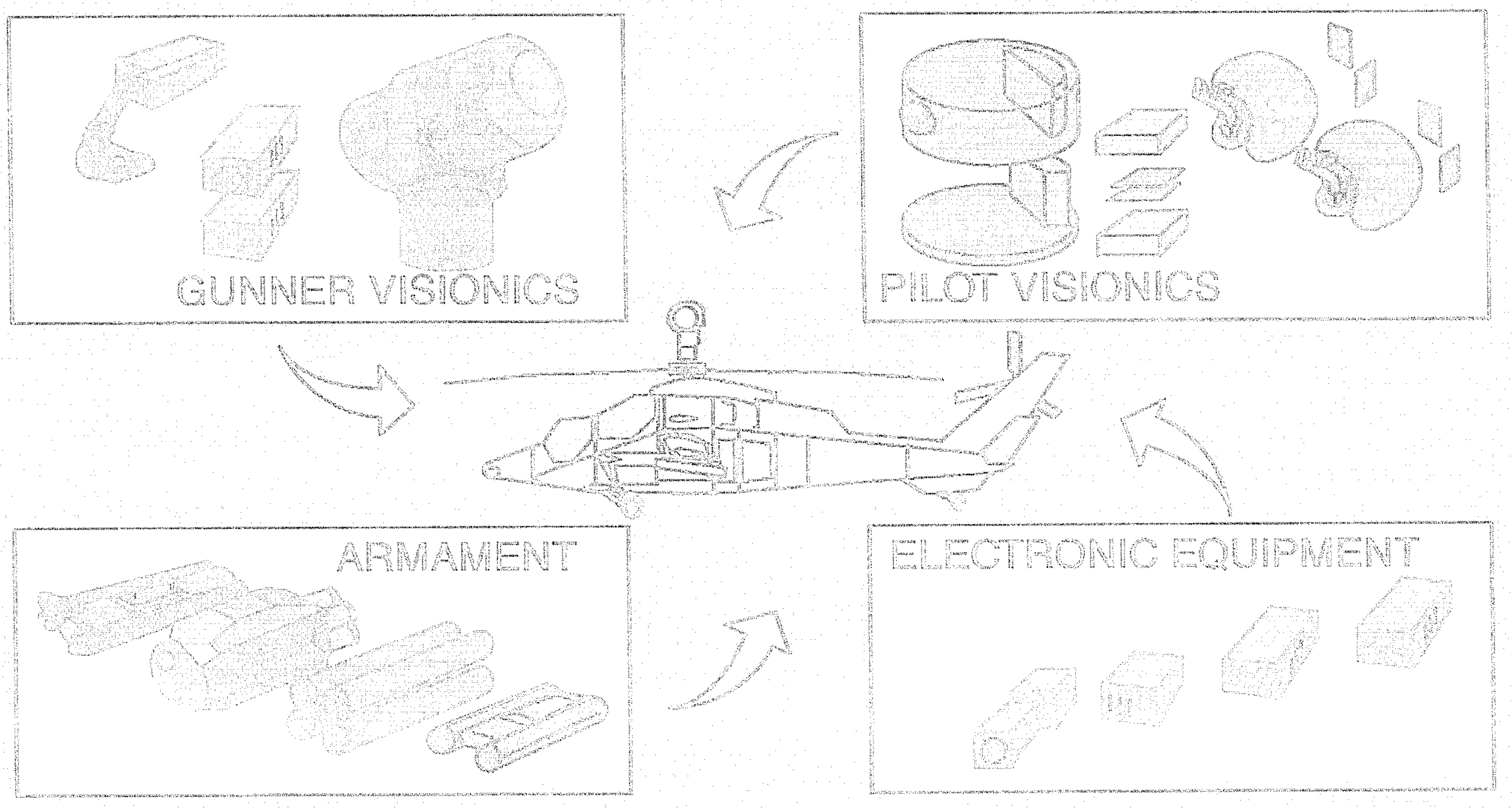
GUNNER VISIONICS
PILOT VISIONICS
ARMAMENT
ELECTRONIC EQUIPMENT

EI-93-05182-JAN92

FIGURE 8

ANTI-TANK

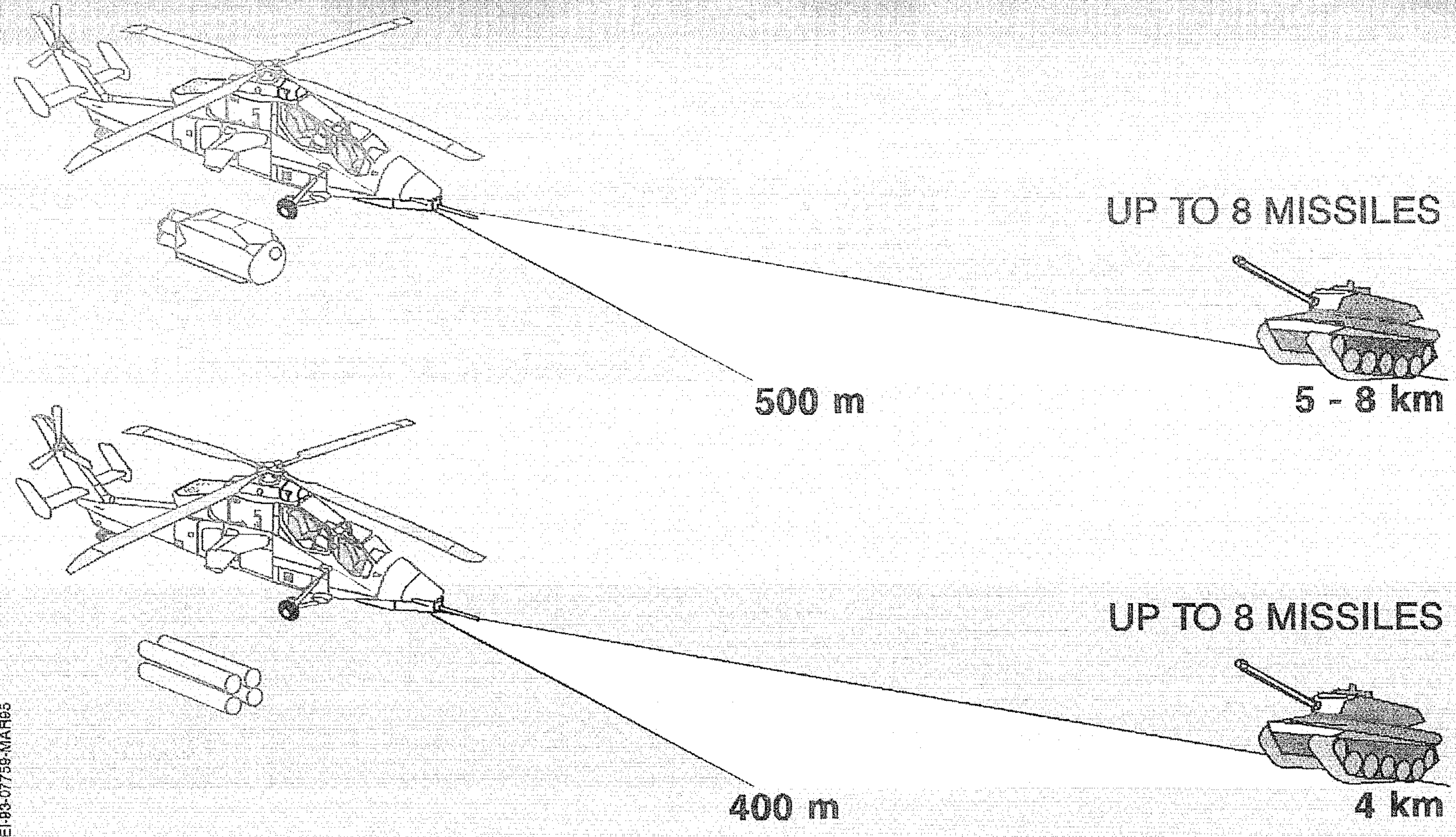

UP TO 8 MISSILES

500 m

5 - 8 km

UP TO 8 MISSILES

400 m

4 km

EI-83-07759-MAR95

FIGURE 9

eurocopter

THIRD GENERATION ANTI-TANK

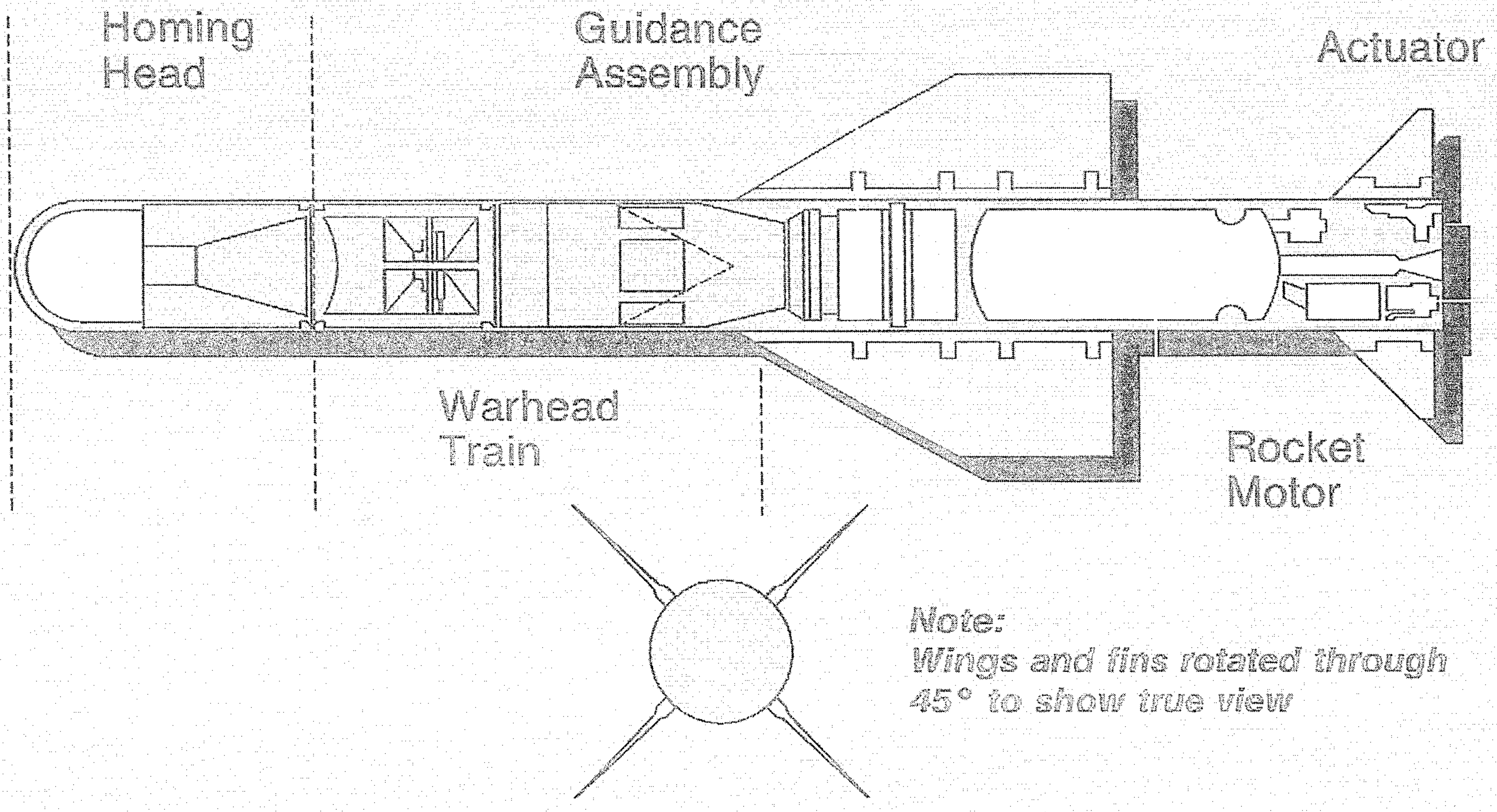
Homing
Head
Guidance
Assembly
Actuator
Warhead
Train
Rocket
Motor

Note:
Wings and fins rotated through 45° to show true view

EI-83-07487-SEP92

3.2.2 Command and control

A Cougar helicopter can be used as command post either in flight or from the ground.

Its capability to reposition wherever needed gives the commander the best situational awareness in order to make on the spot the most appropriate decisions.

The HORIZON radars guide the attack TIGERS to the target areas according to their classification : tanks, armoured wheeled vehicles, provide radar threat data of hostile air defence (Electronic intelligence ELINT) and advanced warning of enemy helicopters.

The observed scenes can be "live" video-transmitted to the commander who personally checks the correct designation of targets.

Linked to a redundant communication network and whatever the helicopters locations, the encryption systems PR4G maintain permanent and secure chains of command liaisons. Data links between TIGERS and HORIZONS supply updated informations displayed on cockpit colour multifunction screens. Man machine interface has been optimised to reduce crew workload. The huge amount of data which are stored in the computers can be erased in case of emergency.

3.3 Weapons systems

The integration of sensors and armaments linked via MIL STD 1553 B avionics BUS and controlled by dual computers are the key to precision targeting.

Mission equipment package system architectures and software on armed helicopters increase drastically their single shot kill probability (SSKP). FIGURE 6

3.3.1 Sensors FIGURE 7

. Roof or mast mounted sight

In the TIGER, these sights house passive thermal imager (FLIR camera) TV camera, laser range finder, direct view optics. The thermal imager of the IRCCD generation provides excellent acquisition performance in terms of long range detection (above 10 km) recognition and identification in line with the range of weapons.

The direct view optics with a magnification power greater than 12 times is also of great value for positive identification.

Video recording can be also used for battle damage assessment.

The design of the mast mounted sight above the main rotor minimizes the exposure and provides more time for accurate designation of the right target.

Automatic target tracking is also possible with the FLIR camera.

. Helmet mounted sights and displays

Worn in tactical flight, they provide prepositioning of the main sights in azimuth and elevation for a quicker target designation and aiming of the weapons. In addition they are used for night pilotage with FLIR and integrated vision goggles.

3.3.2 Missiles FIGURE 8

. **TRIGAT** FIGURE 9 is a true fire and forget antitank third generation missile with passive IR seeker. Locked-on before launch (man in the loop) after mast mounted sight acquisition, it can fly up to 8 km on a flat or curved trajectory to kill target from the top.

Ripple firings of 4 missiles on predesignated targets are possible in less than 8 seconds upto 8 km.

. **HOT** is a precision wire guided tandem hollow charge missile with a range of 4 km optically tracked used specifically when pinpoint accuracy is required as in urban areas.

. The new missiles have SSKP of nearly 0.9 even fire at night thanks to IR technology.

Fire control computer software shortens the firing sequence and saves ammunition consumption, key factor for flying machines.

The missiles advanced technology guarantees lethal hits and fired from helicopters, ensures stand-off targeting and firing, against small fixed or moving targets.

4. CONCLUSION

The case we have studied to illustrate the use of helicopters in such an operation considers the draw backs of air power strikes. An air mobile night operation is not only effective on the ground but less politically risky for being immediate and more gradual.

The own nature of helicopter makes it suitable for operations without airfield infrastructure. Modern helicopters can today fly low level at night or in adverse weather better than any other fixed wing aircraft. Therefore their high survivability makes them capable of air strikes. A helicopter task force provides a powerful and flexible combination of intelligence, reconnaissance, attack, supply, rescue capabilities in a single hand. The high technologies used today on the TIGER COUGAR, HORIZON ranges of helicopters in the field of visionics, armaments, avionics, radio communications and radar increase their effectiveness by supplying reliable details and accurate data to the air crews and to the force commander.

When the challenge is to strike and destroy precisely various pinpoint targets, minimizing human losses, avoiding collateral damages, the **helicopter task force is the most mission effective solution for rapid reaction forces**. As a matter of fact, the helicopters can today do all the job of fixed wing aircraft plus all what the fixed wing cannot do.

PRECISION IMAGING STRIKE TECHNOLOGY INTEGRATION LABORATORY (PISTIL)

Thomas F. Reese
Ronald Going
Strike Analysis Branch
Weapons/Targets Integration Division
Weapons/Targets Department
Naval Air Warfare Center Weapons Division
China Lake, CA. 93555-6001, U.S.A.

Approved for public release; distribution is unlimited.

SUMMARY

Precision-guided weapons that employ advanced imaging infrared seekers, data links, and mission computers require detailed mission-planning and rehearsal systems to ensure mission success. Cost to develop these weapons and mission planning systems are rapidly increasing as advanced signal-processing algorithms are employed to increase probability of target detection, acquisition, and recognition, with the ultimate goal of accurate target tracking and precise aimpoint selection for maximum probability of kill and minimum collateral damage.

This paper presents a real-time Precision Imaging Strike Technology Integration Laboratory (PISTIL). PISTIL provides precision-guided weapons developers with many of the tools and data to answer key questions such as the following:

1. Did the mission plan perform effectively?
2. Did the subsystems function satisfactorily?
3. Did the subsystems function at the proper time?
4. Did any evidence of unexpected or marginal subsystem performance exist?

INTRODUCTION

The Precision Imaging Strike Technology Integration Laboratory (PISTIL) stands today at the forefront of major weapon system acquisition support. It is a critical member of the Government/Contractor Integrated Product Team (IPT) environment that provides both parties with the proven benefits of the "smart buyer/smart user" concepts. PISTIL provides essential functions during concept studies, development, test and evaluation, operational evaluation, and Fleet support. PISTIL is a physical embodiment of the "insight not oversight" approach to weapon system acquisition.

MOTIVATION

In our experience, imaging weapon system concepts, designs, and implementations need to be evaluated as early as possible and continue to be re-evaluated throughout the acquisition process. A total weapon system integration environment that includes intelligence collection, mission planning, missile hardware and software, aircraft interfaces, and man-in-the-loop functions is essential in today's world of limited budgets. Deficiencies in any of these areas can cost hundreds of millions of dollars to correct in a fielded system. Hidden defects can cause mission failures and ultimately lives.

Through its unique ability to combine three-dimensional (3D) target images, missile hardware-in-the-loop, and on-site tactical aircraft, PISTIL provides the most cost-effective, timely, and versatile precision-guided weapons evaluation environment possible. Because today's imaging weapons require precise evaluation and verification of the highly sophisticated interactions between imaging seeker missiles, mission planning, controlling aircraft, and target environments, the new PISTIL laboratory is equipped with technological advancement for evaluation of the following:

1. Imaging seeker concepts
2. Adaptive mission-planning concepts
3. Automatic target-recognition algorithms
4. Man-in-the-loop functionality between aircraft and missile
5. Missile real-time software and hardware
6. Intelligence data and mission-planning effectiveness

PISTIL's superior capabilities allow these tasks to be accomplished for a limitless variation of target and attack scenarios.

Paper presented at the AGARD MSP Symposium on "Technologies for Precision Air Strike Operations in Rapid-Reaction and Localised-Conflict Scenarios", held in Seville, Spain, from 16-19 October 1995, and published in CP-576.

COST EFFECTIVENESS

Live missile firings and captive-flight tests are expensive. Targets are often restricted to a limited number of available test sites. Unpredictable environmental conditions complicate test control repeatability problems.

PISTIL's laboratory environment, on the other hand, with its real missile hardware, real data-link hardware, real tactical aircraft, and unlimited target images, is the most cost-effective alternative to captive flights and live firings for imaging seeker missiles. Any combination of target location, weather, time, target type, mission plan and man-in-the-loop can be evaluated in real-time tests using real missile avionics and real tactical aircraft in a laboratory ground test environment. This variety cannot be provided by captive flight or live firings. PISTIL can be used to reduce the number of high-cost, unrepeatable live firings, and captive flights, thus greatly reducing development and lifecycle costs.

SIMULATION TECHNOLOGY

Missile attack scenarios are conducted by running the real mission plan in real missile hardware controlled by a six-degree-of-freedom flight simulation. Target images are provided in real-time using 3D target scene models developed with data from national resources. The PISTIL was the first laboratory to provide this level of image simulation to an integrated missile, data link, and tactical aircraft. The technology for 3D-image modeling and real-time scene injection is continually upgraded to match growing requirements for speed, target complexity, and target fidelity. PISTIL's simulation technology includes the following:

1. A Silicon Graphics Onyx imaging super computer
2. A variety of government and commercial 3D-target-modeling tools
3. A real-time six-degree-of-freedom flight simulation
4. An F/A-18 cockpit simulation (when real F/A-18 not required)
5. A real missile seeker automatic target recognition (ATR) electronics and missile avionics
6. A tactical aircraft mission planning system (TAMPS)-compatible mission-planning system
7. An AWW-13 data link pod
8. Access to tactical Fleet aircraft (F/A-18, A6-E, etc.)

3D-TARGET-MODELING TOOLS

PISTIL has a variety of 3D-target-modeling tools which include

1. SocketSet Photogrametric Workstation from General Dynamics (GDE), San Diego, Calif.
2. Griffon Photogrametric Workstation from Autometrics
3. MultiGen three dimensional modeler from MultiGen Inc.
4. IRGen infrared modeler from Technology Services Corporation
5. Gemini Visualization System from Gemini Inc.
6. Performer Visualization System from Silicon Graphics, Inc.
7. Virtual Application Prototyping System (VAPS) from Virtual Prototypes

These software packages, along with government software, provided the necessary tools to create accurate 3D infrared databases. These databases are then easily traversed in real time for the digital signal injection using the Onyx imaging super computer.

IMAGING SEEKERS

PISTIL can support evaluation of a variety of imaging seekers, including imaging infrared (IR), millimeter wave, laser detection and ranging (LADAR), synthetic aperture radar (SAR), and television. Sensor field of view, resolution, scan patterns, and sensitivity are modeled in real time. The target scene is injected into the seeker video processor to test the target acquisition, tracking, and man-in-the-loop characteristics of the imaging seeker in conjunction with the rest of the missile, data link, and aircraft systems. This technique is applicable for evaluation of current imaging weapon systems as well as future imaging weapon systems currently being evaluated.

FACILITY DESIGN

PISTIL is an integral part of an existing weapon test and integration complex. This complex includes a dedicated ground support facilities, office spaces, and PISTIL. Full facilities are in place and operational to support precision-guided weapons laboratory and testing, ground testing, captive-flight testing, and live firings. Operations are supported by extensive range and instrumentation facilities.

TARGET

PISTIL provides 3D models of ground targets and ship targets. Attack scenarios can be executed from any heading and altitude profile. Time of year, time of day, cloud cover, haze, and temperature are all controlled and can be set at any required condition. Target modeling is integrated with national resources data-collection facilities to provide high-fidelity models for mission-planning evaluations.

DATA ANALYSIS

PISTIL collects real-time data from the weapon system avionics interfaces, launch platform interfaces, man-in-the-loop interfaces, data-link video, seeker video, cockpit video, and six-degree-of-freedom flight simulation. These data are time stamped and correlated for future analysis. Data collected from PISTIL is directly comparable to data collected in captive flights and live firings. Target images collected in captive flight and live firings can be used in the PISTIL to reproduce the flight results.

The PISTIL provides sophisticated data-reduction, data-visualization, and data-analysis tools to assist in the interpretation and reporting of the test results.

REAL-TIME HARDWARE ARCHITECTURE

The PISTIL six-degree-of-freedom flight simulation is executed on a distributed scalable processor architecture (SPARC) multiboard Versa Module European (VME) system (Figure 1). running a combination of VXWorks and Verdix Ada Development Systems (VADS) Works operating systems. Each SPARC board is a full computer system containing Ethernet, serial ports, (SBUS) interfaces, and VME backplane interfaces. Each SPARC single-board computer is allocated to handle the functions of a particular subsystem within the weapons system simulated. For instance, board one performs the launch platform functions, board two the engine models and airframe models, board three the mission computer model, board four the navset model, board five the seeker model, board six the data-link model, board seven the T1 telemetry output channel, and board eight the T2 telemetry output channel. The boards all share truth data on the VME backplane.

Each board that simulates a weapon subsystem is provided with a special weapon system bus hardware interface on the SBUS. The real weapons system components are also connected to this same bus and are interchangeable with the simulator boards. The functions of board one can be switched over to a real launch platform; board three can be replaced with a real mission computer; board five can be replaced with a real seeker electronics unit; and board six can be replaced with a real data link. Boards two, four, seven, and eight are always used in place of the real subsystems.

VIDEO INJECTION SYSTEM

Dynamic target scenes are developed on a Silicon Graphics Onyx Imaging Supercomputer. These scenes are output from the Oynx's Digital Paddle Board Video Interface via a custom scan converter system that formats the video to the input requirements of the particular seeker electronics unit under test. The custom scan converter is a two-board VME-based system, designed to be modifiable to support a variety of video requirements.

The time, position, and line-of-sight data are computed by the six-degree-of-freedom flight, and gimbal simulation is exported to the Onyx over a Scramnet interface. The Onyx renders the scene to be injected, based on the line-of-sight angle from the six-degree-of-freedom flight and gimbal simulation. The seeker electronics unit under test receives this scene and corrects the seeker pointing angle to try to center the track point. This correction translates to a gimbal command changing the trajectory of the flight vehicle being tested.

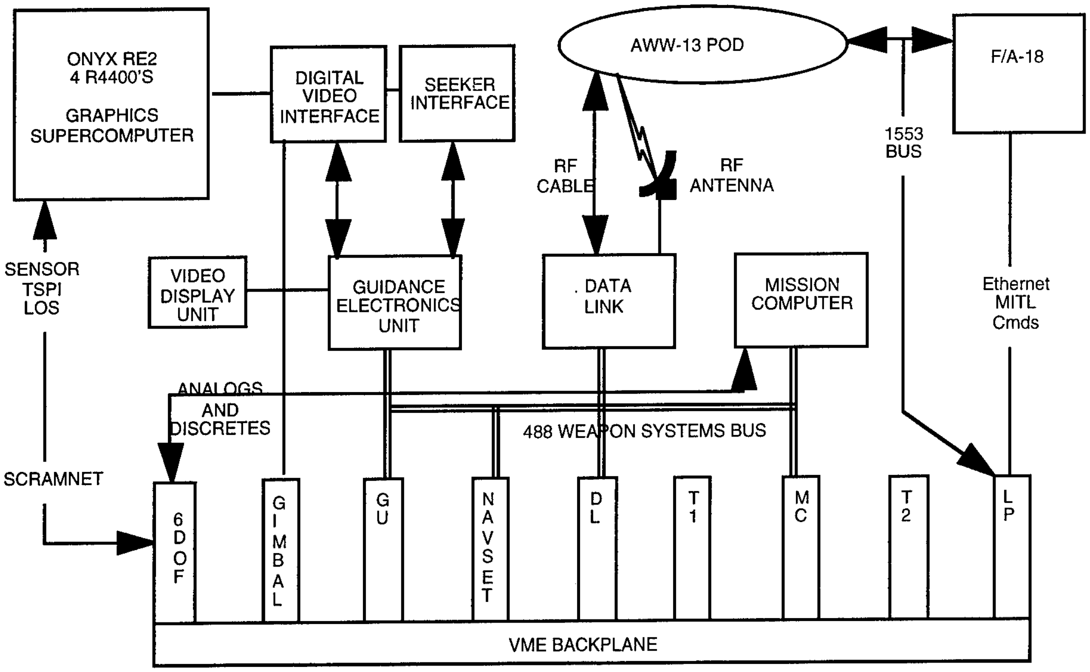
ONYX RE2
4 R4400'S
GRAPHICS SUPERCOMPUTER
DIGITAL VIDEO INTERFACE
SEEKER INTERFACE
AWW-13 POD
F/A-18
1553 BUS
RF CABLE
RF ANTENNA
SENSOR
TSPI
LOS
VIDEO DISPLAY UNIT
GUIDANCE ELECTRONICS UNIT
. DATA LINK
MISSION COMPUTER
Ethernet
MITL
Cmds
ANALOGS AND DISCRETES
488 WEAPON SYSTEMS BUS
SCRAMNET
6 DOF
GIMBAL
GU
NAVSET
DL
T1
MC
T2
LP
VME BACKPLANE

FIGURE 1. SPARC Multiboard VME System.

DATA LINK AND MAN-IN-THE-LOOP FUNCTIONS

A graphical cockpit simulator on a Silicon Graphics 340 VGX is provided to simulate prelaunch cockpit weapon setup and control functions, as well as post-launch man-in-the-loop functions. The simulated cockpit functions are transmitted to the missile pre-launch via a real 1553 hardware interface.

When a real-launch platform is used instead of the simulated-launch platform, the same 1553 interface is used between the real-launch platform and the missile. Man-in-the-loop controls from the stick and throttle are sent through a 1553 bus to the AWW13 data-link pod on the controlling aircraft. The AWW13 pod transmits these RF signals to the missile under flight to allow slewing and designation of the track point of the missile. The missile data-link transmitter sends the seeker scene back to the AWW13 data link pod on the controlling aircraft. The AWW13 pod then relays this scene up to the cockpit video display.

CONCLUSIONS

In this paper, we briefly present a hardware-in-the-loop with a unique architecture for evaluating precision-guided weapons that employ advanced imaging seekers, data links, and mission computers. We describe the functionally of each of the subsystems and the communication links between each of these subsystems. In the course of developing this facility, we discovered many undesirable features within weapon systems and worked with other members of the Government/ Contractor IPT to correct these undesirable features. The PISTIL has proven benefits of the "smart buyer/smart user" concepts.

ACKNOWLEDGMENTS

We would like to thank both present and past PISTIL IPT members for all of their valuable contributions to the Government/Contractor Integrated Product Team. Their creativity, and engineering efforts have resulted in a significant improvement to strike weapons technology.

Precision Strike Concepts Exploiting Relative GPS Techniques

George Schmidt and Roy Setterlund
C. S. Draper Laboratory
M/S 2A, 555 Technology Square
Cambridge, MA 02139
USA

ABSTRACT

Many weapons and weapon carriers will have an avionics suite that includes an integrated INS/GPS (Inertial Navigation System/Global Positioning System) set. This means of navigation motivates examination of whether very high accuracy (~10 ft Circular Error Probable (CEP)) may be obtainable using only this set of weapon avionics operating in a ***relative*** GPS mode, rather than in an ***absolute*** GPS mode where CEP's of 30 to 40 ft would be expected. [Ref. 1] This paper will explain how 10 ft accuracy may be achieved and it will present several different weapon system concepts that exploit such a capability to rapidly attack targets.

Fundamentally, two problems must be solved to achieve an accuracy of 10 ft: (1) target location must be determined to better than 10 ft, and (2), the GPS/INS equipped weapon must be guided accurately to better than 10 ft. This paper will explain how the use of ***relative*** GPS can solve the guidance problem and how the use of ***relative*** targeting in a GPS based coordinate system can solve the target location problem.

The paper begins with a discussion of relative GPS and reports the results of ***actual experiments*** to determine accuracy degradation of relative GPS guidance systems as a function of baseline length and targeting latency. Baseline lengths of up to 540 nmi and latencies up to 15 minutes are considered showing that relative GPS guidance may achieve high accuracy over baselines and latencies useful for tactical applications.

Next, the target location part of the problem is addressed. There must be an accurate sensor that locates the target relative to the GPS reference receiver. The sensor may be on either the launch aircraft or at a remote location. The target could also have been located prior to the mission.

Real-time target location concepts that will be explained include the use of aircraft equipped with an INS/GPS/Synthetic Aperture Radar (SAR) avionics suite to perform a ***real-time relative*** targeting function for weapon initialization. The importance of reasonable aircraft maneuvers to enhance observability and speed up the three-dimensional (3-D) targeting fire control solution will also be addressed. Simulation results for several realistic scenarios will be presented.

Finally, several concepts will be discussed that all make use of highly accurate ***premission relative*** target positioning, i.e., the ability to specify the 3-D location of two points, or localized areas, on the earth relative to each other in a suitable reference frame such as WGS-84. It is of interest to speculate how such a capability could be exploited in a precision strike context. Scenarios involving several existing or planned weapon systems will be described.

1.0 INTRODUCTION

One of the lessons learned as a result of the Gulf War was how effective precision-guided weapons were when employed against a variety of targets. Another lesson was that their effectiveness was constrained by both adverse weather and man-made obscurants, such as smoke. As a result, “All-Weather Precision Strike” was identified by the U.S. Department of Defense (DoD) as a major new thrust for weapon technology development. However, as we all know, any new DoD technology development is subject to the fiscal pressures of the shrinking defense budget. This provides the incentive to seek economical options for providing the high accuracy expected from precision strike weapons with an all-weather capability. The weapon system approaches described in this paper do not require target sensors on the weapon. The primary option for precision strike examined in this paper is through the use of relative GPS.

The nomenclature of navigation techniques that measure one position in relation to another is not consistent in the literature or in common usage, so we begin by defining "relative GPS" as it is used

Paper presented at the AGARD MSP Symposium on “Technologies for Precision Air Strike Operations in Rapid-Reaction and Localised-Conflict Scenarios”, held in Seville, Spain, from 16-19 October 1995, and published in CP-576.

here. By "relative GPS" we mean techniques that compute position corrections by differencing position coordinates, which may be expressed, for example, as latitude, longitude, and ellipsoid height, or as earth-centered Cartesian coordinates. We refer to single receiver position estimation as "absolute GPS". Relative GPS techniques can be used to remove the large, highly correlated common mode GPS errors between two receivers at a particular time and achieve accuracies of a few meters. In this application, one GPS receiver is used in navigating the weapon, whereas the other receiver is involved in the targeting. The key to achieving high accuracy is to require that both receivers use a common set of GPS satellites for navigation. In this way, correlated errors cancel out of the relative navigation solution. Not all error sources are perfectly correlated, however, and the degree of correlation tends to decrease as the distance between the two receivers - the baseline length- increases. Also, the correlated errors themselves change slowly with time, so that if corrections are to be used at some time after they are computed, an additional positioning error will be introduced. The effects of these error sources need to be quantified before relative GPS techniques can be applied to guidance problems. It is the effects of these errors -the spatial and temporal decorrelations- that the experiment reported in Section 2 measures.

The cartoon sequence of Figures 1 through 4 is meant to illustrate the ideas described in the previous paragraph. In Figure 1, two identical receivers are located at true position "B" and they are made to track the ***same*** 4 or more satellites. Although both identical receivers are in error from the true position "B" by an uncertain amount (say 40 ft) due to major error sources such as satellite clock drift, ephemeris errors, and propagation delays, they both read the ***same*** position with the exception of much smaller errors expected to be random and on the order of a few feet. These smaller remaining errors include receiver noise and quantization errors, receiver interchannel biases, and to some degree, multipath.

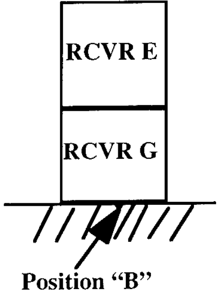

Figure 1. The Relative GPS Concept - 1

In Figure 2, RCVR "E" is now on a weapon whose guidance system receives the broadcast position of RCVR "G". "G" is located at the target. As long as RCVR "E" tracks the same satellites as RCVR "G" and the weapon guidance system follows its commands with small errors, then the weapon will guide to impact at RCVR "G" within receiver noise. Even though the absolute position coordinates of RCVR "G" and RCVR "E" may be incorrect, the "target" position B would be reached essentially perfectly. Clearly, RCVR "G" position would need to be broadcast continuously if both receivers use C/A code only and selective availability (S/A) is turned on. However, the use of GLONASS receivers or P(Y) code receivers may allow targeting to be done with one data transmission of target position and the identity of satellites being tracked by the "targeting" receiver. Thus a central question is: "Can one transmission of RCVR "G" position and the satellites it is using, be sufficient for RCVR "E" to guide the weapon to RCVR "G"?" Alternately stated, the question is: "How far in time prior to impact can the transmission be performed and still achieve better than 10 ft (relative) accuracy at impact?" Experimental results described in Section 2 will answer this question.

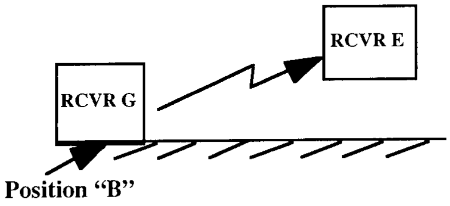

Figure 2. The Relative GPS Concept - 2

In addition, the target location problem needs to be addressed because it is not usually practical to put a broadcasting GPS receiver on the target! The next step in the cartoon sequence is thus to move RCVR "G" some distance away from the target while still maintaining its accurate location relative to that target. Fig. 3 shows the target and receiver locations and the relative location vector between receiver "G" and the target - $\overline{RTL}$.

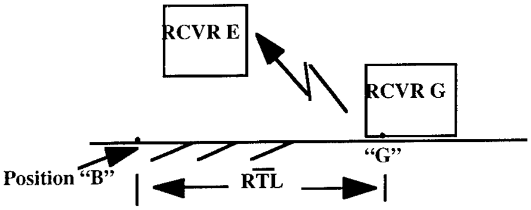

Figure 3. The Relative GPS Concept - 3

Note that now two additional sources of error have been introduced. First, a spatial error in the GPS coordinates of the target because the reference receiver "G" is not located exactly at the target. The central question is: "How far can receiver "G" be from the target and still predict with better than 10 ft relative accuracy what receiver "E" should read at the target?" Experimental results described in Section 2 will answer this question.

The second additional source of error is in the scheme used to measure the *relative* location between the reference receiver "G" and the target. There are various means to determine the *relative* location vector, $\overline{\text{RTL}}$, to the target. In one of the schemes described in Section 3, a high resolution SAR radar is used to locate the target relative to the aircraft in coordinates established by the aircraft INS/GPS system (RCVR "G"). The target coordinates are used by the GPS/INS guided weapon (RCVR "E"). These approaches are summarized in Figure 4.

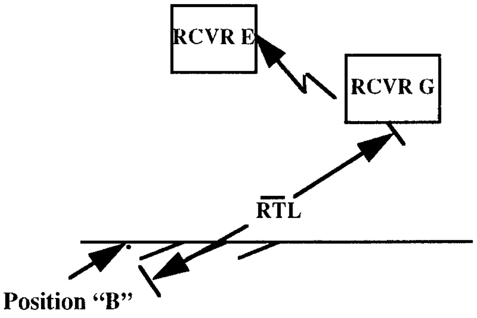

Figure 4. The Relative GPS Concept - 4

In contrast, for the weapons systems described in Sec. 4, in which the reference receiver "G" is located on the ground, the relative location vector $\overline{\text{RTL}}$ is determined prior to the mission.
All of the approaches to be described require the two receivers being able to receive signals from a common set of GPS satellites while possibly separated by ground distances of several hundred miles. Section 5 will show this to be true for separations greater than 540 nmi.

Finally, Section 6 gives some concluding remarks.

2.0 EXPERIMENTAL RESULTS CONFIRMING RELATIVE GPS ACCURACY WITH SEPARATIONS IN TIME AND HORIZONTAL DISTANCE

The experiment was implemented by placing GPS receivers at eleven sites across the continental United States. [Ref. 2] Data was collected in two phases: one on the East Coast conducted in December 1993, and one on the West Coast conducted in March 1994. Figure 5 is a map showing the locations of the receiver sites and baselines used. Table 1 lists baseline endpoints and baseline lengths. Over thirty hours of receiver data was collected for each of the eight East Coast baselines, approximately half of that at a 1 Hz sampling rate,the other half at a 1/30 Hz rate.

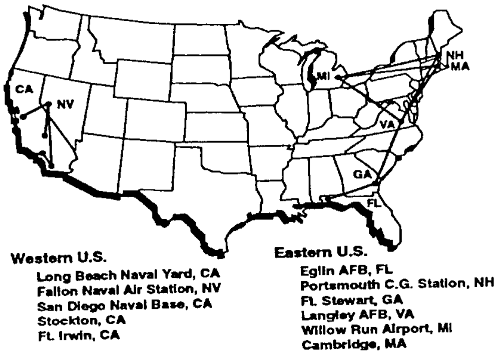

Figure 5 East and West Coast Baselines

Between twelve and sixteen hours of receiver data was collected for each of the West Coast baselines, all of it at a 1/30 Hz rate. The absolute positions were established by independent means. The experiment consists of reading the GPS receiver at one location, adding to its position the relative location vector to a second receiver, and then predicting what the second receiver reads given that it is commanded to use the same satellites as the first receiver.

East Coast Baselines		
Endpoint	**Endpoint**	**Baseline Length (nmi)**
Cambridge, MA	Portsmouth, NH	45
Eglin AFB, FL	Ft. Stewart, GA	263
Langley AFB, VA	Cambridge, MA	400
Langley AFB, VA	Ft. Stewart, GA	405
Langley AFB, VA	Portsmouth, NH	442
Langley AFB, VA	Willow Run, MI	452
Willow Run, MI	Cambridge, MA	552
Willow Run, MI	Portsmouth, NH	558

West Coast Baselines		
Endpoint	**Endpoint**	**Baseline Length (nmi)**
San Diego, CA	Long Beach, CA	80
Stockton, CA	Fallon, NV	152
Ft. Irwin, CA	Fallon, NV	268
San Diego, CA	Fallon, NV	409

Table 1. Baseline Endpoints and Baseline Lengths

To obtain a single value indicator of expected three-dimensional error, we have combined bias and standard deviation in the following way: bias and standard deviation are first computed for each position coordinate (north, east, vertical); the three bias components are combined in a root-sum-square (RSS) sense to give an undirected bias magnitude; similarly, the three standard deviation components are combined in an RSS sense to give an undirected standard deviation magnitude; the undirected bias magnitude and undirected standard deviation magnitude are themselves combined in an RSS sense to give a statistic we call simply the "total error." The total error represents, in a geometrically intuitive way, how a large number of baseline vector measurements would be expected to differ from truth. In the results following, we show the total error bias and standard deviation components separately at first, combined afterward.

Figures 6A and 6b show the bias and standard deviation components, respectively, for the East Coast data as a function of baseline length. Individual data points represent the statistical results of a single data collection session, typically two to four hours in length. Figures 7a and 7b are the corresponding error components for the West Coast data.

Figure 8a is the RSS combination of the bias and standard deviation components of the error for the East Coast data. Figure 8b is the corresponding plot for the West Coast data.

Time delay, Δt, for temporal decorrelation analysis was varied from zero to fifteen minutes in thirty second intervals. Error was again computed as the RSS combination of the bias and standard deviation components measured at each value of Δt. Results for all four West Coast baselines are shown in Figure 9.

The uniform increase in error with increasing time delay and baseline distance indicated by this plot immediately suggests a plane as a representative surface. A least squares fit has been performed on these data, and the deterministic equation of the resulting plane is

$$E(\Delta l, \Delta t) = E_0 + A\Delta l + B\Delta t$$

where Δl is the baseline length in nmi, Δt is the time delay in seconds, $E(\Delta l, \Delta t)$ is the error in ft, and E_0, A, and B are constants with the following values:

$E_0 = 7.6$ ft $A = 2.7 \times 10^{-3}$ ft/nmi
$B = 4.4 \times 10^{-3}$ ft/sec

The results of this experiment show that targeting error grows slowly and linearly with baseline length and targeting latency. The nearly linear behavior of this growth for baseline lengths on the order of 540 nmi and times of flight up to fifteen minutes indicates that the relative GPS navigation technique will give acceptable relative navigation accuracy for precision strike missions. The next part of the problem, relative location of the target will now be discussed.

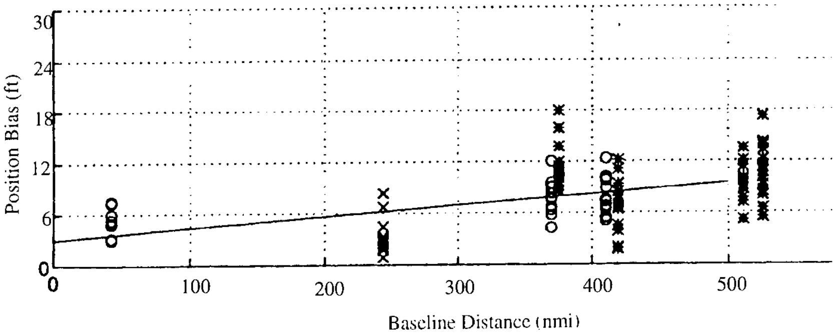

Figure 6a. Bias Component of Error, East Coast Data

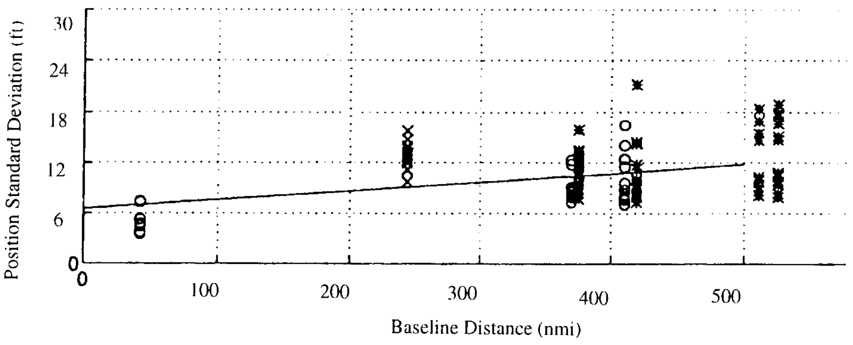

Figure 6b. Standard Deviation Component of Error, East Coast Data

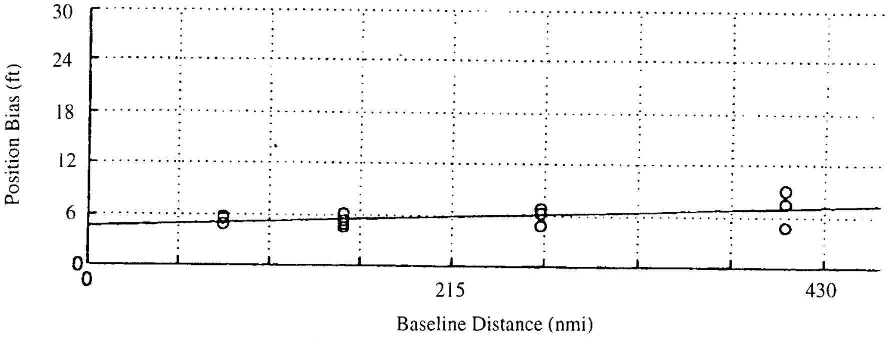

Figure 7a. Bias Component of Error, West Coast Data

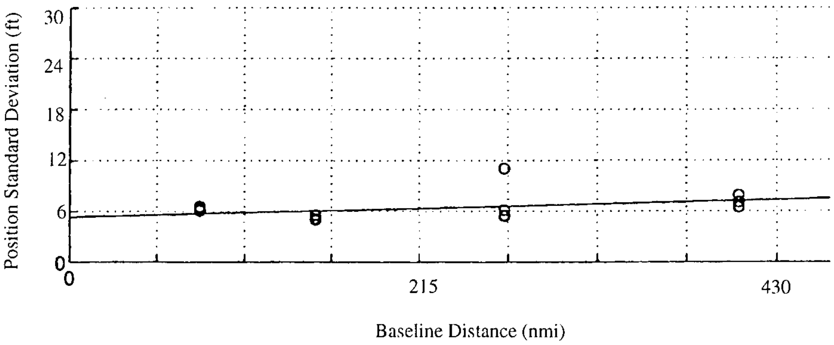

Figure 7b. Standard Deviation Component of Error, West Coast Data

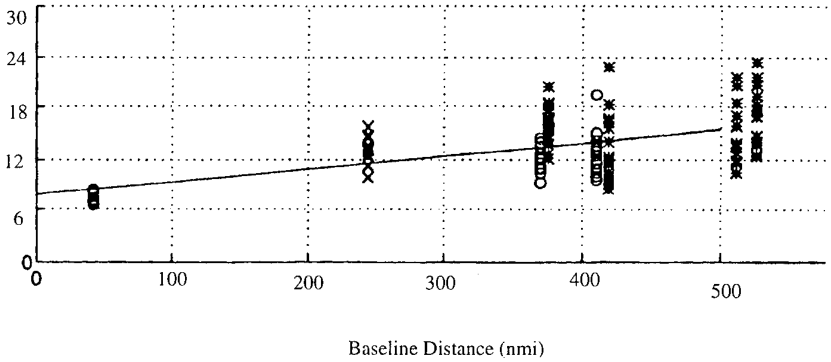

Figure 8a. Total RSS Error, East Coast Data

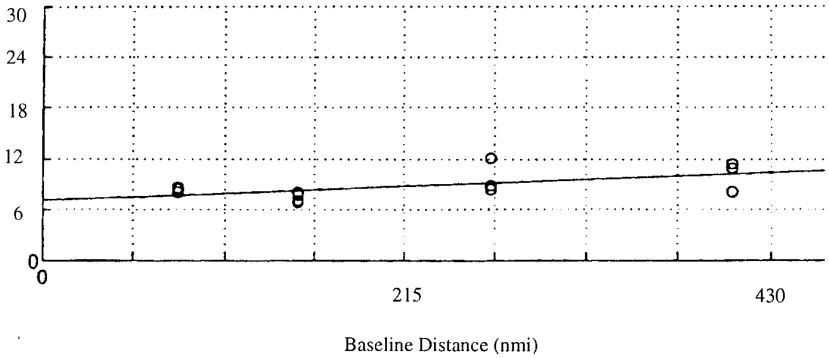

Figure 8b. Total RSS Error, West Coast Data

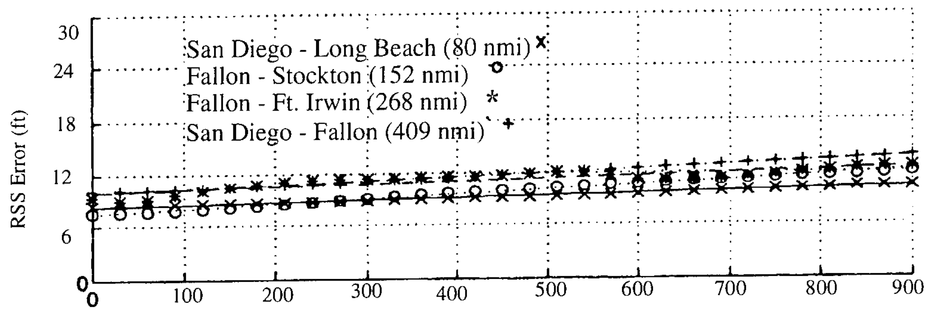

Figure 9. Total RSS Error vs. Time Delay, West Coast Data

3.0 REAL TIME RELATIVE TARGET LOCATION TECHNIQUES

In Section 2 it was shown that a GPS/INS guided weapon, using the same set of satellites as a reference receiver, will be able to maintain precision strike accuracies over long flight distances and flight times. The next part of the problem is to determine the target location relative to the reference receiver. This target location, when used by the weapons GPS/INS navigation system,, will result in precision strike accuracy even though it can be substantially in error in an "absolute" sense. The target is then determined by adding this relative location to the reference GPS receiver location.

Figure 10 shows one concept in which the relative targeting is done by a foot soldier with a reference GPS receiver and a target location device. The target location device might consist of a laser range finder combined with an attitude determination device. The target location (relative to the soldier) would be added to the GPS location to determine the target location in GPS coordinates. The target location and the satellite set used by the reference receiver would be transmitted to the weapon. The receiver on the weapon would use this set of satellites and the guidance would use the computed target location to achieve precision accuracy.

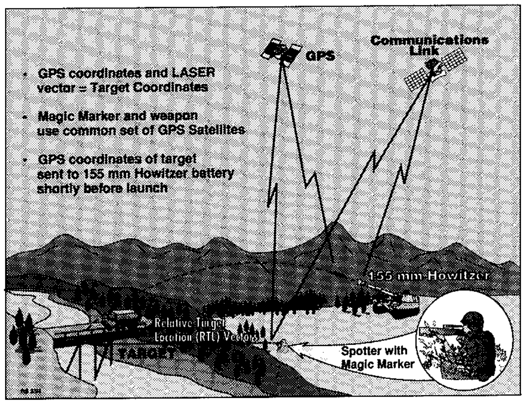

GPS
Communications Link
• GPS coordinates and LASER vector = Target Coordinates
• Magic Marker and weapon use common set of GPS Satellites
• GPS coordinates of target sent to 155 mm Howitzer battery shortly before launch
155 mm Howitzer
Relative Target Location (RTL) Vectors
TARGET
Spotter with Magic Marker

Figure 10. Determining Relative Location

Other implementations might involve the use of a high resolution synthetic aperture radar (SAR) onboard the weapon-carrying aircraft in order to accurately determine the relative target location vector in the aircraft GPS/INS coordinate system. The remainder of this section provides an extensive analysis of this case.

To achieve high 3-D position resolution of ground targets using SAR range and range-rate (Doppler) measurements, SAR uses the velocity vector of the aircraft to create, in effect, an antenna length (or aperture) that is proportional to the velocity of the aircraft times the integration time used in the radar processing. Errors in knowledge of the actual velocity vector directly translate into cross-range errors in the slant plane defined by the velocity vector and the line of sight (LOS) to the target location. GPS provides accurate navigation information that helps the aircraft's Kalman filter sort out the GPS errors, the inertial system errors, the radar errors, and importantly, to relate the SAR Doppler measurement to cross-range position in the slant plane.

As an example, Fig. 11 shows an aircraft trajectory during which a sequence of simulated SAR maps were made. The radar range resolution was set to 3 ft. The aperture length/integration time was adjusted so that each measurement in the sequence also resulted in a radar cross-range resolution of 3 ft. It was assumed that the ARPA GPS Guidance Package (GGP) was the inertial/GPS system on the aircraft. [Ref. 3] An error covariance analysis of a system which used these measurements in combination with GPS/INS navigation to determine target location was performed. The INS errors were those associated with a 1 nm/hr system. The relative GPS errors were modeled as discussed in Section 2. Several results of this analysis are of interest. Figure 12 contrasts the results in target location determination with and without the use of GPS. For this figure, the initial target location error was 500 ft. (1σ) in each of three axes. In the graph on the left, "Without

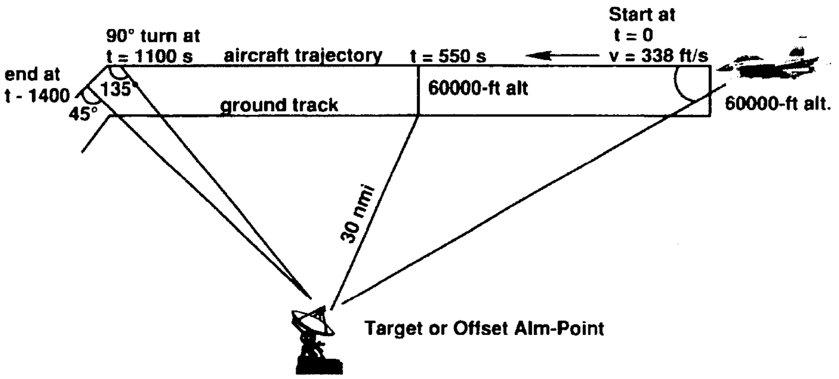
Start at
t = 0
v = 338 ft/s
90° turn at
t = 1100 s
aircraft trajectory
t = 550 s
end at
t - 1400
135°
45°
ground track
60000-ft alt
60000-ft alt.
30 nmi
Target or Offset Aim-Point

Figure 11. Trajectory 1 Geometry

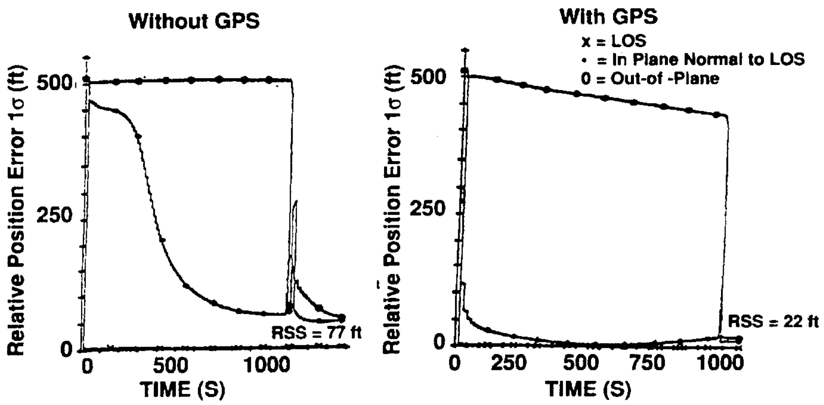

Figure 12. GPS measurements greatly improve SAR performance

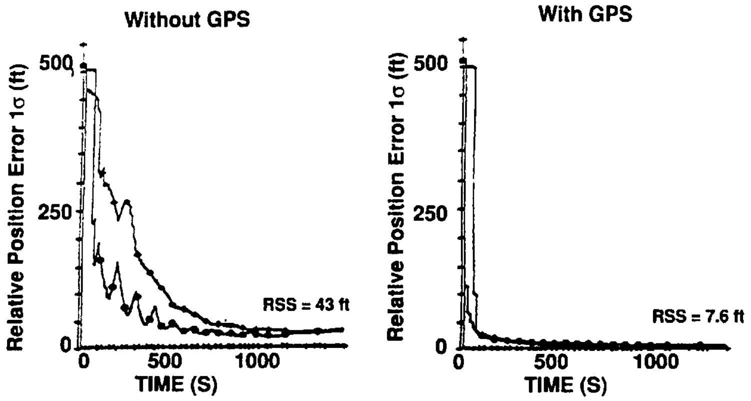

Figure 13. GPS measurements and slant plane changes greatly improve SAR performance.

GPS", the first radar measurement (at t = 0) immediately results in relative target accuracy in the range direction of less than 3 ft. However many more measurements are required to resolve cross-range accuracy. Even at 1000s, the cross-range coordinate is not known to better than about 60 ft. (1σ). This error is primarily due to velocity errors in the inertial system corrupting the relationship between the SAR Doppler measurement and cross-range position. The component of error out of the slant plane is not resolved at all until the slant plane is rotated shortly after 1000s. In the graph on the right, the accuracy provided by GPS velocity measurements greatly aids in translating the SAR Doppler measurement into cross-range position. By about 10 minutes, both in-plane components of target location are accurately measured. Again the third component is not resolved at all until the slant plane is rotated at about 1000s. The GPS aided resolution of this third component is better but still not to the desired level.

The observability of this third component must be further enhanced by slant plane rotations. The idea is to align the measurement directions, either in range or cross-range, along the unresolved direction. There are two approaches to this, one to change the aircraft position, the other is to change the aircraft velocity. It takes much less time to change the aircraft velocity, so this was the approach used here. A series of dive and climb maneuvers, (porpoising) were incorporated into the flight plan. These maneuvers rotate the slant plane by rotating the velocity vector. Figure 13 shows the resulting target determination accuracy. Again the graph on the left shows errors when GPS measurements have been forgone. The graph on the right shows errors when GPS measurements are included. In this later case, accurate measurements are achieved relatively quickly. After about 20 minutes the RSS errors are 7.6 ft. Although perfectly feasible in terms of SAR processing (and aircraft capability), there seems to be a desire in the SAR community to fly straight and level. Practically speaking this undoubtedly simplifies processing algorithms which even so require enormous computing resources. Perhaps a more practical scenario for target location and subsequent weapon delivery is shown in Figure 14. On its way to the target, the aircraft executes a dogleg and altitude change, thus dividing the trajectory into three segments with different slant planes. SAR measurements are made along the dogleg with the SAR beam squinted quite far forward, first + 20 deg, then at - 20 deg. For this study both the range and cross-range resolution was 8 ft. Table 2 shows resulting target location accuracy for two variations. In the first, Case 1, six SAR maps were made, two for each segment of

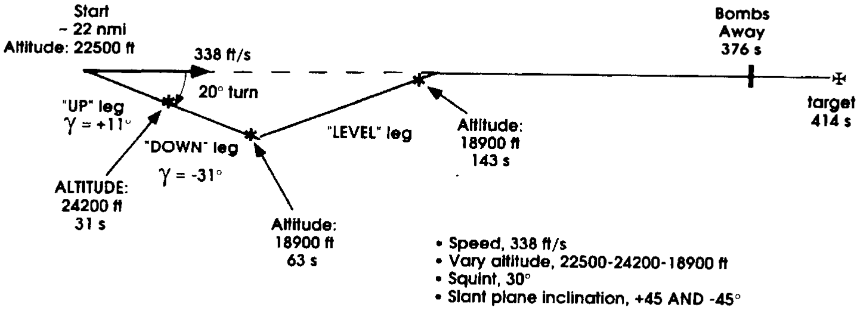

- Speed, 338 ft/s
- Vary altitude, 22500-24200-18900 ft
- Squint, 30°
- Slant plane inclination, +45 AND -45°

Figure 14 Trajectory 3.

1 σ Relative errors, ft
LOS = Along the line-of-sight to target
CR = Perpendicular to LOS in the slant plane
Norm = Perpendicular to the slant plane
FWD = Forward
CRR = Cross range at impact

Case	SAR Measurement Conditions	"Up" Leg $\gamma = +11^{\circ}$ Plane Inclination +45° Altitude: 24,200 ft			"Down" Leg $\gamma = -30^{\circ}$ Plane Inclination -45° Altitude: 18,900 ft			"Level" Leg $\gamma = -0^{\circ}$ Plane Inclination -45° Altitude: 18,900 ft			Bomb Impact	
		LOS	CR	Norm	LOS	CR	Norm	LOS	CR	Norm	FWD	CRR
1	2 at end of each leg	8.0	49.1	500	5.7	31	32	No measurement			9	21
2	Continuous	4.0	51	500	2.7	32	33	1.9	15	21	5	15

Table 2. Trajectory 3 results.

the trajectory. For Case 2, a sequence of several measurements was made along each segment with the aperture time adjusted to yield an 8 ft. cross-range error for each measurement. The last measurement was made at t = 143s. At t = 376s, a guided bomb was launched. The bomb GN&C system included a GPS/INS reference receiver locked to the same satellites as the receiver on the aircraft and used the target coordinates determined by the GPS/INS/SAR system.

The resulting bomb impact errors shown in Table 2 demonstrate the efficiency of relative GPS/INS navigation and target determination by this system at weapon delivery time. The next section analyzes weapon delivery scenarios for which the relative target vector has been determined premission.

4.0 RELATIVE TECHNIQUES EMPLOYING GROUND-BASED RECEIVERS

In this section, we shall consider how various existing or planned GPS-guided weapons could exploit an hypothetical capability to accurately determine 3-D relative target location vectors that are determined prior to the mission. We shall make the explicit assumption that someday we may have the capability to accurately determine these vectors to an accuracy of less than 10 ft (1σ per axis) over distances up to, say, 540 nmi (1000 km).

Such a capability would allow one to provide relative (or absolute if a surveyed point is used) targeting information on many targets over reasonably large potential theaters of conflict. For example, Figs. 15 and 16 show how only a few cooperative receivers located in "friendly territory" could provide coverage of nearly the entire Middle East and parts of northern Africa when used in a relative GPS mode. Of course, we might expect increasingly better accuracy as the distance between the cooperative ground-based receiver and target is shortened.
We shall now illustrate how several, somewhat different, existing or planned weapon systems could exploit such a capability.

First, consider the cruise missile scenario shown in Fig. 17. Here, a ground-based receiver has been located with respect to a target. It will be necessary for the ground-based receiver to update the cruise missile shortly before its arrival at the target. It is not certain how "short" this time must be to be consistent with our accuracy goals. However, the results of Section 2 indicate that several minutes are permissible.

So, a few minutes before impact, we transmit from the cooperative receiver to the weapon the receiver's indicated position and the set of satellites it is using to form its navigation solution. A communications relay (satellite or aircraft) might be used if there were line-of-sight constraints.

It is also assumed that prior to launch we store the relative vector from the cooperative receiver to the target in the cruise missile's flight computer. Then, on receipt of the short data message from the cooperative receiver, the cruise missile ensures it is tracking the correct set of satellites and then adds the indicated position of the cooperative receiver to the $\overline{\text{RTL}}$ vector—thereby making an estimate of

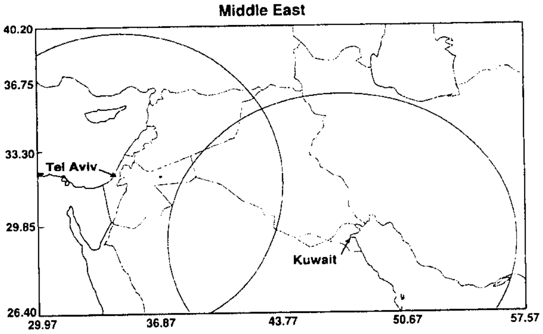
Middle East
40.20
36.75
33.30
29.85
26.40
29.97
36.87
43.77
50.67
57.57
Tel Aviv
Kuwait

Figure 15. 540 nmi "coverage" for two cooperative GPS receiver/transmitter.

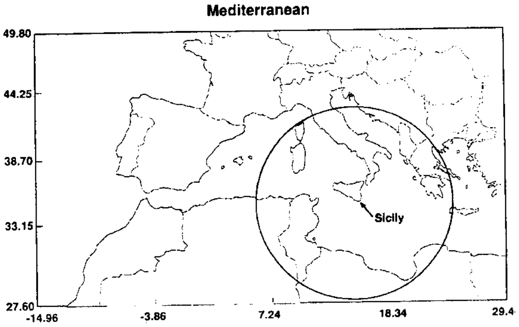
Mediterranean
49.80
44.25
38.70
33.15
27.60
-14.96
-3.86
7.24
18.34
29.4
Sicily

Figure 16. 540 nmi "coverage" for one cooperative GPS receiver/transmitter.

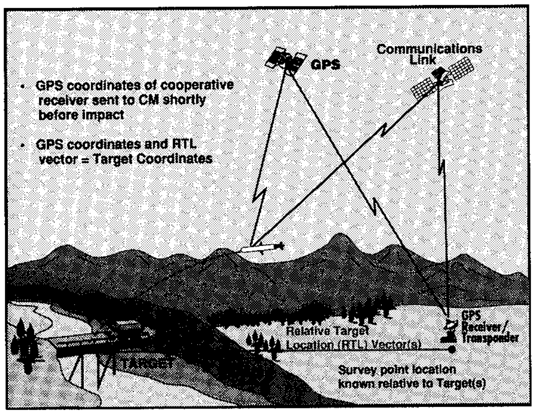
GPS
Communications Link
• GPS coordinates of cooperative receiver sent to CM shortly before impact
• GPS coordinates and RTL vector = Target Coordinates
GPS Receiver/ Transponder
Relative Target Location (RTL) Vector(s)
TARGET
Survey point location known relative to Target(s)

Figure 17. Cruise missile precision strike concept employing relative GPS.

the indicated GPS position of the target and steers itself to that location.

This scheme would appear to be relatively easy to implement in the Tomahawk weapon system, for example, since future planned upgrades include both"time-of-arrival" control and a communications link.

An equally simple scenario can be mechanized for the envisaged Joint Direct Attack (or Standoff) weapon system (JDAM, JSOW). Fig. 18 illustrates this concept. The slight difference in this scenario from that of the cruise missile is that the communication would probably go from the cooperative receiver to the aircraft carrying the weapons. This is feasible due to the relatively short time of flight of the JDAM weapon. Thus, just before launch of the weapons, the A/C receives the targeting data, computes the indicated GPS coordinates of the target(s) and downloads these new coordinates and the set of satellites to be tracked into the JDAM computer.

The ship-based Navy can also take advantage of this relative targeting technique just as well for precision shore bombardment. Fig. 19 illustrates this scenario. It could be possible to locate a receiver in Italy, for example, and have the ship in the Mediterranean Sea while holding targets in northern Africa at risk.

Possibly the simplest scenario might involve the Army's extended range (ER) version of the Army's Tactical Missile System (ATACMS) [Ref. 4]. An ER-ATACMS battery could set up on one of these cooperative sites. Then the GPS receiver in the weapon itself could act as the "cooperative" receiver—thus, not requiring even a communications link, since cooperative receiver and weapon receiver are one in the same—and do the targeting by adding on to its own indicated position the relative target location vector just before launch and then using the same GPS satellites to navigate from there to the target.

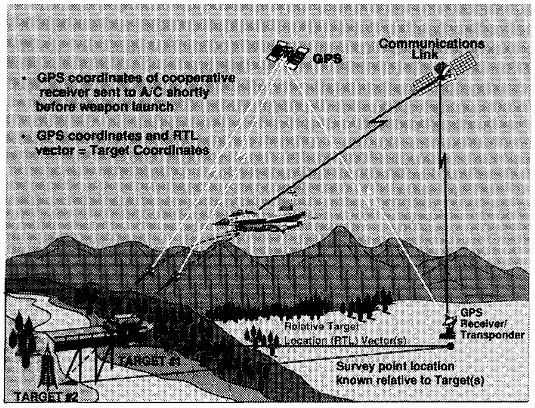
GPS
Communications Link
• GPS coordinates of cooperative receiver sent to A/C shortly before weapon launch
• GPS coordinates and RTL vector = Target Coordinates
GPS Receiver/ Transponder
Relative Target Location (RTL) Vector(s)
TARGET #1
Survey point location known relative to Target(s)
TARGET #2

Figure 18. JDAM precision strike concept employing relative GPS.

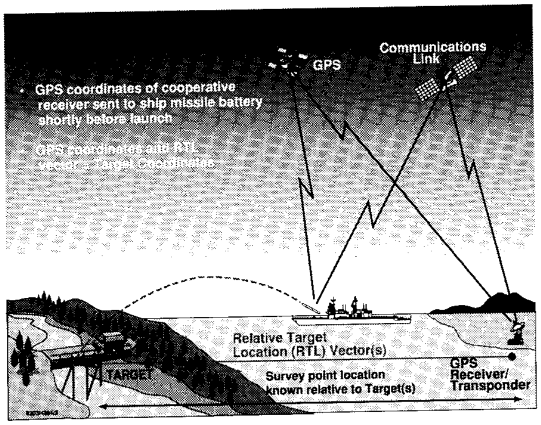
GPS
Communications Link
• GPS coordinates of cooperative receiver sent to ship missile battery shortly before launch
• GPS coordinates and RTL vector = Target Coordinates
Relative Target Location (RTL) Vector(s)
TARGET
Survey point location known relative to Target(s)
GPS Receiver/ Transponder

Figure 19. Relative GPS for Ship-based precision strike.

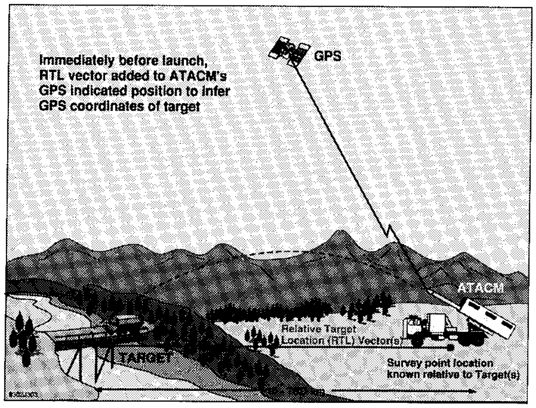
Immediately before launch, RTL vector added to ATACM's GPS indicated position to infer GPS coordinates of target
GPS
ATACM
Relative Target Location (RTL) Vector(s)
TARGET
Survey point location known relative to Target(s)

Figure 20. Relative GPS/ATACMS Scenario

This scenario is shown in Fig. 20. Of course, a separate cooperative receiver can also be used as in the other scenarios, thereby allowing the ATACMS battery to set up where ever it pleases (now, however, a communications link is required between the cooperative receiver and the ATACMS battery).

Variations on these scenarios can be applied to many other existing or contemplated GPS-guided weapon systems. For example, the SAR equipped aircraft of Section 3 could be used to image off-set aimpoints (rather than the target). The points could be in friendly territory and have been mapped relative to the target prior to the mission. (See Figure 21.) In some tactical situations it might even be conceivable to include the reference station and the target in the same SAR image.

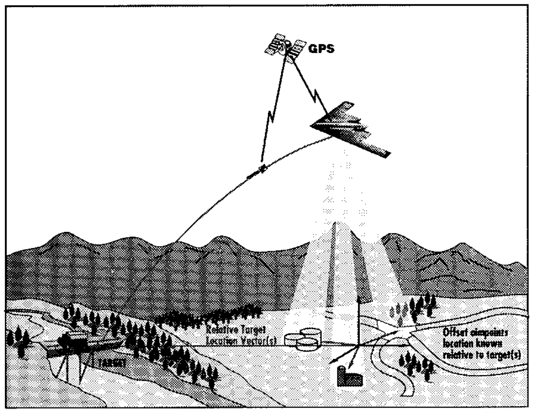
GPS
Relative Target Location Vector(s)
Offset aimpoints location known relative to target(s)
TARGET

Figure 21. Relative GPS/Bomber Scenario

5.0 GPS OBSERVABILITY ISSUES

This section addresses the important issue of GPS satellite availability as a function of (1) target-to-receiver separation, and (2) the time interval between when the target location is estimated and when the weapon actually arrives at the target.

In other words, is it reasonable to expect that as the weapon approaches the target that both it and the cooperative GPS receiver located "far" from the target will have a sufficient number of common satellites in view to enable a relative GPS mechanization? A study was undertaken to address this important issue.

The study assumes that the full constellation of 24 GPS satellites. A simulation was written to model the orbital motion with respect to the earth. In the simulation, pairs of receivers were located at various latitudes (0 to 90 deg) and at various orientations (i.e., N/S or E/W, etc.) with respect to each other. Time was advanced in increments so as to let the geometry evolve for a long enough period so that all the behavior patterns could be observed. Both distance and "time delay" between receivers were varied, the process is illustrated for one location in Figure 22. Table 3 summarizes the results of the study. If, for example, we update the Tomahawk's aimpoint coordinates 5 minutes before impact using data computed from a receiver located 945 nmi away from the target at 60 deg latitude, the table indicates that there will never be a condition with fewer than 4 satellites in view common to both receivers.

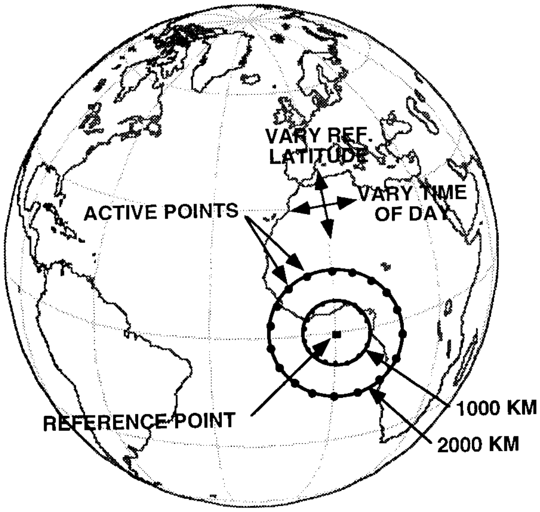

Figure 22. Reference and Active Receiver Locations

Reference Latitude, Degrees - North	Time Delay (Minutes)	Minutes Number in View for Zero Separation	Max. Separation with four satellites in View (nmi)
0	0	6	1458
	5	6	1296
	15	6	1377
	30	6	1080
30	0	5	1350
	5	5	1188
	15	4	918
	30	4	324
60	0	4	918
	5	4	945
	15	4	702
	30	4	432
90	0	7	1836
	5	7	1944
	15	6	1836
	30	6	1458

Two specific examples:

Latitude	Time Delay (min)	Sep. Distance (nmi)	Min. # of Common Satellites	Average #	Average GDOP
30	15	540	4	6.2	4
60	15	540	4	6.5	3.9

Table 3. Summary of Results

High accuracy, however, is not guaranteed solely by having a set of four or more common satellites in view. Satellite constellation geometry (PDOP) is also important. On rare occasions, the geometry may be such that a change in the attack time by +/- a few minutes may result in a substantial improvement in accuracy (as when a new satellite appears over the horizon and has a dramatic effect on the available constellation geometry). This rare condition can be predicted weeks ahead of time if the approximate target location and time of attack are specified, thus allowing the mission planners to either select times with extremely favorable GPS geometry or to avoid the very rare instances of poor geometry. Draper has developed a prototype software/simulation tool for analyses and fire control applications involving these issues. Again, it should be emphasized that instances of poor geometry are, indeed, the rare exception.

6.0 CONCLUDING REMARKS

This concept paper has addressed several potential methods for achieving high accuracy (~10 ft CEP) using GPS/INS weapons. The approaches all revolve around a low-cost weapon navigation system (i.e., no terminal seeker on the weapon) and were variants of relative GPS guidance schemes. In a sense, removal of the terminal seeker on the weapon is allowed by determining the relative location vector using the sensor on the launch aircraft in real time, or by some other premission means of determining the relative target location vector. Simulated accuracies were shown to have promise for achieving the high-accuracy goals. Actual experimental results were presented confirming the theory of relative navigation between receivers separated by long baselines and also separated in time.

ACKNOWLEDGMENTS

The authors wish to express their thanks to several members of the Technical Staff at Draper Laboratory who have contributed to the ideas and work reported in this paper: Dennis Brown, Barry Fink, Richard Greenspan, Frank Mullen, and Richard Phillips. We also wish to thank Ms. Dianne Bennett, Ms. Anna Massa, and Ms. Julie Merrell for preparing this paper for publication. We also acknowledge support by the Advanced Research Projects Agency, ASTO, in providing funding to present this paper.

REFERENCES

[1] [JPO 1] *GPS Joint Program Office System Segment Specification for the User System Segment,* SS-US-200, 31 January 1979.

[2] Mullen, F., Fink, B., and Setterlund, R., "Verification of Relative GPS Targeting Concept", *Proceedings of the 22nd Joint Services Data Exchange,* Scottsdale, AZ, October 1994, Section 5A.

[3] Ebner, R. and Rickords, T., "The Status of the Global Positioning System Guidance Package", *Proceedings of the 22nd Joint Services Data Exchange,* Scottsdale, AZ, October 1994,

[4] "Extended Range ATACMS", *Aerospace Daily*, 5 January 1993, pg. 8.

CARRIER PHASE GPS TIME, SPACE, POSITION INFORMATION DEMONSTRATION (CAPTIDE)

Gregg D. Costabile, Jesse Fowler, Timothy Elbert, David Reiter, III
39 FTS/CAX
601 W Choctawhatchee Ave, Suite 45
EGLIN AFB, FL 32542-5720
UNITED STATES

1.0 SUMMARY

This paper presents a discussion and results of a flight test to obtain Time, Space, Position Information (TSPI) using carrier phase (or kinematic) GPS. A carrier phase capable GPS receiver was installed on board an F-16 aircraft and flown in conjunction with an INS/differential GPS guided weapon test program. The carrier phase TSPI data was compared to the position solution from existing test range TSPI sources, including: four high-dynamic Contraves cinetheodilites operated at 30 frames per second, two FPS-16 radars, the aircraft position system solution, an INS/GPS position measurement pod on board the aircraft, and a post-mission Kalman smoother based software algorithm called "test data optimal processor". The carrier phase and test range solutions were also compared to the INS/DGPS test items. A series of aircraft manuevers were conducted to collect truth data to compare the carrier phase GPS position with the "truth" position. This was the first experiment known to the authors which utilized the carrier phase observable in an aircraft environment where high accuracy TSPI was available to evaluate the accuracy of the carrier phase technology.

2.0 INTRODUCTION

When determining the accuracy performance of any item under test, an analyst desires truth source accuracy an order of magnitude better than the test item to assess its performance. Determining the accuracy of navigational systems operating in a dynamic environment is becoming more difficult as technology evolves. Current inertial navigation / differential GPS systems are capable of navigating to within one meter of an intended position. A scoring system capable of determining position to within 10 centimeters is therefore required to quantify such a test item's navigational performance. This presents significant challenges for current scoring systems.

To quantify the accuracy of a carrier phase GPS system, truth accuracies an order of magnitude better than the carrier phase system are required. Overall carrier phase position accuracy is on the order of 1 to 4 centimeters[1]. This means a truth source capable of determining position to within 1 and 4 millimeters is required to quantify carrier phase position accuracies in high-dynamic applications. Imagine tracking a point on a high performance aircraft performing a high-g turn, or even an airliner on final approach to within 1 and 4 millimeters! Clearly we have approached the state of the art in position determination using existing technologies. The best the CAPTIDE test could hope to do was qualify carrier phase performance to conclude such a system was at least as good as existing position determination technologies. This was the goal of the CAPTIDE program.

3.0 BACKGROUND

The **C**arrier **P**hase GPS **TSPI** **De**monstration (CAPTIDE) was conducted under the auspices of the Exploitation of Differential GPS for Guidance Enhancement (EDGE) program[2]. As a result, CAPTIDE was not permitted to influence the test method or schedule of EDGE. Aircraft manuevers or data collection efforts specific to evaluating CAPTIDE were not possible.

The EDGE test program at Eglin AFB, FL provided the means to assess the performance of a carrier phase GPS system employed in a dynamic environment. The EDGE weapon was an inertially guided, differential GPS (INS/DGPS) aided weapon which was employed from an F-16, Block 50D aircraft. The expected accuracy for this weapon system was between one and three meters. Time-Space-Position Information (TSPI) resources were used on the EDGE program to measure the test item's position accuracy. These resources included four Contraves cinetheodilite cameras, two FPS-16 radars, aircraft INS and aircraft system position solutions, and INS/DGPS TSPI pods which were carried on aircraft stations 2 and 8 (see figure 1). On one of the test missions (captive carry 4), data collected from the four cinetheodilite cameras, two FPS-16 radars, and the aircraft system solution were processed by a Kalman smoother software algorithm called the test data optimal processor (TDOP). The TDOP TSPI solution was the most accurate TSPI solution available at Eglin AFB. Its accuracy was quoted to be between one and three feet[3] and was better than any of the TSPI solutions (cinetheodilites, FPS-16 radar, etc.) used independently.

Paper presented at the AGARD MSP Symposium on "Technologies for Precision Air Strike Operations in Rapid-Reaction and Localised-Conflict Scenarios", held in Seville, Spain, from 16-19 October 1995, and published in CP-576.

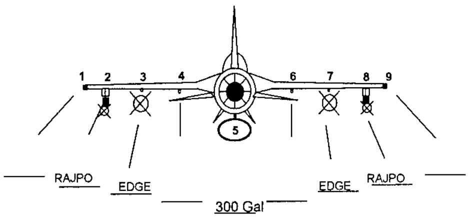

Figure 1 - F-16 Aircraft External Stores Configuration

After successful integration of the system into the F-16 aircraft, the CAPTIDE system was flown on six subsequent EDGE captive carry flight test missions. These captive carry missions were test sorties which did not release the EDGE test item from the aircraft, but were specifically designed to evaluate weapon system performance and function prior to the drop missions. Data analysis efforts for CAPTIDE were focused on three of the six captive carry missions.

4.0 TEST ITEM DESCRIPTION

The CAPTIDE system consisted of the carrier F-16 aircraft, an Ashtec Z-12 GPS receiver with 6 megabytes of extended memory with associated antenna, preamp, and cabling, a laptop PC to communicate with the receiver under an autonomous power source and to extract data post-mission, and an Ashtec Z-12 ground reference receiver with associated cabling, power source, and antenna located directly over a surveyed location. The receiver occupied 385 cubic inches of volume and required 800 milliamps of 28 volt dc power.

The CAPTIDE data reduction software consisted of an off-the-shelf Ashtec product, Precise Differential GPS Navigation (PNAV), and various MATLAB routines written by EDGE personnel. The PNAV software was used to resolve the carrier phase integer ambiguities and provided the carrier phase solution. Default PNAV filter values were used for all carrier phase data reduction; forward and backward data smoothing was used for all data reduction.

4.1 Carrier Aircraft

The test aircraft used for this program was an F-16D, Block 50 aircraft with block 50D avionics. The carrier phase receiver was installed in the ammo bay just aft of the cockpit. The 30 millimeter gun and ammunition barrel were removed to provide adequate space for test instrumentation. F-16 flight test vibration data were analyzed to choose the most suitable location for the commercial receiver hardware. This commercially available receiver was intended for ground use and not specifically designed for an airborne environment. The ammo bay area was chosen because it provided lower vibration levels throughout most of the aircraft's flight regime with respect to any other suitable location on the aircraft. Additionally, the receiver was mounted in a fixture which in turn was shock mounted to the aircraft fuselage. A bracket mounted on the fixture provided stress relief for the power and communications cabling. A cable was run from the receiver to an access panel under the left leading edge wing strake. This arrangement provided a convenient method to insure the system was functioning properly prior to takeoff, and to extract data after the aircraft landed. A laptop PC was used to interface with the receiver via an RS-232 connector at the access panel. The receiver's antenna was mounted on the turtle deck directly above the ammo bay and directly behind the aircraft canopy.

5.0 TEST METHODOLOGY, ANALYSIS, AND RESULTS

The following data analysis methodology was used to assess the performance and accuracy of CAPTIDE. The reported filter values from the CAPTIDE system were qualified via the truth data (TDOP) generated on the fourth captive carry mission. From this baseline, confidence was gained in the CAPTIDE receiver values. CAPTIDE data from the first captive carry mission were used to evaluate the system in a high-dynamic environment. This evaluation investigated filter settling times after the receiver was shielded from the GPS satellite vehicles by the host aircraft (during rolls and wind-up turns), and investigated system performance at extended reference receiver / test receiver baseline separations. Captive carry six generated the data to evaluate the system in a medium dynamic environment and showed the utility of carrier phase GPS for this particular application. The flight profiles and test resources for these missions provided the data to qualify the performance of the carrier phase GPS system for TSPI applications. Data from the INS/DGPS TSPI pods were not of sufficient accuracy to qualify carrier phase GPS performance.

5.1 Captive Carry 1 (CC1)

EDGE captive carry 1 (CC1) was a limited compatibility flight profile mission designed to demonstrate the flight-worthiness of the EDGE weapon system hardware. The test points executed on this test mission are shown in Table 1.

POINT	ALT (ft)	MACH	REMARKS
1	15 K	0.80	3g WUT*, WLSS**, 0g Pushover, 2g L&R 180 deg rolls
2	15 K	0.80	4g WUT, WLSS, -.5g Pushover, 2.5g L&R 180 deg rolls
3	5 K	0.85	Same as Point 2

4	9 K	0.95	Same as Point 2
5	< 1 K	0.90	Speed Soak, 30 minutes

Table 1 - Captive Carry 1 Test Points

* WUT - Wind up turn
** WLSS - Wings level side-slip

This mission was conducted to insure EDGE test item structural and electrical integrity throughout the expected test program flight envelope. The results showed both EDGE weapons and the CAPTIDE system maintained structual and electrical integrity. However, the CAPTIDE receiver's circuit breaker tripped prior to takeoff on all test missions after captive carry six. Subsequently, CAPTIDE data were available for six missions only.

The TDOP position solution was not generated for the first test mission. The aircraft flew over the W151 test range located south of Eglin AFB over the Gulf of Mexico. Filter sigmas, phase residulas, and chi-squared values generated in the receiver were used to investigate the navigation solution quality of the carrier phase system.

The baseline separation of the receiver on board the aircraft and the reference receiver was 30 to 100 statute miles (26 to 87 nautical miles) for most of the compatibility flight (top plot, Figure 2). Notice just before the 79,000 second time epoch the CAPTIDE radial sigma was less than 2 feet for baseline separation distances approaching 100 miles. The aircraft began a series of roll manuevers just after the 79,000 time epoch (Figure 3); the receiver lost lock and the radial sigmas increased significantly. The latter segment of figure 2 reveals that separation distances less than 20 miles produced filter sigmas to less than one foot.

The receiver manufacturer recommends baseline separation distances be kept to less than 10km to maintain carrier phase level accuracies. Since no submeter (level of accuracy), independent TSPI resource was available at 30-100 mile baseline sparations, the reported radial sigma values could not be qualified (see conclusions). The sudden decrease in the radial sigma value just after the 82,000 time epoch was a result of the post-mission data processing software fixing the carrier phase integer ambiguities for about three minutes.

The use of dual frequency receivers, to allow for measurement and compensation for ionospheric delays, and the incorporation of higher order terms in the double difference algorithm baseline estimation to account for geometric errors, should allow a carrier phase based scoring system to achieve < 1 foot accuracy at the baseline distances experienced during CC1[4].

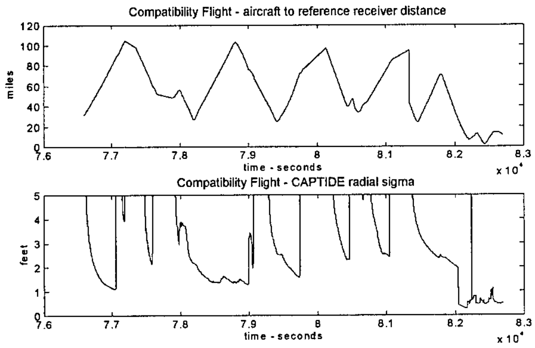

Figure 2 - Compatibility Flight - CAPTIDE separation distance and sigma vs time

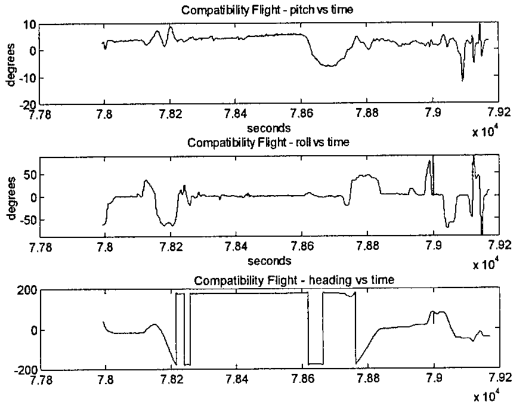

Figure 3 - Compatibility Flight - Aircraft Pitch, Roll, and Heading vs time

Figure 3 is the pitch, roll, and heading dynamics for the aircraft during selected portions of the compatibility flight. Examination of Figure 3, in conjunction with the bottom plot of Figure 2, illustrate the effect of dynamics on the carrier phase solution. The pilot performed a wind-up turn and a 180 degree loaded roll just after the 79,000 time epoch (see the roll and pitch channels of Figure 3). The receiver lost lock at this time due to the aircraft sheilding the CAPTIDE antenna from appropriate GPS satellite vehicles. The corresponding time in Figure 2 gives an indication of CAPTIDE filter settling time after the manuever was completed. The other discontinuities in Figure 2 indicate loaded rolls or wind-up turns and provide additional insight into CAPTIDE filter settling times.

5.2 Captive Carry 4 (CC4)

The objective of the fourth captive carry (CC4) mission was to quantify the accuracy of the EDGE weapon system by collecting the most accurate possible TSPI data available from range truth resources (the TDOP solution) and comparing that data with the weapon's navigation solution. Additionally, the TDOP data and the test item data were used to assess the performance of the CAPTIDE system in a low dynamic environment. Twenty-five passes were accomplished. Data reduction and analysis showed twenty passes yielded useful data. The flight path geometry was chosen to optimize the accuracy of the TDOP solution. The test aircraft flew each pass between 260 and 325 knots indicated airspeed (KIAS), straight and level, at approximately 7,000 feet above ground level (AGL).

The aircraft flew a right turn, oval "racetrack" pattern during CC4. Bank angles in the turns were limited to 30 degrees to prevent the CAPTIDE receiver from losing lock on any GPS satellite vehicle. This maneuver limitation was acceptable to the EDGE test program. A typical CC4 data run is illustrated by Figure 4, which is typical of all runs. The aircraft flew over Eglin test range B70[5] on a 237 degree heading. The top plot of Figure 4 shows the locations of the Contraves cinetheodilite camera sites (B-141, B-120A, etc.) with repect to the aircraft ground track. The separation distance between adjacent camera sites was about two miles. The bottom plot shows a typical altitude profile. The baseline separation between the ground reference receiver and the aircraft never exceeded 25 miles during this mission.

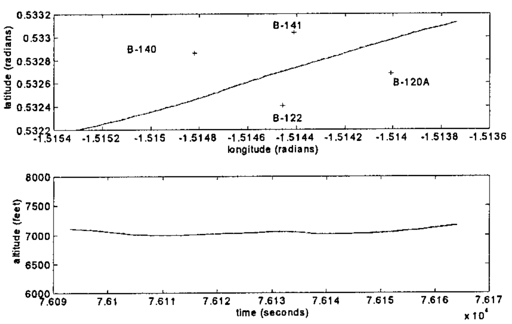

Figure 4: CC4 pass 14 - Ground Track / Altitude vs time

Figure 5 is a comparison of the TDOP and CAPTIDE north, east, and altitude position differences for pass 1. This data is typical of all passes. The upper plot in Figure 5 indicates close agreement in the latitude measurement between TDOP and CAPTIDE. The middle plot shows a periodic oscillation between TDOP and CAPTIDE in the longitude measurement, which is discussed below. The bottom plot shows a bias in the altitude measurement between TDOP and CAPTIDE. The altitude bias changed rather significantly between passes (see Table 2). Based on the collected data, the source of the altitude bias was not conclusively determined.

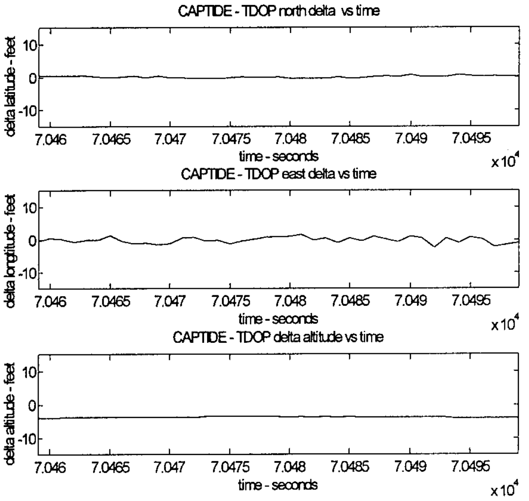

Figure 5 - CC4 TDOP/CAPTIDE Position Differences (pass 1)

Table 2 contains the average position differences between the TDOP and CAPTIDE position solutions for each pass that yielded valid data. The average north position differences were as expected but the variation in east position differences, and the magnitude of the differences in altitude required additional analysis.

Pass #	North	East	Altitude	Radial
1	0.237	-0.177	-3.824	3.836
2	0.107	-0.631	-2.476	2.557
4	0.232	-0.915	-3.607	3.729
6	0.112	-0.925	-3.677	3.793
7	-0.180	-0.968	-3.667	3.797
8	0.422	-0.277	-1.715	1.787
9	-2.790	-0.026	-9.008	9.431
10	-2.350	0.284	-10.060	10.335
14	-0.603	-2.386	-8.664	9.007
15	-0.115	-3.073	-8.534	9.071
16	0.180	-3.594	-8.164	8.922
17	0.441	-0.581	-4.771	4.826
18	0.665	0.085	-4.805	4.852
19	0.226	-0.498	-4.675	4.707
20	0.384	-0.539	-4.125	4.178
21	0.473	-0.601	-4.401	4.467
22	0.340	-0.466	-4.310	4.348
23	0.885	-0.691	-4.339	4.482
24	0.114	-0.893	-4.254	4.348
25	0.045	-0.835	-3.498	3.596

Avg.	-0.059	-0.885	-5.129	5.304

Table 2 - CC4 TDOP/CAPTIDE Average Position Differences (ft)

Figure 6 further illustrates the discrepancy between the TDOP and CAPTIDE longitude measurements. The upper plot in Figure 6 shows the difference in position (in feet) between successive CAPTIDE measurements and the corresponding TDOP measurements. CAPTIDE data was available at a 1 Hz data rate, TDOP was available at 25 Hz. The middle and bottom plots are the first difference in east position (x[t] - x[t-1]) for CAPTIDE and TDOP respectively. Notice at time 70491 the top plot indicates agreement between CAPTIDE and TDOP. At the next time epoch, CAPTIDE (middle plot) senses that the magnitude of the first difference in east position changes by about 2 feet. TDOP (bottom plot) does not sense this change and as indicated by the top plot the solutions disagree by about 2 feet. At the next epoch, 70493, TDOP "catches up" and compensates for changes at both epochs, and as indicated by the upper plot the solutions are in close agreement. The data in Figure 6 is typical of all the data generated during CC4.

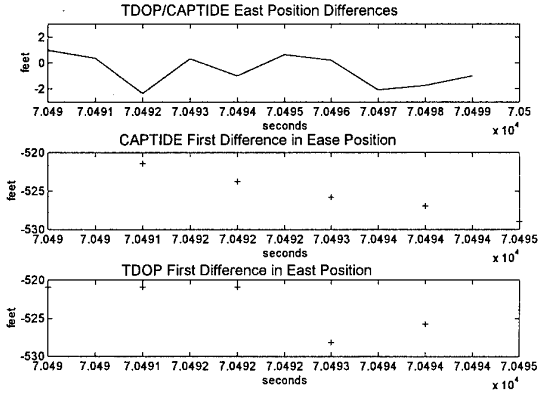

Figure 6 - CC4 pass 1 TDOP/CAPTIDE east position differences / CAPTIDE east 1st difference /TDOP east 1st Difference

Figure 7 illustrates the separation distance, the radial sigma, and the Kalman flag values for pass nine. Notice the radial sigmas reported by the receiver (middle plot) were between .1 and .3 feet for this pass; this was typical data for all passes. The Kalman flag indicated if the receiver solution fixed integer ambiguities. A value of zero indicated an integer-free solution, a value of one indicated an integer-free solution.

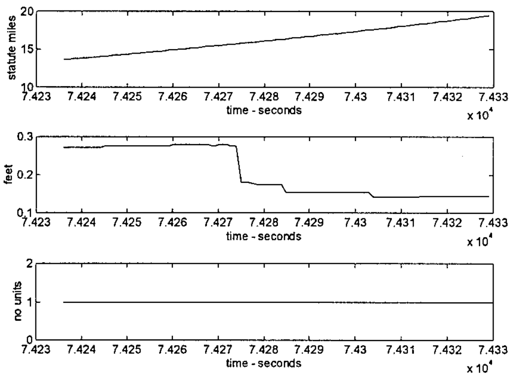

Figure 7 - CC4 Pass 9 - Baseline separation (top plot), Radial sigma (middle plot), and Kalman flag (bottom plot) Vs time

A statistical analysis was conducted on the data to further qualify the CC4 CAPTIDE performance and show biases between TDOP and CAPTIDE. The difference between the CAPTIDE and TDOP position for each data point was determined (for north, east, and altitude). From this data, circular error probable (CEP), CEP RMS, spherical error probable (SEP), and SEP RMS were computed. The CEP shows the 50% data circle centered on the mean of the data set , which in this case is the North-East position deltas between TDOP and CAPTIDE. That is, on the average, 50% of all the data will lie within this circle. The radius of this circle is an indication of randomness in the data set. The CEP RMS is a statistical representation of the data set about the origin, not the mean. The CEP RMS plot is also a 50% circle. That is, on the average, 50% of the data lies within this circle. CEP combined with CEP RMS gives an indication of the biases in the systems. If the system had no biases, the mean of the data set would be zero, and the CEP and CEP RMS circles would be identical. If a system bias exists, then the difference in the CEP and CEP RMS numbers give an indication of the bias. Figure 8 shows the difference in CAPTIDE and TDOP north-east position for the entire CC4 data set and depicts the total CEP and CEP RMS probability circles. The radius of this CEP circle was 1.44 feet with the origin located at -.929 feet east, -.119 feet north. The radius of the CEP RMS circle is 1.61 feet (origin at 0 feet east, 0 feet north). These values, as well as the SEP values, are reflected in the Table 3 totals.

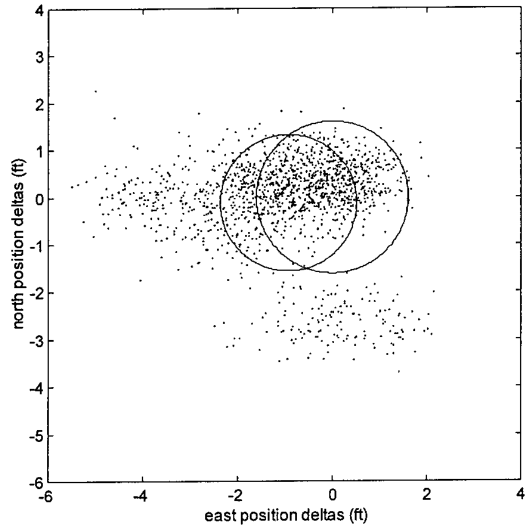

Figure 8 : Total CEP/CEP RMS Statistics

SEP and SEP RMS are similar to CEP and CEP RMS, but include the altitude channel as well. Table 3 contains the circular error probable (CEP) and spherical error probable (SEP) statistics for each of the valid CC4 data passes as well as the total for all data points.

Pass #	CEP	SEP	CEP RMS	SEP RMS
1	0.726	0.713	0.784	2.644
2	0.707	0.750	0.841	2.008
4	0.928	0.999	1.148	2.858
6	0.804	0.900	1.035	2.796
7	0.834	0.883	1.079	2.825
8	0.896	0.871	1.011	1.764
9	0.853	0.868	2.278	6.601
10	0.761	0.748	1.994	6.893
14	0.834	0.818	1.948	6.138
15	0.857	0.846	2.126	6.225
16	0.710	0.691	2.414	6.286
17	1.044	1.099	1.215	3.510
18	0.798	0.773	0.996	3.331
19	1.070	1.133	1.152	3.407
20	0.884	0.953	1.038	3.026
21	0.743	0.906	0.988	3.131
22	0.886	1.009	1.014	3.104
23	0.635	0.649	1.174	3.247
24	1.018	1.182	1.212	3.255
25	1.060	1.200	1.229	2.884
Total	1.442	2.450	1.607	4.292

Table 3 - CC4 TDOP/CAPTIDE Statistics (ft)

5.3 Captive Carry 6 (CC6)

The sixth EDGE captive carry mission (CC6) was designed to evaluate the guidance function and assess overall system performance of the EDGE test item. The aircraft flew trajectories on this mission which mimicked the EDGE weapon flight path of an actual weapon free-flight. The weapon impact angle terminal constraint dictated the weapon trajectory. Three different flight profiles were accomplished on this test flight as shown in Table 4.

POINT	ALT (ft)	MACH	REMARKS
1	30 K	0.80	88,000' simulated release, 14 deg at 5.92 nm, 46 deg at 2.30 nm, 15K' target altitude
2	25K	0.80	88,000' simulated release, 14 deg at 8.4 nm, 35 deg at 3.1 nm, 8K' target altitude
3	20 K	0.80	88,000' simulated release, 30 deg at 8.4 nm, then shallow out dive to pass over target at 10 deg, 5K' target altitude

Table 4 - Captive Carry 6 Flight Profiles

The first point was accomplished twice, the second point three times, and the fourth point four times. The first two points were designed to simulate a horizontal attack, or an attack against a bunker type target. For instance, on the first test point the aircraft ingressed at 30,000 feet altitude and 0.80 Mach. At 88,000 feet downrange from the target the EDGE weapon was (simulated) launched, the weapon acquired GPS satellites and began navigating without influence from the host aircraft. At 5.9 nautical miles downrange from the target, the host aircraft pitched over to 14 degrees nose low. At 2.3 nautical miles downrange from the target the host aircraft pitched over to 46 degrees nose low. The pilot then attempted to fly directly "through" the target located at 15,000 feet altitude, which was directly over an actual target on the ground. Similar actions were accomplished on points two and three.

Figure 9 illustrates typical dynamics encountered during this flight in the pitch, roll, and heading axes. CC6 provided an excellent opportunity to ascertain CAPTIDE performance under the dynamics expected for INS/GPS weapons.

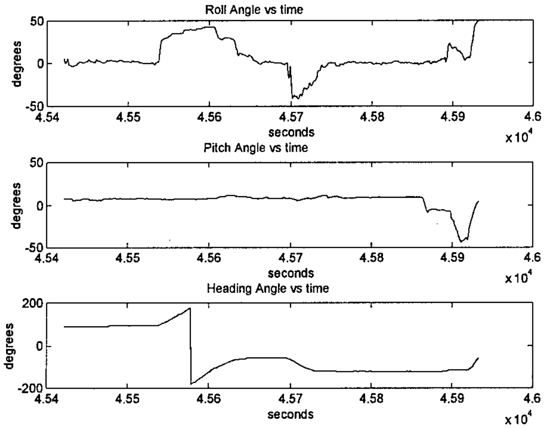

Figure 9 : CC6 pass 1 - Roll, pitch, and heading Vs time

As in the compatibility flight, TDOP data was not generated for comparison with CAPTIDE; therefore, the filter's radial sigma value is presented as an indication of CAPTIDE performance.

Figure 10 presents the radial sigmas and number of tracked satellites for a typical CC6 pass. Comparison of the CC6 (Figure 10, top plot) and CC4 (Figure 7, middle plot) radial sigma values indicates the uncertainty in the radial sigma value is higher for CC6 than it was for CC4. The aircraft banked up to and beyond 60 degrees a number of times during this mission, which resulted in loss of satellite track. The carrier phase integer ambiguities were not fixed at any point during CC6. This is likely the cause of the higher radial sigma values reported in CC6 with respect to CC4.

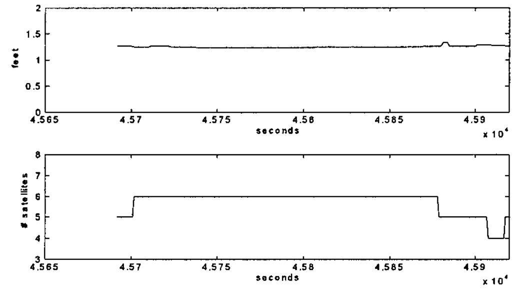

Figure 10 : CC6 pass 1 - Radial sigma (top plot), Number of satellites (bottom plot) Vs time

The position data from the CAPTIDE system helped to uncover a navigational issue in the EDGE test item. Comparison of CAPTIDE and EDGE position solutions helped to reveal a discrepancy in the EDGE navigation solution.

6.0 CONCLUSIONS AND RECOMMENDATIONS

The reported radial sigmas in CC1 at long baseline separation ranges could not be qualified. Truth source data of sufficient accuracy was not available to allow a reasonable assessment of the carrier phase position solution. Review of the receiver's filter sigmas and phase residuals, comparison with the available INS/DGPS TSPI pod information, and comparison with the EDGE test item showed the carrier phase solution was not completely erroneous; it agreed with the other navigation sources to within 5 meters. The test aircraft returned to the same location it left; the carrier phase solution showed this was the case. A more specific and controlled experiment is required to better qualify carrier phase performance at baseline separations greater than 15 miles.

CAPTIDE appeared to provide data as good as TDOP in the horizontal (north-east) plane. However, the vertical plane contained unresolved biases. If these vertical biases can be resolved, it appears a CAPTIDE type system can provide TDOP TSPI accuracy levels as long as the test item antenna can maintain line-of-sight to the GPS satellite vehicles.

CAPTIDE presented a viable and useful alternative to classical test range TSPI methods for this program. Position data from CAPTIDE was available within hours after the aircraft landed. The high accuracy TDOP data required the following processing: developed 17,000 feet of film, read each film frame with a data reader, processed the raw cinetheodilite data through a smoothing algorithm, integrated data from the cinetheodilites, FPS-16 radars, and aircraft to provide the final TDOP solution. This process, rushed, took 10 days. Data analysis and comparison of the CAPTIDE solution with other positioning instruments (EDGE weapons, TDOP, INS/DGPS TSPI pods, etc.) indicated the carrier phase data is of sufficient accuracy to score INS/DGPS type weapon systems. The cost of the carrier phase system for this type of application was also attractive.

The advantages of the CAPTIDE system included the following: fast data reduction time, accuracy, all weather capable, and it was not limited by the placement of range TSPI resources. The limitations of the CAPTIDE system included: requires power and space on board the test item, not currently suitable for aircraft control and vectoring purposes, and not currently suitable for flight safety purposes (flight termination system purposes).

7.0 REFERENCES

1. Wells, D., "Guide to GPS Positioning", Canadian GPS Associates, May 1987, Section 9.8, Carrier Phase Beat Ambiguity

2. Costabile, G., "Exploitation of Differential GPS for Guidance Enhancement (EDGE) Test and Evaluation Report", AFDTC-TR-95-031, August 1995
3. Freeman Mathematics Briefing, Aug 1994
4. Shi, J., Cannon, M.E.: "High Accuracy Airborne GPS Positioning: Testing, DataProcessing and Results", IEEE Position Location Navigation Symposium (PLANS), Las Vegas, NV, May 1994
5. AFDTC Technical Facilities, Vol II, "Land Test Areas", December 1991

Multifunction Millimetre Wave Radar for Future Military Navigation

M.Pirkl
H.J. Roschmann
F.J. Tospann
Airborne Systems Division
Daimler-Benz Aerospace AG
89070 Ulm, Germany

SUMMARY

The development of avionic systems for future military aircraft has to take into account the changes of modern scenarios to reach the highest degree of mission efficiency at an affordable budget. New strategic challenges, such as localised conflicts in out of area scenarios, demand a new set of functions for airborne radar, communications and EW technologies.

In *future military transport aircraft* or helicopters the crew must be assisted under bad weather conditions to solve specific operational problems. Several tasks, such as runway detection, landing, low level flight, ground mapping, and ground movement, have to be fulfilled. To provide independence from ground based or satellite systems an autonomous sensor environment will be of advantage. Also to unmanned aerial vehicles some of these functions can be applicated.

To provide these new functions an Enhanced Vision System is proposed. As the vision sensor of the EVS a millimetre-wave (mmW) radar is presented. The modern mmW radar technology is regarded as a mature approach for military use. The mmW radar operates in *Ka- band* around 35 GHz. A key component is the *frequency scanning antenna* that avoids mechanical rotation of the antenna unit. The FMCW radar technique is used due its performance advantages for military applications (LPI, ECCM). Additionally it uses pure semiconductor technology. The digital part of the radar consists of a modern scaleable signal and data processing unit. New software algorithms, including image processing techniques, present a radar image that bridges the gap between real beam airborne radar and SAR - technologies.

The functional requirements are discussed and result in system requirements. Thus the the proper type and design of an EVS sensor could be identified. The realized demonstrator with technical performances and test results is presented. The outlook shows future developement activities within the specific sensor technology.

LIST OF SYMBOLS

2-D	two dimensional
3-D	three dimensional
CAT	instrument approach category
CFAR	constant false alarm rate
CFIT	controlled flight into terrain
DGPS	differential global positioning system
ECCM	electronic counter counter measures
EVS	enhanced vision system
EW	early warning
FFT	fast Fourier transformation
FLIR	forward looking IR sensor
FMCW	frequency modulated continues wave
FSA	frequency scanning antenna
GPS	global positioning system
HDD	head down display
HGS	head-up guidance system
HUD	head-up display
ICAO	International Civil Aviation Organisation
IF	intermediate frequency
ILS	instrument landing system
INS	inertial navigation system
IR	infrared
LNA	low noise amplifier
LPI	low probability of intercept
MMI	man machine interface
mmW	millimetre wave
NavD	navigation display
NPA	non precision approach
PA	precision approach
RF	radio frequency
RVR	runway visual range
SAR	synthetic aperture radar
STC	sensitive time control
TA	terrain avoidance
TF	terrain following
UAV	unmanned airborne vehicles
VCO	voltage controlled oscillator

Paper presented at the AGARD MSP Symposium on "Technologies for Precision Air Strike Operations in Rapid-Reaction and Localised-Conflict Scenarios", held in Seville, Spain, from 16-19 October 1995, and published in CP-576.

1 INTRODUCTION

The present changes of the airforce's task, i.e. in localised conflict scenarios, demand both new strategies and thus new equipment to meet these new requirements. The air forces find new tasks in such conflicts due to their capabilities of reconnaissance and operations. Thus the airborne sensor equipment plays a key role in localised conflicts due to their abilities in navigation, reconnaissance, self protection and air strike support.

The particular navigation technology of aerial vehicles, such as military transport aircraft, has to cover new functions in an all weather environment:

- autonomous landing and take-off aid at unsupported airports (e.g. without ILS),
- autonomous ground movement with obstacle warning at such airfields (note that airfields could be very busy in out of area operations),
- ground mapping for navigation to assist the pilot in controlled flights into terrain (CFIT),
- ground mapping for correlation with terrain data bases,
- assistance in low level flight operations (TF, TA).

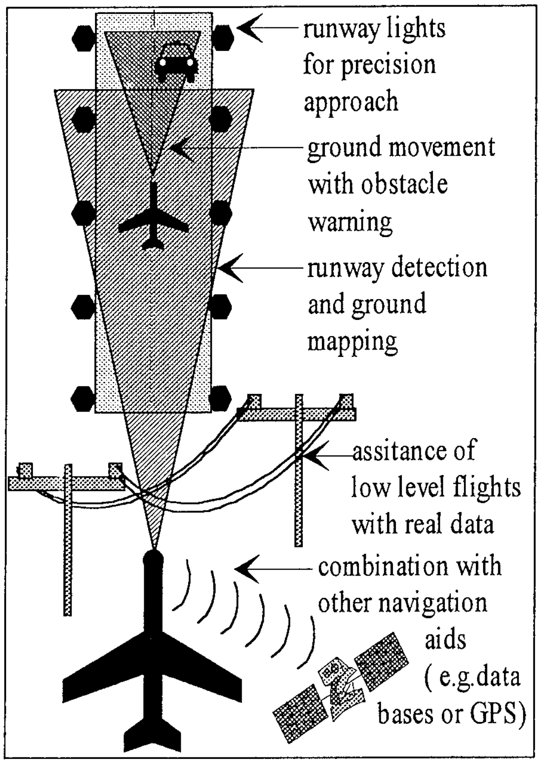
runway lights for precision approach
ground movement with obstacle warning
runway detection and ground mapping
assitance of low level flights with real data
combination with other navigation aids (e.g.data bases or GPS)

Fig. 1 : Some important functions for a military EVS - system

These functional requirements demand airborne forward-looking sensors with extended technical features:

- adverse weather operations (rain, fog, night)
- simple man machine interfaces
- support to other navigation systems, as GPS and databases
- high resolution scanning properties with low outer dimensions
- high information update rate, i.e. high scanning rates
- LPI and ECCM techniques
- HUD for airborne navigation (take off and landing)
- HDD or NavD (ground movement and ground mapping).

A well-established technique for fighter aircraft is the use of head-up displays (HUD) to reduce frequent turning of the head from the window to the instruments. Additionally this HUD does not suffer the adaptation of eyes [ref.1]

Also for civil flight operations a head-up guidance system (HGS) without forward looking sensors is an established equipment that enables ...

- precision approaches without autoland systems,
- reduced sight minimas for landing and take off,
- an optimized man machine interface.

A HGS is reality since a couple of years and assists crews in several commercial airlines [ref.2]. Until now, however, the extension to an EVS suffers the availability of appropriate forward looking sensors that have the following properties [ref.3]:

- electronic scanning with an information update rate > 10Hz
- field of view ± 15° azimuth, 24° elevation
- all weather capabilities
- affordable price.

There are two enhanced vision sensors, that are will be discussed here:

- FLIR
- mmW radar

Both sensors show their specific premises and drawbacks. Due to the weather penetration only a system with a mmW radar can be used [ref.4]. A combination of both sensors could give the best choice. Today FLIR sensors show a mature state of development and also the technology of mm-wave radars come up and can be installed into airborne systems with high performance and affordable prices.

A mmW radar is proposed with superior performance due to ...

- electronic scanning antenna,
- advantageous waveform,
- highly flexible processing architecture,

which are inevitable demands for an EVS radar.

In a first step a demonstrator was realized that confirms the system study and will fulfil the broad span of the needs mentioned above.

2 SYSTEM REQUIREMENTS

2.1 Weather requirements

In civil aviation the weather is classified in categories (CAT) which are listed below. This classification is widely used for the description of adverse weather conditions.

CAT	runway visual range	vertical sight	decision height
I	550m	60	60 m
II	350m	30	30 m
IIIa	200m	0	12 m
IIIb	125 (50)m	0	6 m
IIIc	0	0	0

Table 1: ICAO categories for all-weather operations

The weather classification for civil aviation will be applied to military aviation to discuss equal weather conditions. An EVS sensor should fulfil the requirements to enable an EVS for at least CAT Iia operation.

2.2 Range and azimuth coverage for EVS systems

low level flight:	5 km, 30°
ground mapping	5 km, 30°
takeoff and landing	3 km, 30°
ground movement:	1 km, 90°

2.3 Selecting the proper EVS sensors

In fighter radars the extraction of targets is one of the main features. For the mmW radar, however, the *imaging capabilities* are the essential drivers. So *doppler information is not required* from the sensor.

For evaluating the *range information* that is inevitable for functions such as correlation with data bases, ground mapping, and ground movement an *active sensor* (a radar), is necessary.

Due to the *all weather requirements* of this type of airborne sensor a *microwave radar* meets this demand. Note that the lower the operating frequency the better will be the weather behaviour and also the larger will be the size of the radar.

For *best resolution* in azimuth (or elevation if needed) at a given antenna aperture an *optical sensor* like FLIR or laser radar is superior. On the other hand it suffers the adverse weather conditions and thus could be used only as an additional sensor.

If *airborne obstacle warning* is essential in a high degree (TF operation), a *3-D radar* enables contour flights and even detects wires. In a similar way as mentioned above a microwave radar should be used for adverse weather conditions. On the other hand normally the flight path is known due to any reconnaissance activities or databases. So a *2-D radar* will give enough information to enable safe flight operations and is affordable for many applications, for example future military transport aircraft.

Collecting the facts above a *2-D mmW radar* is a good compromise between all these functions. There are two possible frequency ranges: around 35GHz and 94 GHz. The 94GHz range provides a better azimuth resolution. However, it suffers from radom problems and reduced weather penetration. Furthermore the technology is more mature at 35GHz. So the Ka-band range was chosen.

As already mentioned, the mmW radar may be **supported by a FLIR** to give an enhanced performance at night. The best results would be obtained with a well-balanced sensor fusion that will display the optimized data of both mmW radar and FLIR. For example at nightly approach under clear weather the FLIR is chosen due to its superior near field azimuth resolution. On the other hand for ground based obstacle warning or ground mapping mode the FLIR will not give substantial information. The USAF will go a similar way with the new Hercules 2 transport aircraft, where an EVS system with a combination of FLIR and mmW radar will be installed.

The proper *MMI* is a combination of a HUD and a head-down display (HDD) or navigation display (NavD) [ref.5]. For landing and takeoff a HUD will enable the crew to a very ergonomic working. For ground mapping or ground movement the HDD or NavD will be used.

2.4 Military Requirements on Forward Looking Sensors

2.4.1 Low probability of intercept (LPI)

For TF operation a forward looking active sensor is needed. On the other hand every active sensor can be detected. The system has the task to minimize this risk.

A *CW waveform* should be used to give the best LPI performance relative to a given range. Furthermore an intelligent *RF output power management* reduces the emitted power to the needed level. Thus the detection risk will be very low.

2.4.2 *Electronic counter counter measures (ECCM)*

To minimize the effects of electronic counter measures *spread spectrum* waveforms should be used forcing the interferer to use broadband techniques.

Another measure is *to reduce the intermediate and video bandwidths* within the frontend to the lowest values.

2.5 Sensor requirements for a 2-D mmW radar

2.5.1 *Waveform and frequency range*

As shown in 3.3, 2.4.1 and 2.4.2, a FMCW mmW radar provides the best compromise for an all weather imaging sensor.

2.5.2 *Antenna*

There are three different principles for the postulated electronic scanning:

- active phased array
- passive phased array
- frequency scanning antenna

The passive phased array cannot be used due to losses and price. The active phased array is not available within the next 5 - 10 years. Even after that period a reasonable price will not be achieved. So only the frequency scanning antenna (FSA) remains as the candidate for a future mmW airborne radar.

The beamwidths in azimuth should be less than 1° for a proper image of runways or obstacles. Azimuth weighting functions should enhance the image to a resolution of less than 0.3°.

Typical for airborne application is a reversed cosecans^2 shaped beamform in elevation that compensates elevation angle with distance [ref.6]. For ground movement it cannot be used. In pulsed radars a sensitive time control (STC) is used that cannot applied to FMCW radars. A simple highpass following the analogue part of the receiver shows a very similar performance.

2.5.3 *Frontend*

For a CW radar pure semiconductor technology should be used. The available output power of 1W is sufficient for these applications. Because no STC can be used, the complete range and target dynamics have to pass the receiver during ground operation. To reduce harmonic and intermodulation signals a high dynamic range within the receiver is required.

2.5.4 *Signal and Data Processing*

One of the main task within the processing is the FFT - calculation. So a special designed FFT - board is advantageous for an FMCW radar. To integrate all the radar and image processing techniques a high performance processor architecture should be used.

2.6 Comparision of different sensor types

In table 2 several sensor types are surveyed, a 2-D mmW radar (2-D) a 3-D mmW radar (3-D) a Laser radar (Las) and a FLIR (FL). Five quality categories are used: --, -, 0, +, ++. Note that all weather capability is very important.

Parameter / Sensor	2-D	3-D	Las	FL
ground mapping	++	++	-	-
terrain avoidance	+	++	0	-
terrain following	0	++	--	-
airborne obstacle warning	0	+	+	--
ground movement	++	++	0	-
correlation with data base	+	+	-	+
landing aid	++	++	-	-
Cat I approach to non-supported airports	++	++	--	-
weather penetration	+	++	-	-
LPI	+	+	+	++
ECCM	+	+	+	++
maximum range	+	+	-	-
range resolution near field	+	+	+	-
range resolution far field	+	+	+	--
azimuth resolution	0	0	++	++
required processing power	0	-	-	+
aircraft integration	0	-	-	+
cost	+	0	0	+

Table 2: Comparison of different sensor types

3 OPERATIONAL BENEFITS

3.1 General Benefits using an EVS

According to sudies of Flight Safety Foundation an important reason to introduce a HGS is safety. Note, that about 31% of all the aircraft accidents between 1959 and 1989 could or might have been prevented by using this technology. So even in a military aircraft the *security level of crew and aircraft* would improve with HGS during conventional flight operations.

More flights could be done with an EVS equipped aircraft due to the ability of bad weather penetration. So the availability of the fleet becomes more independent of weather conditions. This could be a feature essential for rapid reaction forces.

Deviations from the mission plan can be avoided using an EVS, e.g. landing on another airport with better weather conditions.

An *EVS is also compatible to civil airports*, where a mission could start or end. Without use of autoland facilities the aircraft can land in all weather categories that are permitted at the airport.

3.2 Landing aid

3.2.1 General

The weather conditions for approaches (i.e. runway visual range and decision height, see above) characterize the landing problems of aircraft. Several technologies, such as ILS, MLS or DGPS, are used to enhance the number of flights in adverse weather conditions. They all need additionally ground based equipment.

A large number of airports can be used with an EVS for a nonprecision approach and possibly for a precision approach in adverse weather condition down to Cat I. For Cat IIIb landing conditions (6m decision height, 50m RVR), however, precision approach regulation must be applicated.

3.2.2 Approach to Supported Airports

If there is any Cat I precision approach (PA) technology available a HGS equipped aircraft can use this help. The PA data (for example ILS) will be written into the HUD and the pilot can use this data for approach down to the decision height, even without autoland facilities. This is a certified procedure [ref.7]. With an additional EVS sensor the minima can be lowered. So a Cat IIIb approach is possible at a Cat I airport.

3.2.3 Approach to Not Supported Airports

For non supported airports - which can be typical for crisis reaction forces - a new procedure is proposed [ref.8], which easily makes Cat IIIb precision approaches available.

Along the runway a certain number of reflectors, for example corner reflectors, will be installed in a definite way. They are very robust, inexpensive, easy to install and do not need any maintenance. A quite good number is 12 reflectors, at each side of the runway 6, with a distance of about 200m. The centre of the line between the first two reflectors seen from the landing aircraft represents the touch down point.

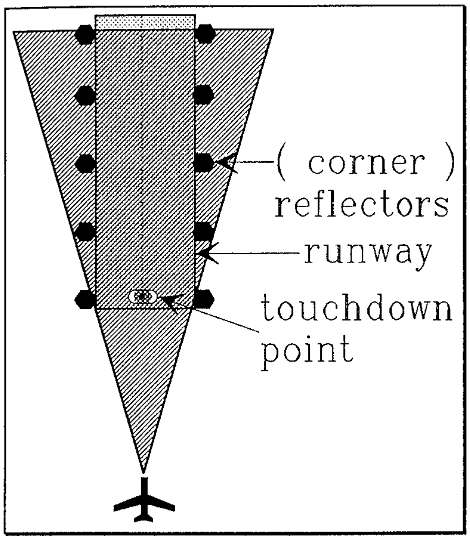

Fig. 2: procedure for a new approach guidance

With a radar such as the proposed mmW radar these reflectors can be detected and tracked during the approach by a Kalman tracker. The known distribution of the reflectors is used for calculating the 3-D aircraft coordinates (x, y, z) relative to the touch down point. So the pilot or the autoland system can evaluate the actual state compared to the computed state hence and control the aircraft.

The simulation of this procedure shows surprising accuracies that can be achieved only with high performance DGPS systems:

distance/accuracies	**Δx / m**	**Δy / m**	**Δz / m**
2500m	< 0.25	< 1.5	< 4.5
1250m	< 0.2	< 1.0	< 2.25
0	< 0.1	< 0.1	< 0.3

Table 3: accuracies with new guided approach

This landing aid can be always available and is not dependent on sophisticated landing aids such as GPS or ILS system. According to the accuracy table above Cat IIIb approaches can be obtained by an EVS equipped aircraft on airports without any installations.

4 REALIZED MMW RADAR DEMONSTRATOR WITH FREQUENCY SCANNING ANTENNA

A ground based demonstrator was realized to evaluate the system study and the critical components.

4.1 Building Blocks

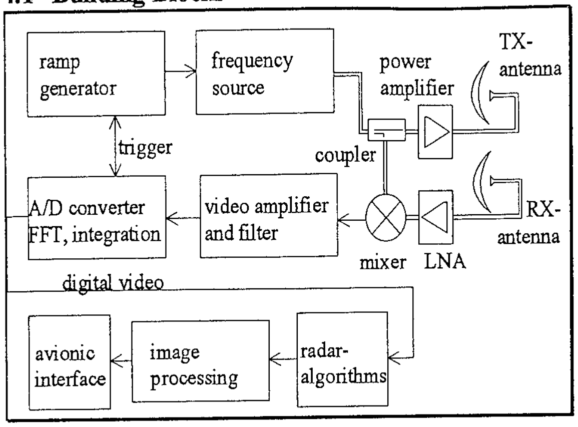

Fig. 3: simplified block diagram of the radar

Since a high degree of TX-RX isolation is required two antennas are used. For optimum performance the low noise amplifier (LNA) and the power amplifier are mounted close to the antenna.

The power amplifier is a custom made circuit with four parallel working amplifier chips with MESFET devices and enables an output power of 1.2W. The cascade of LNA, mixer and receiver shows a noise figure of 3.5 dB.

After the video amplifier and A/D conversion the signal is processed by FFTs and is fed to an integration algorithm that smoothes the image considerably. Radar algorithms, such as CFAR and azimuth weighting, will be used to extract the required information. Image processing techniques, such as denoising and edge extraction, gives additional performance to the operator.

4.2 Frequency Scanning Antenna

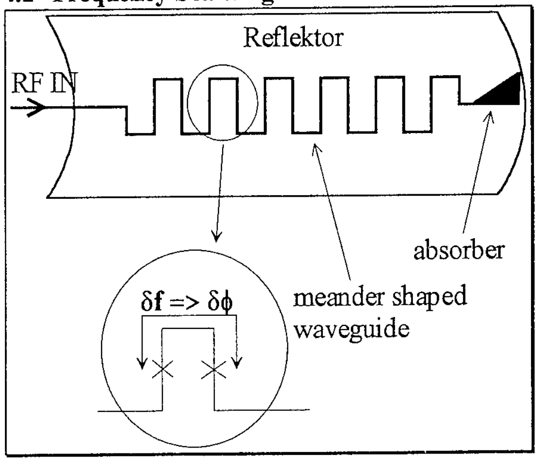

Fig. 4: frequency scanning antenna

The frequency scanning antenna [ref.6] is the key element of this sensor. It consists of a feed, an absorber, and a reflector that enables the elevation shape. The feed consists of a meander shaped waveguide with radiating slots in every branch. The frequency change df is transformed in a phase change dϕ between two radiating slots. This results in a frequency scanning of the beam. The design of the slots enables the proper beamforming. It is a challenging task to get to a minimum loss and low sidelobe levels.

The realised antenna covers 41° within a 1.8GHz sweep and has a 1.2° azimuth beamwidth (one way) at a -30dB sidelobe level. The antenna loss is 2dB as the result of a 7m meander waveguide, which only could be reached by using compensated corners within the meander line. The dimension of a single antenna aperture including reflector is 70 • 15 • 15 cm^3. Two antennas of this size can be integrated even in small aircrafts such as Dornier 328, which is a 30 seat turboprop.

4.3 Combing FSA and FMCW Principles

Both principles need a frequency sawtooth ramp, the FMCW for the ranging and the FSA for azimuth scanning. It is an easy task to combine both demands in only one frequency scan (frequency sweep Df within frame time Dt) and take portions (df, dt) for FFT analysis.

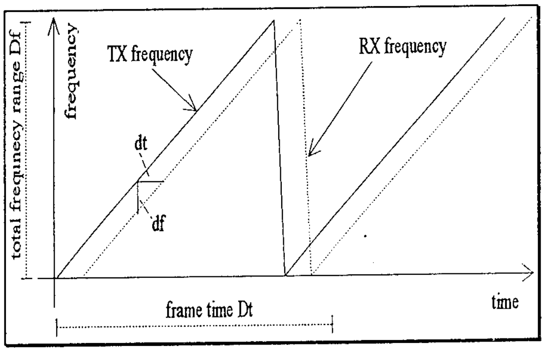

Fig. 5: waveform

So in one frequency scan the antenna covers the azimuth coverage and enables a sufficient number of FFTs for ranging (e.g. the number of hits).

Using this waveform a frequency source can be used achieving a reasonable price. Moreover it is a spread spectrum technique, because the received information is distributed over a large frequency span. Additionally the frequency changes if the interceptor is not in centreline with the flight path that makes a small-band interference impossible.

4.4 Frequency source

There are two design drivers for a frequency source for this radar:

- high linearity of the sweep
- low noise frequency generation

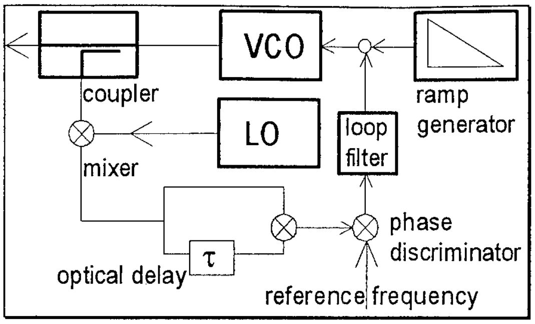

Fig. 6: frequency generator with high linearity

The VCO is a low noise broadband Gunn - oscillator with varactor tuning. The linearizer circuit within this frequency generator includes a downconverter (LO + mixer) and an optical delay line. This delay line consists of a 1200m optical fibre. The delayed and undelayed signals are mixed and give a frequency proportional to the frequency slope of the generator. Stabilised with a reference frequency a linearity of better than 0.0001 is achieved.

4.5 Signal and Data Processing

A flexible processor technique, developed especially for airborne radars, is used.

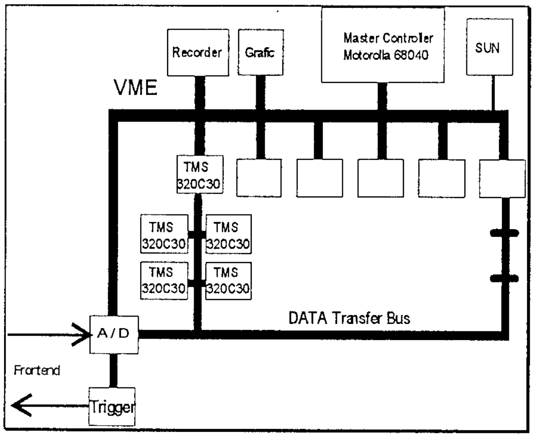

Fig. 7: processor architecture for demonstrator

It consists of a certain number of processing elements and it is scaleable up to 32. Every processing element consists of one master processor (TMS320C30 of TI) and 4 slave processors. The processing elements communicate via a high speed data transfer bus. So a computing power of up to 6 GFlops can be achieved which is more than sufficient for all these tasks. In typical applications a 68000 master controller will be used. For an enhanced vision system 6 processing elements are needed. For both demonstration tasks and documentation a recording unit is used with a magneto optical disk. Instead of the avionic interface a simple VGA monitor is used for the demonstrations.

An information update rate of 16Hz is realized. That meets the requirements for an airborne radar.

At the end of the year a special designed board will be available that is optimized for FFT processing. This FFT - board will replace 4 processing elements for the specific task.

4.6 Software

Following the well-known FFT *a sliding integration* is used that smoothes the picture considerably. Weighted by a factor among 0.5 and 5 the last image will be added to the new one.

A *weighting algorithm* is used to enhance the azimuth resolution. It determines the centre of gravity of all the hits per target. So the image can be sharpened by a factor of 5.

A special designed *area CFAR* - normally used to optimize target behaviour - is successfully applied to this radar. To detect obstacles on the runway and to denoise the image it is a very helpful tool.

There are several *image processing algorithms* that can be applied to the radar image. *Edges*, for example the borderlines between grass and runway, can be *extracted* to prepare additional information. A *Hough transformation* will be applied for drawing lines between runway lights or reflections from wires. For further denoising the radar image a spatial *wavelet transform* can be used. Both techniques will be developed until the end of the year and applied to the mmW radar.

It is a complex task to integrate *classification* techniques. One can define a variety of different classes for the radar image, e.g. grass, forest, runway, wires and so on, and apply artificial intelligence operations to the image. The first research results are promising and give hope for a future realization of this package. Obviously a large amount of computing power will be necessary additionally to implement these procedures into a real time system.

Since the radar delivers data in amplitude and range over angle they must be transformed into azimuth over elevation coordinates for the HUD. It needs a substantial amount of computing power and thus must be computed by signal processors.

4.7 Technical Data of the Realised 2-D Demonstrator

principle of operation	**2-D FMCW radar with FSA**
centre frequency	Ka - Band
total RF bandwidth	1.8 GHz
video bandwidth	600 kHz
RF output power	0.5 W
noise figure	3.5 dB + antenna loss
polarisation	horizontal
azimuth beamwidth	1.2° one way
vertical beamwidth	24° inverted cosec^2 characteristic
polarization	horizontal linear
az. field of view	41°
range resolution	6.5 m
information update rate	16 Hz
maximum displayed range	3.5 km
detection range of a person	> 5 km
weight antenna+ frontend	10 kg *
weight processor	10 kg *
size antenna + frontend	$70 * 50 * 30\ \text{cm}^{3*}$
size processor	$50 * 40 * 40\ \text{cm}^{3*}$

* = target value

4.8 Military Properties

4.8.1 Electronic Support Measures

The ESM ranges, where the radar could be detected will be calculated by

$$\boxed{R_{esm} = \sqrt{\frac{P \cdot G \cdot \lambda^2}{(4 \cdot \pi)^2} \cdot \frac{1}{MDS}}}.$$

Equ. 1: ESM range

(radiated power P, antenna gain G = 31dB, wavelength λ = 8.5mm). The minimum detectable signal (MDS) for a broadband ESM receiver is

- for a simple ESM receiver -40 dBm
- for a standard ESM receiver -60 dBm
- for a high performance receiver -80 dBm

P	simple ESM RX	standard ESM RX	high perf ESM RX	radar range vs. 1m^2
.1	23m	230m	2.3km	6.9km
.5	52m	520m	5.2km	10km

Table 4: ESM ranges for different ESM receiver and radar range against a 1m^2 target

It can be observed that the radar range for small targets (a person shows an RCS of about 0.1 - 1 m^2) is higher than the ESM range. This is a major advantage of an FMCW radar. Furthermore at the moment ESM receivers are not available for mmW signals. Note that atmospheric problems that are not included into the ESM equation would further reduce the ESM range. Thus the radar could be assigned as a *very quiet sensor*.

4.8.2 Interference

If the jammer is located 1km away from the radar the following interference powers are necessary:

Type of interference	radar detection of interferer	complete interference
interference power of antenna mainlobe	-12 dBm	63dBm
interference power of antenna sidelobes	18 dBm	93dBm

Table 5: required interferer level against mmW radar for 1 km distance between radar and jammer

A sidelobe level of -30dB is achieved and is used for the calculations. The mainlobe could be interfered by a selective interferer; however, the probability of interference is very low. In this case only one azimuth cell will be disturbed. For interfering the sidelobes a broadband interferer must be used with an extended output power. This will not be available within the next couple of years.

So the necessary interference levels are so high that an interference seems to be very unlikely.

5 TEST OF DEMONSTRATOR

The demonstrator was tested at some ground based scenarios:

5.1 Test at Airports

To study behaviour of taxiways, runways and obstacles the demonstrator was tested at small and large airports in southern Germany during fall, winter and spring. The contrast between grass and runway is always good and hence the runway can be easily identified. Furthermore if runway lights are available they additionally can be taken for the identification.

5.2 Test at Sea

To study behaviour of seaclutter and landclutter, tests were made at lighthouses. The area CFAR mechanisms were very impressive and could be optimized for different scenarios. Small and big vessels could be identified in strong seaclutter and even the number of masts or other topics could be evaluated.

5.3 Test with Wires

At mmW frequencies the world is similar to the optical world only if the object dimensions are larger than some 10cm. However, if object dimensions are close to the sensor wavelength (diameter <1cm, such as thin wires), the world dramatically changes. An optical view of a long wire turns at mmW frequencies to a set of minima and maxima that depend on the wavelength, the diameter of the wire and the type of wire [ref.9]. To receive a confident reflection of the wires the radar has to detect even these minima. With the mmW radar the sensitivity was sufficient to detect these minima.

6 OUTLOOK

6.1 3-D Radar

For helicopter applications a 3-D radar was studied that gives enhanced performance for the following functions:

- terrain avoidance
- terrain following
- airborne obstacle warning
- weather penetration

6.2 Image Processing

Due to the high information update rate image-processing techniques as mentioned above can be implemented to the radar data. This is a new technology that until now was reserved to optical images. But with an imaging radar this technology comes into new platforms and there will be done a many research activities

6.3 mmW Technology

To reduce the size of the radar by 50% a reflected power canceller will be developed that enables the radar to use transmit and receive functions with only one antenna. This technology is proven in X-band applications [ref.10].

7 CONCLUSION

A radar is presented, that bridges the gap between conventional radars and SAR technology. The technical key features of the FMCW mmW radar are the frequency scanning antenna and the flexible signal processor.

This radar supports an EVS that provides new functions for military aircraft, especially landing, takeoff aid, and ground movement at adverse weather conditions. Additionally this radar enables a new procedure for complete autonomous landing aid down to CAT IIIb conditions. Advanced military properties (LPI and ECCM) assist these functions and give an important self protection to the aircraft.

The system was studied deeply, verified in a ground based demonstrator, and tested at typical scenarios. The radar is regarded as an advantageous sensor for new military aircraft.

8 ACKNOLEDGEMENTS

The authors would like to thank T.G. Liem, Dr.K.Solbach, Dr.W.Gruener, S.Smith, and A.Brokmeier, for substantial contributions and discussions to that project.

9 REFERENCES

1. N.N., "Designers Target the One - Screen Display", Interavia Aerospace Review, February 1991, pp 45
2. Sweetman, B., "Out of the Fog", Air Transport World, March 1995, Reprint, Penton Publishing Inc.
3. Helgeson, M. et al., "Diplay Processing for a Synthetic Vision System (SVS) Utilizing the VME Environment, 1992 IEEE - AES Symposium, pp. 532 - 537
4. M.Burgess & D.Hayes, "Syntetic Vision - A View In the Fog", IEEE AES Systems Magazine, March 1993, pp. 6 - 13
5. H.Moeller, "Synthetic Vision for Enhancing Poor Visibility Flight Operations", IEEE - AES Systems Magazine, March 1994, pp. 27 - 33
6. M.I.Skolnik, "Introduction to Radar Systems", New York, McGraw Hill Book Company, 1962, p.60, pp 311 - 312
7. P.Proctor, "HGS offers Airlines Safety Economic Edge", Reprint of Aviation Week and Space Technology, December 12/19 1994
8. F.J.Tospann, W.Grüner, "Verfahren zur Landehilfe für ein Flugzeug", German Application Note # 195.13.440.0
9. H.H.Al-Khatib, "Laser and Millimeter-wave Backscatter of Transmission Cables", SPIE Proceedings, Vol.300 Physics and Technology of Coherent Infrared Radar, 1981, pp. 212 - 229
10. P.D.L.Beasley et al., "Solving the Problems of a Single Antenna Frequency Modulated FMCW Radar", IEEE International Conference, 1990, pp. 391 - 395

FRIEND IDENTIFICATION BY IR PICTURES ON HELMET MOUNTED DISPLAYS

G. Balzarotti, L. Fiori, B. Midollini

FIAR S.p.A.
Via G.B. Grassi, 93 -20257 Milano - Italia

SUMMARY

In certain operational scenarios -such as peace operations in localised but high density conflict areas- pictures generated by performant infrared sensors and appropriately processed can be considered and highly desirable for *friend identification.* Nevertheless in these circumstances the situation requires an adequate man-machine-interface to allow an operationally effective and rapid use by the Pilot that could now be offered by high performant integrated helmet mounted sights.

This paper wishes to outline and analyse the aspects of visual identification of known objects as they are seen by a thermal imager and displayed on the visor of a helmet.

The problem of the magnification as well as the reduction of the contrast due to the ambient light are evaluated.

An analysis of the *performance prediction* is carried out with the aim to tentatively give a theoretic answer to "Can the identification via IR pictures on Helmet Mounted Displays be really effective?".

1. INTRODUCTION

The visualisation of infrared images onto the visor of Helmet Mounted Displays (HMDs), for both navigation and tactical operation, is one of the most recent and promising applications of optronics systems in the military field: thermal cameras with steerable Line of Sight (LOS) and advanced HMDs are nowadays basic elements of the avionics in both fixed and rotary winged modern aircraft.

An accurate visualisation of the IR image can support the pilot during navigation in adverse conditions, providing also important information about ground threats, otherwise not detectable by naked eye or by other sensors.

However, if on one side HMDs for navigation purposes present indisputable benefits, on the other hand the use of such devices for ground targets recognition and identification could give rise to some perplexity about their true effectiveness, especially when compared to traditional Head Down Displays (HDD).

In the initial phase of defining the characteristics of the equipment to be used for this specific function, one of the problems to face is the performance prediction, necessary to evaluate the system potentiality. Even if for IR imaging systems traditional methods are broadly accepted, allowing to estimate equipment characteristics and to perform their comparison, in this case some of the parameters must be properly redefined. The use of a virtual display for IR video presentation must be considered and defined with great care if reliable results are sought. A dedicated analysis should also be devoted to the case when *objects* to be analysed are *limited in number* and *well known* to the operator.

The factors that have an impact on performance will be analysed in this paper and, for some of them, an estimation of weight will be made by implementing a dedicated test.

2. PERFORMANCE PREDICTION METHODS

Before entering a detailed analysis, we would like to briefly summarise the main guidelines of the most common method used for performance evaluation, i.e. the IR Static Performance Prediction Method [1,2,3].

Such method is based on the evaluation of the Minimum Resolvable Temperature Difference

Paper presented at the AGARD MSP Symposium on "Technologies for Precision Air Strike Operations in Rapid-Reaction and Localised-Conflict Scenarios", held in Seville, Spain, from 16-19 October 1995, and published in CP-576.

(MRTD) of the imaging system and on the criteria that the recognition and identification are linked to the number of lines or pixels resolvable on the target.

The MRTD considers the characteristics of the system spatial resolution and the sensitivity to the radiation, together with the human factors of visual sensitivity. Resolution is included by the Modulation Transfer Function (MTF) of all the elements of the visual chain, starting from the thermal camera optics, up to the human eye. For particularly high resolution systems the MTF of the atmosphere[4] and of the local air turbulence must be included too, in order not to underestimate the effects of image decorrelation.

The camera sensitivity to the IR radiation is included in the Noise Equivalent Temperature Difference (NETD) parameter, which allows to synthesise in one number the noise, the sensitivity and the signal losses. The eye integration time and contrast sensitivity are also taken into account by the MRTD parameter.

The evaluation of the MRTD function has been automated by procedures and modelling[5] of all the elements of the visual chain, in order to create a common basis for the apparatus assessment. Having correctly evaluated the elements of the chain, the MRTD easily provides the minimum resolvable temperature as a function of the spatial frequency of a sequence of lines (bars) when these are converted into video signal.

The visual range is then evaluated considering that for recognition the target must have a dimension on the display sufficient to include at least 3-4 cycles, and that the target-background temperature difference (attenuated by the atmosphere) must be equivalent to the value of the MRTD for the relative spatial frequency. The same approach is used for identification range, considering in this case that at least 6 cycles on the target are necessary.

The method allows a quick evaluation of the performance (even with some limits, see as an example reference 1) for the whole range of equivalence temperature variation - radiance variation.

3. HYPOTHESIS AND PARAMETERS

On the basis of the static performance evaluation method previously described, we have analysed the FLIR-HMD system in order to suitably tune the parameters. The analysis has been focused on the characteristics of the configuration schematically shown in Figure 1.

It is not task of this work to analyse the characteristics of existing systems, thus the FLIR and HMD used have been considered as *ideal* or, better, *well performing*. In other words, we have assumed that the available technologies provide the predicted performance (e.g. the FLIR has a good detector responsivity correction and the HMD has a constant performance on the whole display).

4. MODELLING

In the prediction model it is necessary to consider the human eye with all its characteristics and limitations. The eye MTF model is usually represented by the expression:

$$(1) \qquad \mathrm{MTF}_{\mathrm{eye}} = e^{-\frac{\left(\mathrm{Ln}\left(\frac{r}{r_c}\right)\right)^2}{2\sigma^2}}$$

where: r is the spatial frequency and r_c, the spatial frequency at which the MTF presents the maximum value, is function of the display luminance as follows:

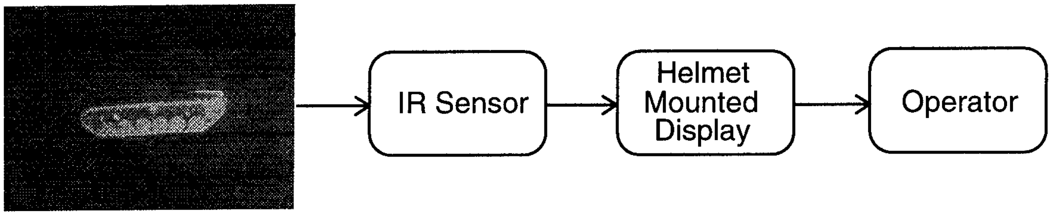

Figure 1. The FLIR-HMD system.
The main elements to be considered for performance evaluation are shown

$$r_c = 0.055 \cdot \mathrm{Log}(\text{display luminance}) + 0.14$$

The correct formulation of the transfer function is certainly one of the hardest tasks, due to the parameters variability and the different usable test methods[6]. Furthermore, equation (1) is appropriate to be applied in the case of traditional displays, i.e. for:

near vision (display distance: 40-80 cm);
biocular vision;
white light sensitivity.

In the case of virtual displays the image is focused at infinity, so the MTF should be characterised for *remote vision*. That is not obviously equivalent to the angle scaling normalisation performed on the parameters to take into account the different eye-display distances: in this case a true variation of the resolution capability of the eye, due to the *accommodation*, is involved.

Visual acuity varies with the distance from the object: roughly, it increases when the distance goes from 20 cm to 1m and decreases again thereafter[7]. Visual acuity is constant for distances from 4 m to infinity if the ambient light is greater than 200 lux.

Biocular visual acuity is generally higher than that of each eye[7]: such result is probably due to the image interpretation performed by the brain. Current HMDs usually allow biocular image presentation, but monocular or partially biocular HMDs are still in use. Furthermore, there are thesis showing that presentations of image on one eye and symbols on the other might be beneficial in terms of pilot's workload. Thus, in all cases where the IR image is not presented to both eyes, we will have to refer to the monocular visual acuity.

Also, MTF evaluation is based on white light vision. Due to technological reasons and to problems of reproducibility, displays for HMDs use, on the contrary, yellow-green phosphors CRTs: high efficiency P43 and P53 phosphors are generally employed in order to obtain a high luminance, particularly for symbology presentation during day operations.

With a normal luminance value, the visual acuity is maximum in the hot region of the light spectrum (red or yellow) and decreases towards the blue light. White light, on the other hand, is the most comfortable.

The P43 phosphor presents an equivalent wavelength of about 540 nm and spectral band of about 10-15 nm[8] for the main emission peak. The peak of P53 is at 544 nm and the spectral band is of 20 nm.

The small bandwidth might have also a negative influence on the visual acuity: components too much localised might, in fact, handicap the capability of correct focusing especially when operator is required to alternate focus for cockpit management[9].

The above can be summarised as shown in Table 1.

The total difference between vision with virtual displays in binocular mode and vision with traditional ones has been estimated as -2/10 (Snellen fraction) in the metric scale.

Such difference has to be introduced in the expression (1) of MTF_{eye} by decreasing the critical frequency r_c. For a monocular case a further loss (-0.5/10, -1/10 depending on conditions) should be included.

Other factors which have an impact on visual acuity are: object and ambient illuminance, contrast, observation time, mean of display (reflection, transparency), operator's workload. Such factors, which obviously have an impact also on vision with traditional displays, must be carefully evaluated for the specific application.

For continuing the analysis we had to make some assumptions on the system configuration: the evaluation of the display readability has been

DIFFERENCE	VISUAL EFFECT
near/remote vision	perceivable
monocular/binocular vision	perceivable
monochromatic/white light	just perceivable
monochromatic bandwidth	just perceivable

Table 1.

therefore performed considering as a reference a HMD equipped with P43 high luminance phosphors CRTs, able to present in raster mode over 3000 nit peak value.

Since the HMD is a transparency display, the characteristics of ambient illuminance have a strong impact on performance: we assumed to range from sunny day to dark night. The scene reflectivity has been set for fields and forest background with maximum reflectivity of 0.5. For the luminance which reaches the pilot, we have considered to include both ambient light, as perceived through the visor in a 60 degrees radius eye's field of view, and the component produced by the CRT.

The eyes luminance threshold has been computed by the following formula (LJND = Luminance Just Noticeable Difference):

$$\mathrm{LJND} = \frac{\mathrm{Log(contrast\ ratio)}}{0.0051} RCS$$

where:

$$\text{luminance contrast ratio} = \frac{\text{foreground luminance}}{\text{background luminance}}$$

The unitary LJND specifies the luminance contrast ratio necessary to detect a small object in a short excursion search time, when the mean scene luminance level is 10000 nit. At such luminance the eye threshold level is 0.0051. For other luminance values, the formula is corrected by the CIE factors of Relative Contrast Sensitivity (RCS). Some values are reported in Table 2 for reference.

With scene illuminance from 100 to 1000 lux, typical of an overcast day, we obtain good operative conditions: the contrast ratio ranges from 5 to 35 and 40-50 grey levels are perceptible.

LUMINANCE (cd/m^2)	RCS VALUE
10 000	1.00
1 000	0.83
100	0.62
10	0.36

Table 2.

When the ambient light is below 100 lux, i.e. for operation during twilight and night, it is necessary to increase the display background luminance, to the detriment of contrast: in fact, if background goes below the visible threshold and the signal stays at a high level of luminosity, it is possible to have a loss in performance with difficulty in focusing the image (empty field myopia phenomenon). The maximum contrast ratio considered acceptable has been 30-35; after such value the background has been increased in order to maintain the mean luminance at a level sufficient not to penalise the eye sensitivity threshold level.

With ambient illuminance of 10 lux the use of 10-20% of luminance available from the display as uniform background allows to maintain the image contrast ratio at optimal levels (8-10) while keeping the RCS value over 0.6, hence providing an almost complete grey scale.

Over 1000 lux the contrast ratio drops below the minimum acceptable level (3-4) and at 10000 lux the number of perceivable contrast levels (about 10) is no longer sufficient even if, in that case, eye threshold reaches the minimum level. In this condition it is necessary to insert a dark visor with transparency of the order of 10-20%. Table 3 summarises the hypothesis.

For a more accurate evaluation of the readability of the picture, the visual capability to

CONDITION	SCENE ILLUMINANCE	HYPOTHESIS
full day light	> 2000 lux	use of dark visor transmission: 10-20%
cloudy sky	100-2000 lux	use of clear visor use of full display contrast dynamics
twilight and night	< 100 lux	clear visor decrease of video dynamics to create a luminance offset

Table 3.

discriminate different colours should also be taken into account. In our case we have to distinguish between P43 phosphors yellow-green signal with the spectrum suitably weighted with the optical characteristics of visors and background.

The colour discriminating capability of the eye could be numerically evaluated by the Chromatic Just Noticeable Difference (CJND):

$$\mathrm{CJND} = \frac{\text{chromatic shift}}{0.0042} \cdot \mathrm{RCS}$$

where the *chromatic shift* is evaluated as the *distance* between the colours "true signal" and "background" in the CIE 1976 coordinates. The mean square of LJND and CJND provides the value of the Perceived Just Noticeable Difference (PJND), which represents a more exhaustive measure of the readability, taking into account not only the luminosity difference but also the chromatic one.

Usually the chromatic perception is significant: considering only the LJND is thus a pessimistic evaluation. In our analysis, having examined specifically the use of HMDs in air to ground applications and due to the great variety of background colours involved, we have chosen not to consider the chromatic variation.

Moreover, we must remind that the relations shown among LJND, CJND and PJND represent a considerable simplification of the psycho-physical processes connected to vision and their accuracy decreases in case of great contrast variations or significant chromatic differences.

Eye-display characteristics are now defined and we can run the usual algorithm for Static Performance Prediction making some assumptions on IR sensor parameters. The data are summarised here below.

OPTICS	
Horizontal Field of View [deg]	30
Vertical Field of View [deg]	30
Optics Diameter [mm]	11
Optics Transmission	0.8
Wavelength of MTF computation [µm]	9

IMAGE FORMATION	
Frame Rate [Hz]	25
Scan Efficiency	0.75
Number of Scanned (Sampled) Lines	576

DETECTORS	
Number of Parallel (Scanning) Detectors	288
Number of Serial Detectors (TDI)	4

DISPLAY	
Type of Display	CRT
View Angle [deg]	30
Magnification	1
Spot Size [mrad]	0.6

TARGET SIZE	
Horizontal Target Size [m]	3.5
Vertical Target Size [m]	3.5

CRITERIA FOR RECOGNITION	
Δt of target [K]	2
Number of Line Pairs for Probability=50%	3

CRITERIA FOR IDENTIFICATION	
Δt of target [K]	2
Number of Line Pairs for Probability=50%	6

ATMOSPHERE	
Extinction Coefficient σ_1 [km^{-1}]	0.2
Extinction Coefficient σ_2 [km^{-1}]	1

The evaluation has been performed considering first a traditional display, and then introducing the penalising factors relevant to virtual displays. The Field of View used is compatible with the purpose of navigation, and a unitary magnification has been considered in order to be able to overlap the IR image with the real scene.

The results, presented Table 4, show a very little difference in range for the two cases. This demonstrates that the virtual displays do not penalise recognition and identification performance. The actual limitation should be found in the limit resolution achievable with wide field of views.

To this purpose, we have had a new run of the program supposing to operate with detector and display suitable for doubling the system resolution, keeping however the 30° Field of View and the unitary magnification.

The results are shown in Table 5: also in this case the impact on range induced by virtual displays is very limited.

The next step has been to investigate the possibility of having a magnification, giving up the hypothesis of overlay.

		RANGE [m]	
		$\sigma_1 = 0.2\ \text{km}^{-1}$	$\sigma_2 = 1\ \text{km}^{-1}$
RECOGNITION	**Real Display**	625	617
	HMD	600	578
IDENTIFICATION	**Real Display**	310	309
	HMD	296	290

Table 4.

		RANGE [m]	
		$\sigma_1 = 0.2\ \text{km}^{-1}$	$\sigma_2 = 1\ \text{km}^{-1}$
RECOGNITION	**Real Display**	1232	1145
	HMD	1110	1027
IDENTIFICATION	**Real Display**	610	587
	HMD	547	526

Table 5.

		RANGE [m]	
		$\sigma_1 = 0.2\ \text{km}^{-1}$	$\sigma_2 = 1\ \text{km}^{-1}$
RECOGNITION	**Real Display**	2501	2154
	HMD	2301	1973
IDENTIFICATION	**Real Display**	1249	1166
	HMD	1147	1063

Table 6.

The presentation of a magnified picture of targets on the helmet visor is not without inconveniences, especially in a single seat aircraft: the possibility to produce an unacceptable discomfort to the pilot is, in fact, high. Nevertheless, the function is, under suitable conditions, realistic and attractive[10,11].

Performance have been evaluated with a 4x magnification and results are summarised in Table 6: ranges are very interesting in this case, the loss presented by the HMD should be weighted with the benefits coming from the presentation of images onto the visor.

5. RECOGNITION AND IDENTIFICATION CRITERIA

Up to now we have not considered a true target, but a sequence of bars: the target in Figure 1 should have been drawn as shown in Figure 2.

The method for performance prediction based on the number of lines on target (Johnson Criteria) was conceived in the Sixties to evaluate the performance of image intensifier systems when identifying tanks and soldiers, and has been extended over the years.

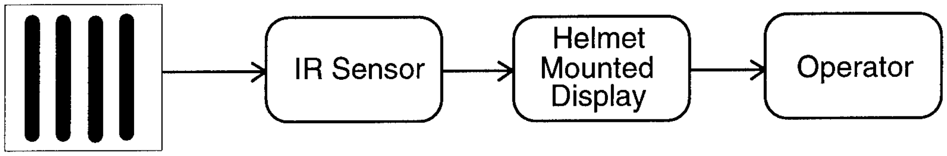

Figure 2. Performance evaluation tests for IR systems are usually based on bars-type targets

One criticism to the Criteria we could mention here is that probably it is the silhouette which allows the recognition process to take place, rather than the resolution contents of the image. Furthermore, the IR image is different from the one in the visible waveband: few hot areas in the image are sometimes sufficient to determine the object.

There are works which analyse the problem of perceptions of IR image on the basis of more appropriate operative approaches, taking into account not only the picture quality but also statistic and observer's decision[12]. On that line we planned a simple test to verify the weight of knowledge of objects in the probability of recognition and identification: *"friends"*, with an appropriate training, can be considered "well known" *objects*.

6. THE TEST

The test has the aim to verify if the acquaintance with object leads to a significant improving of the recognition and identification probability.

A sequence of symbols and simple synthetic images (in the following called *objects*) with very limited contrast level are presented on a TV display. Objects have been created so to be easily interpreted in suitable conditions.

Some objects are presented during the test more than one time, others only once: the observer gets acquainted with repeated objects and should be able to identify them more easily.

The test has used 254 objects, as shown in Figure 3. Twelve of them are repeated ten times, the others only once. For information, the object at line 4 and column 6 is the griffin of the FIAR logo.

As background, we wanted to reproduce a typical operation scenario: the objects have thus been displayed overlapped to an IR image taken from a aerial sequence (see Figure 4).

The image was obtained by sampling a video registration, but the dynamic is however quite good, as shown in the histogram of Figure 5a.

The intensity level of objects has been adjusted to reach a low contrast level.

Figure 5.b shows the histogram of the 100 x 100 pixels area containing the objects and Table 7 summarises the main parameters involved.

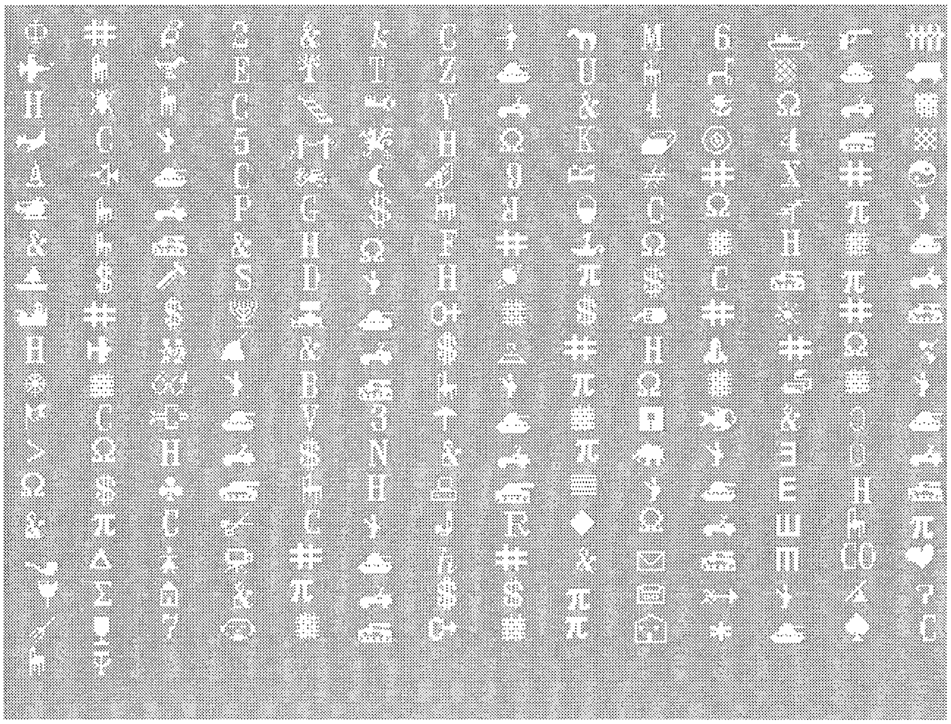

Figure 3. The sequence of objects used in the test

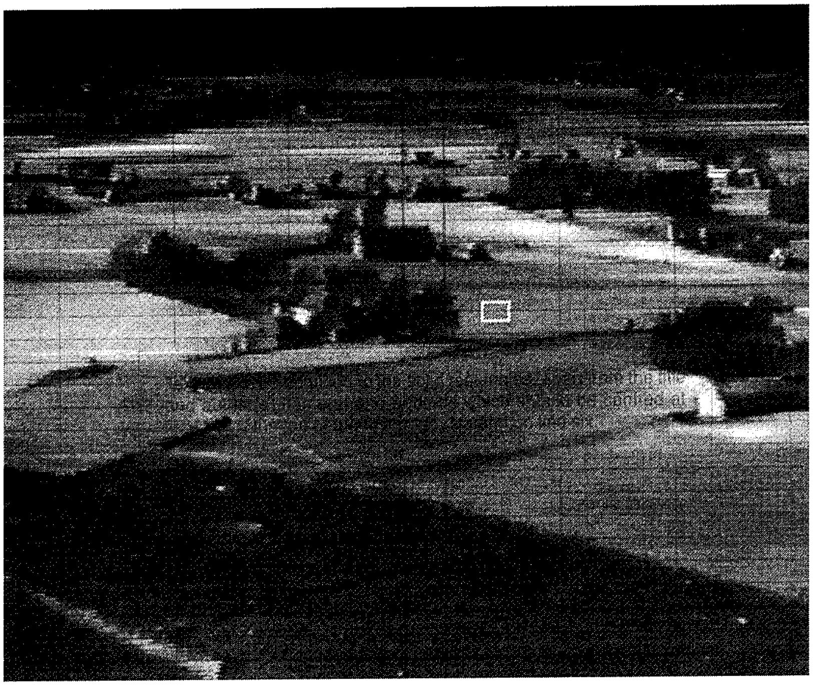

Figure 4. The image used as background in the test.
Objects to be identified have been positioned in the rectangle here highlighted

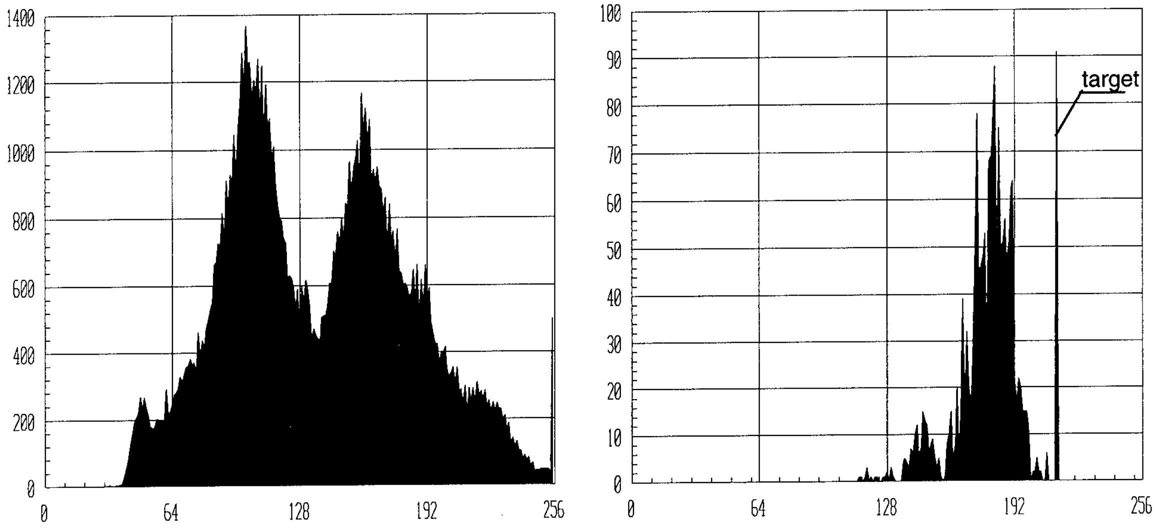

a

b

Figure 5. Grey level histogram of the background picture (a)
and of the 100x100 pixels sector including object (b)

Number of Pixels per Object (mean value)	59.6
Background Mean Level (relative)	0.7
Background Levels Standard Deviation (relative)	0.06
Object-background Inherent Contrast Ratio	1.19
LJND	4

Table 7

Images have been presented on a monochrome monitor, P1 green phosphor (x=0.209, y=0.736, medium persistence), CCIR 50 Hz interlaced video, luminance equal to 30 nits, ambient light 290 lux. The observers have been let free to find their own most comfortable view distance, in order to reduce the effect of viewers' ammetropy. Presentation time for each object has been set equal to 2 seconds after which the observer had to identify the object. For each object, the observer was informed of the result of the identification (i.e. correct or incorrect).

It must be pointed out that, with respect to a static TV image, we have in this case a deterioration of the signal to noise ratio due to the fact that the image is frozen.

7. OBJECT SHAPE

Just few general notes before presenting the test results.

Choosing the objects of the sequence has revealed a critical task: alpha-numeric characters, in suitable contrast conditions, should be identifiable with only five resolved elements (see Snellen's chart); characters and numbers, in fact, are unambiguously determined by not more than five vertical or horizontal contrast elements (actually, less than five for the horizontal direction) as shown in Figure 6.

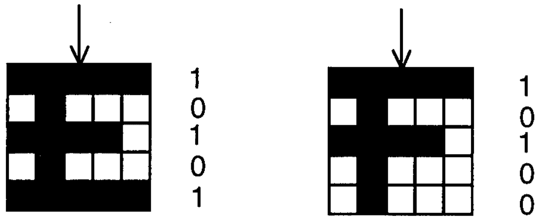

Figure 6. Snellen's Letters can be clearly defined by 5x5 elements

Though it is possible to create objects with similar characteristics (e.g. for verifying children visual acuity), it has been rather difficult to find a good variety of objects presenting the same characteristics and, at one time, which the observers are familiar with.

The use of real IR images (as the ones shown in Figure 7) would have been difficult to perform and, also, would be too specific (ambient temperature, time of the day, status of the object): such employment would have been useful to create a file of samples, but would not have met the objectives we had.

Thus, we have decided to use synthetic symbols limited to an equivalent area of 12 x 12 pixels.

In the test, we have tried to optimise the interpretability rather than dimensions. Thus, the number of pixels composing each symbols is not constant: objects have an average dimension of about 60 pixels, with a minimum of 20 for the simplest characters and a maximum of 120 for more complex objects.

Figure 8 shows the histogram of the pixels distribution in the objects.

Objects composed by a lower number of pixels should probably be considered separately due to their higher probability to be identified.

One of the reasons of the wide spread of the histogram is that different kinds of objects require, beyond any artistic capability of the authors, a different number of elements to be clearly depicted: it has been mentioned that a character in a simple font, for example, should be drawn with at least 5x5 visually resolved elements to be unambiguously identified among other characters.

Similar considerations are valid for more complex objects: the minimum number of elements for an appropriate identification *is a function of the object itself.* A tank could be properly identified only when some characteristics appear evident to the viewer and for that reason a very detailed image would be necessary (great number of resolved elements); a lower level of details could be necessary for identifying a tank with specific macroscopic characteristics.

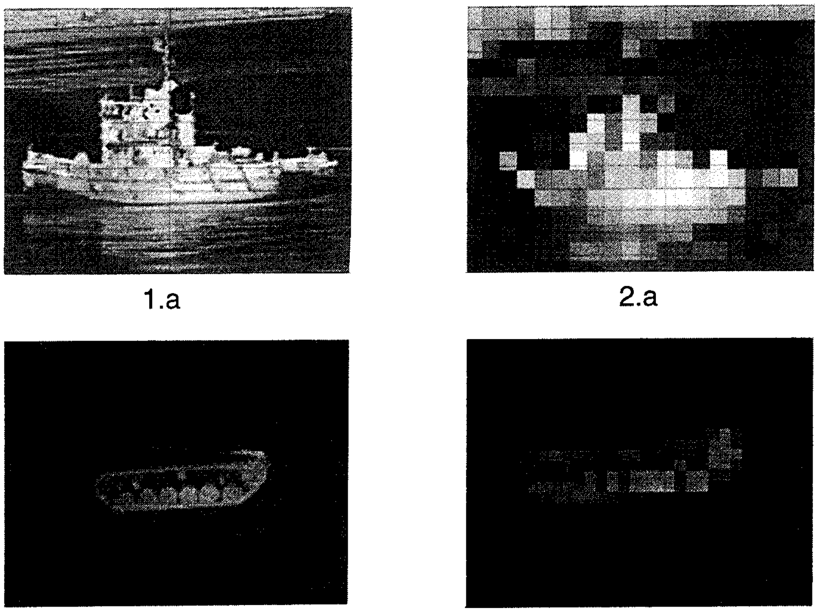

1.a 2.a

1.b 2.b

Figure 7. IR images (1.a and 1.b) and the resizing (2.a and 2.b) performed to obtain a dimension suitable for the test

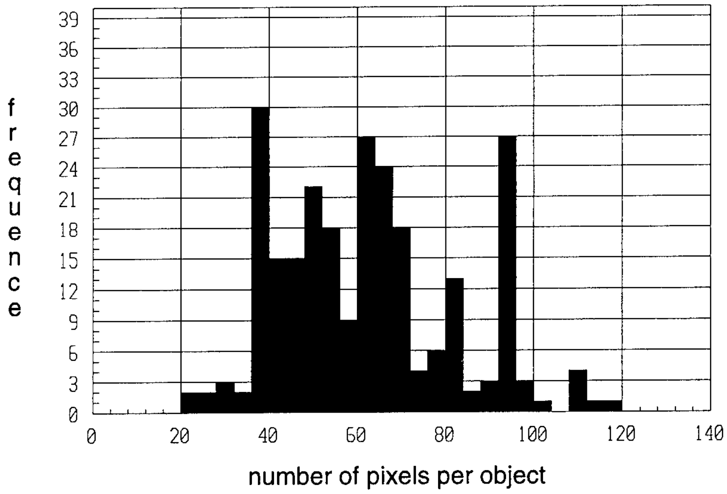

Figure 8. Histogram of objects' pixels distribution

Evaluating the vision system performance is necessary to know the *Identification-Recognition characteristic size* (within the meaning defined above: *minimum number of resolved elements for an unambiguous Recognition-Identification in an optimum environment*) for each target-object.

The *Identification-Recognition characteristic size* depends from many factors, and surely from

waveband
aspect ratio

For an improvement in the consistency of the performance assessment it is therefore necessary to build up, by means of appropriate trials, a wide data file with the Identification-Recognition target characteristic sizes for all objects under interest, in different aspect angle, producing a file as shown in Table 8.

The probability of a right assessment could be significantly low if the image of objects on the HMD does not reach at least the characteristic size.

OBJECT	TARGET CHARACTERISTIC SIZE					
	Recognition			Identification		
	front aspect	rear aspect	side aspect	front aspect	rear aspect	side aspect
a						
b						
c						
...						

Table 8.

NUMBER OF SAMPLES	25
Correct Assessment of Objects (relative frequency)	0.55
Correct Assessment of Single Shot Objects (relative frequency)	0.40
Correct Assessment on First Appearance of Repeated Objects (rel. freq.)	0.41
Correct Assessment of Repeated Objects (relative frequency)	0.74

Table 9.

7. TEST RESULTS

Notwithstanding the limited number of samples, information provided by the test can be considered interesting for the homogeneity of results. A summary is shown in Table 9.

During the test it was evident the learning phase of observers in identifying repeated objects: while the global identification percentage is 0.55, the percentage relevant to repeated objects is 0.74.

The set of repeated objects can be considered homogeneous with the other objects: for their first appearance, in fact, the identification percentage (0.41) is very close to the percentage of correct assessment of *single shot objects* (0.40).

Considering that the repetition of objects is a training for the observers, we can extrapolate the rate of correct assessments for known/other objects by dividing the score relevant to *repeated* objects and the score for *single shot* objects (1.8 in our test).

The difference in assessment of known and other objects should be taken into account for tuning the results of performance prediction shown in Tables 4, 5 and 6.

The above, even if cannot generate rules, is sufficiently meaningful to justify further studies.

8. ACKNOWLEDGEMENTS

A special thank to Dr. Paolo Cantoni for having carefully carried on the test and to all the colleagues who devoted their time to undergo it.

9. REFERENCES

1. "The Infrared & Electro-Optical System Handbook", Vol 4, SPIE Press 1993, Michael C. Dudzik Editor
2. "Definition of Nominal Static Range Performance for Thermal Imaging Systems" STANAG 4347, 1988
3. J.M. Lloyd "Thermal Imaging Systems", Plenum Press, New York, 1975
4. F. Lei, H.J. Tiziani, "Atmospheric Influence on Image Quality of Airborne Photographs", Opt Eng. 32(9), September 1993
5. "Calculation of Minimum Resolvable Temperature Difference (MRTD) for Thermal Imaging System", STANAG 4350, 1988
6. "A comparison of Models Predicting Thermal Imager Performance", PANEL IV, RSG 7 AC/243 July 1981
7. E. Gil Del Rio, "Optica Fisiologica Clinica", Ediciones Toray, Barcelona 1980
8. "Optical Characteristic of Cathode Ray Tubes", Publication no.116-A Electronic Industries Association EIA, Dic. 1985

9. J.C. Kotulak, S.E. Morse, W.E. McLean, "Does Display Phosphor Bandwidth Affect the Ability of the Eye to Focus", Helmet Head Mounted Displays and Symbology Design Requirements, SPIE Proceedings, April 1994
10. H.D.V. Boehm, R. Schramner, "Requirements of a HMS/D for a Night-Flying Helicopter", Aerospace Sensing Helmet Mounted Display, SPIE Proceedings, April 1990
11. G. Balzarotti, L. Fiori, R. Malfagia, "Presentation of IR Picture on Helmet Mounted Displays", Helmet Head Mounted Displays and Symbology Design Requirements, SPIE Proceedings, April 1994
12. J.S. Sanders, M.S. Currin, C.E. Halford, "Visual Perception of Infrared Imagery", Opt. Eng. 30(11), November 1991

TARGETING FOR FUTURE WEAPON SYSTEMS

P.R.C.COLLINS and P.GREENWAY
British Aerospace (SRC), Filton, UK
D.R.EDMONDSON and M.A.GREEN
British Aerospace (BASE), Plymouth, UK

British Aerospace, Sowerby Research Centre,
FPC 267, P.O. Box 5,
Filton, Bristol, BS12 7QW,
England.

SUMMARY

In future weapons systems, accurate target selection and location is required to maximise warhead effectiveness and minimise collateral damage. To help achieve this there should be available significant information about the target location from a variety of sources, eg. satellite imagery, surveillance data and intelligence information. On board the vehicle there will normally be a navigation system which has a good estimate of its position and often there will be an E-O (Electro-optical) sensor which produces imagery of the terrain ahead and the target. There is also available an increasing level of computational power and software techniques including fast image processing systems. Using a model from a preprepared database of terrain features matched to features extracted from such an image it is possible to estimate the sensor position and hence the target position. We discuss here a "proof of principle" system which demonstrates a robust mechanism for achieving this. We describe an implementation using data gathered from a camera moving across a terrain model and results are presented.

1. INTRODUCTION

The successful operation of a future weapon system will depend on a number of factors. Of these, the terminal miss distance is probably the most important. In order to achieve acceptable performance, the weapon system must be equipped with a high performance targeting system which is capable of allowing reliable location of the target to occur. By integrating some of the technologies which have recently emerged, future weapon systems can be designed which will allow accurate selection of the correct target, minimising the possibility of collateral damage.

The rapid growth in high resolution satellite image data, combined with advances in the processing power of mission planning workstations, means that the targets can be selected and appropriate image features extracted which will characterise the target. Processing power is now such that many image processing techniques, once considered to be computationally too complex, are straightforward to implement in real or near real-time applications. Thus, salient target features can be extracted from high resolution images to allow automatic target recognition (ATR) to be performed.

Fundamental to the success of the target recognition process is the availability of accurate navigation information. Emerging navigation technologies which fuse information from an inertial navigation system (INS), the Global Positioning System (GPS), a terrain reference navigation (TRN) system, such as TERPROM [1], [2], and a scene matching area correlation (SMAC) system, for example AUTONAV [3], will provide accurate pointing information to the weapon system enhancing the opportunity for locking-on to the target. A suitable framework for the integration of navigation data is discussed in [4] where details are given of the BRAINS integrated navigation filter.

In order for future weapon systems to be effective the ATR system must exhibit a considerable degree of robustness to system errors and variations in operational scenario. Image Database Fusion (IDF) is a robust method of enhancing the performance of an imaging system through the exploitation of other sources of information. The primary image processing technique used in IDF is Model Matching. The objective of model matching is to discover the 3D position of an object (the model), with respect to the seeker reference frame, by performing a match between corresponding model and image features. In IDF, the model is derived from remotely sensed data and contains information about potentially observable features which might be extracted from an image obtained from a sensor (eg. FLIR) on an aircraft. Embedded in this extended model is information about specific targets, for example their known or estimated position and features which characterise them.

Section 2 of this paper reviews briefly the navigation requirements for targeting future weapon systems, whilst Section 3 examines the various image processing modes which can be considered.

The main part of the paper (sections 4-8) concentrates on the IDF processes and discusses results obtained

Paper presented at the AGARD MSP Symposium on "Technologies for Precision Air Strike Operations in Rapid-Reaction and Localised-Conflict Scenarios", held in Seville, Spain, from 16-19 October 1995, and published in CP-576.

from simulated trajectories on a physical, scale model terrain where both remotely sensed and seeker images were simulated. Finally, some conclusions are drawn and possible areas of future work identified.

2. NAVIGATION REQUIREMENT

A weapon system will have a series of requirements, perhaps the most significant of which will be the need to arrive at the target area and subsequently designate the target for a given mission. A need for a small miss distance has a significant influence on the navigation requirements.

The navigation system requirements are dictated by the desired weapon effectiveness or target kill probability. For some categories of target, such as airfield runways, the overall weapon effectiveness may be met by navigating directly to the target. This normally requires the fusion of the outputs of a suitable set of navigational sensors such as INS, TRN and GPS in an integrated navigation filter. However, for airborne weapon systems such as TIALD (Thermal Imaging Airborne Laser Designator) this direct approach is liable to be at high speed and at low level. It is thus likely that the target will only be visible for the final few seconds just prior to weapon delivery. The problem is magnified when the target is either a hardened aircraft shelter (HAS) or enemy military communication centre. For a successful kill, pin-point hits are required at high incidence angles. This may well require a system incorporating some form of automatic aim point refinement. ATR will play a major role in minimising time over the target area.

3. IMAGE PROCESSING REQUIREMENTS

Navigation considerations have established the need for automatic target recognition for weapon systems such as TIALD. An element of technical risk must be associated with the complex nature of the computer vision tasks required for ATR, as no 100% guarantee of successful target designation can be given. However, significant progress is being made on the "Image Understanding Environment" (IUE) and other ATR, navigation and guidance applications of image processing [5].

As ATR technologies mature so the risk factor will be reduced. A hierarchy can be postulated in which increasing levels of autonomy are gradually introduced into the actions of the image processing. The following image processing options are possible:

3.1 Man in the Loop Only Operations

In this mode a human operator would be responsible for acquiring the target from an image which could be enhanced to maximise the chances of target recognition. The major issues in MITL operation are explored in References [6] and [7]. Using information from the aircraft's navigation system, a rough search region could be delineated within the image, helping to reduce operator workload. From the algorithmic viewpoint the human vision system is one of the best available image processors. Hence this can be regarded as a baseline recognition system for judging other ATR systems.

3.2 Target Cueing to Aid Man-In-the-Loop Operations

As a first step towards the low risk introduction of autonomy, target cueing can be considered in which a number of candidate objects are presented to the operator who must then select a target to be engaged. The exact form of cueing required may vary with target type. For large fixed land targets the operator could be cued with primitives, such as line fragments, which would help to enhance the location of the target. Alternatively, it may be that a reliable algorithm, perhaps based on model matching, can be introduced to interpret scene primitives to allow the fixed land target to be recognised and then cued to the operator.

3.3 Fully Autonomous ATR

In this mode, the algorithms must locate the target without any operator intervention making it the highest technical risk option.

In all cases the image processing function would be supported by the navigation system, which will allow sightlines to the predicted object location to be calculated. In this way levels of confidence can be ascribed to regions of pixels within the imager FOV. In effect the navigation system is providing a check on the possible false acquisitions of the image processing algorithms. Navigation information must be included in any model matching scheme, to allow perspective transformations to be performed. Further, an on-board culture database combined with the navigation system outputs can provide the ATR system with a priori information which can be used in the recognition procedure.

4. IDF CONCEPT

There are a wide variety of possible targets for weapon systems. Many types of target which are to be recognised and designated have complex 3D structures. However some will present few, if any, recognizable features directly associated with the target. Most such targets are likely to be fixed (at least within the time span of available intelligence information) and their positions could be found from the recognition of landmarks either in the immediate vicinity of the target or along the approach path. In a more general situation such techniques as scene segmentation, analysis, labelling and understanding could be more appropriate [8].

We are concerned here with a scenario where there is knowledge of the sensor location in the real world, available from navigation system data. There is also a good knowledge of the absolute locations of many (fixed) objects within the scene, from intelligence and satellite data. This makes the use of image and database fusion (IDF) techniques worthy of prime consideration.

The key image processing problems which need to be solved are all related to the fact that the types of objects which are to be recognised and located can have complex 3D structures. The constituent features may or may not be visible depending on the direction from which we approach the target and may or may not be unique to a particular target or part of the scene.

In computer vision studies it has often been found that the best method of dealing with problems of this kind is to match line based features to a 3D Model. The model provides a simple way of relating different features by means of their spatial inter-relationships. Thus, if we observe in an image a set of features which match the spatial arrangement of features in the model, it is probable that we have found an example of that model (or part of the model) in the image. This approach is called *Model-Matching.*

Model-matching is a well established image processing technique at the Sowerby Research Centre (SRC). In previous studies, a video image of an object in the real-world (typically a mechanical assembly) was matched with a 3D CAD (Computer Aided Design) model of that object. The software performs the model matching, translating and rotating the model until an exact correspondence has been achieved and the model projection can be overlaid on the image of the object. With suitable calibration, this allows us to make deductions about the relationship between the image and the real-world. We can estimate the position and orientation of the object relative to the camera or of the camera relative to the object, and hence its location in the real world.

It is apparent that the model-matching paradigm could, with some important modifications, be applied to the location of a sensor on board an aircraft from its imagery of the world. The problems to be solved are essentially as before with one main difference being that in an aircraft the sensor would be constantly moving. Another important difference is that the models represented would be kilometres in extent instead of millimetres. The study of the extraction of positional information, from the combination of sensor imagery, navigation data and a database of feature locations and characteristics, was undertaken in the production of a prototype Image Database Fusion (IDF) system.

Model-matching is a very flexible technique. It is robust with respect to "noise" in the data caused by poor imagery or partial obscuration of the target. It is also capable of locating many types of target and, unlike many correlation techniques, it allows freedom of approach to the target from any altitude or bearing. These are very desirable characteristics for an airborne target acquisition system.

However, unconstrained model-matching is computationally expensive. There are usually six degrees of freedom in the matching process; the roll, pitch and yaw of the sensor, and the latitude, longitude and altitude of the sensor. In addition, if the sensor is not rigidly fixed with respect to the vehicle, extra degrees of freedom must also be taken into account.

The problem only becomes tractable when use is made of the navigational information available on the platform. By using this information, the model-matcher can be constrained in the extent, within these degrees of freedom, that it has to search in order to find a match. Consequently, the use of information from the vehicle's navigational systems is a key element of IDF. The navigation systems are used to give an estimate of the vehicle's current position. The IDF software searches for features in the image, matches the features with the current model, and can track the model in subsequent frames. If this fix is accurate, IDF can immediately designate the target. However, it is expected that the position and orientation output from IDF will become yet another input to an integrated navigation system.

Generally, model-matching has not been proven in a highly dynamic situation such as IDF. It is normally used in applications where the sensor is in a fixed position. Thus the model matching problem for IDF is doubly difficult; not only do we want to find a 3D target in 3D space, we also need to be able to track its position over a sequence of frames once it has been found.

5. IDF PROTOTYPE SYSTEM

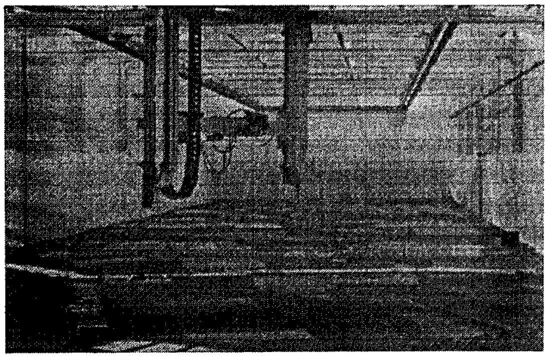

Figure 1: SRC Terrain Model

The prototype IDF software processes a digitised image from the SRC terrain model and an estimate of

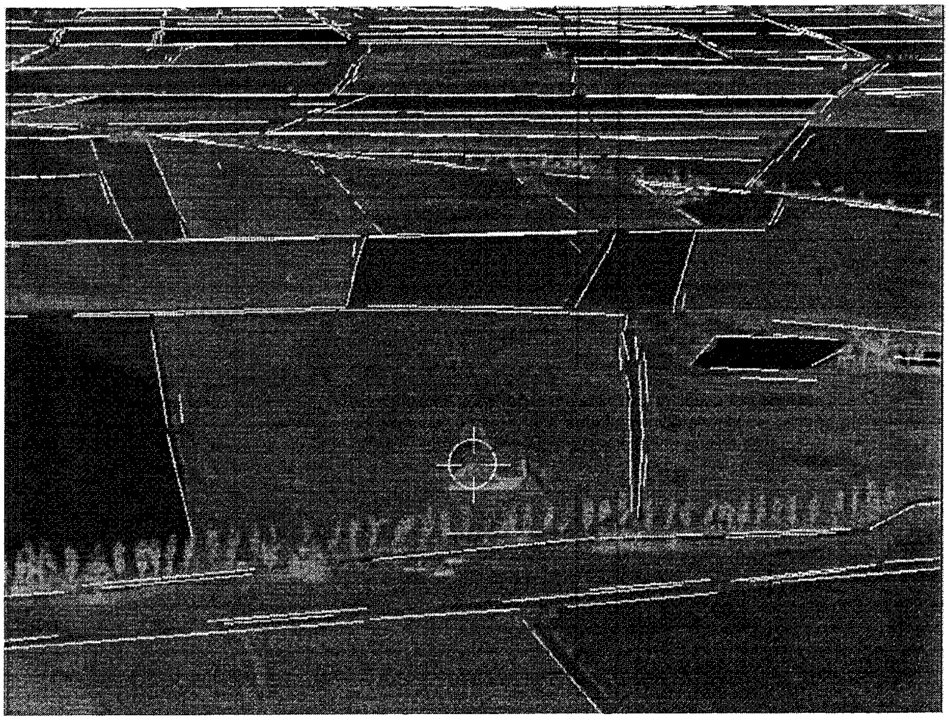

Figure 2: The view from the FLIR sensor, with an overlay of database features and target designator (in this case a H.A.S.)

the camera position or position estimate derived from earlier processed frames, which can be degraded by Gaussian noise. Features from the appropriate part of of the database are projected into the current image and a local search is made to detect features having good matches in orientation and strength. The camera position and orientation is then optimised to give a least squares error match between the projected and detected features.

The least squares error minimisation technique does not require that all database features should be visible or detected in the image. It is robust with respect to errors and distortions in the image or the database and gives a best estimate of position and orientation based on the available information. The target itself can be wholly or partially obscured provided it can be located with respect to the features in the database.

5.1 SRC Terrain Model

The SRC physical terrain model facility (see Fig.1) was used in this study. The terrain model is a 300:1 scale model of a 25 square kilometre area of the west German plain. A five-axis overhead gantry system carries a video camera over the model enabling a wide variety of flight scenarios to be simulated experimentally. By a combination of special paint schemes and video inversion, pictures of the terrain model can provide a realistic simulation of Infra-Red imagery. The terrain model was used in three distinct ways.

It was used to gather a realistic sequence of flight data and imagery. Fig.2 illustrates a typical image, with IDF overlays, from the end of a sequence along a trajectory shown in Fig.4 (This image is discussed further in later sections).

An image database which simulated an overhead view of the target areas as seen from a 'satellite' was produced. This was constructed from a collection of images taken vertically over different parts of the model. The pixel resolution on the ground was approximately one metre (real world scale) but distortions at the edges of individual images, where they meet, was much greater (about 5m). Fig.3 shows such a collection of images with database features added, as discussed below.

A Model database of terrain landmarks was obtained from the image database. In a real IDF system the landmarks which would be used in the Model Database would be constructed using available maps, satellite, or other reconnaissance data either in advance or during mission planning.

In the current study, as a terrain model was used, genuine navigational inputs were not available. Consequently,the positions of the robot gantry which carried the CCD camera over the terrain model were used as the basis for the 'navigational data'. This required careful measurement of the camera position on the gantry and the gantry motion.

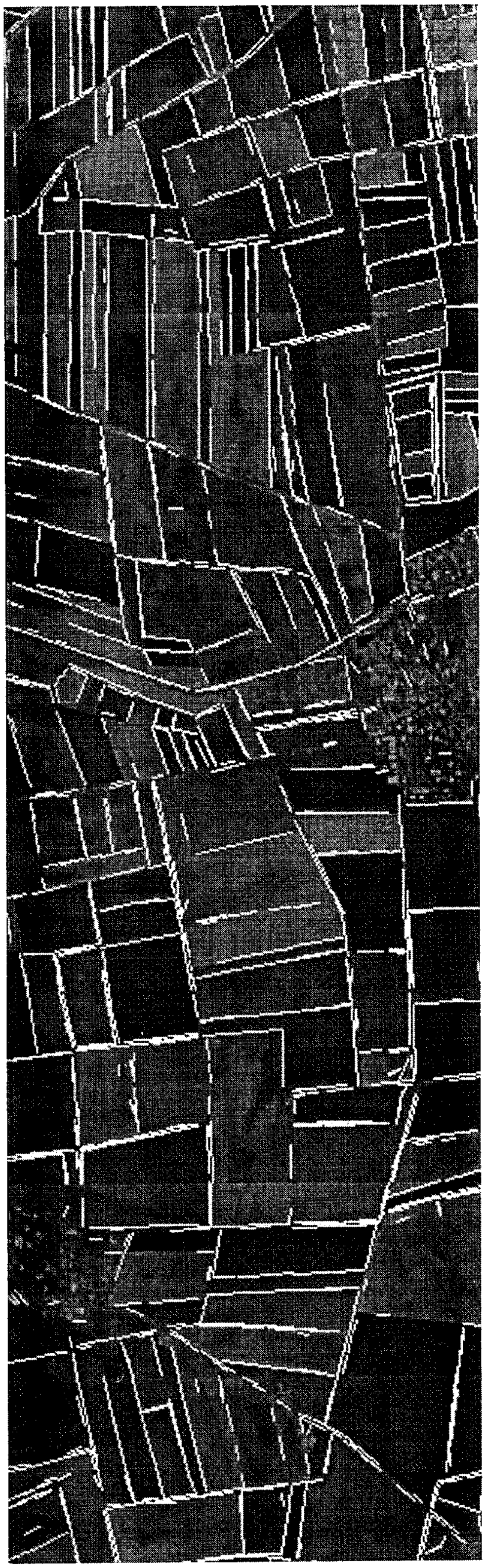

Figure 3: The 'satellite' view of the SRC Terrain Model with database overlay.

5.2 Landmark Database

The landmark features were extracted automatically in the following way: an edge map of the image was obtained using the Canny operator; the edges were then approximated by fitting straight lines. By altering the various parameters of the programs used to perform these operations it is possible to select the most significant line segments in each image. Part of the database is illustrated in Fig.3 in which the extracted line segments are shown superimposed on the 'satellite' imagery. This database format can easily be extended to include point features, texture patches or even region based segmentations.

In the IDF implementation, the model database contains a description of terrain covering several kilometres in extent. However because of the restricted Field of View (FOV) of the sensor only a small percentage of the database is visible in any given image. The model database software can query the database to determine what is theoretically visible from the sensor from any 3D position over the terrain in question.

The database is organised around landmarks (groups of features with some meaningful relationship to each other). Given this database structure, it is possible to build a very information-rich description of the world in the database as an arbitrary number of landmarks is permissible. Techniques for the efficient implementation of the database were not considered in this study, but this is an important issue for future work.

The database used for IDF is essentially two dimensional. Although height information can (and should) be included where available, it is not required on a per feature basis but only at a low spatial frequency to allow for gross terrain height variations. It could thus be a subset of the data available for existing terrain following systems. It is intended that the majority of data should be automatically extracted from satellite or other reconnaissance data by simple and fast computer processing. This enables new information to be processed and included during mission planning. Where detailed three dimensional data is available, e.g. for the target itself, this could be included in the database and should be used by the IDF algorithm and give improved performance. The prototype system has successfully been used with no height information at all. Currently height information on a grid spacing of 300m x 150m is being used, with a vertical resolution of approximately 1m.

5.3 Landmark Selection

A key to achieving the successful operation of the IDF system could be the careful choice of *appropriate* landmarks and landmark features for the IDF model-matcher to work with. This choice can be made either in database preparation or mission planning. In the current IDF study two feature types (lines and points) were implemented and used although development has been predominantly line based. This gave good results for the type of terrain studied, but a real system may need to implement a wider range of feature types. The database format, in its current form, is capable of coping with additional types. If necessary, this could easily be extended.

One issue affecting the choice of landmarks concerns obscuration due to atmospheric effects; landmarks far away are more difficult to see than ones nearby. Another concerns landmarks which are nearest the vehicle; these will be seen at the bottom of the camera's FOV and will appear to be moving much more rapidly than objects further away. The main difficulty here is likely to be a higher degree of motion blur for these landmarks. This will have consequences for the algorithm used to detect these landmarks. A third issue concerns the perceived *importance* of a landmark; it may be worth investing different amounts of computer resources on different landmarks. Some may be more "information rich" than others. Lastly, we need to consider the density and distribution of landmarks across the imagery. The accuracy obtained will depend upon this distribution.

5.4 Data Fusion for Positional Measurements

IDF requires inputs from the aircraft's navigation systems so that it can estimate the position of the sensor in the database reference frame. This prediction is used to query the model database and project the landmarks into the image. The model-matching software then calculates the position and orientation of the sensor relative to the world given the original prediction as a starting point. There is a requirement for a data fusion process to monitor the current positional estimates from the various systems (GPS, INS, TERPROM, IDF etc) and continually provide IDF with the best prediction of the current position and orientation of the vehicle. This has not been addressed here

5.5 Sources of Error

Several effects may introduce error into IDF estimates if care is not taken to avoid or allow for them. Motion blur may make the measurement of the position of features more inaccurate. A secondary motion problem can appear when the image is composed of two interlaced fields, if the sensor moves significantly in the time taken to capture the two fields. General vibration and buffeting of the vehicle has similar effects to motion blur. The effect of inaccurate attitude measurement is more significant in situations where the FOV is narrow and the sensor look-down angle is very shallow.

6. IDF PERFORMANCE ESTIMATION

It is worth restating that in IDF the goal is to jointly estimate position and sensor orientation by a least squares fit of the observed image features to a known database. This is a more difficult problem than estimating the target position within the image (which would be a much simpler problem for IDF). The accuracy of this estimation at any time will depend upon the geometry of the sensor sightline and the features which appear within the field of view.

This examination of performance estimation deals not with IDF itself but an idealised system which optimally utilises all available information. It may be developed from IDF in the future, or it may be impossible to fully achieve, but it indicates a limit on the achievable performance.

It should be pointed out that the image processing problem of range ambiguity does not apply when matching to a model of known size. Provided there is a reasonable estimate of relative orientation available, the estimation of range from a pair of features depend on their range, separation and the accuracy of measurement of the angle between them in the image.

For features at long range any database inaccuracies and sensor position inaccuracies have little effect on sensor orientation determination. However sensor position estimation is poor using features at long range. When features at shorter ranges are processed sensor position estimation accuracy improves until limited by database inaccuracies, image blurring, image measurement and model matching accuracies and the availability of a suitable range of features.

In order to obtain an estimate of the errors some approximate values are used, which are thought to give an example of typical system parameters, in sample calculations.

In this work a nominal sensor is chosen, of approximately 30° field of view and 1mR (milli Radian) pixel size. The achievable feature location accuracy is difficult to assess especially for larger features. It may well be several pixels but equally sub pixel resolution is achievable under appropriate conditions. Averaging over edgels within a line feature or over a number of features will improve accuracy but conversely line features only provide accurate positional information in one direction and information from a number of features must be combined to fix an image position in two dimensions. These complexities will be ignored and at present for sample calculations the feature location accuracy will be taken as approximately equal to the pixel size of 1mR. A suitable average over an assumed feature distribution could be used for more accurate estimate.

Note that in practice the various errors are not independent and various correlation mechanisms exist and may tend to average out errors in various orientations.

6.1 Orientation Accuracy

The estimate of sensor orientation obtained from features at long range will depend upon the feature location accuracy and feature distribution. In pitch and yaw it should be the same as the feature location accuracy, here taken as 1mR, probably improved by averaging over a number of features. The roll accuracy will be reduced by the sine of the angle off boresight, here a maximum of 15°, giving an expected accuracy of about 4mR.

6.2 Positional Accuracy

The positional accuracy of IDF will be mainly determined by the features at shortest range, in the bottom of the image, provided that there is a large range coverage within the field of view. Orthogonal to the sightline the error will be the feature location accuracy multiplied by the range. Detectable feature offsets resulting from an orientation error of 1mR at 600m would be 0.6m and this accuracy might be approachable if position vs. orientation ambiguities can be avoided.

Along the sightline the fractional error in range is the feature location accuracy divided by the sine of the angle of the feature off boresight or about 0.004. At 300m height above ground and a 30° FOV, with the top of the image viewing horizontally, the bottom of the image will view the ground at an angle of 30° below the horizontal and at a range of 600m. This gives an estimated 3m error along the sightline relative to the database, with database errors possibly significant. By looking at several images in different directions in succession this position accuracy could be improved and equalised across the three dimensions.

Note that at a speed of 300m/s at a 25Hz frame rate sensor motion per image is 12m. Lateral motion is 6m at 30° from the velocity vector (or 3m at 15° when looking forwards along the velocity vector). This is a maximum motion of 10 pixels per frame at 600m range and could need further attention.

Motion blur may well be a limiting factor. Its effects will depend on sensor type and sightline geometry. However it may well be possible to accurately locate a line feature edge when blurred.

6.3 Effect of varying depression angles.

The previous section provides a mechanism for estimating the errors for an "IDF like" system. It considers a situation in which the range variations within the field of view will be large compared with the range from the sensor to the closest feature. If this is not true it strongly affects the estimation of expected errors.

Notice that here the yaw and azimuth estimation should be similar to those above, at low depression angles. However as the depression angle increases not only will range variations within the field of view decrease but, especially in elevation, the features at different ranges are more widely separated within the image and effects such as roll inaccuracies will degrade azimuth performance. Eventually the geometry can approach a view of a patch of features on the ground for which there is be substantial position vs. orientation ambiguity. In particular the error mechanisms are likely to be substantially different in low level flight and when looking or diving down from a high angle.

When there is a large depth of field of view (e.g. in low level flight at low depression angles) the position and orientation accuracy should be limited by the accuracy of feature location within the scene (subject to image blurring and database accuracy).

In a dive with a small range variation within the field of view the position and orientation accuracy will change and position vs. orientation ambiguities will begin to appear (primarily in lateral position and azimuth). If accurate position information is available (e.g. from the navigation system) then these ambiguities should be resolved to give accurate orientation and vice versa. Position accuracy along the sightline and roll about it remain a direct function of range and angle off boresight of the appropriate features.

However during the final dive towards the target the estimation of the position and orientation of the sensor may well be of secondary interest since the location of the target within the image for use in guidance and aim point refinement is likely to be of more importance for system effectiveness. The accuracy of target position within the image should be a direct function of the range and matching accuracy and the database accuracy.

7. PROTOTYPE SYSTEM RESULTS

Fig.4 shows a generic trajectory along which image data has been gathered from the terrain model. The trajectory starts at about 300m and pulls up and then levels out at about 600m before diving towards a target. The diagram (Fig.4) also shows the position estimates which IDF produced from individual image frames while tracking along the trajectory with no smoothing. An enlargement of part of the trajectory is shown in fig.5 with a 5m circle shown for reference.

Although IDF is designed to be used in a tightly coupled filter integrated with a navigation system, the prototype system was in fact able to track the trajectory from the initial frames to the end point using only information from the images and the database and with no smoothing filter. With a small amount of smoothing IDF could track unaided in the presence of injected noise at a level of 3m and 0.1° on all axes. The image in Fig.2 was taken from the end of such a run and shows accurate targeting.

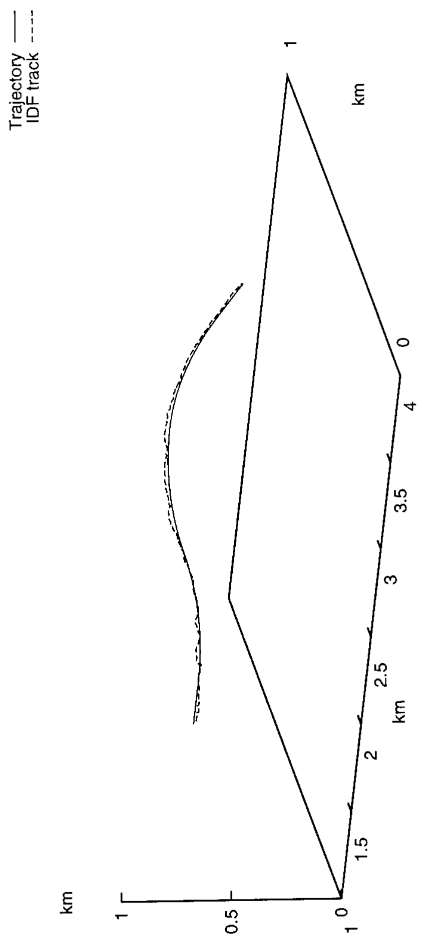

Figure 4: An IDF trajectory over the Terrain Model

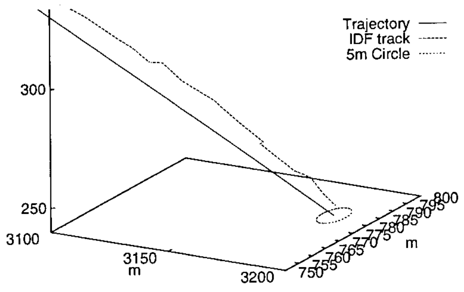

Figure 5: An IDF trajectory over the Terrain Model Enlargement

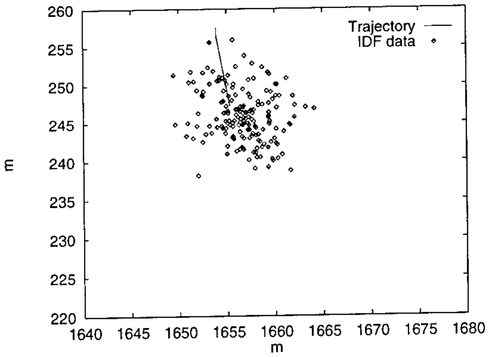

Figure 6: IDF on a line trajectory over the Terrain Model

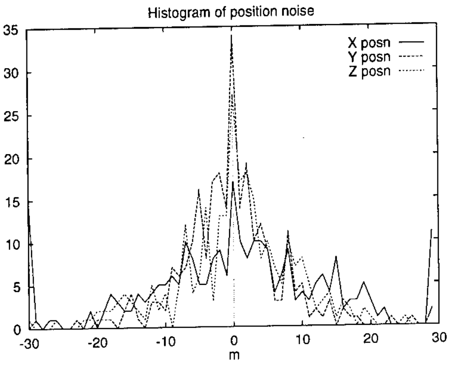

Figure 7: IDF position noise histogram

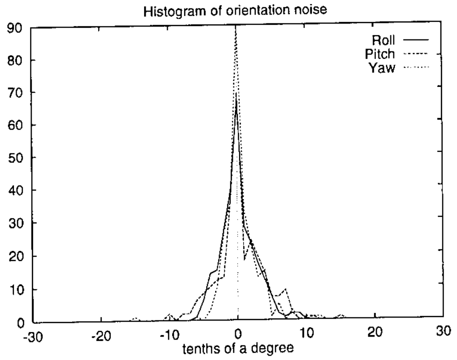

Figure 8: IDF orientation noise histogram

Fig.6 shows IDF using images from another trajectory consisting of a straight line at a constant height of about 300m diagonally across the model but viewed directly along the trajectory in order to view deviations from it. The deviations are predominantly vertical tending to confirm the major error is along the optical axis.

The noise levels achieved were, as predicted, worse along the camera line of sight. IDF noise levels were in general comparable with those predicted above. Differences from predicted levels were generally of the same order as variations between frames with different feature distributions. Results were sometimes better than the predictions perhaps showing significant gains from averaging over a larger number of feature positions. The accuracy achieved was dominated by uncorrected radial distortion in the camera lens. The accuracy levels achievable were found to be about 4m rms laterally and 8m rms along the sightline. When large levels of noise were injected into the initial search start point the noise on the position and orientation estimates seemed non Gaussian, as might be expected if there were occasional substantial mismatches in the initial feature association. Plots of error histograms are shown in Fig.7 and Fig.8. Fig.7 shows the histogram of positional errors in metres over 170 frames of a flat trajectory. Fig.8 shows the corresponding histogram of orientation errors in roll, pitch and yaw in tenths of a degree. This is the subject of ongoing study.

8. CONCLUSIONS

A prototype system has been developed, and has been used to demonstrate the principal benefits of IDF. These are:-

1. it can *automatically* pin-point large fixed unbounded targets.
2. it uses available information about the vehicle's current position and refines this with respect to visible landmarks. The target position is calculated with respect to these landmarks.
3. it does not require detailed information concerning the target other than its geographical location.
4. it is a Line Of Sight (LOS) system; its accuracy increases as range to the target decreases.
5. it can be used for aim-point refinement: once a large target is located using the methods described, IDF can use a more detailed 3D model of the target to identify particular features of the target.
6. it could be performed in real-time using currently available technology.
7. it is stealthy; it does not rely on systems such as GPS, and it emits no radiation.

Planned future work includes studies into how new feature extraction techniques might improve the accuracy of the positional data obtained from IDF and a comparison of alternative model matching strategies.

BASE also hopes that a demonstration of a simulator may be provided by using the SRC Terrain Model. The gantry and camera would be controlled by the IDF software locating and tracking its chosen target. If successful, hardware would be produced capable of being used on flight trials.

Acknowledgements

The authors wish to thank the members of BAe (Dynamics) Ltd. with whom they have had useful discussions on the weapons system aspects of this paper.

References

1. Dale R.S. TERPROM - automatic precision navigation and guidance in all-weather. In *Guidance-Control-Navigation Automation for Night All-Weather Tactical Operations*, volume AGARD CP 387 Ref 19.
2. Grey D.M. and Dale R.S. Recent developments in TERPROM. In *Advances in Techniques and Technologies for Air Vehicle Navigation and Guidance*, volume AGARD CP 455 Ref 12.
3. Navigation system. UK Patent Application 9316472.1.
4. Robins A.J. *Recent Developments in the TERPROM Integrated Navigation System.* American Institute of Navigation, 1988.
5. *DARPA Image Understanding Workshop, New York.* Morgan-Kaufmann, 1988 - 93.
6. Carver E.M. RPV reconnaissance systems: The image interpreter's task. In *Remotely Piloted Vehicles Sixth International Conference*, Bristol UK. 6-8 April 1987.
7. Carver E.M. Human factors issues in fibre optic data link systems. In *Fibre Optics in Guided Flight, Royal Aeronautical Society*, March, 1993.
8. W.P.J. Mackeown, P. Greenway, B.T. Thomas, and W.A. Wright. Contextual image labelling with a neural network. In *IEE Proc. Vision, Image Signal Processing*, volume 141, No 4., pages 238–243, August 1994.

Digital Video Compression for Weapons Control and Bomb Damage Indication[1]

Charles D. Creusere
Gary Hewer

Naval Air Warfare Center Weapons Division
China Lake, CA 93555
USA

SUMMARY

The goal of this paper is to familiarize the reader with the major image and video compression technologies in the context of weapons control (WC) and bomb damage indication (BDI) applications. Toward this goal, we discuss the operation and limitations of the four major still image compression techniques: discrete cosine transform (DCT), wavelet transform, vector quantization, and fractal. We then consider the broader problem of implementing video compression algorithms which use the previously discussed still image compression algorithms as basic building blocks. Some of the techniques examined here are motion estimation, motion compensation for prediction and interpolation, and 3-dimensional subband coding. Finally, we discuss the major characteristics of digital video compression and transmission systems, concentrating on the impact they have on WC and BDI system performance. Many of these characteristics are desirable in every compression application (e.g., good image quality) but some of them are especially important for low-cost remote-sensing platforms (e.g., a low-complexity video encoder). In addition, some characteristics like video latency are important for the weapons control application but not for the BDI application. Within this framework, we discuss the various image and video compression technologies available and highlight those which are particularly good or bad for WC/BDI applications.

1. INTRODUCTION

Recent advances in computational hardware and signal processing theory have made the transmission of real-time digital video possible. Thus far, there have been two driving applications in this field: (1) video broadcast via such media as CDROM, terrestrial radio frequencies (RF), and satellite RF and (2) video teleconferencing. The key paradigm for video broadcasting which is opitimized by the MPEG standards [1], [2] is to make the receiver as cheap as possible since there are many receivers but only a few transmitters. For video teleconferencing, on the other hand, the goal is to make the system as symmetric as possible because every system must be able to both transmit and receive video in real-time. In addition, broadcast video is generally expected to be of very high quality (MPEG 1 video should look at least as good as that of a standard VCR, for example) while a considerable amount of degradation is accepted in teleconferencing video.

The paradigms for military remote-sensing video are considerably different from those of either broadcast or teleconferencing video. First and foremost, the transmitter and, consequently, the video encoder, must be as low in complexity as possible while the decoder complexity is far less important. Reducing the complexity of the encoding translates into reduced space, weight, and power requirements on the sensor platform. At the very least, relaxing these requirements reduces the cost of the complete system, but it can also be the enabling factor which makes the system possible in the first place. The issue of transmitter complexity and its associated costs becomes even more important for weapons control and bomb damage indication (WC/BDI) applications where the transmitter is expendable. Currently, analog video datalinks derived from the NTSC television broadcast standard are used, but these suffer from a variety of shortcomings including low resolution, jamming/intercept vulnerability, and a lack of flexibility to varying video data types (e.g., Ladar, SAR, IIR, etc.). Digital video transmission can overcome all of these shortcomings, albeit at a higher transmitter cost.

In this paper, we study a number of compression technologies and evaluate their suitability for WC/BDI applications. In Section 2, we introduce the notation and terminology which will be used throughout this paper while Section 3 discusses the four most common still frame compression technologies. Still frame compression is studied both for its own sake and because it forms the basis of the video compression strategies introduced in Section 4. Section 5 analyzes the ability of the various algorithms presented in the earlier sections to satisfy the WC/BDI compression requirements. Finally, conclusions are presented in Section 6.

2. NOTATION AND TERMINOLOGY

Throughout this paper, the terms *compression* and *coding* are synonymous and will be used interchangeably. We use the word *coding* to describe the compression process because an actual bit stream describing the image is output by the compression algorithm. Historically, this process is referred to as *source coding*, a term which originates from Shannon's original work on information theory [3]. Consistent with this terminology, we refer to the part of the algorithm which performs compression as the *encoder* and the part which performs decompression as the *decoder*.

---

[1] Unclassified, Distribution Unlimited

Paper presented at the AGARD MSP Symposium on "Technologies for Precision Air Strike Operations in Rapid-Reaction and Localised-Conflict Scenarios", held in Seville, Spain, from 16-19 October 1995, and published in CP-576.

variable bit rate, and, thus, getting the coded image through a fixed bit rate channel requires either that we iterate the coding process (changing a quality factor until the desired bit rate is achieved) or that we use a large buffer with some form of feedback control from the quantizer. This later approach is the one taken in the MPEG standards.

As regards the WC/BDI problem, DCT-based methods have much to offer. First and foremost, the complexity of a still-frame DCT-based encoder is very low because the complexity of the 8x8 DCT is very low. In addition, the algorithm scales linearly with the dimensions of the image, and it is highly parallelizable. Finally, a great deal of commercial hardware is available which can be easily leveraged for military applications. The only real drawback of a DCT-based coding algorithm is its performance at low bit rates-- the boundaries between the 8x8 blocks appear in the reconstructed image. Consequently, for low bit rate transform coding, transforms which maintain spatial locality and yet have overlapped blocks are preferable. Such transforms are often called modified lapped transforms (MLT) or multirate filter banks [7] and certain members of this general class can be used to efficiently implement discrete wavelet and wavelet-packet decompositions.

2.3 Wavelet and Wavelet-Packet Transforms

Wavelet and wavelet-packet transforms are two members of the general class of subband coding methods. While other forms of subband coding have been discussed in the literature at great length [8], a general consensus has formed over the past few years that wavelet and wavelet-packet techniques offer the best in coding performance.

The block diagram of one level of a 2-dimensional wavelet transform is shown in Fig. 2 where L and H indicate lowpass and highpass filters respectively and the subscripts v and h indicate the direction in which the filter operates (vertical or horizontal). The downward-pointing arrow followed by the 2 represents the down-sampling operation in which every other sample point is discarded-- this maintains the same sampling density in the wavelet domain as existed in the original image. To get a true wavelet transformation, the decomposition of Fig. 2 is iteratively applied, first to the original image and then to the low-low band at each successive level until, in the limiting case, there is only one pixel remaining in the final low-low band. A mapping of wavelet coefficients is shown in Fig. 3 for a 3-level wavelet decomposition where the two capital letter indicate the frequency band (e.g., HL corresponds to a high-low band) and the subscript indicated the scale of that band. In this figure, lower scale numbers correspond to finer edge features in the image while higher number correspond to subsampled coarse features. Note that all of the bands represent different resolutions of edge features except the final low-low band which contains all of the remaining low frequency image content. The wavelet coefficient mapping illustrated in Fig. 3 can be converted perfectly back into the original image if the correct filters L and H are used in Fig. 2. The conditions on these filters were first presented in [9] and later used by Daubechies in her compactly-supported (i.e., having a finite impulse response filter bank implementation) orthogonal wavelets [10]. In order to show the equivalence between this discrete wavelet transform (DWT) and the continuous wavelet transform, Daubechies required her filters to have an additional quality called regularity which is somewhat related to the number of zeros which filter L has in the frequency domain at π. Relaxing the orthogonality constraint, perfect reconstruction biorthogonal wavelets and filter banks have also been created [11], and these have been shown in recent years to be the most effective for image compression applications [12].

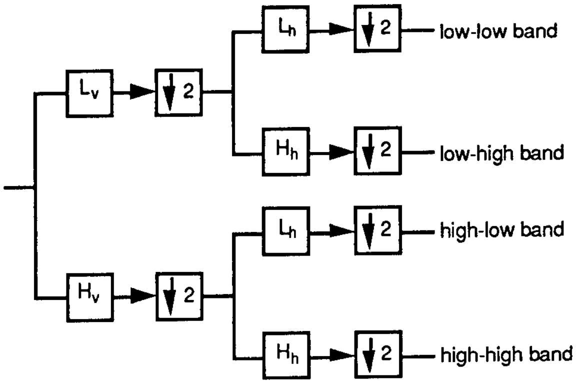

Figure 2: 4-band, 2D wavelet decomposition.

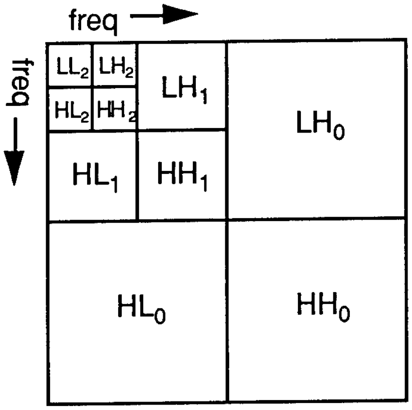

Figure 3: Wavelet coefficient map.

Early wavelet compression algorithms followed the same format as the DCT-based coder illustrated in Fig. 1: transform, quantize, and losslessly encode [13]. This methodology generated better results with a wavelet transform than with a DCT, but the difference was only on the order of a few decibels in PSNR improvement. It was not until the advent of the Embedded Zerotree Wavelet (EZW) algorithm developed by Shapiro [14] that a vast improvement in still frame compression quality was realized over DCT-based methods like JPEG. The most important concept introduced in this algorithm is that of forming zerotrees of wavelet coefficients. This idea makes it possible to efficiently exploit the correlation between insignificant coefficients at different scales. This basic concept has since been further optimized using an entropy-constrained quantization approach to achieve some of the best wavelet coding results published to date [15].

In general, there are two forms of coding: lossless and lossy. As the names suggest, *lossless* coding implies that the image produced by the decoder is identical to that which went into the encoder. Unfortunately, the compression ratio that one can achieve using lossless coding is image dependent and is generally not more than 4:1 (4 times fewer bits in the compressed image than were in the original). *Lossy* coding, on the other hand, implies a loss of information in the coding process leading to a degradation in the quality of the decoded image. To accurately characterize the quality of a lossy coder, one must specify a rate-distortion curve-- i.e., the bit rate (compression ratio) of the coded image versus the distortion introduced by the coding process. This distortion is typically measured by either mean squared error (MSE) defined as

$$\mathrm{MSE} \equiv \frac{1}{X \cdot Y} \sum_{m=0}^{X-1} \sum_{n=0}^{Y-1} \left| x(m,n) - \hat{x}(m,n) \right|^2 \qquad (1)$$

or peak signal to noise ratio (PSNR) which is general given in decibels and is defined by

$$\mathrm{PSNR} \equiv 20 \cdot \log_{10}\left(\frac{255^2}{\mathrm{MSE}} \right). \qquad (2)$$

In (1) the original and coded images are given by x(m,n) and $\hat{x}(m,n)$, respectively, and both are X by Y pixels in size. Thus, in later sections when we discuss the *rate-distortion performance* of a coding algorithm, we are simply referring average distortion introduced into the output image as measured by (1) or (2) compared to the number of bits used to represent it in coded form.

3. IMAGE COMPRESSION

3.1 Overview

The objective of still image compression or coding is to reduce the number of bits of information needed to represent a given image by eliminating redundancy in the image (lossless compression) and by introducing distortion into the image in a manner which is acceptable to the viewer [4]. While lossless compression is desirable, the amount of bit rate reduction it can achieve depends on the entropy or information content of the image. Allowing distortion to be added to the image by the compression process results in a loss of information, but it also makes it possible to achieve arbitrarily high compression ratios at the cost of accepting large amounts of distortion. Thus, any lossy image compression algorithm must characterized by a rate versus distortion curve in order to properly characterize its quality.

In recent years, four major coding techniques have dominated the engineering literature, and all of these have become commercially available in some form. The four major approaches are: discrete cosine transform (DCT), wavelet transform (WT), vector quantization (VQ), and fractal. Some of these techniques can also be combined to create a hybrid coding algorithm, the most common approach to this being to combine a transform with VQ. In this work, we give only a brief overview of each of these methods, focusing on characteristics which affect their utility in WC/BDI applications.

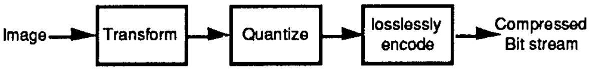

Figure 1: Block diagram of an image encoder.

3.2 Discrete Cosine Transform

Coders based on the DCT are by far the most pervasive today. Included in this group are the motion picture experts group (MPEG) 1 and 2 standards for broadcast video [1], [2], the CCITT H.261 standard for video teleconferencing [5], and the joint photographics experts group (JPEG) standard for still image compression [6]. For these coding algorithms, a separable 2D DCT is performed on each 8x8 block of image pixels. Specifically, the forward transform of the DCT is defined by the JPEG standard as

$$F(u,v) = \frac{C(u)C(v)}{4} \sum_{j=0}^{7} \sum_{k=0}^{7} \left\{ \begin{array}{l} f(j,k)\cos\left[\frac{(2j+1)u\pi}{16}\right] \\ \cdot\cos\left[\frac{(2k+1)v\pi}{16}\right] \end{array} \right\} \qquad (3)$$

where f(j,k) is an 8x8 block of image pixels and

$$C(x) = \begin{cases} \frac{1}{\sqrt{2}} & \text{if } x = 0 \\ 1 & \text{otherwise} \end{cases}. \qquad (4)$$

The inverse transform is similarly defined with the roles of (j,k) interchanged with those of (u,v). Using these relatively small blocks reduces the amount of computation required and preserves a reasonable amount of spatial locality in the transform domain. This second point is important because the underlying statistics of a typical image are highly nonstationary and, therefore, to maximize coding efficiency, bits must be allocated spatially across the image in a nonuniform manner. In addition, since non-overlapping blocks of the image are transformed, the entire process is easily parallelized. The use of nonoverlapping blocks is also the Achilles heel of such algorithms at low bit rates, however, because block boundaries begin to appear in the reconstructed image. These artifacts begin to emerge in JPEG-coded images as the compression ratio is increased above 20:1.

Figure 1 shows a block diagram of the complete transform-based image encoder in its simplest form. In the figure, each block of the image is first converted into its frequency components by the transform (defined by (1) for the DCT). After transformation, the blocks of coefficients are quantized with varying numbers of bits being allocated to different frequency components. The distribution of bits amongst the frequency components can be either fixed for all time or it can be adapted and transmitted to as side information-- this second approach generally provides superior performance. After quantization, the coefficients are losslessly encoded either by using run-length and Huffman coding or by using an arithmetic coder. The purpose of the lossless coding is to eliminate any remaining statistical redundancy in the image; thus, if the corruption of 1 bit during transmission causes the reconstructed image to degrade into white noise, the encoder has done an excellent job. It should be noted that the use of lossless coding makes this coder inherently

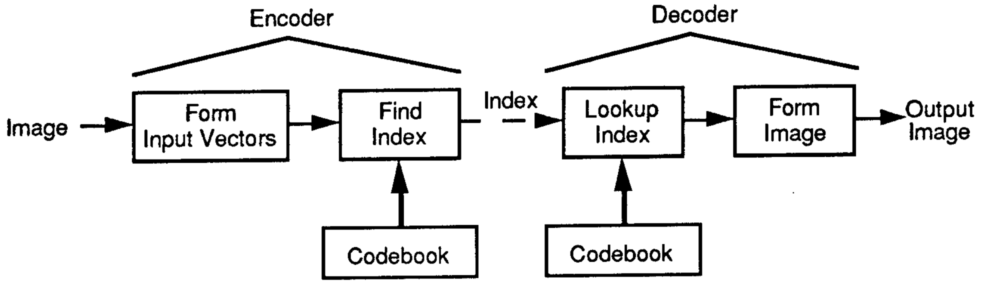

Figure 4: Vector quantization-based encoder and decoder.

A wavelet-packet decomposition uses the basic filtering process described by Fig. 2, but instead of successively subdividing the low-low band, it adapts the decomposition to the image using some criterion. The first work in this field used entropy to determine whether or not a given band was further subdivided [16] while later work optimized the decomposition in a rate-distortion sense [17]. These methods are very computationally expensive compared to a standard wavelet transform because of the added need to adaptive the decomposition, but, when combined with the zerotree concept, they deliver excellent rate-distortion performance on difficult images [18].

In terms of the objective PSNR (or equivalently MSE) distortion measure, wavelet-based coding algorithms outperform DCT-based algorithms at all bit rates. This difference, however, only becomes visually perceptible at lower bit rates and even this is mostly because of the serious blocking artifacts which appear in the DCT-coded image. Thus, for higher bit rate applications (e.g. less than 20:1 compression ratios) there is little perceptible advantage to using a wavelet-based over a DCT-based coder, but there is a considerable increase in computational complexity. The computational complexity of a DWT for an NxN image is kN^2 where the constant k depends on the exact filters used in Fig. 2 and the number of levels of the wavelet decomposition. For the very low complexity 5/3 biorthogonal wavelet [11] with 5 levels of decomposition k is 30 while for the allpass wavelet (the most computationally efficient wavelet having good filter quality) it is 7 [19]. The complexity of the block based-DCT, on the other hand, is also kN^2 but with k less than one, giving it a considerable computational advantage. At very low bit rates, however, the perceptual quality of a wavelet-coded image is far better than that of a block-based DCT. In such situations, the image coded with the DWT is generally blurred, suffering from ringing or blocking artifacts at sharp edges within the image. The exact nature and extent of these artifacts depend on the lengths and smoothness of the wavelet filters used in the decomposition. For shorter biorthogonal wavelets, such distortions are not severe, and reasonable image quality can often be attained down to compression ratios of 100:1.

3.4 Vector Quantization Methods

A Vector quantizer groups L input samples (in this case pixels) together into an input vector **x** and measures the Euclidean distance,

$$d = \sum_{k=0}^{L-1} (x(k) - c_i(k))^2 , \tag{3}$$

between that vector and a set of codevectors $\mathbf{c}_i$ in what is called the codebook. The index i of the codevector with the smallest Euclidean distance (i.e., the one most similar to the input vector) is then transmitted to the receiver which then looks up this index in its own codebook to find an approximation to the original input vector. The encoder and decoder for this process are illustrated in Fig. 4. Note that the encoder and decoder must have access to exactly the same codebooks and that the quality of this method is directly dependent on the quality of the codebook.

The motivation for this technique comes from an observation in Shannon's landmark paper [3] that by allowing the size of the coded vector to grow to infinity, the efficiency of the coder could achieve the theoretical bound--i.e., the vector could be coded with the absolute minimum number of bits. Unfortunately, infinite length vectors are difficult to work with in practice, and this theoretical observation provides no clues as to how one might actually design the vector quantizer. An algorithm called the generalize Lloyd or LBG (Linda, Buzo, and Gray) algorithm [20] has been developed to design VQ codebooks, but it is only guaranteed to converge to a locally optimal solution. As the dimension of the input vector and the size of the codebook increase, it becomes more and more difficult to find good solutions using this algorithm. This problem becomes especially obvious when one directly applies VQ to image compression because the input vector are reasonably large (typically 4x4 or 8x8 groups of pixels) and the codebooks are very large (many thousands of codevectors). Even worse, however, is the huge variety of possible input sequences. The VQ codebook design process tries to distill out of a sequence of training vectors the essential "truths" of that sequence-- i.e., the fundamental feature blocks that best describe a set of images. Unfortunately, the space of all possible image sequences is simply too broad for such a method to be effective. On smaller, narrowly defined image sets, though, such techniques may prove to be very useful.

In order to overcome some of the limitations of this unstructured VQ approach, numerous researcher have studied ways to add structure to the VQ coder. Some approaches which have been found to be useful for image compression include mean-gain-shape VQ [21], transform VQ [22], [23], product code VQ [24], and multiresolutional VQ [25]. All of these techniques allow a priori knowledge about the input source to be included into the coding model, simplifying and robustifying the design. In addition, if the VQ is forced to have a binary, tree-structured codebook, the search complexity for a codebook of size M can be reduced from M Euclidean distance comparisons to just $\log_2 M$. The decoder operation is simply a table lookup operation, so the encoder search represents all of the complexity in a conventional VQ implementation. From the perspective of the WC/BDI problem, it is unfortunate that most of the complexity resides in the expendable encoder. If vectors of size 4x4 are used, each Euclidean distance calculation requires 32 operations, making the total complexity $2 \cdot M \cdot N^2$ operations for an image of size NxN. While this is quite high (M is generally greater than 1000), the structure of this search process is very regular and, consequently, well suited to VLSI implementations.

Despite their theoretical advantages, the performance of most VQ codering algorithms on images taken from outside their training sets lags that of transform-based coders. It should be noted, however, that vector quantization is actually a superset of all of the other image coding techniques discussed in this paper. For example, a coder with identical rate-distortion performance to the JPEG coder can be implemented using a full search VQ on 8x8 blocks of image pixels-- the DCT, quantization, and lossless compression can be implicitly incorporated into the VQ codebook. Even fractal coding, which is discussed in the next section, can be implemented in a VQ framework. Of course, it is generally more efficient to implement transform and fractal coders explicitly than it is to use a VQ formulation.

3.5 Fractal Methods

Fractal coding methods are based on the assumption that natural images have fractal characteristics-- i.e., that the same basic features appear in different spatial locations and at different scales throughout the image. While a fractal coder also uses transformations, it is far different than those discussed above because the transforms themselves and not the transform coefficients are what is transmitted to the decoder. A fractal-based encoding algorithm is shown in Fig. 5. Basically, a number of mappings must be devised which map all of the blocks of the image to other, smaller blocks of the image. Going from large to small blocks results in a contractive mapping which is a necessary condition to ensure convergence in the decoder when the mapping is iterated. Overlapping is allowed in both the domain (original) blocks and the range (translated and contracted) blocks and the Collage Theorem is used to smoothly fuse blocks together. If the mappings are designed properly, an approximation of the original image can be reconstructed in the decoder by iteratively implementing these mappings (starting from any arbitrary image) until convergence is achieved. An excellent, in-depth treatment of fractal coder design is presented in [26].

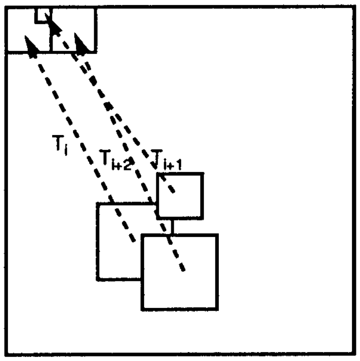

Figure 5: Block mappings for iterative fractal encoder.

While fractal coding algorithms are amongst the most mathematically elegant, they do have their drawbacks. The first and foremost of these is that their encoder complexities are extremely high. By contrast, the complexity of a fractal decoder is almost trivial, but, unfortunately, this asymmetry is exactly the opposite what is needed for still frame compression in WC/BDI applications. In addition, the rate-distortion performance of fractal coders has been found to be generally inferior to that of DCT- and wavelet-based coders. Some impressive claims of good image quality at compression ratios of 1000:1 have been made, but these have not been well substantiated in comparative tests on large, diverse sets of natural images.

4. VIDEO COMPRESSION

4.1 Overview

In video coding algorithms, both interframe and intraframe redundancy are removed from an image sequence. To remove intraframe redundancy, one of the still image compression algorithms discussed in the last section is often used. The most common video coding schemes use block-based motion-compensated prediction to create a residual image which has very low energy and can, therefore, be coded with very few bits . A generic encoder is shown in Fig. 6 while the corresponding decoder is shown in Fig. 7. Most of the video coding algorithms using motion-compensation fit into this framework, including MPEG 1 and 2. Comparing the figures, one notes that the video encoder actually contains a complete copy of the still frame decoder in its feedback loop. Excluding the still frame encoder and decoder, the two most complex blocks in Fig. 6 are the motion estimation and rate buffer blocks. By effectively estimating the motion and compensating for it in the feedback loop, a residual image with little energy is formed, and this can be coded by the still frame encoder with very few bits. As a general rule, however, the better the motion estimate is, the more complex the estimator must be. The rate buffer, on the other hand, does not require a lot of computational processing power to implement: it is complex because it must dynamically adjust the quantization in the still frame encoder so that a constant bit rate can be output without buffer over- or underflows. Performing this operation well requires large amounts of

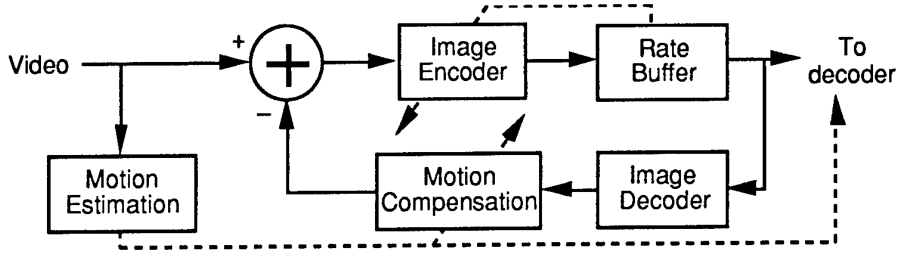

Figure 6: Generic video encoding system.

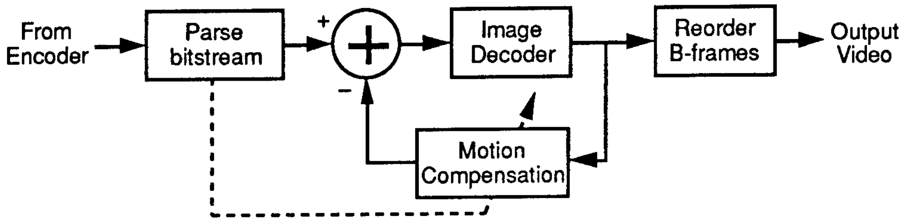

Figure 7: Generic video decoding system.

hand optimization in the design process and a lot of logic circuitry in the buffer controller. A number of possible rate buffer implementations have been proposed in [27]-[29].

4.2 Video Encoding and Decoding

The video encoder described by Fig. 6 can produce three different types of video frames: I-frames, B-frames, and P-frames. A typical mix of such frames is shown in Fig. 8. An I-frame is coded only using information from within that frame (i.e., intraframe coded), and, consequently, allows a clean break-in or resynchronization point within the video sequence. It is very important to have these break-in points to allow the receiver to resynchronize in the event of an uncorrected transmission bit error. The density of I-frames determines how many seconds of video are corrupted in the event of a transmission error. A P-frame, on the other hand, is the prediction residual from the last P- or I-frame in the sequence-- it has no dependence on future frames. Obviously, P-frames do not offer break-in points and errors from past frames will propagate into them. The last standard kind of frame is a B-frame which is bidirectionally predicted from both past and future frames. The highest compression is achieved with B-frames, but they cannot be used to predict future frames because they, themselves, depend on future frames

By comparison, the operation of the video decoder as shown in Fig. 7 is quite simple with its most complex element being the still frame decoder. The reordering block is needed only if bidirectionally predicted frames are used and, while it increases the memory requirements of the decoder, it has no impact on its computational complexity. Note that the decoder shown in Fig. 7 does not support the use of motion-compensated interpolation to fill in discarded frames. Using this interpolation greatly increases the computational complexity of the decoder with no cost to the encoder, making it well suited to the remote-sensing paradigm.

4.3 3D Subband Coding

Another video compression technology which has shown much promise in recent years is motion-compensated 3-dimensional subband coding. A 3D subband decomposition transforms the sequence not only in the two spatial dimensions but also in the temporal dimension, creating a time-frequency-space mapping of the sequence. In theory, this decomposition alone should be able to capture and localize motion information, but recent work has found that the addition of global motion compensation greatly improves performance [30], [31]. The video encoding and decoding algorithms shown in Figs. 6 and 7 also describe the basic structure of a motion-compensated 3D subband coder where the 'image encoder' and 'image decoder' blocks now process sets of images. Obviously, this also forces other blocks in the system, most notably the motion compensation block, to process sets of image frames as well.

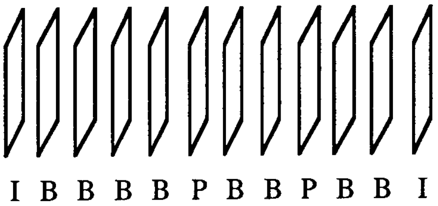

Figure 8: Typical mix of coded frames. I-frames, P-frames, and B-frames are intra, unidirectionally- predicted, and bidirectionally-predicted frames, respectively.

4.4 Motion-Compensated Interpolation

An important technique for improving the perceptual quality of compressed image sequences is bidirectionally motion-compensated interpolation. This approach is illustrated in Fig. 9. First, the past and future frames are reconstructed, and these are used along with motion information to interpolate the missing frames. In Fig. 9, for example, the interpolated frame I_1 is a linear combination of 4/5ths the past frame and 1/5th the future frame where each of these have been motion compensated before being combined. To perform the motion compensation, the past frame is moved forward along the motion vector(s) while the future frame is moved backward along it (them). If multiple vectors are used in a block-based compensation scheme, overlapping and non-covered areas in the interpolated images must be considered. Bidirectional interpolation does not truly add any new information to the image sequence, but it does increase its perceived quality by maintaining a sharp, smooth blending of true image frames, simulating a far higher frame rate than was actually transmitted. Note that bidirectional interpolation is a part of the bidirectional predictive coding used in Fig. 6 and 7-- the bidirectionally interpolated image forms the estimate which is subtracted from the original image to create the differential update (B-frame) in the encoder. The MPEG coding algorithm also allows for the use of motion-compensated interpolation in the decoder [1].

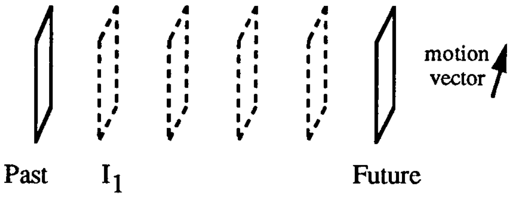

Figure 9: Motion compensated interpolation.

4.5 Motion Estimation

The motion estimation process is truly the heart of video compression in that it has a very large effect on the efficiency of the system and pn the quality of the resulting output. The most common method currently used is block-based motion estimation where blocks of pixels from the past frame are compared with blocks in the current frame in under to determine where they moved. Using these vectors, one can then compensate the past frame in Fig. 6 for the motion (e.g., move the blocks to their new locations) before subtracting it from the current frame [32]. The most common way to determine the movement of the blocks is to use full-search block matching in which a spatial-domain correlation is performed between a block in the previous frame and a region around that block in the current frame. This is computationally expensive, and it often results in poor motion estimates when displacements of less than one pixel are involved. To overcome this second problem, one can interpolate the blocks to achieve subpixel accuracy, but this further increases the computational complexity. Faster spatial correlation methods such as the three point search have been developed to reduce the computational complexity [4], but these only converge to the optimal motion vector if the error surface is convex (which is not often the case).

Another class of motion vector estimation methods are those based on frequency domain correlations. For example, block matching can also be done by taking the fast Fourier transforms (FFTs) of the past and current blocks, multiplying them, and then taking the inverse FFT. This has the advantage over spatial domain correlation in that subpixel accuracy can be achieved simply by zero padding in the transform domain. Another approach is to perform the frequency domain correlation over the entire frame and then do block matching at the correlation spikes to determine which blocks moved where. This has proven to be especially effective for high quality interpolation using a variant frequency-domain method called phase correlation [33]-[35]. Finally, we note that, thus far, pixel based methods like optical flow [36]-[38] have not been widely applied in image coding because of the high cost associated with coding the flow vectors.

5. WC/BDI TRADEOFFS IN VIDEO CODERS DESIGN

The most important features in a video coding algorithm designed for weapons control and bomb damage indication applications are low encoding complexity, low latency, acceptable quality, flexible data type, and robustness to channel errors. All of these can be simultaneously achieved as long as one does not also constrain the bit rate. Of course, all realistic channels have bandwidth constraints, so perfectly satisfying all of these constraints in the same system is impossible. Instead, one must study the tradeoffs associated with different design decisions.

5.1 Encoding Complexity

5.1.1 Still Frame Encoding

The conventional video encoder shown in Fig. 6 contains a still frame encoder and decoder. In the case of a DCT- or wavelet-based algorithm, the inclusion of this feedback loop doubles the complexity of the video encoder. Using instead a non-symmetric still frame scheme like VQ or fractal coding greatly reduces the cost of adding the decoder to the feedback loop but greatly increases the basic cost of the encoder, leading to a net increase in computational complexity over a transform-based system. Given this along with our earlier discussion about still-frame coding algorithms, we conclude that the best choice is a transform coder, although which one depends very much on the bit rate at which the system is designed to operate. Because both the forward and inverse transforms must be performed, the computational advantage of the block-based DCT over the wavelet transform becomes even more pronounced. On the other hand, if too few bits are allocated to code each I-frame, severe artifacts are introduced into the sequence by the transform, and these will only be exacerbated in the differentially coded frames. Consequently, despite its computational complexity, wavelet-based coders are preferable at lower bit rates.

5.1.2 Video Encoding

As pointed out in the last section, the feedback loop in Fig. 6 adds a great deal of computational complexity to the system. If subpixel interpolation is used in the motion-compensation block, the encoder complexity is increased even more. If the motion compensation can instead be performed in the transform domain, the still frame decoder block can be eliminated, greatly reducing the complexity. While this has been recently proposed [39], the idea is not yet proven. Better still would be the elimination of the entire feedback loop, but this would make it much more difficult to exploit temporal redundancy in the sequence.

5.2 Low Latency

The need for low latency is most obvious in the weapons control problem-- if the delay between when the image was acquired and when it is viewed by the pilot becomes too great, then by the time the pilot's control input gets to the weapon it might be too late to update the weapons course. The latency issue is simplified, however, because the pilot does not directly control the weapon: he simply performs the final target selection. Thus, a few seconds of latency in the video may be acceptable as long as a frame motion history is maintained in the weapon so that it knows where a spot designated in a past frame has moved to in the current frame. The issue of exactly how much latency can be tolerated for weapons control depends largely on the speed and maneuverability of the weapons as well as the speed of the target. Since man-in-the-loop control is generally only used for ground targets and with relatively slow weapon platforms, it is likely that considerable delay can be tolerated.

For the BDI problem, the requirements for video latency are less severe, but they still exist. Consider, for example, an encoder which introduces a latency of 2 seconds into the video stream. With such an encoder we will lose, on the average, the last second of video which, if the BDI sensor is mounted on the weapon itself, could be critical information. Thus, latency must be considered in this application as well.

5.3 Acceptable Quality

While objective measures like MSE (or, equivalently PSNR) roughly characterize image quality, it is well known that they have many flaws. It is for this reason that human perceptual evaluations have formed the cornerstone of HDTV evaluation. The same holds true for WC/BDI applications but with a twist: it is not important that the video 'look good', but rather it is only important that the video be usable. Thus, pilots and analysts must be able to examine the video to recognize targets and to assess damage. A highly compressed image appears to be blurrier than the original, but the actual distortion is highly nonlinear. This means that subjective evaluations with the actual users of this video are necessary-- evaluations which must be performed within a statistically valid framework to be meaningful. In other words, the evaluation must do more than simply asks for opinions; it must assess the ability of the subject to correctly perform his job. Little such data currently exists, making it impossible to accurately characterize the image quality required of a future WC/BDI system.

5.4 Flexible Data Types

Logistically, it would make sense to use common, scalable image and video compression algorithms for all resolutions and types of sensors. Visible and imaging infrared (IIR) sensors are the most likely candidates for WC/BDI compression, but one might wish to use the same datalink to also transmit Ladar and SAR images for other applications. Thus, it makes sense to design flexibility into the system. In a general sense, just using a digital communications system greatly increases the flexibility over older analog system which had frame rates and resolutions built directly into the waveform. To achieve the best compression performance on all data types, however, it is important that the encoder be fully adaptive-- i.e., that it not depend on a priori knowledge about the image set. Such knowledge is invariably sensor dependent and is unlikely to generalize well. This a priori information often appears in a coding algorithm in the form of VQ codebooks, nonuniform scalar quantizers, Huffman lookup tables and arithmetic coder models. These last two are only a problem if they are fixed rather than being image adaptive.

5.5 Robustness to Channel Errors

The RF environment is a noisy one because every electronic device radiates some RF energy at some frequencies. In the military arena, this unintentional radiation is compounded by the problem of intentional jamming by the enemy. The process of compression or source coding as it is called by Shannon extracts redundancy from the input signal. If the source coding is optimal (i.e., all redundancy has been extracted) then a single bit error in transmission will turn the reconstructed signal at the receiver into noise. To protect the compressed signal, it is necessary to add redundancy back into it in such a way that errors can be detected and/or corrected. This is called channel coding. Shannon has shown that the optimal transmission signal (in terms of bit rate and robustness to channel errors) can be achieved by using separate source and channel coding [3]. The two most common forms of channel coding used today are the block-based Reed-Solomon and BCH codes and the infinitely extending convolutional codes [40]. Recently, research has begun on joint source-channel coding in an effort to decrease the complexity of the complete system [41], but such efforts are still in their early stages.

The other major factor affecting both the bit throughput and the signal robustness is the analog modulation. Using advanced modulation techniques like quadrature amplitude modulation (QAM) [42] or vestigial sideband modulation (VSB) [43], it is possible to robustly transmit 20 Mbits/sec of digital data over a single 6 MHz analog television channel. Even using MPEG 1 compression with its nominal bit rate of 1.5 Mbits/sec, one can transmit 13 digital channels in the space currently used for one analog channel. These advanced modulation schemes are optimized for Gaussian noise because that is generally a reasonable model for noise sources in such RF channels. Thus, while a Gaussian noise jammer is very hard to overcome for an analog video transmission

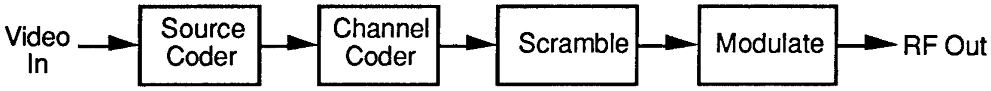

Figure 10: Complete video transmission system.

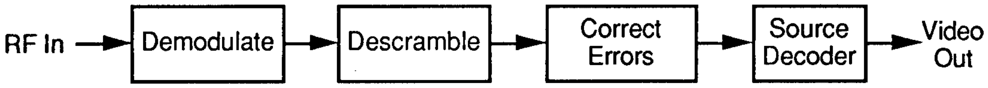

Figure 11: Complete video receiver.

system, it is actually the best case for a digital system. For the digital system, long burst errors are the worst case, but this problem can be minimized by scrambling the bit stream as it leaves the channel coder. Complete diagrams of the transmitter and the receiver are shown in Figs. 10 and 11.

Unfortunately, little work has been done so far in characterizing interference sources in the military environment and quantifying their effects on the quality of digitally transmitted video. It is quite possible that unintentional RF radiation from the aircraft could be a greater problem than intentional jamming from the ground. Ultimately, one or more video transmission systems must be rigorously demonstrated in a realistic RF environment before these questions can be convincingly answered.

6. CONCLUSION

We have discussed a wide range of image and video coding algorithms, analyzing their suitability for weapons control and bomb damage indication applications. In the course of this investigation, we have concluded that while block-based DCT algorithms are superior for high bit rate, high quality video applications, wavelet-based algorithms are the better choice for low bit rate, reduced-quality video. Before actual systems can be adopted, however, there are still many questions which must be answered. Of these, the two most important are what level of video quality is required for the weapons control and BDI applications and how does the battlefield RF environment affect the video datalink. Once these questions have been answered, the problem of constructing a new digital video compression and communications system will be bounded, allowing the many engineering tradeoffs associated with such a system to be made and ultimately resulting in the introduction of this technology onto the battlefield.

REFERENCES

[1] D.J. LeGall, "The MPEG video compression algorithm: a review," *SPIE Vol. 1452 Image Proc. Algorithms and Techniques II*, 1991, pp. 444-457.

[2] K. Challapali, et. al., "The grand alliance system for US HDTV," *Proceedings of the IEEE*, Vol. 83, No. 2, Feb. 1995, pp. 158-174.

[3] C.E. Shannon, "A mathematical theory of communications," *Bell Systems Technical Journal*, Vol. 27, 1948, pp. 379-423, 623-656.

[4] A.N. Netravali and B.G. Haskell, *Digital Pictures: Representation and Compression*, Plenum Press, NY, 1988.

[5] "Video coder for audio visual services at px64 Kbits/sec," Recommendation H.261, The Consultative Committee on International Telephony and Telegraphy, 1990.

[6] G.K. Wallace, "Overview of the JPEG (ISO/CCITT) still image compression standard," *SPIE Vol. 1244, Image Proc. Algorithms and Techniques*, 1990, pp. 220-233.

[7] P.P. Vaidyanathan, *Multirate Systems and Filter Banks*, Prentice Hall, Englewood Cliffs, NJ, 1993.

[8] J.W. Woods and S.D. O'Neil, "Subband coding of images," *IEEE Trans. on Acoustics, Speech, and Signal Proc.*, Vol. ASSP-34, Oct. 1986, pp. 1278-1288.

[9] M.J.T. Smith and T.P. Barnwell, "Exact reconstruction techniques for tree-structured subband coders," *IEEE Trans. on Acoustics, Speech, and Signal Proc.*, Vol. ASSP-34, No. 3, June 1986, pp. 434-440.

[10] I. Daubechies, "Orthonormal bases of compactly supported wavelets," *Comm. on Pure and Applied Math.*, Vol. XLI, 1988, pp. 909-996.

[11] I. Daubechies, *Ten Lectures on Wavelets*, SIAM, Philadelphia, PA, 1992.

[12] M. Lightstone and E. Majani, "Low bit-rate design considerations for wavelet-based image coding," *Proc. of the SPIE Symposium on Visual Comm. and Image Proc.*, Sept. 1994.

[13] M. Antonini, et. al., "Image coding using wavelet transforms," *IEEE Trans. on Image Proc.*, Vol. 1, No. 2, April 1992, pp. 205-220.

[14] J.M. Shapiro, "Embedded image coding using zerotrees of wavelet coefficients," *IEEE Trans. on Signal Proc.*, Vol. 41, No. 12, Dec. 1993, pp. 3445-3462.

[15] Z. Xiong, K. Ramchandran, and M.T. Orchard, "Joint optimization of scalar and tree-structured quantization of wavelet image decompositions," *Proc. of the 27th Annual Asilomar Conf. on Signals, Systems, and Computers*, Nov. 1993, Pacific Grove, CA, pp. 891-895.

[16] R.R. Coifman and M.V. Wickerhauser, "Entropy -based algorithms for best basis selection," *IEEE Trans. on Info. Theory*, Vol. 38, No. 2, March 1992, pp. 713-718.

[17] K. Ramchandran and M. Vetterli, "Best wavelet packet bases in a rate-distortion sense," IEEE Trans. on Image Proc., Vol. 2, No. 2, April 1993, pp. 160-175.

[18] Z. Xiong, K. Ramchandran, M.T. Orchard, "Wavelet packet-based image coding using joint space-frequency quantization," *Proc. Int. Conf. on Image Proc.*, Nov. 1994, pp. 324-328.

[19] C.D. Creusere and S.K. Mitra, "Image coding using wavelets based on perfect reconstruction IIR filter banks," submitted to *IEEE Trans. on Circuits & Systems: Video Technology*, revised March 1995.

[20] Y. Linde, A. Buzo, and R.M. Gray, "An algorithm for vector quantizer design," IEEE Trans. on Communications, Vol. COM-28, Jan. 1980, pp. 84-95.

[21] M. Lightstone and S.K. Mitra, "Entropy-constrained mean-gain-shape VQ for image compression," *Proc. of the SPIE VCIP*, 1994.

[22] P.H. Westerink, et. al., "Subband coding of images using VQ," IEEE Trans. on Communications, Vol. 36, No. 6, June 1988, pp. 713-719.

[23] M. Antonini, et. al., "Image coding using VQ in the wavelet transform domain," *Proc. Int. Conf. on Acoustics, Speech, and Signal Proc.*, 1990, pp. 2297-2300.

[24] M. Lightstone, D. Miller, and S.K. Mitra, "Entropy-constrained product code VQ with application to image coding," *Proc. Int. Conf. on Image Proc.*, Nov. 1994.

[25] A. Gersho and R.M. Gray, *Vector Quantization and Signal Compression*, Kluwer Academic Publishers, Boston, MA, 1992.

[26] A.E. Jacquin, "Fractal image coding: a review," *Proceedings of the IEEE*, Vol. 81, No. 10, Oct. 1993, pp. 1451-1465.

[27] C.T. Chen and A. Wong, "A self-governing rate buffer control strategy for pseudoconstant bit rate video coding," *IEEE Trans. on Image Proc.*, Vol. 2, No. 1, Jan. 1993, pp. 50-59.

[28] M.R. Pickering and J.F. Arnold, "A perceptually efficient VBR rate control algorithm," *IEEE Trans. on Image Proc.*, Vol. 3, No. 5, Sept. 1994, pp. 527-532.

[29] K. Ramchandran, A. Ortega, and M. Vetterli, "Bit allocation for dependent quantization with application to multiresolution and MPEG video coders," *IEEE Trans. on Image Proc.*, Vol. 3, No. 5, Sept. 1994, pp. 533-545.

[30] J.-R. Ohm, "Three-dimensional subband coding with motion compensation," *IEEE Trans. on Image Proc.*, Vol. 3, No. 5, Sept. 1994, pp. 559-571.

[31] D. Taubman and A. Zakhor, "Multirate 3-D subband coding of video," *IEEE Trans. on Image Proc.*, Vol. 3, No. 5, Sept. 1994, pp. 572-588.

[32] M. Bierling, "Displacement estimation by hierarchical blockmatching," *Proc. SPIE Visual Comm. Image Proc.*, Vol. 1001, 1988, pp. 942-951.

[33] M. Goetze, "Generation of motion vector fields for motion compensated interpolation of HDTV signals," *Signal Proc. of HDTV*, Elsevier Science Publishers, North-Holland, 1988, pp. 383-391.

[34] G.M.X. Fernando and D.W. Parker, "Motion compensated display conversion," *Signal Proc. of HDTV*, Elsevier Science Publishers, North-Holland, 1988, pp. 393-399.

[35] Th. Reuter and H.D. Hoehne, "Motion vector estimation for improved standards conversion," *Signal Proc. of HDTV*, Elsevier Science Publishers, North-Holland, 1988, pp. 345-354.

[36] J.L. Barr, D.J. Fleet, and S.S. Beachemin, "Systems and experiments, performance of optical flow techniques," *Int. Journal of Computer Vision*, Vol. 12, No. 1, 1994, pp. 43-77.

[37] G. Hewer, C. Kenny, and W. Kuo, "Wavelets, curvature, and chaining issues with application to optical flow," *Proceedings of the SPIE Conf.*, vol. 2277, San Diego, CA, July 1994, pp. 253-264.

[38] G. Hewer, C. Kenney, W. Kuo, and L. Peterson, "Curvature and aggregate velocity for optical flow," *Proceedings of the SPIE Conf.*, vol. 2567, San Diego, CA, July 1995.

[39] H. Ito and N. Farvardin, "On motion compensation of wavelet coefficients," *Proc. Int. Conf. on Acoustics, Speech, and Signal Proc.*, May 1995.

[40] R.E. Blahut, *Theory and Practice of Error Control Codes*, Addison-Wesley Pub. Co., Reading, MA, 1983.

[41] T.P. O'Rourke, et. al., "Robust transmission of compressed images over noisy Gaussian channels," *Proc. Int. Conf. on Acoustics, Speech, and Signal Proc.*, May 1995.

[42] L. Goldberg, "IC opens 500-channel frontier to cable systems," *Electronic Design*, Vol. 42, No. 23, Nov. 7, 1994, pp. 71-80.

[43] R. Citta, et. al., "The digital spectrum compatible HDTV transmission system," *IEEE Trans. on Consumer Electronics*, Vol. 38, Aug. 1991, pp. 101-107.

Exploitation of Differential GPS for Guidance Enhancement (EDGE) High Gear Program

Capt John L. Dargan
Gary Howell
Tim Elbert
David Gaskill

ASC OL/YU
102 West D Avenue, Suite 168
Eglin AFB FL 32542-6807

SUMMARY

History was made on May 23, 1995 as an Air Force F-16 dropped a modified GBU-15 from an altitude of 25,000 feet and a down range distance of 87,000 feet against a vertical target. The modified GBU-15, incorporating a differentially corrected INS/GPS navigation scheme, became the first seekerless, autonomous, Inertial Navigation System (INS)/Global Position System (GPS) weapon to successfully attack a vertical target, impacting within 2 meters of the target aimpoint. This historic flight was accomplished in the middle of a successful six-drop test program conducted at Eglin Air Force Base, Florida.

The EDGE program was designated an Air Force Materiel Command High Gear Program, allowing streamlined acquisition and reporting procedures, in response to the Joint Direct Attack Munition (JDAM) plan for adding precision capability to its baseline GPS-guided munition. A precision-capable, seekerless, autonomous, INS/GPS weapon is a force multiplier in that fewer weapons are needed to strike the target and future host aircraft can be designed to be smaller and more "stealthy" since less weapon carriage is required.

EDGE met its objective to demonstrate the navigation accuracy improvement potential of differential GPS (DGPS) for guiding air-to-ground munitions through an end-to-end weapon system implementation of DGPS using a DGPS reference receiver network, a modified GBU-15 glide bomb, and a Block 50 F-16D launch aircraft.. Results show precision navigation accuracy is attainable through DGPS. This paper provides additional details on EDGE system implementation and results from ground, captive, and free-flight tests.

INTRODUCTION

The EDGE program was initiated in response to the Joint Direct Attack Munition (JDAM) plan for adding precision capability to its baseline GPS-guided munition. The objective of EDGE was to demonstrate the navigation accuracy improvement potential of Differential GPS (DGPS) with a goal of improving current GPS-guided munition accuracy from about 13 m circular error probable (CEP) to less than 5 m. In order to more readily assess EDGE navigation performance, other weapon system errors were mitigated as much as possible such that navigation error became the dominant weapon error source.

Weapon system errors can be divided into three major sources: guidance errors (including aerodynamic and autopilot error sources), target location errors (TLE), and navigation errors (both INS and DGPS error sources). Errors due to the implementation of the EDGE guidance algorithm, the autopilot algorithm, and aerodynamic uncertainties were approximately 30 centimeters. Target location error, normally a significant weapon error source, was also reduced to 30 centimeters. This was accomplished through a survey of EDGE target locations by the Defense Mapping Agency (DMA). Thus, navigation was the dominant error source for EDGE, and any system error assessed during testing could be attributed primarily to navigation.

Overall, the EDGE objective and goal were accomplished, demonstrating precision navigation accuracy is attainable through DGPS. Static ground testing, captive flight testing, and free flight testing were used to assess navigation accuracy through an end-to-end weapon system

Paper presented at the AGARD MSP Symposium on "Technologies for Precision Air Strike Operations in Rapid-Reaction and Localised-Conflict Scenarios", held in Seville, Spain, from 16-19 October 1995, and published in CP-576.

implementation of DGPS using a DGPS reference receiver network, a modified GBU-15 glide bomb, and a Block 50 F-16D launch aircraft. The demonstration culminated with the modified GBU-15 using DGPS guidance to attack both horizontal and vertical test targets located on the Eglin Air Force Base (AFB) test range.

Numerous systems integration and functionality tests were conducted in support of the EDGE program. The focus of this paper is on the implementation, integration, and performance of the DGPS reference receiver network and the weapon INS/GPS navigation system.

EDGE SYSTEM

Overview

As illustrated in Figure 1, the EDGE system concept consisted of a DGPS reference receiver network, an Improved Data Modem (IDM), a Block 50 F-16D launch aircraft, and a modified GBU-15 glide bomb. This concept was used to test the end-to-end weapon system implementation of DGPS.

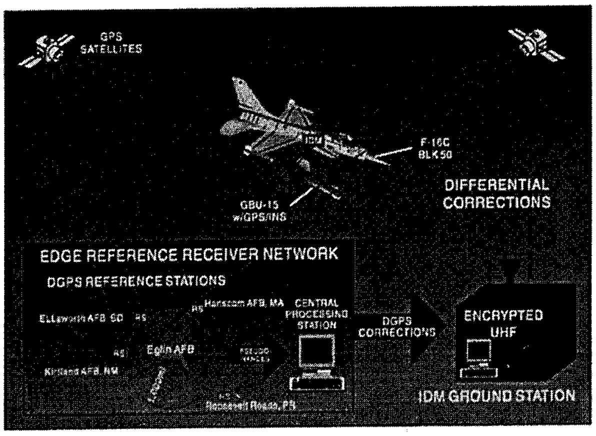

Figure 1: EDGE System Concept

The DGPS reference receiver network contained four, 12-channel P/Y code reference receivers located at sites which surrounded the theater of operation, the Eglin AFB test range, by approximately 1000 nautical miles. The reference receiver network produced "theater-wide" pseudorange corrections that removed most of the GPS space and control segment clock and ephemeris ranging errors. These pseudorange corrections were computed for all GPS satellites in view of the network and were accurate for up to thirty minutes. The reference receiver network provided the corrections to an Improved Data Modem ground station which transmitted them via a UHF data link to the launch aircraft. This single transmission to the aircraft occurred several minutes prior to weapon launch. The launch aircraft then passed the corrections via the 1553 bus to the GBU-15 Integrated Flight Management Unit (IFMU) where they were stored for use after weapon launch. The IFMU contained a strapdown INS that was tightly coupled with a five-channel P/Y code fast acquisition GPS receiver. A navigation Kalman filter was used to reset the INS. Once the aircraft launched the GBU-15, the IFMU GPS receiver entered acquisition mode and acquired five satellites on P/Y code. The receiver then began updating the navigation Kalman filter with pseudorange measurements. These measurements, however, were differenced with the respective pseudorange corrections prior to being input to the filter. This process continued throughout the 100-second weapon flight duration, thereby enhancing navigation accuracy. Additional details on the EDGE subsystems are contained below.

EDGE DGPS Reference Receiver Network

Classical DGPS typically involves a single reference receiver located on a surveyed benchmark which compares its ranging measurements to the satellites with a calculated range based upon the receiver's surveyed location. The difference between the measured range and calculated range is the differential pseudorange correction. This correction can then be given to a user-receiver miles away to improve its navigation accuracy.

The classical DGPS correction removes most of the satellite clock and ephemeris error, the ionospheric and tropospheric delay errors, and the Selective Availability (SA) clock dither error. Because the SA clock dither varies so frequently, classical DGPS corrections must be generated every six seconds to remain accurate. Also, since tropospheric and ionospheric errors are relatively constant over distances only up to 100 - 200 miles, the distance between the reference receiver and user-receiver is usually limited to this distance.

The EDGE "theater-wide" technique for differential correction generation is similar to classical DGPS with two main exceptions.

Since authorized, Department of Defense (DoD), L_1/L_2 GPS receivers were used in the EDGE weapons, the effect of SA did not have to be accounted for in the differential corrections. Thus, EDGE corrections needed only be generated once every thirty minutes to retain accuracy. Secondly, EDGE corrections removed only the satellite clock and ephemeris errors, leaving the authorized, DoD, L_1/L_2 weapon receiver to remove its own tropospheric and ionospheric delays. As such, the distance between the EDGE reference receivers and the EDGE weapon was not limited to 100 - 200 miles.

The EDGE reference receiver network surrounded the theater of operations, Eglin Air Force Base (AFB), with four Ashtech 12-channel P/Y-code reference receivers located over 1000 miles away. This ensured any satellites used by the weapon receiver were visible first to the network and guaranteed the network could generate corrections for all satellites visible to the weapon receiver. These four reference receivers were located at Roosevelt Roads Naval Station, Puerto Rico, Hanscom AFB, Massachusetts, Ellsworth AFB, South Dakota, and Kirtland AFB, New Mexico. The reference receiver stations also included a weather sensor which provided temperature, pressure, and humidity data. Each P/Y-code reference receiver made ranging measurements to all satellites in its view. These measurement data along with integrated carrier data, the satellite navigation message, and weather sensor data were transferred via telephone land lines to a central processing station at Eglin AFB. Although the reference receivers were authorized, SA was not removed from the measurement data transferred via the land lines. Instead, SA was removed from the data once it was received at the central processing station. This avoided the requirement for classified land lines. This central processing station, a Sparc 20 computer, performed several functions on these measurement data leading up to the generation of differential corrections, as shown in Figure 2.

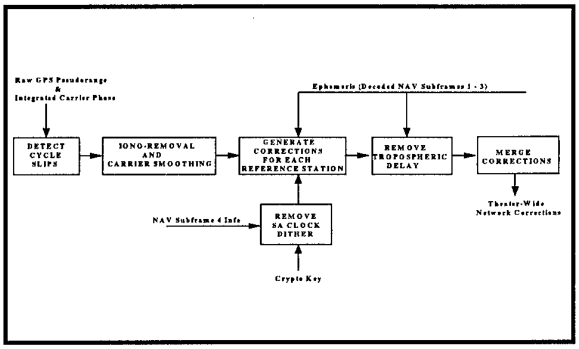
Raw GPS Pseudorange & Integrated Carrier Phase
Ephemeris (Decoded NAV Subframes 1 - 3)
DETECT CYCLE SLIPS
IONO-REMOVAL AND CARRIER SMOOTHING
GENERATE CORRECTIONS FOR EACH REFERENCE STATION
REMOVE TROPOSPHERIC DELAY
MERGE CORRECTIONS
Theater-Wide Network Corrections
NAV Subframe 4 Info
REMOVE SA CLOCK DITHER
Crypto Key

Figure 2: Central Processing Station Functional Flow Diagram

First, integrated carrier phase cycle slips were detected. Integrated carrier phase measurement data are highly accurate but with an unknown constant of integration (integer number of cycles). A cycle slip occurred when the GPS receiver momentarily lost count of the carrier cycles received, thereby providing a false measurement. Cycle slips were detected by comparing the difference between the L_1-P and L_2-P integrated carrier phase measurements. Sudden jumps in this difference were due to cycle slips. Any detected cycle slips were later corrected in the carrier smoothing process.

Next, ionospheric delay was removed from the pseudorange and the integrated carrier phase by combining L_1 and L_2 P-code measurements and L_1 and L_2 integrated carrier phase measurements, respectively. Since combining these measurements increased the overall measurement noise and effect of multipath, carrier smoothing was used to mitigate these repercussions.

Carrier smoothing is a process that takes advantage of past data to help estimate current values. Carrier smoothing was accomplished by applying a weighted average difference (between the pseudorange and integrated carrier phase in the past) to the current integrated carrier phase measurement. This resulted in a more accurate estimate for the absolute pseudorange.

Prior to calculating "theater-wide" differential corrections, pseudorange corrections were calculated for all satellites in view for each of the four respective reference receiver stations. Selective Availability clock dither was removed from the reference receiver measurement data prior to calculating the corrections. This was accomplished through the use of a combination of subframe 4 information and a GPS group-unique variable (GUV).

Next, tropospheric delay was modeled using temperature and pressure data and satellite elevation angle. Once determined, these delays were removed from the carrier-smoothed pseudorange corrections for each reference station prior to the correction merging process.

Finally, once the corrections were generated for each reference station, they were merged to form a single set optimized for the theater test location using a weighted least-squares process which took into account reference network geometry and individual correction quality.
When a satellite was visible by three or fewer stations, an averaged correction was used weighted by correction quality; when all four stations viewed a satellite, a geographical weighted average was calculated. This geographical weighted average involved a weighted least-squares process, which calculated the rate of change of correction with respect to north and east and determined the optimum correction for the network center (Eglin AFB).

Theater-wide correction quality was determined through the use of an independent quality monitor located on Eglin AFB. This quality monitor was an Ashtech 12 channel P/Y-code GPS receiver which was located on a surveyed point. The "theater wide" differential corrections were applied to the navigation solution of this static receiver. The difference between the differentially corrected navigation solution and the surveyed location was the error in the differential correction. Testing and analysis showed the "theater-wide" differential corrections had a one-sigma ranging error of 0.5m. Combining the differential correction errors with the weapon receiver ranging errors resulted in the error budget shown in Table 1.

Table 1: EDGE DGPS Error Budget

	SOURCES			
ERRORS	DGPS Correction Errors	Correction Distribution Errors	Weapon GPS Receiver Predicted Errors	TOTAL (1σ)
Carrier-smoothed measurement error*	0.15 m		1.0 m	1.01 m
Residual tropo delay	0.2 m†		0.5 m	0.54 m
Latency of corrections		0.37 m		0.37 m
Correction round-off		0.05 m		0.05 m
Displacement from virtual RR		0.0 m		0.0 m
RMS range error contributions	0.32 m	0.37 m§	1.1 m	1.2 m (UERE)
	Correction Error = 0.5 m			
	HORIZONTAL DILUTION OF PRECISION			1.5
	HORIZONTAL TARGET CEP			**2.1 m**

* Includes code noise, multipath, & residual iono
† Projected tropo error with integrated carrier phase
§ Based on 30-min correction update rate

Improved Data Modem Ground Station (IGS)

The differential corrections generated by the central processing station were formatted and provided to the IGS via an RS 232 interface. This formatted correction message was 64 bytes in length and included pseudorange corrections for 12 satellites, the satellite id numbers, the standard deviation for each respective correction, and the issue of data ephemeris used in generating each correction. After receipt of this message, the IGS encrypted it and transmitted it via a UHF data link to the improved data modem (IDM) receiver on the aircraft. After this one-time transmission was received and decrypted by the aircraft IDM receiver, the correction data were transferred via the 1553 bus to the weapon where they were stored for use after weapon launch.

EDGE Weapon

The modified, 2,000 pound GBU-15, shown in Figure 3, had the infrared (IR) seeker removed from the guidance package and replaced with the INS/GPS hardware.

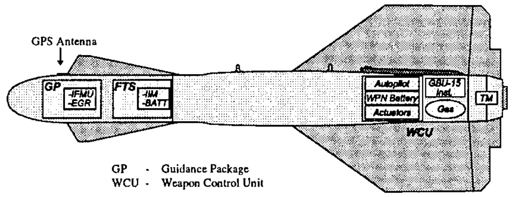
GPS Antenna
GP
-IFMU
-EGR
FTS
-IM
-BATT
Autopilot
WPN Battery
Actuators
GBU-15 Inst.
Gas
TM
WCU
GP - Guidance Package
WCU - Weapon Control Unit

Figure 3: EDGE Modified GBU-15 Layout

The GBU-15 weapon control unit: analog autopilot, gas bottle, and fin actuators were not modified for EDGE. The INS/GPS guidance package interfaced with the weapon control unit through the existing autopilot interface by emulating the commands to the autopilot as if they originated from the IR guidance module. The primary elements of the EDGE guidance package were the Integrated Flight Management Unit (IFMU) and the GPS receiver. The IFMU was manufactured by Honeywell and was based upon their GG1308 ring laser gyro (RLG). The GPS receiver was manufactured by Interstate Electronics Corporation (IEC) and was augmented with a fast acquisition capability. Additional details on these two guidance package elements are provided below.

Integrated Flight Management Unit (IFMU)

The IFMU served as the master navigation system for the weapon and provided all the weapon I/O functions which included: aircraft 1553B interface, telemetry interface, autopilot interface and weapon GPS receiver interface. Additionally, algorithms performing the transfer alignment, inertial navigation, integrated INS/GPS navigation guidance, application of pseudorange differential corrections, weapon system health monitoring and weapon event sequencing were all performed within the IFMU. The IFMU included a system processor, power supply, analog/discrete I/O boards, and a HG 1700 Inertial Measurement Module (IMM). The IFMU's 17 lb. weight and 7.00 x 7.63 x 10.40 inches dimensions allowed for easy integration into the nose of the weapon. The IFMU architecture is shown in Figure 4.

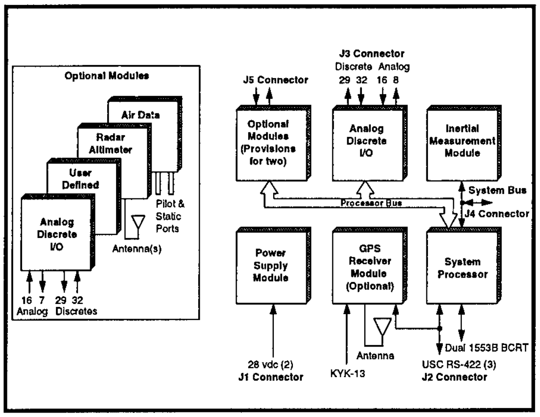
Optional Modules
Air Data
Radar Altimeter
User Defined
Analog Discrete I/O
Pilot & Static Ports
Antenna(s)
16 7 29 32
Analog Discretes
J5 Connector
J3 Connector
Discrete Analog
29 32 16 8
Optional Modules (Provisions for two)
Analog Discrete I/O
Inertial Measurement Module
System Bus
Processor Bus
J4 Connector
Power Supply Module
GPS Receiver Module (Optional)
System Processor
28 vdc (2)
J1 Connector
KYK-13
Antenna
Dual 1553B BCRT
USC RS-422 (3)
J2 Connector

Figure 4: Honeywell IFMU Architecture

The HG 1700 IMM performed the inertial sensing function and was comprised of a triad of Honeywell GG1308 ring laser gyros and Sundstrand RBA 500 vibrating silicon accelerometers. The error budget for these sensors is shown in Table 2.

Table 2: IMM Sensor Error Budget

Sensor	Error	Model	1-σ	Correlation
RLG	Bias	Gauss-Markov	1.0 deg/hr	3 hours
	Scalefactor	Gauss-Markov	50 ppm	3 hours
	Orthogonality	Gauss-Markov	10 arc-sec	3 hours
	Random Walk	Gauss-Markov	0.125 $\text{deg/hr}^{1/2}$	
	Quantization	n/a	2.76 arc/sec	
RBA-500	Bias	Gauss-Markov	1000 μ g	3 hours
	Scalefactor	Gauss-Markov	100 ppm	3 hours
	Orthogonality	Gauss-Markov	10 arc-sec	3 hours
	Misalignment	Gauss-Markov	20 arc-sec	3 hours
	Nonlinearity	Gauss-Markov	22 μ g's $/g^2$	3 hours
	Random	Noise	0.025 $\text{ft/sec/hr}^{1/2}$	

GPS Receiver

The weapon GPS receiver, manufactured by IEC, was a five channel, fast acquisition, P/Y code receiver housed in a SEM-E form factor. The receiver was comprised of four circuit cards which included: the RF down converter circuit card, the tracking & I/O circuit card, the navigation processor circuit card, and the fast acquisition circuit card. The receiver dimensions of 6x6x1 inches allowed it to physically reside inside the IFMU.

Communication between the receiver and IFMU occurred via an RS-422 interface. As such, the receiver accepted time, position, velocity, attitude, and ephemeris data from the aircraft via the IFMU. With this information and time accurate to within 10 milliseconds, the receiver would acquire satellites within 5 to 10 seconds.

For maximum GPS satellite coverage, two antennas were placed on the munition, as shown in Figure 2. One in front of the forward strakes and the second antenna behind the tail. GPS satellites were acquired on the front antenna. After acquisition, the receiver multiplexed between the L_1 and L_2 frequencies to measure the ionospheric delay on the signals from the five satellites being tracked. The receiver then multiplexed between the antennas depending on the satellite visibility on the front antenna. The receiver was capable of only one type of multiplexing at any given time. It could frequency multiplex and then antenna multiplex, or vice versa. However, it could not simultaneously frequency multiplex and antenna multiplex. It was critical for the receiver to complete its L_1/L_2 multiplexing for all five channels prior to transitioning to antenna multiplexing. Failing to do so would not allow ionospheric delay to be measured for all five satellites, hence degrading navigation accuracy.

EDGE INTEGRATED NAVIGATION SYSTEM

Blending GPS data with the differential corrections and the IFMU inertial navigation solution provided a highly accurate integrated solution that was the key to demonstrating the navigation accuracy improvement potential of DGPS. This integrated system is illustrated in Figure 5.

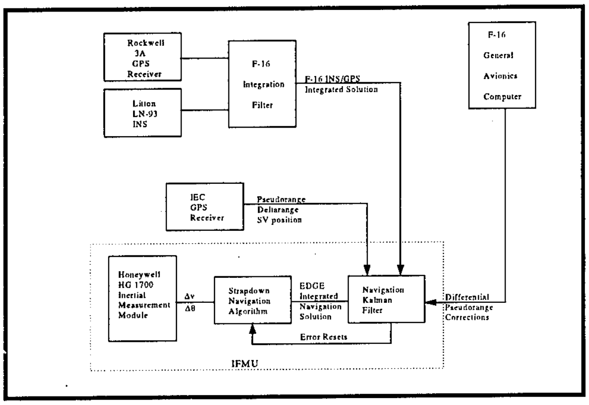
Rockwell 3A GPS Receiver
Litton LN-93 INS
F-16 Integration Filter
F-16 INS/GPS Integrated Solution
F-16 General Avionics Computer
IEC GPS Receiver
Pseudorange
Deltarange
SV position
Honeywell HG 1700 Inertial Measurement Module
Δv
Δθ
Strapdown Navigation Algorithm
EDGE Integrated Navigation Solution
Navigation Kalman Filter
Differential Pseudorange Corrections
Error Resets
IFMU

Figure 5: EDGE Integrated Navigation System

The IFMU contained the HG 1700 Inertial Measurement Module, the strapdown navigation algorithm, and the navigation Kalman filter with measurement data from an IEC GPS receiver or integrated F-16 INS/GPS solution for transfer alignment. The F-16 navigation solution was derived from the integration of a Litton LN-93 INS with a Rockwell 3A GPS receiver.

The IFMU exercised two basic modes during EDGE flight testing, an INS aided mode for transfer alignment and a GPS aided mode after weapon launch. Prior to weapon launch, the strapdown inertial navigation solution was coarsely initialized with the master F-16 INS/GPS data. Further processing of the F-16 data through the Kalman filter refined the orientation of the IFMU with respect to the local level frame. Differential corrections were not used in this initialization from the F-16 data. After initialization, the weapon was launched utilizing tightly coupled INS/GPS data aided with differential corrections. The differential corrections were passed from the F-16 General Avionics Computer (GAC) to the IFMU independent of the F-16 integrated navigation system. The IEC GPS receiver transferred P/Y-code pseudorange, delta-range, and satellite positions to the IFMU. Software in the IFMU subtracted the differential corrections from the respective pseudorange measurements transferred from the GPS receiver prior to being input to the Kalman filter. The Kalman filter provided resets to the IFMU inertial solution. These resets included sensor bias compensation as well as position, velocity and attitude corrections. The filter operated at a 5.12 second update rate and had a variable configuration dependent upon the mode of operation of the IFMU.

Transfer Alignment

Transfer alignment occurred utilizing the INS aided mode of the IFMU. In this mode 15 error states were modeled in the Kalman filter. These states were: 3 integrated velocity, 3 velocity, 3 attitude, 3 gyro biases, and 3 accelerometer biases. Measurements during transfer alignment consisted of the difference between the IFMU and F-16 integrated local level frame horizontal and vertical velocities over the 5.12 second Kalman cycle.

Integrated velocity measurements were formed by integrating the 50 Hz F-16 velocity data and differencing these integrals with integrated IFMU velocity. IFMU velocities were integrated at a 100 Hz rate over the same 5.12 second interval the F-16 data was integrated. Additionally, the latitude and longitude of the IFMU were slaved to the F-16 latitude and longitude by time aligning the data and correcting the IFMU position error by the measured quantity. The reset logic built into the Kalman filter was used to accomplish this slaving of latitude and longitude.

GPS Aiding

At weapon launch the integrated velocity error states were reconfigured as position error states and GPS clock phase and clock frequency states were added to the filter for a total of 17 states. After the receiver acquired five satellites the filter began processing of the GPS line of sight measurements. Only the pseudorange measurements along with their corresponding differential corrections were processed by the filter. These measurements for the five channels were provided to the filter at a 1 Hz rate. Typically, five line of sight measurements per channel were collected during the 5.12 second Kalman cycle. As such, these measurements were prefiltered with a least squares filter to reduce noise and provide the Kalman filter with only one 5.12 second measurement for each satellite tracked.

The measurement noise on the differentially corrected GPS measurements was initially set very high at 469 ft^2. This caused the filter to deweight the influence of the measurements and weight the inertial system model more heavily. After the receiver measured the ionospheric delay for each of the five satellites being tracked, the filter lowered the noise on the differentially corrected pseudorange measurements to approximately 25 ft^2. In turn, this allowed the influence of the differentially corrected GPS measurements to be more pronounced as they became the primary driver for the filter error estimation. As such, the effect of differential GPS on weapon navigation accuracy could now easily be determined.

EDGE Guidance Law

The guidance law developed and flown on the EDGE vehicle provided steering signals that resulted in target impacts along a programmable impact vector. Local level coordinate frame guidance commands were computed at a 25 Hz rate based upon the weapon velocity vector, weapon to target line-of-sight vector, and the specified impact vector. The EDGE guidance law aligned these three vectors based upon the following equation:

$$\gamma_c = k_2 \left[T \times k_1 \left[\frac{\vec{R}}{|\vec{R}|} - \frac{\vec{V}}{|\vec{V}|} \right] \right]$$

where γ_c = Guidance command vector
$\vec{T}$ = Impact unit vector
$\vec{R}$ = Weapon to target range vector
$\vec{V}$ = Weapon velocity vector

To minimize miss distance, the gain k_1 was scheduled based upon the range to the target and was used to eliminate the impact vector constraint when the range became small, thus avoiding geometry induced high dynamics in the end-game. When $k_1 = 1.0$ and the angles between the vectors are small, the guidance law reduces to classical proportional navigation.

TEST RESULTS

Assessment of the EDGE integrated navigation system accuracy was accomplished along with a multitude of systems integration and functionality testing at Eglin AFB. The systems and functionality testing included stand-alone testing of the differential correction network, laboratory bench testing of the IFMU and GPS receiver, mobile van testing of the IFMU and GPS receiver, static navigation ground testing, and captive and free flight testing of the total integrated system. Although the functionality and stand-alone tests were important in the overall EDGE integration effort, this paper focuses on the testing used to assess the navigation accuracy improvement potential of differential GPS for guiding air-to-ground weapons: static navigation ground testing, captive flight testing, and free-flight testing.

Static Navigation Ground Test Results

In order to verify the performance of the EDGE weapon navigation solution using the aircraft interfaces and initialization uncertainties that would be seen during flight test, a static navigation test was performed. This test also allowed verification of the Quality Monitor station, and quantification of the navigation performance improvement of a differentially corrected EDGE weapon over a non-differentially corrected EDGE weapon.

The test involved locating a Block 50 F-16 on a surveyed point, mounting two EDGE weapons on the aircraft (one on each wing), and sequenced through 20 simulated launches. A common GPS antenna placed over a surveyed marker provided RF inputs to both EDGE weapon GPS receivers. One of the EDGE weapons was provided differential corrections from the EDGE wide area differential GPS reference receiver network via Improved Data Modem (IDM) link to the aircraft. The other EDGE weapon operated without differential corrections. Operational aircraft avionics (INS, GPS) were used to initialize the EDGE weapons prior to each simulated launch. Ten minute navigation runs were performed after each simulated launch and navigation data collected from both the differentially corrected and non-differentially corrected EDGE weapons. The test set-up is depicted in Figure 6.

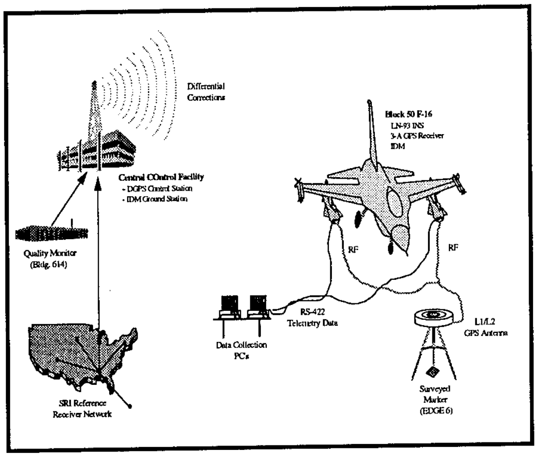
Differential Corrections
Central COntrol Facility
- DGPS Control Station
- IDM Ground Station
Quality Monitor (Bldg. 614)
SRI Reference Receiver Network
Block 50 F-16
LN-93 INS
3-A GPS Receiver
IDM
RF
RF
RS-422 Telemetry Data
Data Collection PCs
L1/L2 GPS Antenna
Surveyed Marker (EDGE 6)

Figure 6: EDGE Static Navigation Test Set-up

The results of the static navigation test, shown in Figures 7 and 8, are compared at 100 seconds after simulated launch since this is the nominal time of weapon flight for an actual drop test.

Table 3 summarizes the static navigation test results and clearly indicates differential corrections improve performance.

Table 3: Static Navigation Test Position Error Summary

	Horizontal Position Error (feet)		3D Position Error (feet)	
	mean	σ	mean	σ
Differentially Corrected Weapon	6.3	3.6	8.8	5.5
Non-differentially Corrected Weapon	12.8	8.5	20.3	12.3

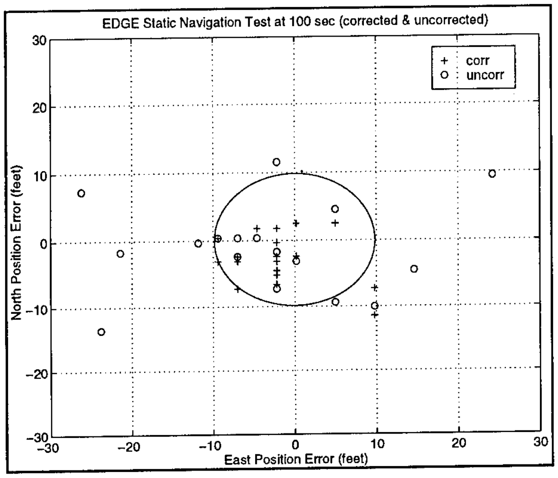

Figure 7: Static Navigation Test Horizontal Position Error

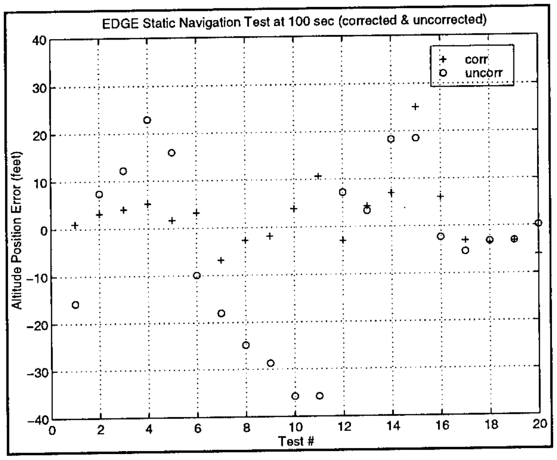

Figure 8: Static Navigation Test Altitude Error

Captive Flight Test Results

Six captive flight tests were conducted as part of the EDGE demonstration. The majority of these tests assessed system functionality and compatiblity. However, one captive flight test was designed specifically to quantify the accuracy associated with the EDGE guidance system and to compare a differentially corrected system solution with a non-differentially corrected system solution. To accomplish this, two identical EDGE weapons were mounted on the F-16. The weapon on the left wing received differential corrections while the weapon on the right wing did not. Twenty five straight and level passes were then flown with this configuration through an optimal Time Space Position Information (TSPI) corridor on the test range to provide the data for this analysis. From the total 25 passes, five passes were eliminated for the corrected weapon and nine were eliminated for the non-corrected weapon due to weapon GPS receiver tracking errors caused by F-16 fuselage masking of the weapon GPS antennas.

The highest quality TSPI available at Eglin AFB, the Test Data Optimal Processor (TDOP), was used for assessing position of the weapons under captive carriage. TDOP is a Kalman Smoother used to integrate Eglin range assets and provide high accuracy TSPI data for comparison with data from the system under test. Eglin range assets for TDOP input included cinetheodilites, radars, and aircraft inertial velocity. The TDOP position solution is accurate to within 0.5 feet.

Figure 9 depicts the average horizontal per pass "miss distance" of the EDGE differentially corrected system solution compared with the TDOP solution. The average miss distance across all passes was 12.03 feet. The average horizontal per pass "miss distance" of the non-differentially corrected system solution compared with the TDOP solution was 29.958 feet and is shown in Figure 10.

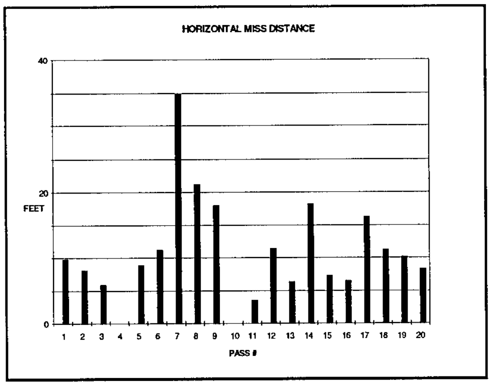

Figure 9: Differentially Corrected Horizontal Miss Distance

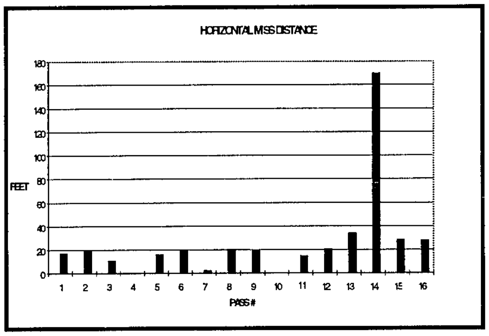

Figure 10: Non-Differentially Corrected Horizontal Miss Distance

Free Flight Test Results

The six EDGE free flight tests were broken into three distinct groups. Free flights 1 and 2 attacked horizontal targets with an impact angle of 85 degrees. Free flights 3 and 4 attacked vertical targets with an impact angle of 20 degrees. Free flights 5 and 6 were executed under an operational scenario in which the target coordinates were received from an operational source (i.e. not DMA surveyed). This scenario consisted of two F-16s in trail, each carrying a differentially corrected EDGE weapon, that launched its weapon against the same horizontal target within three seconds of one another. Thus, free flights 5 and 6 were launched three seconds apart and attacked the same horizontal target using the same operationally derived target coordinates. However, free flight 6 was deemed a no-test due to a satellite acquisition anomaly in the weapon GPS receiver that caused the differential corrections not to be used. In essence, free flight 6 was more representative of a normal GPS guided weapon instead of a differentially corrected GPS guided weapon. A summary of the free flight launch parameters and test results is shown in Tables 4 and 5, respectively.

Table 4: EDGE Free Flight Launch Parameters

Drop	Time of Flight (sec)	Downrange Distance (ft)	Release Altitude (ft)	Release Velocity (ft/s)	Release Bearing (deg)	Impact Velocity (ft/s)
1	100.2	73,600	30,344	879	237.7	1073.5
2	101.6	72,300	30,533	845	237.4	1077.8
3	95.7	86,900	26,301	944	236.5	968.1
4	103.0	87,700	25,278	907	236.8	915.8
5	89.9	66,600	29,507	883	238.9	1098.6
6	89.2	65,900	29,528	889	238.8	1097.1

Table 5: Flight Test Results Summary

Drop	Target type	Radial error (m)
1	Horizontal	4.1
2	Horizontal	4.0
3	Vertical	1.9
4	Vertical	9.0
5	Horizontal	3.9
6	Horizontal	N/A

Figure 11 shows each weapon impact with respect to the 20'x20'x8' horizontal target. The aimpoint was the center of the target. Excluding the 'no test' that occurred on the sixth drop test, it appears a 4 meter along-track bias exists in attacking horizontal targets. Analysis of flight test data seems to indicate this apparent bias may be largely due to weapon GPS antenna multipath that occurs as the weapon pitches over in the last 20 seconds of flight.

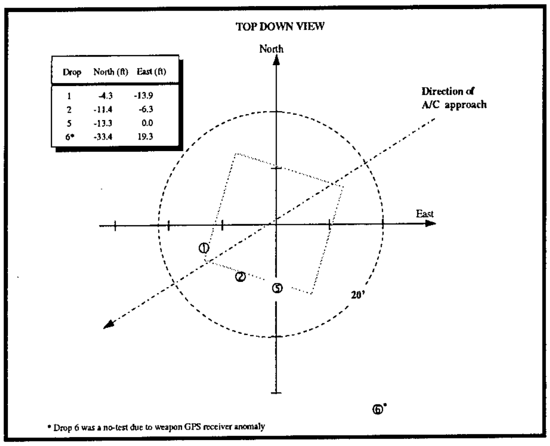

Drop	North (ft)	East (ft)
1	-4.3	-13.9
2	-11.4	-6.3
5	-13.3	0.0
6*	-33.4	19.3

* Drop 6 was a no-test due to weapon GPS receiver anomaly

Figure 11: Free Flight Miss Distances Against Horizontal Targets

Figure 12 shows the weapon impact with respect to the 40'x28' wooden billboard for each of the two drop tests against the vertical target. The aimpoint was the center of the billboard. Numerous hours were spent in analyzing flight test data after completing the fourth drop test. This analysis showed Vertical Dilution of Precision (VDOP) of the satellites tracked by the weapon was higher than normal (over 3.0), and the high humidity in the atmosphere may have contributed larger tropospheric errors. These factors at least partly contributed to the weapon impacting 9 meters short of the target.

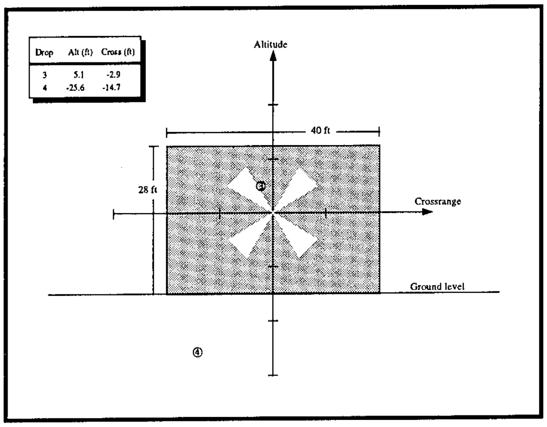

Drop	Alt (ft)	Cross (ft)
3	5.1	-2.9
4	-25.6	-14.7

Figure 12: Free Flight Miss Distances Against Vertical Targets

GUIDANCE RESULTS

The four EDGE drop tests against horizontal targets achieved impact angles within 2.0 degrees of the desired 85 degree impact angle. The two EDGE free flight tests against vertical targets resulted in impact at the specified impact angle of 20 degrees. Miss distances due to the guidance law, weapon control system, and weapon aerodynamic uncertainty were typically under 1.0 foot with a maximum of 1.6 feet. Figure 13 shows the weapon trajectories flown during drop testing, while Figure 14 shows the miss distance contributions due to vehicle control errors for each of the six EDGE drop tests.

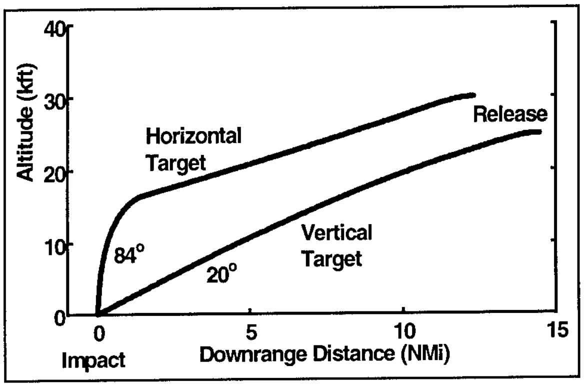

Figure 13: EDGE Weapon Trajectories

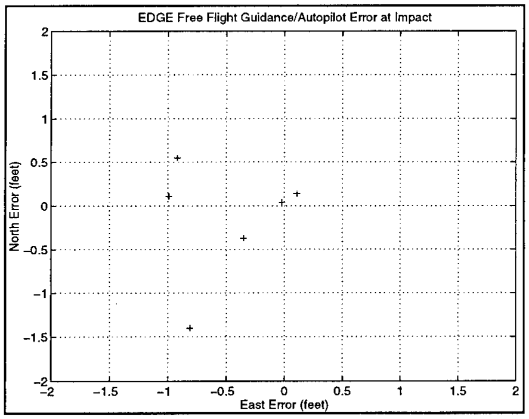

Figure 14: Miss Distance Contributions due to Vehicle Control Errors

CONCLUSIONS

The EDGE program accomplished its objective and goal by demonstrating that 5 meter weapon navigation accuracy is achievable through differential GPS. Static navigation testing demonstrated 2 meter horizontal weapon navigation accuracy is possible with differential GPS. Captive carriage testing resulted with 3.5 meter horizontal weapon navigation accuracy, while free flight testing resulted with 4 meter horizontal weapon navigation accuracy. An apparent 4 meter bias exists when the weapon attacks horizontal targets. Analysis indicates this bias may largely be caused by weapon GPS antenna multipath. As such, antenna multipath mitigation needs to be investigated as the Air Force strives towards near-zero CEP autonomous weapons. Additionally, GPS receiver noise reduction and Kalman filter optimization should be pursued as well.

REFERENCES

[1] Jolley, "A Primer for Differential GPS (DGPS) and the EDGE High Gear Program", May 95

[2] Kohli, "High Performance GPS Receiver for Air Launched Munitions", IEEE, 94

[3] Software Design Document for the DGPS Reference Receiver Network., SRI International, July 95

[4] Synder, "INS/GPS Operational Concept Demonstration (OCD) High Gear Program", IEEE, 1994

LOCALISATION AUTOMATIQUE D'OBJECTIFS
A PARTIR D'UNE CARTE RADAR

JP. MESTRE - R. DE PEUFEILHOUX
THOMSON-CSF
1 Bd. Jean Moulin
78852 ELANCOURT Cedex - FRANCE

Introduction

Une mission d'attaque au sol nécessite, en général, plusieurs acquisitions d'objectif à des fins de navigation (pour recaler la position de l'avion) ou d'attaque (pour désigner l'objectif à traiter).

Le radar de pointe avant est un des moyens utilisables pour ces acquisitions.

La localisation d'un objectif peut être réalisée à partir de cartes SAR acquises au cours de la mission par le radar. La procédure de localisation employée peut être manuelle (le pilote désigne sur la carte) ou **automatique** (le système propose une solution).

Cette communication présente les principales méthodes employées pour réaliser cette fonction, ainsi que les axes retenus par THOMSON-CSF.

1 - L'adéquation de la fonction au besoin opérationnel

1-1 La fonction technique de localisation dans la mission d'attaque au sol

Dans une mission d'attaque au sol, on peut distinguer typiquement deux phases: la navigation et l'attaque.

Dans la phase de navigation, il est nécessaire d'avoir une bonne localisation absolue de l'avion. L'équipement inertiel de base des avions, la centrale inertielle, dérive, il faut donc périodiquement recaler ses informations. La désignation d'un point du sol de coordonnées absolues connues est un des moyens de recalage.

Dans la phase d'attaque, il faut savoir où se trouve l'objectif, donc disposer d'une localisation précise de l'objectif par rapport à l'avion. L'un des moyens d'en disposer est d'effectuer la désignation directe de l'objectif pendant la mission. L'avion désignant peut alors, soit mener l'attaque lui même, soit communiquer cette désignation d'objectif à d'autres qui engageront les moyens nécessaires à son traitement.

Ces deux fonctions opérationnelles, le recalage de navigation et la désignation d'objectif, peuvent donc être réalisées à travers la même fonction technique: la localisation d'un point du sol (amer de recalage ou objectif à traiter) par rapport à l'avion.

1-2 L'évolution du besoin opérationnel

L'attaque au sol avec des armements classiques non guidés s'effectue aujourd'hui, en général, en réalisant une acquisition directe ou indirecte (par l'intermédiaire d'un point additionnel) de l'objectif dans le viseur tête haute de l'avion. On réalisera une acquisition directe dans le cas d'une cible d'opportunité dont on ignore les coordonnées, une acquisition indirecte si l'on connait précisément les coordonnées relatives de la cible à traiter.

Le seul cas où ce type d'acquisition n'est pas impératif est celui du traitement d'objectifs de valeur aux coordonnées absolues bien connues. Ceci dans la mesure ou l'avion attaquant dispose d'un système très performant de recalage continu de son vecteur d'état (position et vitesse) comme, par exemple, une centrale inertielle hybridée GPS, en fonctionnement nominal, sinon la navigation doit être recalée.

L'acquisition d'un point du sol dans le viseur tête haute a des caractéristiques très limitatives:

- temps clair (de jour et de nuit, si équipement supplémentaire adapté),
- courte portée (< 10 km),
- acquisition manuelle,
- avion peu évolutif et quasi aligné (point visé au voisinage de l'axe avion).

Le besoin opérationnel qui doit être satisfait aujourd'hui est très différent:

- tout temps,
- tir à distance de sécurité
- tir toutes altitudes,
- objectif multicible
- réduction de la vulnérabilité de l'attaquant.

Pour satisfaire ce besoin, dans les différentes missions d'attaque au sol, de nouveaux moyens sont employés, les principaux étant:

- des armes plus précises et aux portées supérieures,
- l'automatisation des modes d'attaque,
- les modes de cartographie des capteurs embarqués.

1-3 La localisation d'objectifs à partir d'une carte radar

Les modes SAR des radars de pointe avant offrent des images de haute résolution par tous les temps. A partir de ces images il est possible de désigner un objectif non aligné (ne se trouvant pas dans l'axe de l'avion) à des distances très supérieures à la portée visuelle et compatibles de l'emploi de nouveaux armements guidés ou non.

Par ailleurs, la désignation, qui permet de localiser l'objectif, peut être réalisée soit manuellement, soit automatiquement.

Paper presented at the AGARD MSP Symposium on "Technologies for Precision Air Strike Operations in Rapid-Reaction and Localised-Conflict Scenarios", held in Seville, Spain, from 16-19 October 1995, and published in CP-576.

L'évolution des systèmes d'armes conduit à proposer à l'équipage de nouvelles fonctions d'assistance à l'accomplissement de la mission.

Pour réaliser cette fonction technique de localisation, on peut présenter la carte radar à l'opérateur et lui laisser le soin de trouver, d'identifier puis de désigner la cible. Le système peut également assister l'opérateur dans ces différentes opérations. Cette assistance pouvant aller jusqu'à l'automatisation complète de la fonction, le système proposant une solution à l'opérateur.

Bien sur, l'automatisation nécessite de disposer d'un certain nombre d'informations a priori telles que la connaissance de la région cartographiée, de la cible ou du type de cible à traiter,... La nature et l'importance de ces informations a priori seront précisées dans l'exposé des méthodes à venir.

L'automatisation permet d'alléger la charge de travail du pilote ou de l'équipage qui peut mieux se consacrer au pilotage ou à l'autoprotection, mais elle offre aussi d'autres avantages comme la moindre sensibilité à certaines erreurs liées à l'élaboration et à la présentation de la carte radar.

2 - La présentation des cartes radar

Les cartes radar sont élaborées par le radar de pointe avant de l'avion. Ce sont des cartes SAR, l'utilisation de l'effet doppler pour disposer d'une bonne résolution angulaire nécessite d'élaborer ces cartes, non pas dans l'axe de l'avion, mais sur le côté. La technique d'élaboration utilisée est du type DBS (Doppler Beam Sharpening), l'antenne balayant en repère avion le terrain pendant la prise de carte.

Les principales caractéristiques de ces cartes sont:

- une résolution radiale et angulaire de classe décamétrique,
- un niveau de conformité de l'ordre de la résolution (le radar suppléant, si besoin est, aux insuffisances de la localisation du porteur),
- une taille de carte qui est de quelques NM sur la radiale (selon résolution) et qui peut aller jusqu'à 45° de couverture en azimut,
- une distance d'élaboration de l'ordre de 40 NM,
- un délai d'obtention de quelques secondes.

Ces cartes radar peuvent être prises:

- en virage (tolérance en facteur de charge),
- en évolution dans un plan oblique (en piqué par exemple),
- à toutes altitudes, la taille et la portée de la carte étant limitées à basse altitude.

L'illumination de la région cartographiée est brève et ne nécessite pas une puissance très élevée.

L'ensemble de ces caractéristiques permet de dégager les principaux avantages opérationnels de ces modes:

- mise en oeuvre possible à toutes altitudes,
- mise en oeuvre possible à grande distance,
- possibilité de guider l'avion en évolution pendant la prise de carte,
- moindre indiscrétion électromagnétique.

La localisation d'objectifs à partir de cartes radar permet, outre l'aspect tout temps, la mise en oeuvre de cette fonction dans des conditions de souplesse d'emploi et de minimisation de la vulnérabilité de l'avion.

3 - les traitements possibles

3-1 Principes de traitements de localisation automatique

Le but de la localisation automatique de cible est de déterminer la position de la cible dans un repère lié à l'avion.

Ceci peut se faire de plusieurs manières:

- (a) la plus simple est de connaître la position de tout point de l'image radar dans un repère lié à l'avion et de localiser la cible dans cette image, la position de la cible est alors connue par rapport à l'avion; cette méthode demande une signature de la cible facilement observable et discriminante; la cible une fois reconnue, la précision est très bonne; elle ne dépend que de la précision de la prise de carte; le tir peut se faire sur coordonnées;

- (b) la carte radar peut aussi être recalée sur un modèle de référence par rapport auquel la position de la cible a été préalablement marquée; la détermination de la position de la cible est donc indirecte et il n'est pas nécessaire que celle-ci ait une signature très caractéristique; par contre il faut élaborer, en préparation de mission, un modèle cartographique qui soit superposable à l'image; le tir peut alors se faire sur coordonnées; mais l'identification peut encore être pratiquée en tant que contrôle ;

- (c) si la géométrie de la prise de carte n'est pas parfaitement connue, le recalage de l'image et du modèle de référence avec la carte permet cependant de retrouver la cible mais le tir ne peut pas se faire sur coordonnées; ce ne peut être que la désignation initiale pour un armement équipé d'un moyen de guidage terminal.

Dans les deux derniers cas, le modèle de référence ne coïncidera bien avec la carte radar (supposée parfaite géométriquement) que si lui-même a été relevé parfaitement sur une source reproduisant elle-même exactement la surface terrestre.

La première méthode (a) ne peut être employée que si la signature de la cible a fait l'objet de très importantes études de modélisation auparavant (nombreuses campagnes de mesures pour toutes les présentations, tous les milieux, tous les temps, ...). Ceci n'est guère envisageable pour des cibles de haute valeur du type infrastructures celles-ci ne répondant pas à des caractéristiques standard comme des chars, des shelters (mais pour ces cibles signées se pose le problème de l'ambiguïté car il y a généralement plusieurs cibles sur la zone au même moment).

La troisième méthode (c) nécessite de disposer, pour le tir, d'un armement à guidage terminal.

La seconde méthode (b) est donc la plus générale et la plus adaptée dans le cas qui nous intéresse où l'erreur sur la position des points de l'image dans le repère avion peut être maîtrisée.

C'est donc cette seconde méthode qui est développée ci-après. Les principales fonctions mises en oeuvre dans cette méthode sont détaillées par la suite:

IDENTIFICATION (cas où la cible est dans l'image radar) L'image n'est pas toujours exactement superposable au modèle (ou la cible n'est pas parfaitement localisée dans celui-ci) si bien que la position dans l'image à laquelle devrait correspondre la cible au terme du recalage n'est pas forcément la cible. Un traitement de proximité doit permettre d'identifier celle-ci dans le voisinage du point trouvé.

RECALAGE C'est l'opération qui consiste à mettre en correspondance au mieux la carte radar avec le modèle de référence.

PREPARATION DE MISSION Le modèle de référence est élaboré en Préparation de Mission à partir de données source.

ACQUISITION DE DONNEES SOURCE Les données source sur la cible et son environnement sont rassemblées, géo-référencées et quelque fois prétraitées (exemple: redressement des vues obliques pour obtenir des orthophotos).

Les étapes ci-dessus doivent être étudiées dans cet ordre car plus on descend dans les fonctions plus les degrés de liberté sont grands (par exemple le contenu du modèle ou la nature des données source)

3-2 Les étapes du traitements

3-2-1 Identification

Cette étape se déroule, en temps réel, pendant la mission. Elle intervient après l'étape de recalage.

Le modèle local de cible devant permettre l'identification peut être constitué:

- d'un point brillant (barycentre d'un écho fort sur une surface de taille donnée);
- de la présence d'un contraste fort dans une direction;
- de la présence d'une ombre;
- d'une signature en double polarisation (si disponible).

La recherche se fait dans une zone circulaire qui dépend de la précision de localisation de la cible dans le modèle, de la non-conformité résiduelle de l'image et de l'effet du relief. Cette zone ne devrait pas dépasser un cercle de 50 m autour du point désigné, l'incertitude de localisation ayant été réduite par le recalage.

Compte-tenu de la petite taille de la zone de recherche, une exploration systématique du domaine est possible.

3-2-2 Recalage

Cette étape se déroule, en temps réel, pendant la mission.

Pour recaler la carte radar et le modèle il faut qu'ils aient des éléments communs. Le choix de ces éléments communs est fondamental pour la précision et la robustesse du recalage.

Quatre considérations principales orientent ce choix:

- les éléments doivent pouvoir être extraits de l'image avec une bonne probabilité de détection et une faible fausse alarme;

- les éléments doivent pouvoir être extraits des données source en préparation de mission pour constituer le modèle avec le minimum d'intervention manuelle;

- les éléments extraits de l'image et ceux du modèle doivent se ressembler;

- les éléments doivent être suffisamment nombreux dans la scène.

Les éléments qui paraissent le mieux répondre à ces quatre impératifs sont les segments de droite. Ces éléments sont en général simultanément observables dans les images et les données source. Il est possible de les extraire des images et des données source avec des méthodes maintenant bien rodées. Ils sont suffisamment nombreux dans l'environnement habituel des cibles de haute valeur.

D'autres types d'éléments sont envisageables:

- des points brillants: leur modélisation est possible mais il peut y avoir lors de l'extraction dans l'image un fort taux de fausse alarme (des réflecteurs ignorés en Préparation de Mission donnent aussi des échos forts) et une perte de détection (des réflecteurs prévus peuvent être masqués, mal orientés ou finalement non observables par erreur sur le matériau constitutif). De plus ce type d'amer n'est pas forcément très répandu et la Préparation de Mission comprend une part manuelle importante (interprétation des données source);

- des zones homogènes de même "couleur" dans l'image et dans le modèle: l'intérêt est de permettre le recalage par des algorithmes simples (et des circuits rapides) de corrélation d'images; la difficulté peut provenir de la fidélité de la "couleur" entre image et modèle et de la représentativité du modèle (si celui-ci est obtenu automatiquement à partir de sources non-interprétées comme les images SPOT ou ERS1, on aura une bonne restitution de la géométrie (complète et fidèle) mais des risques de différences radiométriques - dans la "couleur"; si le modèle est construit à partir de fichiers géographiques comme DLMS ou VMAP, il risque d'y avoir d'importants manques dans la géométrie mais la radiométrie est plus fiable); une image de synthèse de la zone est réalisée

- des configurations particulières: alignement d'échos forts ou croisements de routes par exemple; ces structures qui peuvent être extraites de l'image et élaborées en peuvent être extraites de l'image et élaborées en Préparation de Mission (avec interprétation manuelle) ne sont cependant pas toujours présentes dans la scène.

Avant de mettre en oeuvre le recalage, l'étape d'extraction des segments de l'image est cruciale, le but étant de maximiser la détection tout en minimisant la fausse alarme.

Les méthodes classiques d'extraction des segments font en général l'hypothèse que le long d'un segment l'orientation du gradient et quelquefois sa norme demeurent à peu près constantes. Ceci n'est pas toujours le cas avec des images SAR (*Fig A*) dans lesquelles la présence de speckle empêche cette continuité.

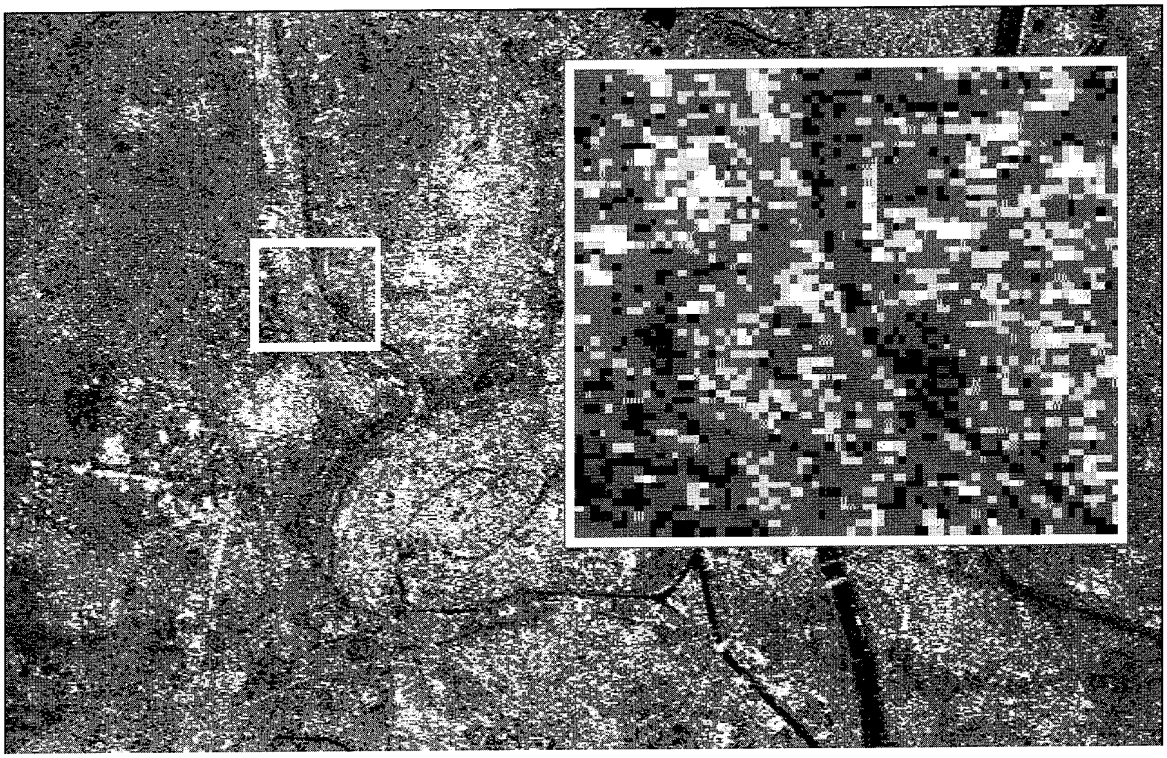

Figure A: Image SAR montrant l'effet du speckle sur les contours

Il est donc parfois nécessaire de filtrer au préalable les images pour retrouver cette continuité. Les filtres les plus utilisables sont ceux qui sont basés sur la nature physique du bruit de speckle (bruit multiplicatif) comme le filtre de FROST [ref 1]. Le filtrage peut aussi être mis en oeuvre lors de la formation d'image (par exemple en sommant plusieurs vues). Pour extraire les segments de l'image on peut procéder directement en recherchant les points de fort gradient et en reliant ceux de ces points qui sont alignés et contigus. Il est aussi parfois utile de s'appuyer pour cette recherche des segments sur les lignes de contours des régions homogènes (figure B).

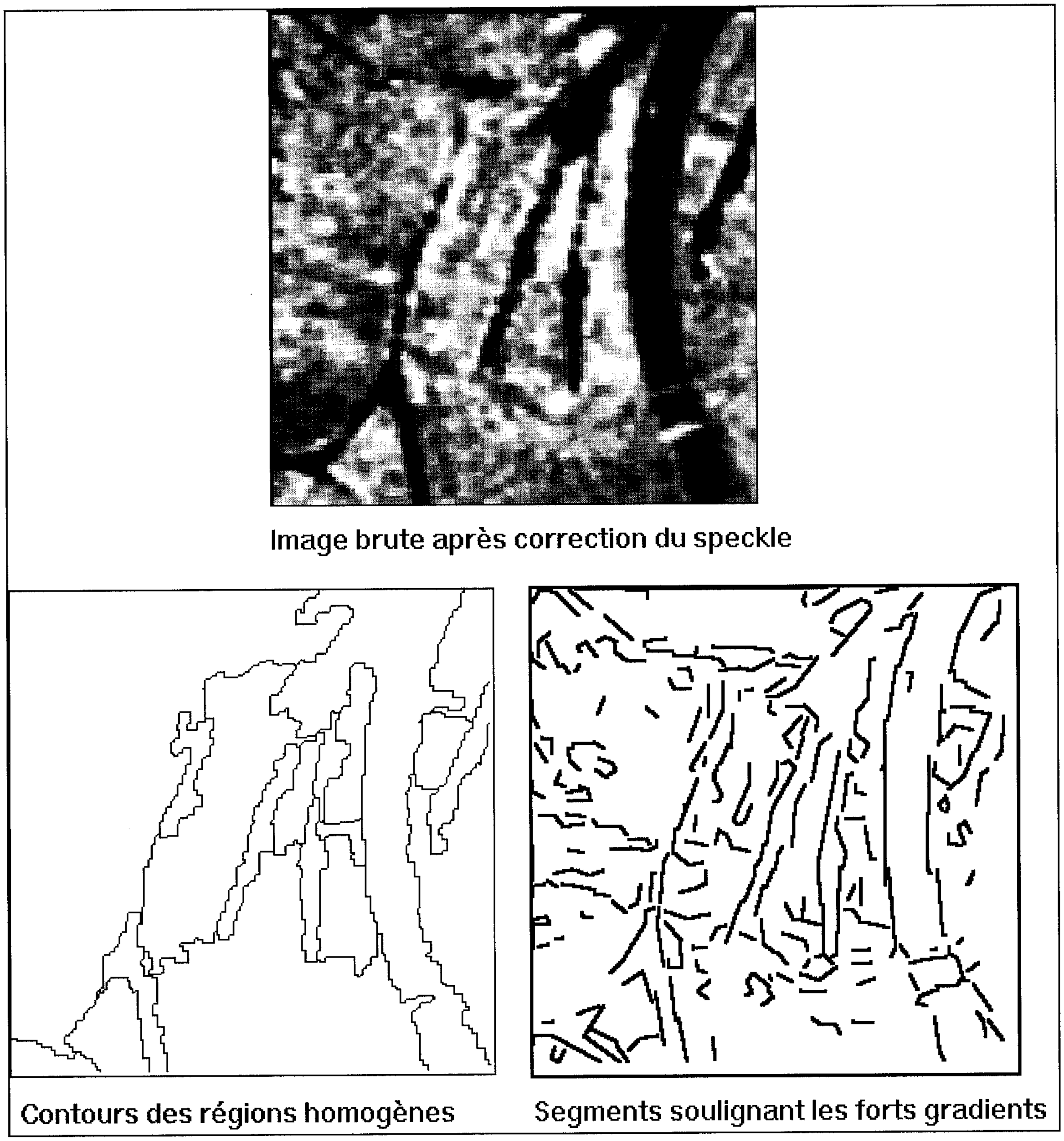

Image brute après correction du speckle

Contours des régions homogènes

Segments soulignant les forts gradients

Figure B: Illustration de l'étape de segmentation

En général le processus d'extraction de segments donne un grand nombre de segments. Une sélection est nécessaire pour limiter la combinatoire de la mise en correspondance. Cette sélection parmi les segments extraits peut être favorisée par la prise en compte d'une information a priori sur la longueur et l'orientation des segments à extraire. Cette information a priori peut être facilement calculée à partir des segments du modèle pour ne retenir que les segments qui ont des orientations compatibles de celles du modèle, la sélection sur la longueur est plus délicate car on n'est jamais sur d'extraire de l'image un segment sur toute la longueur qu'il a dans le modèle. On peut aussi tenir compte du fait que plus les segments extraits sont longs plus ils ont de chance de correspondre à de vrais amers naturels présents dans le modèle; on favorise donc dans la sélection les segments longs.

Pour la méthode de mise en correspondance des segments extraits de l'image avec ceux du modèle plusieurs choix sont possibles qu'on peut regrouper en deux grandes catégories:

- les méthodes globales (*dites **prédiction-vérification d'hypothèses***); plusieurs instances de déplacement entre image et modèle sont envisagées, chacune donne lieu au calcul d'un coût et l'instance donnant le coût minimal est retenue; les instances recouvrent le domaine possible des variations soit systématiquement avec la précision variations soit systématiquement avec la précision cherchée soit par une approche pyramidale qui permet de limiter l'exploration systématique au seul niveau le plus haut de la pyramide; les méthodes globales sont très couteuses en temps de calcul et la fonction distance n'est pas toujours simple à mettre au point; une des distances les plus utilisées est la distance de CHAMFER; les performances sont bonnes si les segments sont assez isolés et si la distorsion entre image et modèle est faible;

- les méthodes accumulatives dans lesquelles la transformation est déterminée de manière progressive en accumulant des fragments d'évidence: à chaque intégration d'un fragment d'évidence la transformation cherchée s'affine et son domaine d'admissibilité est réduit (méthode dérivée de la transformée de HOUGH); le fragment d'évidence est ici l'appariement d'un segment image avec un segment modèle, appariement basé sur l'orientation commune et éventuellement d'autres critères (longueur, sens du contraste,...). Si la transformation cherchée est une translation, chaque appariement possible conduit à un certain nombre de translations potentielles (en quelque sorte on peut dire que l'appariement "vote" pour certaines translations); à la fin de l'intégration des appariements, la translation potentielle la plus souvent rencontrée (celle qui a eu le plus de "votes") est retenue; l'ensemble des translations potentielles constitue ce qu'on appelle la nappe d'accumulation (figure C).

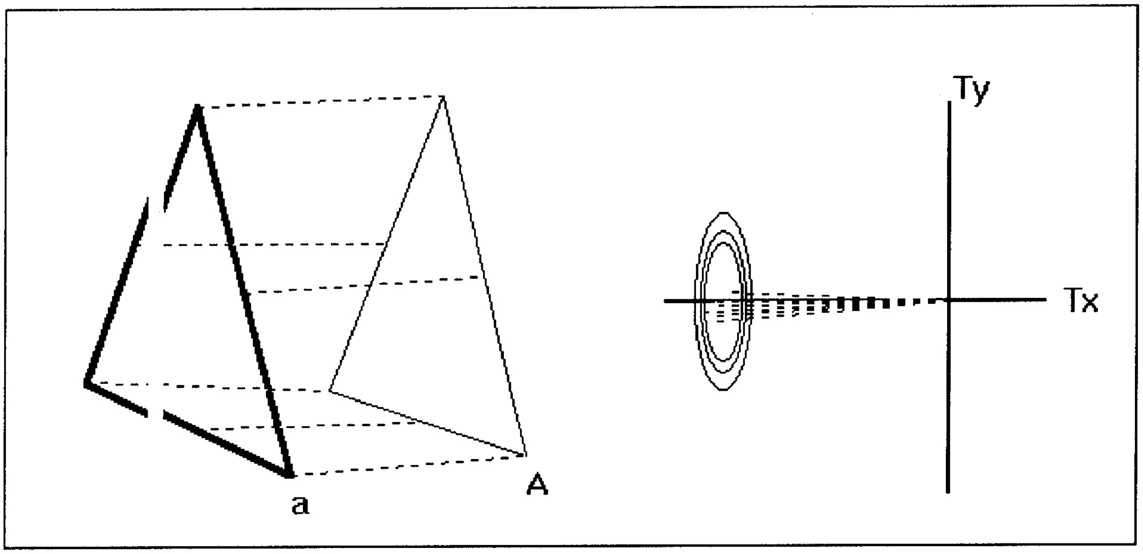

Les segments fins correspondent au modèle de référence, les segments épais sont ceux extraits de l'image radar (les segments homologues sont, en général, de taille et d'orientation différentes).

Toute translation [Tx,Ty] (trait en pointillé) qui fait correspondre, au moins partiellement, un segment du modèle avec un segment de l'image est reportée dans la nappe d'accumulation et le niveau courant du point (Tx,Ty) augmente.

Figure C: Construction de la nappe d'accumulation

En réalité la bonne transformation n'est pas systématiquement donnée par le pic le plus haut de la nappe d'accumulation, il peut en effet y avoir des fausses alarmes dues à des conjonctions fortuites non stables. Il faut donc que le pic soit suffisamment marqué pour donner une bonne précision mais pas trop isolé des autres pics de hauteurs voisines. La détection du bon pic est associée au calcul d'un indicateur de confiance, celui ci est basé sur la configuration du pic principal et des pics voisins, ainsi que sur les caractéristiques des segments modèle et image mis en correspondance.

L'ordre dans lequel sont faits les appariements est relativement indifférent puisque ceux-ci sont traités indépendamment les uns des autres (le vote se fait dans l'isoloir) par contre les critères d'appariement et la manière dont sont déterminées les translations potentielles pour un appariement ont une influence sensible. Par exemple un segment court extrait de l'image, qui, comme on l'a dit, a de fortes chances d'être un artefact, ne sera apparié à un segment modèle que si la condition d'orientation commune est respectée avec une très faible tolérance; par contre si le segment est plus long la tolérance d'appariement sur l'orientation sera plus grande. Il est aussi envisageable de ne pas considérer des segments isolés mais des couples de segments; cela a pour effet de diminuer fortement la fausse alarme dans la nappe d'accumulation mais le nombre de couples est beaucoup plus grand que le nombre de segments et cela augmente donc le temps de calcul.

Pour la mise en correspondance des segments, THOMSON-CSF a retenu une méthode accumulative.

L'organigramme général de ce dernier type de méthode (accumulative) est donné à la figure D

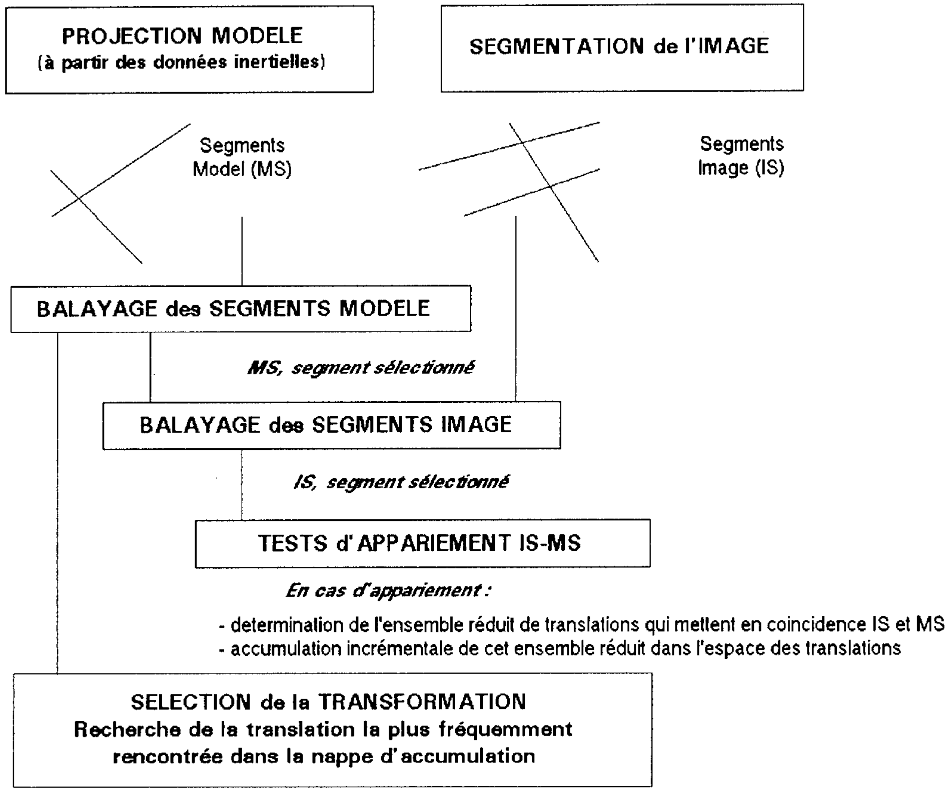
PROJECTION MODELE
(à partir des données inertielles)
SEGMENTATION de l'IMAGE
Segments Model (MS)
Segments Image (IS)
BALAYAGE des SEGMENTS MODELE
MS, segment sélectionné
BALAYAGE des SEGMENTS IMAGE
IS, segment sélectionné
TESTS d'APPARIEMENT IS-MS
En cas d'appariement :
- determination de l'ensemble réduit de translations qui mettent en coincidence IS et MS
- accumulation incrémentale de cet ensemble réduit dans l'espace des translations
SELECTION de la TRANSFORMATION
Recherche de la translation la plus fréquemment rencontrée dans la nappe d'accumulation

Figure D: Organigramme de la méthode accumulative

3-2-3 Préparation de Mission

Cette étape se déroule avant la mission

La préparation de mission consiste à extraire, des données source, les primitives utilisées dans le recalage (avec d'éventuels attributs). On a vu que les segments sont parmi les plus intéressantes de ces primitives.

Les questions à résoudre concernent:

- l'emprise au sol du modèle; celle-ci dépend beaucoup de la taille de l'image par rapport à la dynamique de recherche (l'incertitude de localisation) il est fondamental de savoir si on doit chercher l'image dans le modèle (taille de l'image petite par rapport à la dynamique de recherche) ou si l'on doit chercher le modèle dans l'image (taille de l'image grande par rapport à la dynamique de recherche); dans le premier cas l'emprise du modèle doit être telle que l'image soit toujours dans le modèle quelle que soit l'erreur de navigation; dans le second cas le modèle peut être réduit à un petit motif suffisamment étendu cependant pour qu'il soit unique dans la dynamique de recherche; dans le cas qui nous intéresse la taille de l'image radar est toujours supérieure à la dynamique de recherche.

- la sélection des primitives; il est toujours délicat de trouver des règles de sélection qui assurent le meilleur fonctionnement. Mais des règles simples peuvent cependant être appliquées, par exemple pour les segments, il paraît clair que le linéaire cumulé doit être supérieur à un seuil, que le pourcentage de segments longs doit être fort et que tous les segments ne doivent pas être dans la même classe d'orientation;

- l'attribution des primitives ; en considérant toujours l'exemple des segments, l'attribut le plus simple à renseigner, quand il est pertinent (par exemple pour les transitions terre-eau, pour les limites de bois, de vallées) est le sens du contraste le long du segment; cette indication peut éviter lors du recalage de faire de faux appariements;

Mais d'un point de vue opérationnel la question majeure est souvent le degré d'automatisation de la chaîne de préparation de mission; de ce point de vue, comme on l'a déjà souligné, la constitution du modèle à base de segments est automatisable que ce soit à partir de fichiers géographiques numériques (l'élaboration est alors tout naturellement automatique) ou à partir d'images spatiales du type SPOT (figure E);

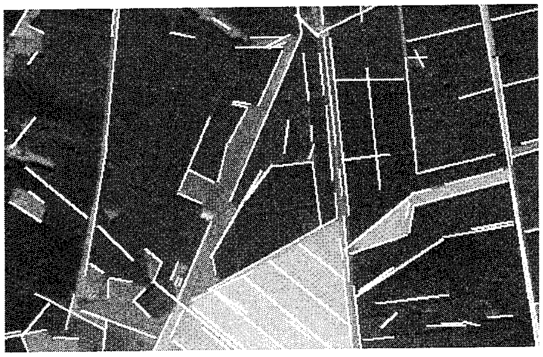

Figure E: Image SPOT segmentée

Dans ce dernier cas l'intervention manuelle de l'opérateur est limitée à un contrôle de validité du modèle automatique et au renseignement des attributs de contraste pour quelques segments.

Une dernière étape avant mise en forme du modèle est la validation. Celle-ci est en général automatique et utilise, quand c'est possible, le même algorithme de recalage qu'à bord: des instances d'images sont découpées dans le modèle (en extension ou en réduction suivant les cas) et les segments de ces instances sont mis en correspondance avec le modèle; ce dernier n'est validé que si l'auto-corrélation présente un pic bien marqué et bien démarqué des possibles lobes secondaires.

La mise en forme du modèle à embarquer ne pose pas de problème particulier; s'agissant de données du type objet (plutôt que pixels) le volume est faible.

3-2-4 Acquisition de données source

La préparation du modèle nécessite la disponibilité de données source qui doivent être à jour, très précises (mieux que 10 m pour une précision de localisation du même ordre), soigneusement référencées et dans lesquelles la cible est observable (cas d'une cible fixe géoréférencée).

De telles données source existent ; on peut ainsi citer parmi les données les plus utilisables :

- les images SPOT dont les caractéristiques principales sont la couverture mondiale et la bonne résolution (10 m) ; la localisation géographique absolue peut poser des problèmes dans les régions où manquent des points d'appui de coordonnées bien connues ;

- les images HELIOS ; ce satellite d'observation militaire qui vient d'être lancé en Juillet dernier par la France, avec la coopération de l'Italie et de l'Espagne, doit fournir des images optiques de bien meilleure résolution que SPOT ;

- les images ERS1 qui ont une résolution moins bonne que celle de SPOT mais qui ont l'avantage d'être des données SAR donc plus facilement comparables aux cartes élaborées par les radars de pointe avant ;

- les fichiers géographiques numériques ; les fichiers DLMS, de couverture et de contenu limités, devraient être remplacés dans un proche avenir par les données VMAP de couverture mondiale et très complètes (plus de 10 thèmes sont prévus : routes, hydrographie, côtes, relief, zones urbaines, aéroports, voies de chemin de fer, ...) ; cependant la précision de 10 m ne sera sans doute effective que dans quelques régions ;

- les images de reconnaissance aérienne (comme celles du radar de surveillance et de reconnaissance RAPHAEL en service dans l'armée de l'air francaise) qui ont une bonne résolution mais qui ne sont acquises que sur certaines zones. Ces images ont des caractéristiques analogues à celles élaborées par le radar de pointe avant, ceci facilite notablement le choix et le renseignement des primitives qui vont constituer le modèle de référence. Dans le cas où la zone visée n'est pas accessible aux avions de reconnaissance, un SAR spatial peut être utilisé pour l'acquisition des données source.

3-3 Avantages de la méthode présentée

Les principaux avantages de ce type de méthode basé sur la mise en correspondance, par technique accumulative, de segments extraits de l'image avec des segments d'un modèle de référence élaboré en Préparation de Mission sont:

- la robustesse (conséquence du choix des primitives),
- la possibilité de mise en oeuvre en temps réel (maitrise du temps de calcul)
- la souplesse d'évolution
  . adaptation aisée à des modes de cartographie de caractéristiques différentes (résolution de classe métrique par exemple),
  . ajout de primitives autres que les segments (points brillants par exemple) .
- le "filtrage" des déformations résiduelles de l'image radar.

4 - Les applications de la fonction

Les applications de la localisation automatique sont multiples.

La première qu'il faut citer est l'acquisition d'objectifs fixes de coordonnées connues, c'est le cas des amers de recalage ou des cibles qu'on sait positionner précisément dans leur environnement (grace à une reconnaissance préalable à la mission). Dans ce cas la fonction donne directement la position estimée de l'objectif, celui ci et/ou son environnement recalé peuvent être directement superposés à la carte radar (ainsi que la qualité du recalage calculée par le traitement). L'opérateur dispose ainsi des éléments permettant de juger la pertinence du traitement.

La deuxième application est l'aide à l'acquisition de cibles déplacables (mobiles à l'arrêt, franchissement, PC de campagne,...) ou mobiles.

Dans ce cas l'application comporte deux étapes:

- le recalage qui va permettre de visualiser sur la carte radar des éléments caractéristiques de l'environnement qui peuvent être très utiles pour l'acquisition de certaines cibles. On pourra visualiser, par exemple, les taxi way, les voies routières ou ferroviaires, les cours d'eau,...

- l'identification qui permet l'acquisition directe de certaines cibles (shelters, chars, bateau,...) en utilisant un modèle local de celles ci. Il faut noter qu'à cause du principe SAR, seule une cible déplacable (donc fixe quand on l'observe) peut être localisée précisément.

La dernière application que nous citerons est celle présentée dans la communication ASTRID. Il s'agit de coopération radar et optronique qui peut être envisagée pour tout type de cibles. Le radar effectue une prélocalisation et transmet une direction à rallier à un capteur optronique petit champ qui va permettre de confirmer la présence de la cible et éventuellement d'en améliorer la localisation. L'avion de combat RAFALE disposera d'un radar et d'un capteur optronique en pointe avant utilisables en Air-Sol, le radar ayant plusieurs modes SAR et l'optronique des modes d'imagerie visible et infrarouge.

ASSOCIATION DE CAPTEURS OPTRONIQUES DE NOUVELLE GÉNÉRATION AUX SYSTÈMES DE NAVIGATION ET D'ATTAQUE

J. JOFFRE - E. JULLIEN
JP. BERNOVILLE - R. GOULETTE - Y. LE GUILLOUX
SAGEM S.A.
Division Navigation et Défense
27 rue Leblanc
75512 PARIS Cedex 15
FRANCE

Sommaire :

Les capteurs infrarouge ont été intégrés sur des avions d'armes depuis une vingtaine d'années. On distingue principalement parmi ceux-ci les capteurs frontaux (FLIR généralement montés en pod de navigation), dédiés au pilotage de nuit et les pods de désignation, utilisés en phase terminale d'attaque air-sol.

Alors même que le besoin de navigation de nuit existe pour assurer une permanence de la menace aérienne [1], on constate que la généralisation des systèmes infrarouge n'a pas été réalisée dans les avions d'arme.

L'évolution technologique a abouti récemment à la réalisation de capteurs à hautes performances, occupant un volume réduit, donc intégrables en cellule, et susceptibles de remplir les deux fonctions principales de la mission : navigation et attaque.

L'apparition de l'imagerie optronique de nouvelle génération utilisant les détecteurs IRCCD permet ainsi une avancée importante dans les missions de frappe Air/Sol.

L'objet de cet article est de préciser les principes et caractéristiques de capteurs IRCCD en France, et leur apport tout au long d'une mission de nuit. Pour cela, il décrit les travaux réalisés par SAGEM avec le soutien des Services Étatiques :

- la caméra thermique IRIS,
- l'intégration réalisée sur MIRAGE 2000,
- l'aide au pilotage de nuit,
- les méthodes de recalage de navigation par imagerie infrarouge,
- l'apport concernant l'attaque air-sol de nuit.

Mots clé : – caméra thermique,
– IRCCD,
– recalage de navigation,
– traitement d'images,
– détection de contours
– couplage Inertie/Infrarouge

Liste de symboles :

– CCPI	Calcul Continu du Point d'Impact
– CCPL	Calcul Continu du Point de Largage
– FLIR	Forward Looking Infra Red
– GPS	Global Positionning System
– IRCCD	Infra Red Charged Coupled Device
– IRLS	Infra Red Line Scanner
– SMT	Système Modulaire Thermique
– TDI	Time Delay Integration
– VTH	Viseur Tête Haute

1 CAMÉRA IRCCD IRIS

SAGEM a débuté le développement de la caméra IRIS en 1988. Elle a été le premier utilisateur du détecteur IRCCD 288x4 (8-12 microns) à couplage direct de la Sofradir.

SAGEM a conduit son développement avec les principes suivants :

- la caméra devait être conçue de façon modulaire. Les fonctions critiques devaient être intégrées dans des modules communs aux diverses applications envisagées,
- le bloc senseur comprenant le détecteur et le système de balayage devait être le plus petit possible pour pouvoir se loger avec grande facilité dans la partie utile des applications,
- les modules communs devaient être capables de supporter les environnements militaires des 3 Armes,
- la caméra devait être capable de s'interfacer suivant différents standards vidéo, sorties numériques et analogiques (STANAG 3350 et RS 170) et liaisons numériques (RS 422, 1553, ARINC),
- l'information vidéo devait être numérisée à la sortie du détecteur (codage sur 12 bits) permettant ainsi un traitement d'images pour non seulement les corrections de non-uniformité ligne à ligne, mais également l'amélioration d'image et tout autre traitement de l'information vidéo. Les paragraphes suivants sont une application de cette possibilité de traitement interne de l'image.

1.1 Description des modules

1.1.1 Bloc senseur

Il comprend :

- le détecteur 288x4 associé à un refroidisseur,
- l'optique de focalisation,
- le système de balayage horizontal en dents de scie permettant de fournir une trame de 288 lignes,
- le système d'entrelacement vertical permettant de décaler l'axe optique d'un demi-détecteur pour réaliser la deuxième trame,
- l'électronique nécessaire pour commander les phases du CCD et l'adaptation des informations vidéo issues du détecteur.

Paper presented at the AGARD MSP Symposium on "Technologies for Precision Air Strike Operations in Rapid-Reaction and Localised-Conflict Scenarios", held in Seville, Spain, from 16-19 October 1995, and published in CP-576.

1.1.2 Électronique déportée

Fonctionnellement, elle doit comporter au moins 2 cartes au standard VME et format double Europe qui assurent :

- la conversion analogique/numérique du signal vidéo issu du bloc senseur, le traitement des non-uniformités, la mise à disposition sur un bus vidéo numérique de l'image,
- la conversion numérique/analogique de cette information pour la mise au bon standard vidéo (STANAG 3350 ou RS 170).

Ce format double Europe, au standard VME, permet de s'adapter directement, au moins pour les développements en laboratoire, à des cartes de traitement d'images ou à des processeurs déjà développés par ailleurs.

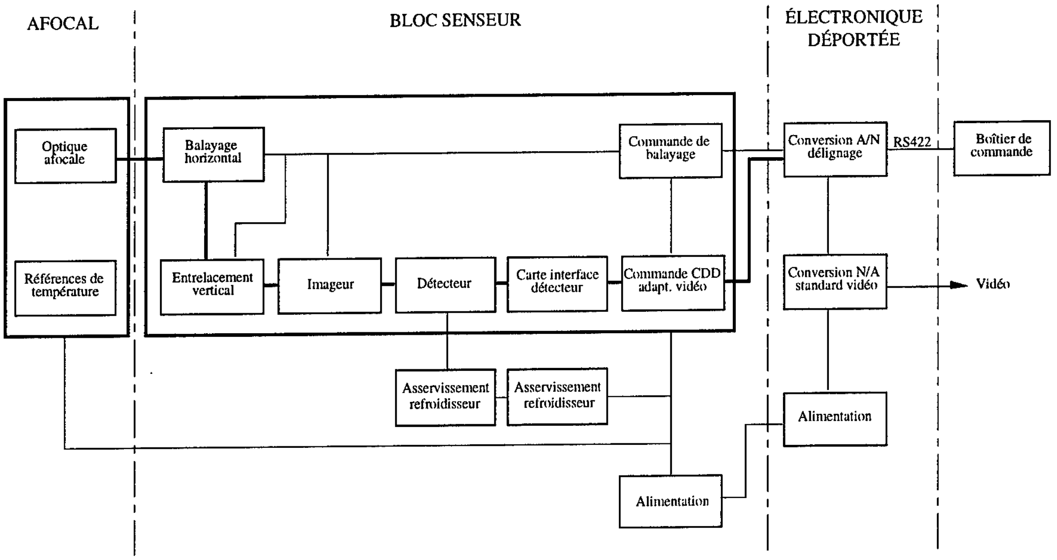
AFOCAL
BLOC SENSEUR
ÉLECTRONIQUE DÉPORTÉE
Optique afocale
Références de température
Balayage horizontal
Entrelacement vertical
Imageur
Détecteur
Carte interface détecteur
Commande de balayage
Commande CDD adapt. vidéo
Asservissement refroidisseur
Asservissement refroidisseur
Alimentation
Conversion A/N délignage
RS422
Boîtier de commande
Conversion N/A standard vidéo
Vidéo
Alimentation

1.2 Principales caractéristiques des modules communs

- Formats :
  nombre de points par ligne : 768,
  nombre de lignes : 575 entrelacées, fréquence trame : 50 Hz } STANAG 3350,
  nombre de lignes : 480 entrelacées, fréquence trame : 60 Hz } RS170.
- Champ du bloc senseur sans afocal : 14,4° x 10,8°.
- Champ instantané de chaque détecteur (IFOV) : 0,58 mrd x 0,65 mrd.
- NETD : < 0,045 °C.
- Non uniformité < 2 NETD sur toute l'image (à 1 σ).
- Temps d'intégration de chaque pixel $\leq 20\ \mu$s.
- Temps de refroidissement du détecteur à 77 K : 5 mn pour une température ambiante de 20 °C.
- Puissance électrique : 120 W.

1.3 Traitement d'image de premier niveau

1.3.1 Correction des non uniformités ligne à ligne [2]

Chaque trame est réalisée par le balayage horizontal de la barrette de 288 détecteurs (en fait, 4 détecteurs en ligne fournissent une information avec un rapport S/B amélioré par 2 grâce au TDI). Chaque ligne ainsi générée a son propre biais et son facteur d'échelle qu'il faut identifier pour avoir une image homogène.

Le balayage du miroir horizontal permet de voir à chaque trame, en bords de champ droit et gauche, deux références de température ; l'une, positionnée à la température des points chauds de l'image, l'autre à celle des points froids. On obtient ainsi 2 références dans la température de scène qui permettent de calculer les coefficients de biais et de facteur d'échelle de chaque détecteur.

Après la conversion analogique/digitale, la correction suivante est appliquée :

$$S'_i = a_i\ S_i + b_i$$

où : S_i est l'information brute
a_i et b_i sont respectivement les coefficients de gain et de biais

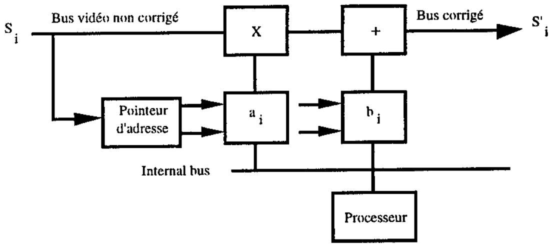
S_i
Bus vidéo non corrigé
X
+
Bus corrigé
S'_i
Pointeur d'adresse
a_i
b_i
Internal bus
Processeur

On obtient ainsi une non uniformité inférieure ou égale à 2 NETD sur toute l'image (à 1 σ).

Cette qualité de "délignage" est importante d'une part pour le pilotage (il ne faut pas faire apparaître des lignes que le pilote pourrait confondre avec l'horizon), et pour les traitements d'images ultérieurs qui vont justement rechercher des lignes dans l'image.

1.3.2 Amélioration de la résolution de l'image [4]

La qualité optique du bloc senseur et celle de l'afocal correspondant à l'application sont définies pour fournir une FTM (Fonction de Transfert de Modulation) de l'ordre de la limite imposée par la diffraction.
La FTM est aussi limitée par la taille des détecteurs et la fréquence d'échantillonnage.

Ainsi, la FTM globale de l'ensemble est mathématiquement déterminée par des lois physiques connues. Pour améliorer l'image, il faut compenser l'atténuation des fréquences moyennes et hautes. La caméra IRIS possède en option une carte spécifique réalisant cette transformée inverse par un filtrage de Wiener.

Aspect théorique :

Si $g(x,y)$ est l'image obtenue à partir de l'image originale ou idéale $f(x,y)$, on peut modéliser le phénomène de la façon suivante :

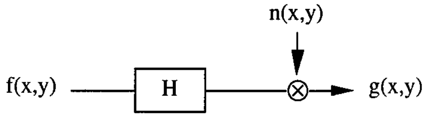

Où H est la fonction de transfert optique de la caméra
$n(x,y)$ est le bruit apporté par l'ensemble du système (optique et électronique).

La solution au problème au problème d'amélioration de $g(x,y)$a été donnée par Wiener en proposant la fonction inverse :

$$Wk(x,y) = FT^{-1}\left(\frac{1}{h(u,v)} \bullet \frac{|h(u,v)|^2}{|h(u,v)|^2 + k}\right)$$

où k est un paramètre d'optimisation pour compenser le bruit,
$h(u,v)$ est la fonction de transfert de la caméra dans le domaine fréquentiel.

L'image restaurée est de la forme :

$$fre(x,y) = Wk(x,y) \otimes g(x,y)$$

Ce filtrage de Wiener est réalisé dans la caméra IRIS en temps réel à l'aide d'un convolueur 7 x 7. Les coefficients utilisés sont déterminés à partir des mesures de la fonction d'étalement de point (équivalente à la réponse impulsionnelle, mais en 2 dimensions).

1.4 Applications de la caméra IRIS

Le premier prototype de la caméra IRIS a été réalisé pour un développement exploratoire aéronautique. Il a effectué ses premiers vols sur Nord 260 au CEV en 1990. La caméra a été installée dans le nez de l'avion. Ces premiers essais ont fourni les premières images IRCCD du capteur 288x4 de la Sofradir. La caméra IRIS a depuis lors été utilisée dans une grande variété d'applications, chacune d'entre elles ayant ses spécificités propres. Son architecture modulaire, sa petite taille et sa faible consommation permettent de l'installer dans différentes configurations.

1.4.1 Applications Marine

La caméra thermique IRIS a été choisie par la Marine française en 1989 pour le périscope du sous-marin nucléaire nouvelle génération "LE TRIOMPHANT".

La caméra IRIS a aussi été retenue par la Marine danoise en 1990 pour les mâts optroniques de ses sous-marins d'attaque.

Les contraintes spécifiques de ces programmes étaient :

- la dimension du bloc senseur qui devait être compatible du diamètre du périscope
- deux modes de fonctionnement imagerie et veille (balayage interne de la caméra arrêtée)
- la grande distance entre le bloc senseur et l'électronique déportée qui devait être supérieure à 40 mètres.

Ces systèmes sont les premières applications opérationnelles de capteurs IRCCD.

1.4.2 Application terrestre

La caméra thermique IRIS a été choisie par Euromissile en 1991 pour le programme d'amélioration du système d'armes ROLAND. SAGEM est responsable du développement du viseur complet qui intègre la caméra IRIS-G. Dans cette application, il y a aussi deux modes de fonctionnement : le mode imagerie et le mode veille.

La qualité de l'image doit être compatible avec les traitements pour la détection et la poursuite de cibles distantes (avions ou hélicoptères) jusqu'à 20 km. L'information vidéo numérique est transmise sur 12 bits au calculateur de veille et de poursuite.

Les caméras IRIS G sont en cours d'intégration avec le Viseur GLAIVE.

1.4.3 Application hélicoptère

Le maître d'œuvre du Viseur Principal du programme hélicoptère "TIGRE HAP" a aussi sélectionné la caméra IRIS. Les contraintes spécifiques de cette application sont les environnements mécanique et thermique sévères et l'intégration d'une stabilisation fine dans la caméra pour assurer les performances de portée en petits champs.
IRIS a également été retenue pour le viseur principal de l'hélicoptère ROOIVALK.

1.4.4 Application Drone

La caméra IRIS doit équiper le Drone SPERWER pour lequel la SAGEM a été très récemment retenue par l'Armée de Terre Hollandaise.

1.4.5 Application aéronautique

Nous allons décrire plus précisément l'intégration de la caméra IRIS dans le MIRAGE 2000 B.O.B. (Banc Optronique Biplace) du Centre d'Essais en Vol.

Cette intégration a été réalisée avec le soutien du STTE, Service Technique des Télécommunications et Équipements, rattaché à la Direction des Constructions Aéronautiques de la DGA.

2 INSTALLATION DANS L'AVION

2.1 Intégration dans le MIRAGE 2000

Le MIRAGE 2000 dispose d'un Viseur Tête Haute (VTH) capable de présenter une image vidéo Raster au standard CCIR. Le champ de l'image vidéo projetée en tête haute est de 18°x24°.

La caméra IRIS a donc été dotée d'un afocal permettant d'adapter son champ à celui du VTH. Le bloc senseur avec son afocal et l'électronique déportée sont installés en soute en avant du train d'atterrissage.

La caméra est harmonisée avec le VTH de manière à projeter une image collimatée qui se superpose très exactement avec le monde extérieur. Avec 768 points par ligne et un champ horizontal de 24°, des pixels de taille carrée, on obtient dans l'espace objet une résolution de 0,55 mrd, tout à fait compatible avec la résolution de l'œil.

Le traitement d'amélioration d'images permet de fournir une finesse d'image qui donne toute satisfaction au pilote.

Dans les applications aéroportées, les variations de dynamique de la scène quand l'avion pointe vers le ciel (en général très froid) ou vers le sol (plus chaud) sont très importantes. Le contrôle automatique de gain et de niveau moyen de l'image a des constantes de temps adaptées aux missions typiques d'un avion militaire en particulier en utilisant les informations d'attitude (couplage IR. Inertie).

2.2 Installation dans un avion d'armes

L'installation dans l'avion est simple, il suffit de trouver en pointe avant le volume nécessaire pour loger le bloc senseur et son afocal. Dans la plupart des avions, il y a une soute pour un télémètre laser ou des provisions pour des équipements optionnels. Elle peut être aménagée pour recevoir en plus le bloc senseur grâce à son volume réduit. La partie qui doit dépasser du fuselage est celle du hublot de sortie; elle doit permettre de passer le champ vertical sous le fuselage sans vignettage. Avec un champ de 18°x24°, la taille de la pupille est très petite (diamètre = 16 mm).

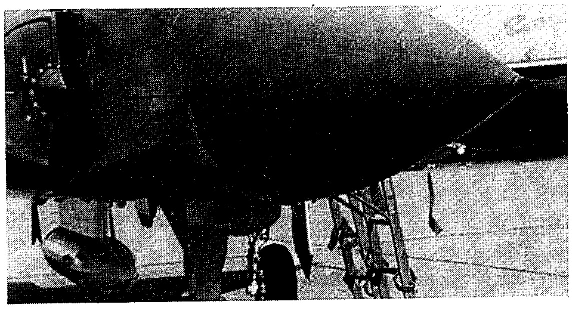

L'intérêt d'une telle installation par rapport à une installation en pod est évident ; en particulier parce que la caméra est rigidement fixée à la même structure avion que le VTH.

Listons quelques avantages:
- absence de vibrations relatives,
- harmonisation par rapport au VTH invariante suivant les différents points du domaine de vol,
- tous les points d'emport sont disponibles pour l'armement,
- enfin, la traînée aérodynamique est modifiée beaucoup plus faiblement (pratiquement inquantifiable en subsonique).

Tous les avions peuvent être prédisposés, comme pour les pods, pour recevoir la caméra. Si les contraintes budgétaires ne permettent pas d'équiper tous les avions, les caméras pourraient être tout aussi facilement installées d'un avion à un autre, comme cela est fait pour les pods.

Le couplage au système d'arme peut être très simple. Pour une installation de démonstration de capacité du FLIR dans un avion mono ou biplace, il suffit, outre l'installation optico-mécanique déjà décrite précédemment, d'installer une liaison vidéo vers le boîtier générateur de symbole du VTH et vers les moyens d'enregistrement (magnétoscope). La mise en œuvre de la caméra peut être faite par un petit boîtier de commande en banquette.

3 AIDE AU PILOTAGE

3.1 Apport de la caméra IRIS

Ce type d'installation a été réalisé depuis de nombreuses années dans différents avions d'arme. Mais par rapport aux équipements précédents, l'apport de cette caméra est dans la très grande qualité de l'image. La résolution thermique, quelques centièmes de degrés, et la résolution spatiale permettent de fournir une image infrarouge d'une qualité aussi bonne que celle d'une image dans le visible. Par rapport aux matrices CCD visibles 768x575 lignes, on peut même considérer que pour ce qui concerne la résolution spatiale, l'image infrarouge est meilleure. En effet, le système, tel qu'il a été conçu, comporte un suréchantillonnage de 1,7 en balayage horizontal et de 2 en vertical (entrelacement de deux trames continues). La topologie des matrices CCD a pour conséquence que le facteur de remplissage est toujours inférieur à 1.

3.2 Portée

Les portées en infrarouge dépendent bien évidemment des conditions atmosphériques, des tailles et des températures de cibles. En simplifiant à l'extrême, on peut considérer que les portées fournies par la caméra IRIS sont, pour ce qui concerne le paysage, du même ordre de grandeur que celles en visible de jour, pour des conditions atmosphériques données. Par ailleurs, l'imagerie infrarouge apporte une information spécifique qui est la mise en évidence des points chauds. A titre d'exemple, une cheminée d'usine peut être détectée en grand champ par bonne condition atmosphérique à plus de 13 nautiques, alors qu'en visible on ne l'aperçoit qu'à 2 ou 3 nautiques.

Toutes conditions étant égales par ailleurs, les simulations montrent que l'amélioration en portée par rapport aux systèmes SMT français de la génération précédente, apporte un gain en portée de 40 à 50 %.

C'est cette avancée technologique des capteurs et de leur mise en œuvre qui donne aujourd'hui un regain d'intérêt pour l'utilisation de caméra infrarouge dans les avions d'armes.

3.3 Incrustation de la symbologie

L'incrustation de la symbologie du VTH est réalisée par le boîtier générateur de symboles. Avec un tel système, on peut reconduire de nuit les procédures de navigation et d'attaque au sol classique qu'on ne pouvait faire que de jour sur la plupart des avions mono ou biplace actuels.

3.4 Couplage avec les jumelles de vision de nuit

L'utilisation de l'imagerie vidéo avec le champ fixe dans le VTH n'est certainement pas suffisante pour assurer un pilotage de nuit dans de bonnes conditions. Si le pilote a, de nuit, une parfaite vision du monde extérieur à travers le VTH, par contre il n'a aucune vision pariétale ; celle-ci étant très utilisée pour les références attitudes avion et notion de hauteur en pilotage à vue. Le champ de vision est donc trop petit pour assurer un pilotage avec la sécurité suffisante surtout à basse altitude [1]. Les pilotes ont l'impression de voler dans un tunnel et les manœuvres en latéral sont dangeureuses à basse altitude. Le couplage avec les jumelles de vision de nuit résout actuellement le problème.

On peut faire de la navigation de nuit par temps clair, à basse altitude (à quelques centaines de pieds). Certes l'imagerie visualisée dans le VTH de nuit ne donne pas la même vision du sol que de jour, et elle n'est pas stéréoscopique, mais à l'expérience (50 vols sur MIRAGE 2000 et MIRAGE III dans des conditions atmosphériques et des scènes variées), la réalité du relief semble être très bien ressentie par les pilotes grâce à la qualité de l'image qui permet une bonne interprétation en 3D et au déplacement de l'avion par rapport au sol. La notion de hauteur et de vitesse est donnée par le défilement pariétal du sol obtenu grâce aux jumelles de vision de nuit.

3.5 Besoin en précision de position horizontale

Néanmoins, pour assurer une sécurité suffisante à très basse altitude, il est nécessaire de conforter le pilote par une aide à la navigation dans le plan vertical [1], par exemple une ficelle de vol ou un suivi de terrain sur fichier, automatique ou non. Cela nécessite une précision importante dans le plan horizontal qui est fournie par la centrale à inertie recalée par divers moyens.

La caméra I.R. peut servir au recalage grâce aux méthodes présentées ci-après. Ainsi, le couplage inertie/infrarouge possédant ses propres moyens de recalage permettant le pilotage pour la navigation de nuit est un système autonome.

4 RECALAGES DE NAVIGATION

4.1 Introduction

Les systèmes de navigation et d'attaque des avions d'armes utilisent tous comme référence de position, de vitesse et d'assiette, des centrales à inertie.

Les précisions classiques de ces centrales, en inertie pure, sont de l'ordre 0,5 à 1 Nm/h en position et de 0,6 à 1,2 m/s en vitesse ; ce qui correspond à des gyroscopes de la classe de 0,5 à 1/100°/h .

Les erreurs sur les informations d'attitude sont très faibles. Elles sont de l'ordre de 0,5 mn à 1 mn d'arc, soit $1{,}5.10^{-4}$ rd ou $3\ 10^{-4}$ rd, donc meilleur que l'ordre de grandeur de la précision d'harmonisation et de codage des angles d'attitude.

Cette grande précision sur les informations d'attitude est une propriété essentielle de l'inertie qui va nous servir grandement dans le recalage par traitement d'images.

De façon classique, les erreurs de la centrale sont corrigées tout au cours du vol grâce à des informations fournies par des recalages de position. Ces informations alimentent un filtre de Kalman qui fournit en temps réel la meilleure estimée de la position, de la vitesse et des attitudes de l'avion.

La navigation de nuit va bénéficier de la précision en position horizontale pour la ficelle de vol.
Les calculs de balistique effectués pour la désignation du point d'impact en CCPI ou de l'instant de largage si la cible a été précédemment désignée (CCPL), vont bénéficier prioritairement des informations recalées de vitesse.

4.2 Moyens actuels

Aujourd'hui, ces recalages de position peuvent être réalisés :

- de façon manuelle de jour et par bonne visibilité : par passage à la verticale au-dessus du point dont les coordonnées sont connues, et par désignation avec un réticule de ce même point (triangulation ou télémétrie laser ou radar),
- de façon automatique et en tout temps : par corrélation d'altitude, corrélation radar et GPS.
  - La corrélation d'altitude (CORZ) nécessite un modèle numérique de terrain et une radio-sonde ou un senseur équivalent qui mesure la hauteur de l'avion au-dessus du terrain survolé. Le profil de terrain est enregistré pendant le temps durant lequel l'avion survole la région dont le modèle numérique de terrain a été mis en mémoire lors de la préparation de mission.

    Le principe consiste à trouver le maximum de corrélation entre le profil enregistré et un profil extrait du modèle numérique de terrain en faisant déplacer parallèlement à lui-même le profil enregistré sur le modèle numérique de terrain. Le maximum de corrélation donne la meilleure position estimée qui va être introduite dans le filtre de Kalman.

    Cette méthode de recalage est implantée par SAGEM dans de nombreux systèmes depuis plus d'une décennie. L'intérêt de la corrélation d'altitude est d'être autonome, imbrouillable, discrète et précise. Sa précision dépend du modèle numérique de terrain mais elle est classiquement de 60 m pourvu qu'il n'y ait pas d'ambiguïté (nécessité d'une bonne préparation de mission). On peut néanmoins trouver des régions (par exemple terrain plat) où la CORZ n'est pas utilisable.

    Le traitement numérique pour la corrélation peut être réalisé sans difficulté dans le calculateur de la centrale. Il faut par contre une mémoire de masse pour stocker le modèle numérique de terrain.
  - La corrélation Radar nécessite un radar doté de la fonction cartographique adaptée. Cette fonction réalise une prise d'image radar de la zone de recalage que l'on compare avec une image prévisionnelle horizontale issue de la préparation de mission. La précision est de 60 à 80 m. Ce type de traitement peut fonctionner à très haute altitude (30 000 ft). A cause de la complexité de la préparation de mission, du recalage et du capteur, ce type de traitement est implanté dans un très petit nombre d'avions.

- Les systèmes GPS peuvent fournir en continu une information de position dont la précision dépend du code et peut aller de 100 mètres (code C/A) jusqu'à une dizaine de mètres (code P/Y) s'ils disposent des clés nécessaires. Le recalage peut donc, surtout s'il utilise un couplage serré (utilisation des informations de pseudo-distance dans le filtre de Kalman) être très précis. Néanmoins, le GPS n'est pas un moyen autonome et, en cas de conflit, cette information peut ne pas être utilisable, ne serait-ce que pour des raisons de brouillage (le signal reçu est très faible et peut être très facilement brouillé localement).

4.3 Recalage par imagerie infrarouge

Ces 3 procédés de recalage quasiment automatiques utilisent des capteurs très différents. Ils ont chacun leurs contraintes et leurs limitations. Ils laissent la place à un autre moyen qui utiliserait l'imagerie infrarouge pour être utilisable comme eux de jour comme de nuit.

Le recalage par imagerie est un moyen totalement autonome, discret, imbrouillable (à moins de changer l'aspect de la région survolée !).

Ces caractéristiques ressemblent à bien des égards à celles de la corrélation d'altitude. Par contre, ces deux modes de recalage par imagerie ou par corrélation d'altitude sont très complémentaires. En effet, sur un terrain totalement plat la CORZ ne peut pas fonctionner alors que c'est là où les traitements les plus simples de l'imagerie (détection d'amers linéaires) peuvent être appliqués sans problème.

SAGEM a développé depuis plus de 10 ans des techniques de recalage de ses centrales par traitement d'image. La première est basée sur un analyseur infrarouge ventral (Super Cyclope ou Cyclope 2000 de la société SAT). Les autres sont basées sur une caméra infrarouge montée en frontal (FLIR) comme dans le M2000 .

La première technique sera citée essentiellement pour son aspect didactique. Les autres qui concernent le recalage frontal font l'objet de cette présentation.

C'est l'arrivée à maturité de capteurs infrarouge de grande qualité qui permet de proposer le recalage par imagerie frontale sur avions d'armes.

4.3.1 Recalage ventral

L'analyseur monoligne construit son image ligne par ligne en utilisant le déplacement de l'avion. La résolution de l'image est différente au centre et au bord de l'image. L'image, elle-même, dépend de l'attitude de l'avion. Le premier traitement consiste donc à effectuer toutes les corrections pour fournir une image du sol conforme, c'est-à-dire qui peut se superposer à une carte du terrain survolé. Avec une telle image du terrain survolé, on conçoit immédiatement que l'on peut facilement se recaler en cherchant dans cette image des objets dont la position est connue.
Le premier système que SAGEM a développé était basé sur l'idée simple que des lignes droites (routes, voies ferrées, bordures de terrain) étaient facilement détectables dans l'image et caractérisées uniquement par leur orientation par rapport au nord. Très souvent il y a des voies de communication près des objectifs.

Le système de recalage, grâce à la connaissance de sa position estimée, déclenche le processus quand l'avion arrive dans l'ellipsoïde d'incertitude à 3 σ de la position avion centré sur le milieu de la droite de recalage dont il va rechercher l'orientation dans sa base de données.

La connaissance de l'attitude avion, cap en particulier, et de l'orientation de cette ligne droite par rapport au nord, donne immédiatement l'orientation attendue de cette ligne dans l'image.

La résolution de l'orientation d'une ligne droite dans une image de haute résolution (plus de 1200 pixels par ligne) est de l'ordre de grandeur - ou bien meilleure - de la précision en cap de la centrale.

Suivant la position de l'avion, cette ligne dans l'image se déplacera parallèlement à elle-même. Il reste donc à trouver où cette droite se situe dans l'image et on aura une information de position dans la direction perpendiculaire à cette droite. C'est donc un recalage monodirectionnel.

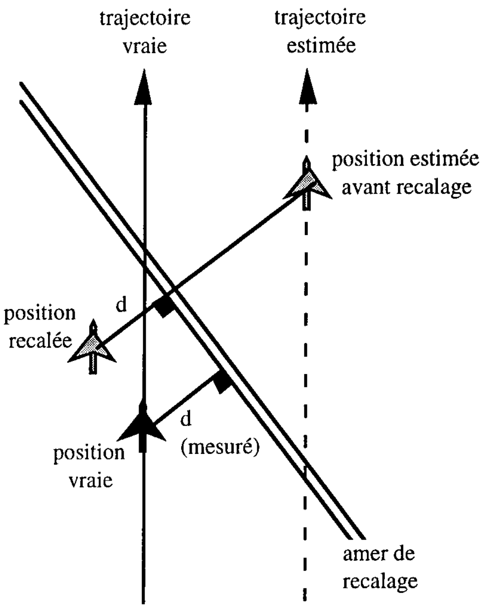

Le filtre de Kalman utilisera cette information pour recaler au mieux la position. Des recalages successifs avec des droites d'orientations nettement différentes permettront d'affiner la position sur les 2 axes.

La précision de recalage est très dépendante de la précision sur la hauteur par rapport au sol, il est donc préférable d'utiliser l'information de la radio-sonde au moment de la prise d'image pour définir la hauteur.

Pour trouver la ligne dans l'image, on effectue une détection de contour (en calculant les gradients X et Y et en effectuant un seuillage).

L'algorithme consiste ensuite à découper l'image en secteurs parallèles à la direction de la ligne recherchée et à accumuler les points de contour dans chaque secteur.

On obtient ainsi un histogramme donnant le nombre de points par secteur. Le maximum de l'histogramme indique celui où se trouve notre ligne recherchée dont la position dans l'image permet d'effectuer le recalage.

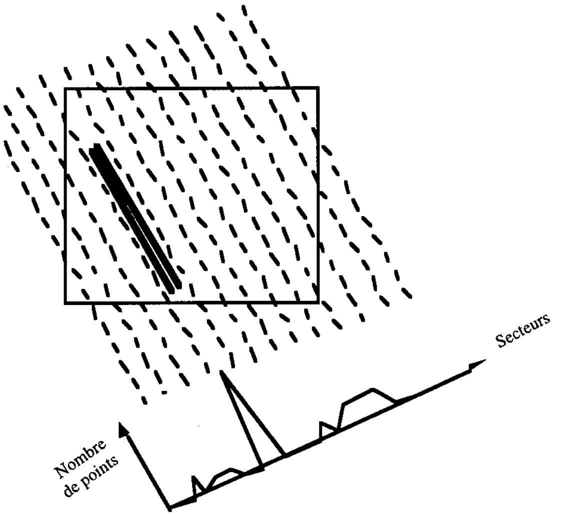

Cet algorithme a été testé en laboratoire sur des images réelles avec des données de navigation enregistrées lors d'essais en vol d'un MIRAGE F1CR. Il n'a pas été utilisé opérationnellement du fait du faible nombre d'avions français équipés d'analyseur monoligne.

4.3.2 Recalage frontal

L'idée est donc d'utiliser la caméra frontale que l'on propose pour les systèmes de navigation et d'attaque jour/nuit pour mettre en œuvre les études que la SAGEM a effectuées durant ces dernières années.

L'axe optique de la caméra est parallèle à celui du VTH. Il est incliné de quelques degrés (-7° pour le M2000) sous la référence horizontale avion.

4.3.2.1 Recalage monodimensionnel

Le problème est un peu plus complexe que celui posé par l'analyseur monoligne car l'image n'est plus conforme à la projection horizontale du terrain.

Regarder vers l'avant a pour conséquence d'obtenir une image en perspective, ce qui rend la géométrie du problème un peu moins triviale mais facilement soluble.

Par contre, le champ (IRLS : 120°, FLIR : 24°), et le nombre de points par ligne (IRLS : 1200, FLIR : 768) conduisent à une résolution moins bonne en frontal, au vu des distances de détection plus importantes.

Alors que dans le cas de l'analyseur monoligne, des droites parallèles au sol l'étaient aussi dans l'image, avec une vue en perspective, des droites parallèles vont se couper dans le plan de l'image au point de fuite (à l'horizon si les droites sont horizontales). Ce point, qui peut être dans ou hors de l'image, est unique pour une direction de droite. Ainsi, connaissant l'orientation de la droite et les 3 angles d'attitude de l'avion, on est capable de calculer les coordonnées de ce point de fuite dans le plan de l'image.

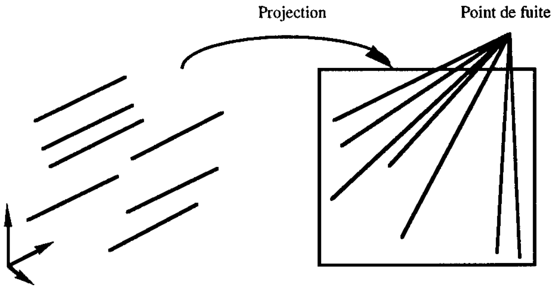

Des lignes parallèles dans l'espace se coupent dans l'image au point de fuite

L'image de la droite de recalage passera forcément par ce point et son orientation dans l'image autour de ce point de fuite va dépendre de la position par rapport à l'avion.

De la même façon que précédemment, on extrait de l'image les contours par des traitements classiques (détection de contour : gradient, élimination des points non maximaux, seuillage, ...).

On effectue ensuite un histogramme de points suivant des secteurs qui ne sont plus parallèles mais qui sont centrés sur le point de fuite.

La présence d'une ligne dans un secteur se traduira par un maximum dans l'histogramme. Tous les maxima locaux de cet histogramme seront considérés comme des droites de recalage possible. Divers tests de cohérence (la largeur de la route par exemple, la position dans l'ellipsoïde d'incertitude) permettent de sélectionner le meilleur candidat. Une bonne préparation de mission ne devrait donner qu'un seul choix possible.

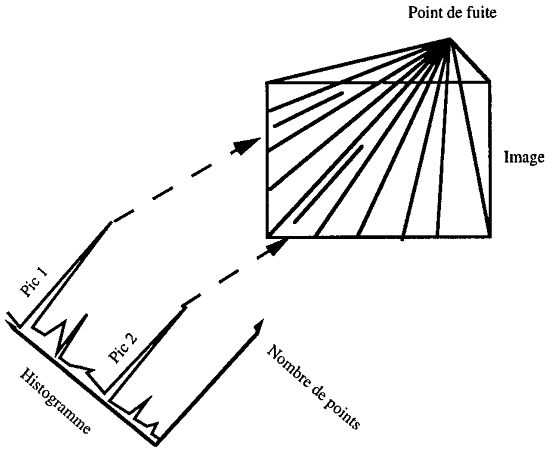

Une fois que l'on a déterminé la position de la droite de recalage dans l'image, connaissant la hauteur au-dessus du sol, on est capable comme dans le cas précédent de positionner l'avion par rapport à cette droite. Nous avons à nouveau un recalage monodirectionnel. Le filtre de Kalman peut fonctionner comme précédemment. Des recalages successifs, avec des droites d'orientation différentes les unes par rapport aux autres, permettront de recaler au mieux la position dans le plan horizontal.
Ces deux types de recalage sont robustes ; le nombre d'informations à stocker en mémoire est très faible (3 coordonnées + 2 orientations + 1 largeur de la droite). Les calculs réalisés sont très faibles par rapport à une corrélation d'images classique et complète. Le taux de détection est très grand du fait de l'assurance que la position avion se trouve à l'intérieur de l'ellipsoïde à 3 σ.

4.3.2.2 Recalage bi-dimensionnel

Néanmoins, le fait d'utiliser uniquement des lignes droites entraîne un certain nombre de réserves de la part des opérationnels. En effet, cette méthode ne peut être utilisée que là où l'homme a modifié l'aspect naturel : création de routes, de voies ferrées, de limites rectilignes de terrain, etc.

Dans des endroits non aménagés ou très montagneux, on peut craindre de ne pas trouver de tels amers. On en revient donc à des recalages avec des amers à 2 (champs, lacs) ou 3 dimensions (bâtiments, ponts, autre super structure simple).

Ces recalages sont bi-dimensionnels et s'appuient sur la connaissance de l'altitude avion.

La forme des amers doit donc être décrite par une suite de vecteurs, formant un contour fermé ou non (on stocke en mémoire les coordonnées des points extrémités de ces vecteurs).

Quand l'avion atteint la position estimée où l'amer est dans le champ de vision, le système gèle une image frontale. Par traitement, il va déterminer les contours de l'amer dans l'image et il va comparer cette image du contour avec celle en perspective obtenue par projection dans le plan image à partir de la description en mémoire de l'amer et la position de l'avion.

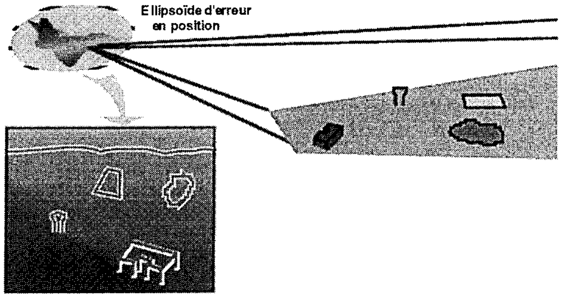

On fera une corrélation d'images entre les deux contours pour les différentes positions possibles de l'avion dans l'ellipsoïde d'incertitude fourni par le filtre de Kalman.

La plus forte corrélation fournira la meilleure estimée de la position avion.

Ce recalage 2D peut fonctionner avec des amers décrits en deux ou trois dimensions. Dans le plan image on se retrouve toujours en 2D.

4.3.2.3 Recalage tri-dimensionnel

On peut aussi utiliser un modèle plus complexe de l'amer pour améliorer la précision de l'information de recalage. Cette méthode sera malheureusement plus exigeante en volume de traitement.

Pour éviter des calculs trop longs, on procède suivant une méthode appelée hypothèse/vérification. Cette méthode consiste à choisir 3 contours dans l'image et 3 segments dans le modèle, orthogonaux entre eux et non contigus, en faisant l'hypothèse qu'ils se correspondent bien un à un. Cela permet de déterminer une position d'où ces segments seraient vus pour se confondre avec ceux de l'image. Si ce point est compatible avec l'ellipsoïde d'incertitude de position, alors on vérifie l'hypothèse qui a été faite en projetant, dans le plan de l'image, le modèle complet de l'amer vu du point supposé et on le compare au contour complet de l'amer dans l'image.

De façon à rendre cet algorithme le plus robuste possible, on garde toujours plusieurs hypothèses possibles que l'on confirme ou non par des traitements de plusieurs d'images successives qui donnent des perpectives différentes.

Dans ce cas, on recale la hauteur sans avoir recours à la radio-sonde.

4.3.2.4 Mise en œuvre

Tous ces algorithmes ont été testés de façon intensive et exhaustive en simulation avec des données réelles (image infrarouge et position avion) prises au cours d'essais en vol.

Avec les recalages 1D ou 2D utilisant la radio sonde, on peut obtenir des précisions décamétriques en position et, de là, des erreurs en vitesse de quelques 1/10 m/s.

L'algorithme en 3D est plus difficile à mettre en œuvre (contours plus courts et plus bruités) et nécessite encore des travaux d'évaluation. Si son intérêt par rapport au recalage 2D peut paraître limité, on peut imaginer d'autres applications (guidage terminal, reconnaissance automatique d'objectifs, ...).

Grâce au soutien du STTE, ces méthodes de recalage 1D et 2D vont être testées sur MIRAGE 2000 dans le courant de l'année 1996.

Le traitement d'image est intégré dans la caméra IRIS et délivre l'erreur de position au filtre de Kalman qui se trouve dans la centrale ULISS.

5 L'ATTAQUE AIR-SOL DE NUIT

Suivant les armements et modes de tir utilisés, le besoin en performances du capteur optronique évolue très sensiblement.

La problématique peut se résumer schématiquement à l'aspect suivant : offrir au pilote des portées de détection, reconnaissance, identification permettant une visée ou une désignation compatibles de la portée de l'armement tiré dans le mode choisi.

5.1 Armements et modes classiques

Les couples modes/armements envisageables, pour lesquels on indique une portée balistique typique de tir, sont les suivants :

- CCPI canon	1000m,
- CCPI roquettes	2000m,
- CCPI bombes	2000m,
- CCPL bombes	3000m,
- CCPL-PI bombes	5000m.

On peut considérer qu'il faut ajouter à cette portée au moins 3000 m (correspondant environ à 10 ou 15 s de vol), pour obtenir la distance minimale à laquelle le pilote doit passer en mode attaque et acquérir visuellement la cible dans l'image IR présentée dans le VTH (sauf dans le dernier mode où le pilote acquiert le point initial).

Dans tous les cas, on supposera que la mission a été préparée, qu'un réticule dans le VTH lui indique la cible, donc qu'il est nécessaire de la détecter en IR mais pas de la reconnaître ou de l'identifier suivant les critères de Johnson. Plus la navigation et la gestion des recalages sont optimisées, et plus le réticule est positionné précisément, ce qui permet au pilote une détection anticipée. On se retrouve avec la même problématique que de jour.

Pour tous les armements tirés en CCPI (mode de tir manuel), les portées sont réduites. De plus, les tirs s'effectuent avec un angle de piqué, et la cible est nécessairement dans le champ du VTH. L'utilisation d'un FLIR grand champ 18°x24° est donc parfaitement compatible de ce mode de tir.

En CCPL direct bombes (lisses, freinées ou à sous-munitions), le pilote doit effectuer une désignation de l'objectif dans le VTH (palier ou piqué), et le tir s'effectue à portée relativement réduite. Le FLIR grand champ est également adapté à ce type de passe.

En CCPL-PI, les portées sont plus importantes (5000 m voire plus), mais la désignation s'effectue sur un point initial dont on connaît la position par rapport à l'objectif. Dans ce cas encore, il suffit au pilote de reconnaître, dans les mêmes conditions qu'en CCPI, ce point qu'il survole en général à faible distance. Une fois encore, un FLIR grand champ permet l'acquisition de ce point initial. Il est donc adapté au CCPL-PI.

La possibilité d'intégrer le FLIR dans la cellule avion est primordiale, afin d'éviter toute erreur d'harmonisation qui se traduirait par une augmentation du cercle d'égale probabilité d'erreur par rapport à la cible.

On peut donc considérer qu'il est possible de reconduire de nuit comme de jour les passes d'attaque préparées CCPI et CCPL, à l'aide d'un FLIR IRCCD grand champ harmonisé avec le VTH.

5.2 Armements moyenne et longue portée

Pour les armements à plus longue portée (armements guidés laser propulsés ou non - 7 à 12 km de portée -, armements futurs largables en stand-off à plus de 15 km), l'utilisation d'un grand champ ne suffit plus.

De plus, dans un contexte de conflit localisé à réaction rapide, la proximité, voire l'enchevêtrement des forces terrestres en présence sont parfois tels qu'il est indispensable de reconnaître, voire d'identifier formellement la cible.

La mission s'apparente alors à de l'appui feu : il est nécessaire d'effectuer un tir de précision n'engendrant pas de dommages collatéraux.

Nos axes de travaux actuels concernent l'utilisation et l'intégration d'un FLIR bichamp. La détection initiale de l'objectif est toujours effectuée en grand champ. Elle peut être assistée par le positionnement d'un réticule en VTH sur le lieu présumé de la cible. Ceci est possible dans le cadre d'une mission preparée où l'on connaît, a priori, cette position.

Une fois la détection initiale effectuée, le pilote passe en petit champ qui pourrait être orientable. L'image agrandie est présentée en visualisation tête basse. Il est nécessaire de pouvoir commander la position du petit champ dans le grand, afin d'éviter toute manœuvre avion inutile pour recentrer l'objectif dans le viseur.

La désignation précise du DMPI (Desired Mean Point of Impact) s'effectue alors en petit champ, et la conduite de tir peut ainsi être initialisée à des distances compatibles des portées recherchées. Là encore, la précision de désignation est d'autant plus importante qu'elle s'effectue à longue distance.

6 CONCLUSIONS

Grâce aux avancées technologiques faites dans les capteurs infrarouge et dans leur mise en œuvre, on peut disposer aujourd'hui, dans les avions d'armes, d'images infrarouge dont la qualité est aussi bonne que celle des images visible et dont l'information peut être très riche.

L'association "caméra IRCCD/jumelles de vision de nuit" permet le pilotage à vue pour la navigation de nuit à basse altitude avec des conditions atmosphériques correctes.

La finesse de la résolution spatiale et thermique permet de faire des traitements pour retrouver avec une très haute probabilité des amers dans l'image. Ceci peut être utilisé pour le recalage du système de navigation.

Les précisions attendues sont du même ordre que celles que l'on obtient avec le GPS. Cette méthode de recalage pourrait en être un substitut quand celui-ci ne serait plus disponible. Ainsi toutes les missions prévues pour utiliser une telle précision de navigation peuvent donc être envisagées, malgré l'absence de GPS.

Les performances obtenues avec la caméra IRCCD IRIS grand champ permettent d'ores et déjà d'effectuer, de nuit comme de jour, toutes les passes d'attaques classiques en CCPI et CCPL, direct ou avec point initial. La caméra frontale est harmonisée avec le VTH. L'installation dans l'avion est simple et peut faire l'objet du rétrofit de nombreux avions.

L'adjonction d'un petit champ orientable devra permettre d'étendre le domaine d'application au tir nocturne d'armements à des portées pouvant atteindre 15 km.

7 RÉFÉRENCES

[1] Colonel C. DORTOMB (EMAA)
"L'attaque de nuit"
(AGARD-MSP Rome Oct 94)

[2] M. BROEKAERT, B. NOEL DU PAYRAT
"Nonlinearity and nonuniformity corrections for the IRIS family of IRCCD thermal imagers"
(SPIE San Diego Jul 1994)

[3] Y. LE GUILLOUX, J.C. FONDEUR
"Using image sensors for navigation and guidance of aerial vehicles"
(SPIE Orlando apr 1994)

[4] P. DUPUY, J. HARTER
"IRIS family of IRCCD thermal imagers integrating long life cryogenic coolers, sophisticated algorithms for image enhancement and hot point detections"
(SPIE San Diego jul 1995)

NAVIGATION SANS INITIALISATION D'UNE BOMBE GUIDEE INERTIELLEMENT

Yves PATUREL
Eric MARTIN
Jean-Thierry AUDREN
SFIM Industries
13, rue Ramolfo Garnier
F-91344 MASSY CEDEX
France

1. SOMMAIRE

La portée des bombes lisses classiques est limitée à 4 à 6 kilomètres suivant les conditions de tir. La sophistication des défenses aériennes rend les missions de bombardement de plus en plus périlleuses pour les pilotes et leurs avions. L'utilisation de bombes propulsées permet d'augmenter la portée des bombes et donc d'assurer une meilleure sécurité des missions. L'obtention d'une précision correcte nécessite un guidage dont le plus sûr et le plus autonome est le guidage inertiel. Cependant, un tel guidage nécessite l'initialisation de la centrale inertielle de la bombe et donc, la fourniture d'informations de l'avion vers la bombe (vitesse, position). Cette contrainte est coûteuse sur les avions de génération précédente pour lesquels les liaisons numériques n'atteignent pas les points d'emport des bombes. Cet article décrit un procédé original, breveté, permettant de larguer la bombe propulsée, guidée sans initialiser la centrale inertielle. Une analyse des performances du procédé a été menée en simulation ainsi qu'une analyse de sa sensibilité aux différentes sources d'erreur. Les modifications nécessaires à la conduite de tir de l'avion sont décrites.

2. LISTE DES SYMBOLES

$\vec{C}$	direction de la vitesse de la bombe
C_{x_0}	coefficient aérodynamique (traînée) de la bombe
$C_{z\alpha}$	coefficient aérodynamique (portance) de la bombe
$\vec{d}$	vecteur additionnel suivant l'axe de largage
e	distance entre position réelle et courbe de consigne
$\vec{g}$	champ de gravitation
$P(t)$	position réelle à l'instant t
$P_c(t)$	position de consigne à l'instant t
$P_c(t')$	position de consigne à l'instant t'
$\vec{P}_{NG}$	position non gravitationnelle de la bombe
R	repère lié à l'engin
R_i	repère initial de l'engin
$\vec{V}$	vitesse de la bombe à l'instant t
$\vec{V}_o$	vitesse initiale de la bombe
$\vec{V}_A$	vitesse calculée par la centrale inertielle
$\vec{V}_{NG}$	vitesse non gravitationnelle de la bombe
$\vec{X}$	axe longitudinal de la bombe
$\vec{X}_i$	axe longitudinal initial de la bombe
α	incidence de la bombe
β	dérapage de la bombe
$\vec{\gamma}_{NG}$	accélération non gravitationnelle
γ_o	angle entre horizontale et axe de la vitesse initiale de la bombe
Δg_z	erreur sur le champ de gravitation
ΔT_l	erreur sur le temps de largage de la bombe
ΔV_o	erreur de vitesse initiale de largage
ΔX_o	erreur de position de largage suivant axe X
ΔY_o	erreur de position de largage suivant axe Y
ΔZ_o	erreur d'altitude de largage
$\Delta\alpha$	erreur sur l'estimation d'incidence
$\Delta\beta$	erreur sur l'estimation de dérapage
$\Delta\gamma_o$	erreur de la conduite de tir sur l'angle de largage
$\Delta\theta_o$	erreur sur l'angle d'harmonisation de la bombe en tangage
$\Delta\psi_o$	erreur de visée de la conduite de tir ou du pilote en cap
$\Delta\psi_1$	erreur d'harmonisation de la bombe en cap
η_c	facteur de charge commandé par l'asservissement de guidage
φ	angle entre la direction de la vitesse à l'instant t et la direction de la vitesse initiale

3. QUEL EST LE PROBLEME ?

Le bombardement est une méthode classique utilisée pour neutraliser des cibles clés en territoire ennemi. C'est un moyen toujours très utilisé dans les différentes sortes de conflit. Cependant ce type d'opérations nécessite de s'approcher suffisamment de la cible. Pour un bombardement basse altitude, la distance à la cible est typiquement de 4 km. Les progrès des défenses antiaériennes rendent ces missions de plus en plus dangereuses pour les avions et donc leur équipage. Aussi tout moyen permettant d'augmenter la distance de tir serait très apprécié des états-majors et des équipages. La distance à la cible est imposée par les lois de la balistique puisque la trajectoire de la bombe dépend essentiellement du vecteur de vitesse initiale et des caractéristiques aérodynamiques de la bombe. Afin d'augmenter cette distance de sécurité, une solution consiste à ajouter un propulseur et un moyen de guidage

Paper presented at the AGARD MSP Symposium on "Technologies for Precision Air Strike Operations in Rapid-Reaction and Localised-Conflict Scenarios", held in Seville, Spain, from 16-19 October 1995, and published in CP-576.

à la bombe. Afin de rester dans le concept et le prix d'une bombe, ceux-ci doivent rester simples et de faible encombrement. Sinon, nous viendrions de réinventer le concept du ... missile!!!

La bombe doit alors être guidée car l'imprécision de la connaissance de la poussée du propulseur ainsi que de l'accroissement de la portée augmentent la dispersion du point d'impact. A moins d'utiliser des récepteurs GPS code Y ou des autodirecteurs, le guidage vers la cible ne peut être effectué que grâce à une centrale inertielle. Le guidage inertiel a l'avantage d'être autonome, tout temps, non brouillable ni leurrable.

En contrepartie, dans sa forme traditionnelle, il doit être initialisé, ce qui nécessite :

- une liaison numérique entre l'avion et la bombe
- des manoeuvres en cap de l'avion.

Ces contraintes présentent d'une part une difficulté opérationnelle et d'autre part l'impossibilité d'utiliser une telle arme sur des avions de bombardement déjà anciens qui ne disposent pas de liaison numérique jusqu'aux points d'emport des armes. SFIM Industries a donc imaginé un procédé de guidage sans initialisation et sans communication avec l'avion. Ce procédé, qui a été breveté, a de plus l'avantage de pouvoir utiliser les conduites de tir de bombardement existantes moyennant des modifications mineures.

4. PRINCIPE GENERAL

4.1. Trajectoire d'une bombe lisse classique

Lors du largage d'une bombe lisse, il n'existe aucun transfert d'information vers la bombe. Le calculateur de l'avion qui délivre l'ordre de largage s'appuie sur la connaissance a priori du comportement de la bombe qui doit être répétable. La trajectoire suivie dépend :

- du vecteur vitesse de la bombe au moment du largage
- de la position
- des coefficients aérodynamiques
- des conditions de l'air ambiant (vitesse de vent, température, pression, ...)

La trajectoire diffère d'une trajectoire parabolique à cause principalement des coefficients aérodynamiques.

Pour un tir à basse altitude, en fonction des caractéristiques de largage (vitesse, angle, ...), la portée varie classiquement entre 4 et 6 kilomètres.

4.2. Notion de trièdre non gravitationnel

Comme première approche, considérons la bombe comme un point matériel soumis à **la seule influence de la gravité**.

Considérons un trièdre d'orientation quelconque mais fixe dont l'origine se trouve sur la bombe et se déplace donc avec elle (voir Figure 1). Si nous nous intéressons aux mesures accélérométriques dans ce trièdre, nous pouvons remarquer qu'elles sont nulles. C'est là une des caractéristiques des mesures inertielles qui provient de la théorie de la relativité générale : on ne peut différencier le champ de gravitation et l'accélération absolue subie. En effet la seule accélération mesurable est l'accélération non gravitationnelle $\vec{\gamma}_{NG}$, différence entre l'accélération absolue $\vec{\gamma}$ et le champ de gravitation $\vec{g}$.

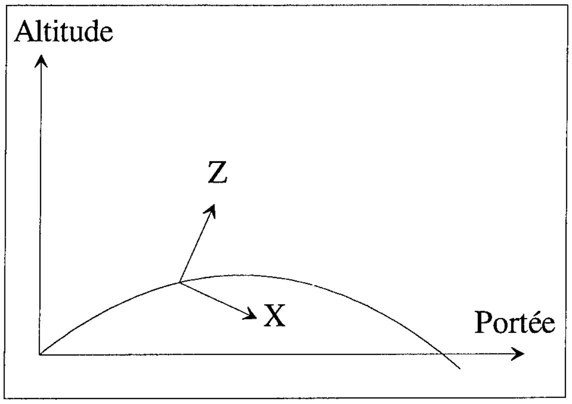

FIGURE 1

Nous appellerons donc **trièdre non gravitationnel** ce repère d'orientation fixe dont l'origine se déplace selon une balistique parfaite. Nous pouvons alors définir

- l'accélération non gravitationnelle :

$$\vec{\gamma}_{NG} = \vec{\gamma} - \vec{g}$$

- la vitesse non gravitationnelle :

$$\vec{V}_{NG} = \int_0^t \vec{\gamma}_{NG}.dt$$

- la position non gravitationnelle :

$$\vec{P}_{NG} = \int_0^t \vec{V}_{NG}.dt$$

où le temps t = 0 désigne l'instant de largage.

Si nous appliquons ces notions à une bombe idéale sans interaction avec l'atmosphère, nous obtenons :

$$\vec{\gamma}_{NG} = \vec{0} \Rightarrow \vec{V}_{NG} = \vec{0} \Rightarrow \vec{P}_{NG} = \vec{0}$$

Si nous appliquons ces notions à une bombe réelle, nous mesurons l'accélération, la vitesse et la position de la bombe réelle dans le repère de la bombe idéale au même instant (voir Figure 2).

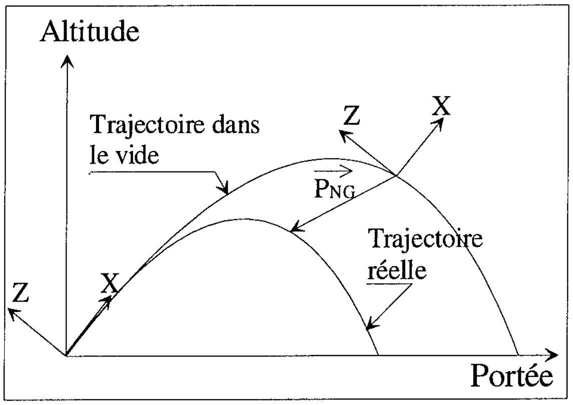

FIGURE 2

4.3. Principe de pilotage dans le trièdre non gravitationnel

La réalisation de mesures dans un trièdre non gravitationnel est extrêmement simple. Il suffit de prendre un trièdre accélérométrique stabilisé dans une orientation quelconque et d'intégrer ces mesures accélérométriques une ou deux fois à partir de l'instant de largage. Ceci est réalisé très simplement avec une centrale inertielle sans aucune procédure d'initialisation.
Si on suppose que la bombe est munie d'un propulseur et d'un système de pilotage, on peut aisément envisager un pilotage asservissant $\vec{P}_{NG}$ à $\vec{0}$ ($\vec{V}_{NG}$ et $\vec{\gamma}_{NG}$ sont alors des mesures destinées à l'avance de phase pour l'asservissement). La bombe réelle suit alors la trajectoire balistique parfaite de la bombe théorique dans le vide.
Hormis l'intérêt scientifique ou technique du phénomène on peut remarquer que :

- aucune initialisation n'est nécessaire (comme pour une bombe lisse classique),
- les effets du vent sont éliminés,
- la trajectoire est allongée puisqu'on élimine alors le freinage aérodynamique.

Bien que déjà intéressant cet allongement n'est pas suffisamment significatif pour présenter un réel progrès opérationnel. Dans les conditions de tir basse altitude avec une vitesse initiale de 300 m/s et un angle de tir de 30 degrés, la portée est de 8 km environ.

4.4. Allongement de la portée par vecteur additionnel

En introduisant à nouveau une notion d'orientation non quelconque du trièdre non gravitationnel, il est possible d'augmenter la portée.

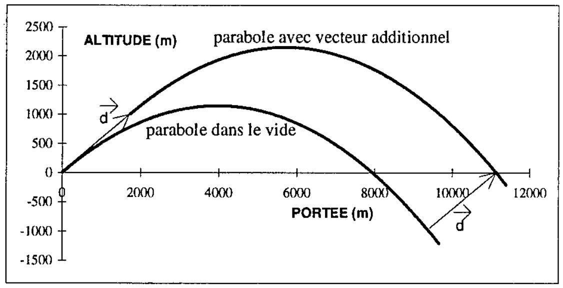

FIGURE 3

Pour cela, on suppose que, lors du largage, l'axe X du trièdre non gravitationnel est aligné sur l'axe longitudinal de la bombe. De plus, au lieu de réaliser l'asservissement sur la consigne $\vec{P}_{NG} = \vec{0}$, on le fait sur:

$$\vec{P}_{NG} = \vec{d} = \begin{bmatrix} d \\ 0 \\ 0 \end{bmatrix}$$

La figure 3 ci-dessus montre comment se place alors le point d'impact. Pour un vecteur additionnel de 2000 mètres et des conditions de tir basse altitude avec une vitesse 300 m/s et un angle de tir 30 degrés (identiques à celles prises précédemment), la portée passe de 8 à 11 kilomètres.

L'initialisation du trièdre dans la bombe est particulièrement simple puisqu'il suffit de prendre comme repère initial le trièdre de la bombe à l'instant de largage.
La connaissance de l'orientation de ce repère par rapport à l'avion est tolérante aux erreurs d'harmonisation puisque celles-ci ne s'appliquent qu'au vecteur additionnel et non à toute la portée. A titre d'exemple, une erreur d'harmonisation de 0.5 degré ne produit qu'une erreur de 17 mètres pour une portée supérieure à 11 kilomètres.

5. GUIDAGE SUR TRAJECTOIRE DE CONSIGNE

5.1. Pilotage 3 axes

Nous avons défini précédemment une bombe "magique" qui suit la trajectoire théorique d'une bombe dans le vide décalée d'une distance $\vec{d}$ de 2000 mètres suivant l'axe initial de la bombe $\vec{X}_i$.
Dans le repère de la centrale inertielle, cette bombe vérifie à chaque instant $\vec{P}_{NG}(t) = \vec{d}$. La trajectoire qu'elle décrit au cours du temps dans le repère terrestre est la courbe de consigne.

Cependant réaliser à tout instant $\vec{P}_{NG}(t) = \vec{d}$ exige un asservissement de la bombe suivant ses 3 axes. Si deux de ces axes peuvent être piloter simplement par des gouvernes aérodynamiques, le troisième nécessiterait de commander la poussée du propulseur. Cette commande augmenterait considérablement la complexité de l'arme et donc son coût.

Si l'on suit à tout instant $\vec{P}_{NG}(t) = \vec{d}$, on suit non seulement la parabole décalée de $\vec{d}$ mais chaque point de la trajectoire est atteint exactement au même instant que celui d'un bombe balistique dans le vide. La bombe est non seulement sur la trajectoire mais aussi exactement à l'heure!
Cette retombée « gratuite » n'est cependant pas nécessaire. Il importe peu en effet que la bombe prenne de l'avance ou du retard sur la trajectoire théorique, l'essentiel étant qu'elle reste sur cette trajectoire.
Le relâchement de cette contrainte de temps a permis alors de ne mettre en oeuvre qu'un pilotage deux axes.
Afin de pouvoir guider la bombe sur sa trajectoire de consigne, il est nécessaire de pouvoir calculer l'écart entre la position réelle et la position de consigne. La courbe de consigne est la trajectoire d'un engin réalisant en permanence $\vec{P}_{NG}(t) = \vec{d}$. L'asservissement se fait sur cette courbe avec de l'avance ou du retard. Pour cela il faut :

- estimer les conditions initiales pour se représenter la trajectoire de consigne
- définir une fonction représentant l'écart entre position calculée et la courbe de consigne

5.2. Estimation des conditions initiales

Si la trajectoire de consigne est connue dans le référentiel de la bombe (elle correspond à $\vec{P}_{NG}(t) = \vec{d}$), obtenir sa position avant ou après nécessite une connaissance locale de la trajectoire de consigne soit une connaissance de la vitesse initiale et de la gravitation dans le repère initial de la bombe. Nous avons donc développé un algorithme d'estimation des conditions initiales.

5.2.1. Principe

L'évolution de l'axe longitudinal $\vec{X}$ de la bombe est mesurée par la centrale inertielle. A l'instant de largage, cet axe correspond à peu près à la direction de la vitesse initiale de la bombe (Voir Figure 4).

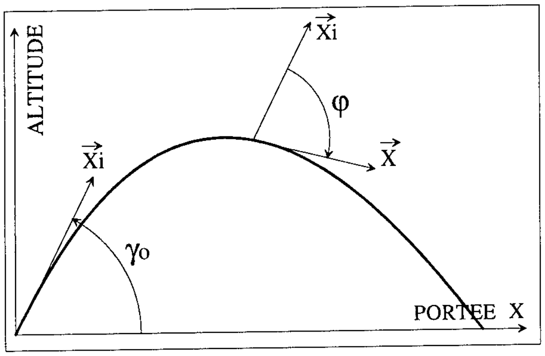

FIGURE 4

Or, pour une parabole, l'évolution de l'angle φ entre la direction de la vitesse et la direction de la vitesse initiale la caractérise et permet de déterminer les vecteurs vitesse initiale $\vec{V}_0$ et gravitation $\vec{g}$ dans le repère initial de la bombe.

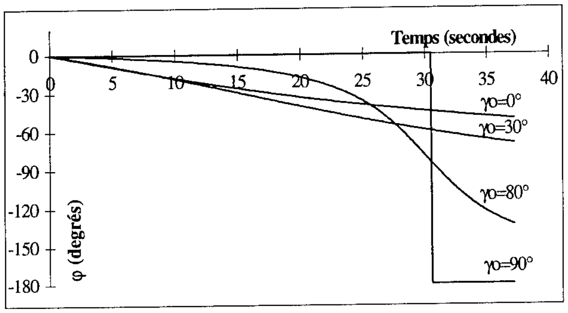

FIGURE 5

On peut voir en effet sur la figure 5 que pour chacune des conditions initiales la forme de la courbe d'évolution de l'angle φ est différent.

5.2.2. Mise en oeuvre

A chaque instant t (l'instant t=0 est l'instant de largage) nous avons :

- le repère de l'engin R dans le repère initial R_i est calculé par la centrale inertielle,
- la direction de la vitesse de l'engin dans le repère engin est évaluée (la direction de la vitesse reste proche de l'axe longitudinal et leur écart est fonction du facteur de charge). Cette évaluation est effectuée grâce à un modèle d'incidence et de dérapage. Ce modèle est déterminé en fonction d'essais qui peuvent être effectués préalablement sur la bombe.

On connaît donc la direction $\vec{C}$ de la vitesse de l'engin dans le repère R_i.

Les équations de la dynamique donnent :

$$\vec{V} = \vec{V}_0 + \vec{g}*t + \vec{V}_A = V*\vec{C}$$

avec

$\vec{V}$: vitesse absolue de la bombe à l'instant t

$\vec{V}_0$: vitesse de la bombe à l'instant initial t=0

$\vec{V}_A$: vitesse fournie par la centrale inertielle

$\vec{g}$: champ de gravitation supposé constant et de module g_o connu.

Disposant alors à chaque instant de la mesure de $\vec{V}_A$ et $\vec{C}$, nous pouvons déterminer $\vec{V}$ et $\vec{g}$ par la méthode des moindres carrés avec contrainte. La contrainte est que le module de $\vec{g}$ doit être égal à g_o.

5.3. Analyse des erreurs sur la restitution des conditions initiales

Une analyse des erreurs de restitution des conditions initiales a montré que pour obtenir une précision suffisante, il était nécessaire que :

- la bombe soit proche de la position en temps sur la courbe de consigne, ce qui revient à avoir une avance ou un retard faible. Cela est obtenu en choisissant correctement les caractéristiques de la bombe et de la consigne (valeur de la poussée, temps de propulsion, ...). Il est par ailleurs nécessaire que ces caractéristiques soient suffisamment reproductibles entre les différentes bombes de même modèle.
- suffisamment de temps se soit écoulé, pour que l'estimation opère sur de nombreuses mesures ; cela élimine les vols trop courts. Cette contrainte n'est pas gênante car les vols courts sont synonymes de distances à l'objectif faibles, ce qui n'est pas le but recherché avec une bombe propulsée, guidée.
- l'incidence soit connue même imprécisément, ce qui nécessite l'élaboration d'un algorithme d'estimation de l'incidence. On remarque que les estimations d'incidence sont d'autant meilleures que les incidences sont faibles, ce qui incite à limiter les facteurs de charge commandés. Une bombe guidée n'est pas un missile, aussi elle n'est pas destinée à subir des facteurs de charge importants. Par ailleurs, la limitation du facteur de charge limite la traînée et donc la taille du propulseur.

5.4. Observateur

L'écart entre la position réelle et la trajectoire de consigne a été pris comme étant la distance entre la position actuelle et la trajectoire de consigne.

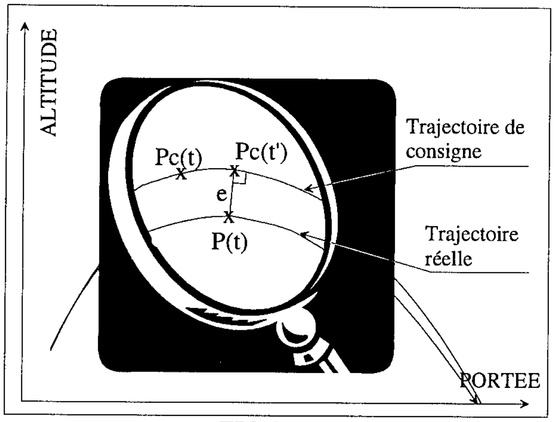

FIGURE 6

On voit sur la figure 6 que, pour obtenir cette distance, on recherche le temps t' pour lequel la trajectoire de consigne était ou sera le plus proche de la position réelle. L'écart e est la distance entre la position de la trajectoire de consigne à l'instant t' et la position à l'instant t .

L'asservissement de guidage maintient l'écart aussi faible que possible. La bombe est alors quasiment sur la trajectoire de consigne avec une avance (ou retard) $\Delta t = t' - t$ par rapport à la trajectoire de consigne.

6. SIMULATIONS EFFECTUEES

Afin de vérifier les performances de ces algorithmes, nous avons mis en oeuvre une simulation complète des algorithmes auxquels sont associés un modèle de bombe et des algorithmes d'asservissement de guidage. Si les algorithmes de principe ont été réalisés tels qu'ils pourraient être implantés, nous avons simplifié le modèle aérodynamique de la bombe, les algorithmes d'asservissement de guidage et les algorithmes de calcul des erreurs des mesures inertielles.

6.1. Schéma général

L'ensemble des fonctions mises en jeu dans le guidage de la bombe sont (voir Figure 7):

- les mesures inertielles qui fournissent les seules données accessibles au calculateur placé dans la bombe
- l'observateur qui est constitué des 3 algorithmes suivants :
    - restitution de l'incidence et du dérapage,
    - restitution des conditions initiales,
    - calcul de l'écart.
- l'asservissement de guidage qui génère les commandes à effectuer
- la dynamique de la bombe qui est modélisée

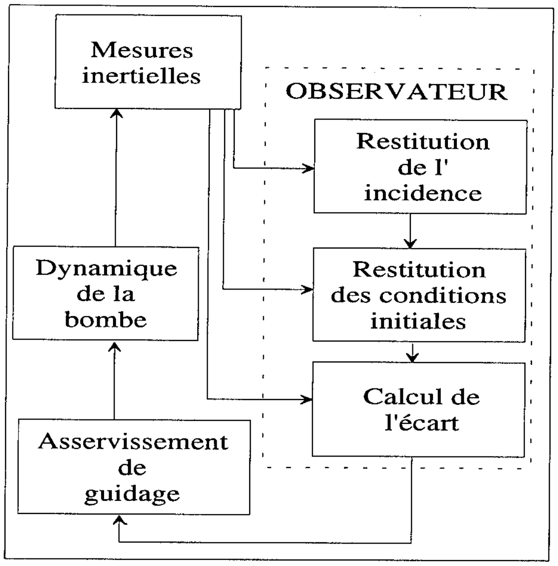
Mesures inertielles
OBSERVATEUR
Restitution de l' incidence
Dynamique de la bombe
Restitution des conditions initiales
Calcul de l'écart
Asservissement de guidage

FIGURE 7

6.2. Modèle de bombe

Le modèle de bombe qui a été utilisé pour ces simulations a les caractéristiques principales suivantes:

- masse : 250 kg
- diamètre : 0.3 mètre
- poussée du propulseur : 3500 N
- durée de la propulsion : 20 secondes
- coefficients aérodynamiques constants $\begin{cases} Cx_0 = 0.3 \\ Cz_\alpha = 6 \end{cases}$

Le système de pilotage qui n'est pas de première importance dans l'évaluation des performances a simplement été modélisé par une réponse du premier ordre avec une constante de temps de 0.38 seconde.

Dans les simulations, il est possible de faire varier ces caractéristiques autour de ces valeurs nominales pour simuler la dispersion des paramètres réels par rapport aux paramètres théoriques :

- masse : tirage d'une variable gaussienne d'écart type 5% d'écart par rapport à la masse nominale
- poussée : tirage d'une variable gaussienne d'écart type 5% d'écart par rapport à la poussée nominale
- coefficients aérodynamiques : tirage d'une variable gaussienne d'écart type 5% d'écart par rapport à la valeur nominale

6.3. Estimateur d'incidence

Dans la réalité de la programmation de ces algorithmes, il sera nécessaire de déterminer un modèle d'incidence qui permettra au calculateur de la bombe d'estimer l'incidence et le dérapage à partir des seules données disponibles, à savoir

- les facteurs de charge sur les 3 axes
- les caractéristiques physiques et aérodynamiques nominales de la bombe

Pour ces simulations, nous avons simulé l'estimateur d'incidence par l'ajout à l'incidence réelle d'un modèle d'erreur. Ce modèle d'erreur est composé de 2 termes :

- le premier est proportionnel à l'incidence elle-même
- le second est un bruit gaussien à moyenne nulle

Les modèles utilisés ont donc été :

$$\Delta\alpha = k * \alpha + b$$

$$\Delta\beta = k' * \beta + b'$$

où

α et β sont respectivement l'incidence et le dérapage,

k et k' sont les coefficients d'erreur proportionnels à l'incidence et au dérapage; en valeur nominale, ces coefficients sont tirés aléatoirement avec une distribution gaussienne d'écart type de 0.15,

b et b' sont des bruits gaussiens d'écart type 0.5 degré.

6.4. Asservissement de guidage

L'écart e entre la bombe et la trajectoire de consigne se décompose, en fait, en deux écarts dans un plan « vertical » XZ et l'autre dans un plan « horizontal » XY, X, Y, Z représentant les axes de la bombe.

Dans chacun des ces plans, le calcul de la commande en facteur de charge est réalisé par un régulateur PID de ce type :

$$\eta_c = (K_1 * e + K_2 * \frac{de}{dt} + K_3 * \int e * dt) / g$$

Les gains K1, K2 et K3 ont été choisis en fonction des caractéristiques de la bombe et des axes concernés. De, plus elles varient au cours du temps:

- en début de vol, la trajectoire de consigne est mal connue car l'estimateur des conditions initiales n'a pas suffisamment de mesures, aussi l'asservissement est plutôt « mou » car on ne cherche pas à se maintenir coûte que coûte sur une consigne peut-être erronée
- en milieu de vol, la trajectoire de consigne est mieux connue, cependant l'impact n'est pas encore proche et il n'est pas nécessaire de se maintenir au plus proche de la courbe de consigne
- en fin de vol, l'impact est imminent et il est alors indispensable de « serrer au plus près » la courbe de consigne.

6.5. Mesure inertielles

Les erreurs de mesure inertielles ont été simulées de façon simplifiées :

- pour les mesures gyrométriques, une dérive aléatoire constante au cours du vol est simulée. Cette dérive est générée aléatoirement avec une distribution gaussienne et un écart type de 10 degrés/heure.
- pour les mesures accélérométriques, un biais constant et une erreur constante de facteur d 'échelle sont simulées sur les 3 axes de mesure. Ces erreurs sont générées aléatoirement avec une distribution gaussienne et un écart type de 10^{-2} m/s^2 pour le biais et de 10^{-3} sur le facteur d 'échelle.

6.6. Résultats des simulations

Les résultats suivants ont été obtenus à partir d'une simulation Monte-Carlo pour laquelle nous avons effectué 100 tirages. A chaque fois, la simulation a calculé l'écart d'impact entre la courbe de consigne et la trajectoire suivie réellement par la bombe. Les différents paramètres caractéristiques de la bombe ont été tirés aléatoirement avec les valeurs décrites aux § 6.2, 6.3 et 6.5.

Cela a été fait pour différents cas de lancement. Trois cas ont été simulés :

Cas n°	Angle γ_o	V_o	Z_o	Portée
1	30°	300 m/s	100 m	11260 m
2	40°	250 m/s	100 m	9160 m
3	0°	300 m/s	6000 m	12490 m

Les résultats obtenus sont les suivants :

Cas n°	Moyenne écart X	Moyenne écart Y	CEP
1	9 m	0 m	13 m
2	15 m	1 m	19 m
3	7 m	-1 m	20 m

Ces résultats montrent que **les performances des algorithmes** permettant le guidage d'une bombe sur son objectif sans initialisation de la centrale inertielle sont **meilleures que 20 m en CEP**. Ils ne prennent pas en compte les erreurs liées à la conduite de tir et à l'imprécision sur la connaissance des paramètres de l'avion au moment du largage.

6.7. Sensibilité aux différents paramètres

Afin de vérifier que les résultats ne sont pas sensibles de façon rédhibitoire à des variations de certains paramètres, nous avons effectué une simulation en ne modifiant qu'un paramètre à la fois. Cette simulation est effectuée sous forme d'un tirage de Monte-Carlo pour lequel seul l'écart-type d'un des paramètres est modifié. Ces simulations ont été réalisées pour chacun des 3 cas de trajectoire décrits au § 6.6. Pour chacun des cas, nous rappelons en caractères gras la valeur nominale utilisée dans la simulation globale décrite au § 6.6.

6.7.1. Sensibilité au modèle d'erreur d'incidence

	Modèle erreur incidence k = 0 % (1 σ) b = 0.1 ° (1 σ)	**Modèle erreur incidence** **k = 15 % (1 σ)** **b = 0.5 ° (1 σ)**	Modèle erreur incidence k= 30 % (1 σ) b = 1.0 ° (1 σ)
Cas n°	CEP (m)	**CEP (m)**	CEP (m)
1	12	**13**	16
2	15	**19**	44
3	9	**10**	12

Il est clair que l'erreur d'estimation de l'incidence influe sur la précision de l'impact. Il est donc nécessaire de soigner les algorithmes de détermination de l'incidence et du dérapage et de valider ces algorithmes par des essais réels sur une bombe.

6.7.2. Sensibilité aux erreurs gyrométriques de la centrale inertielle

	Dérive sur chaque axe 10 °/h (1 σ)	Dérive sur chaque axe 20 °/h (1 σ)	Dérive sur chaque axe 40 °/h (1 σ)
Cas n°	**CEP (m)**	CEP (m)	CEP (m)
1	**13**	13	15
2	**19**	20	21
3	**10**	11	11

On s'aperçoit que les erreurs gyrométriques n'ont pas une influence capitale sur les résultats. Cela est dû principalement au fait que le temps de vol est court.

6.7.3. Sensibilité au biais des accéléromètres de la centrale inertielle

	Biais sur chaque axe 1 mg (1 σ)	Biais sur chaque axe 2.5 mg (1 σ)	Biais sur chaque axe 5 mg (1 σ)
Cas n°	**CEP (m)**	CEP (m)	CEP (m)
1	**13**	26	49
2	**19**	36	64
3	**10**	21	40

Le biais des accéléromètres jouent un rôle important dans les erreurs d'impact. Il est donc nécessaire que la centrale inertielle soit dimensionnée de façon à ce que ce paramètre soit parfaitement maîtrisé.

6.7.4. Sensibilité à la dispersion des coefficients aérodynamiques

	Ecart coeff. nominal / coeff réel 5 % (1 σ)	Ecart coeff. nominal / coeff réel 10 % (1 σ)	Ecart coeff. nominal / coeff réel 15 % (1 σ)
Cas n°	**CEP (m)**	CEP (m)	CEP (m)
1	**13**	13	13
2	**19**	19	19
3	**10**	10	11

Les coefficients aérodynamiques réels jouent principalement sur l'avance et le retard de la bombe par rapport à la trajectoire de consigne. Cette avance ou retard doit rester faible pour obtenir de bonnes performances; cependant, il faudrait des dispersions très grandes entre les différentes bombes pour obtenir des sensibilités significatives.

7. ADAPTATION DES CONDUITES DE TIR

7.1. Quelles modifications pour les conduites de tir ?

Après l'étude des algorithmes qui permettent à la bombe de suivre la trajectoire de consigne, il s'agit de définir les algorithmes de la conduite de tir de l'avion qui permettent de larguer la bombe avec la meilleure précision.

La distance à la cible étant de l'ordre de 10 kilomètres, le pilote aurait des difficultés à effectuer une visée optique. Par conséquent nous préférerons l'algorithme dit « Calcul Continu de Point de Largage » (CCPL) à celui dit « Calcul Continu de Point d'Impact » (CCPI). Dans ce cas, la position de la cible est mémorisée dans le calculateur de la conduite de tir et celui-ci détermine automatiquement l'instant de largage.

Pour cela il calcule à chaque instant la trajectoire de la bombe, en déduit le point d'impact et attend qu'il coïncide avec la cible pour donner l'ordre de largage.

- Pour une bombe lisse classique, la trajectoire est déterminée par intégration numérique à partir des conditions initiales de largage (vecteur vitesse, position) et des caractéristiques aérodynamiques de la bombe.
- Pour une bombe propulsée et guidée suivant les algorithmes décrits ci-dessus, la trajectoire est déterminée à partir des conditions initiales uniquement : la trajectoire de consigne est la courbe définie comme la parabole dans le vide translatée d'un vecteur $\vec{d}$ orienté suivant la vitesse initiale et de module 2000 mètres. La formulation est concise. Les algorithmes de la conduite de tir s'en trouvent simplifiés et leur temps d'exécution est réduit.

7.2. Analyse des erreurs dues aux défauts de largage

Une fois les algorithmes de la conduite de tir connus, nous pouvons calculer les erreurs d'impact de la bombe autres que celles de guidage. C'est à dire avec une bombe guidée parfaitement.

Les principales causes d'erreur sont :

- le système de navigation et de désignation de l'avion,
- l'harmonisation des axes de la bombe et ceux de l'avion,
- les coefficients aérodynamiques (ces paramètres interviennent à ce niveau uniquement pour les bombes lisses traditionnelles et non pour les bombes guidées par ce principe : dans ce dernier cas, les erreurs dues aux coefficients aérodynamiques sont pris en compte au niveau des erreurs de principe - voir § 6.7.4-),
- la répétabilité des conditions d'éjection (uniquement pour la bombe lisse, car pour une bombe guidée inertiellement, les mouvements lors de l'éjection sont réellement mesurés par la centrale inertielle),
- la précision de l'instant de largage
- l'erreur sur la connaissance de la gravité : la gravité varie à la fois en latitude et en altitude suivant une loi qui ne peut être modélisée par le calculateur de la bombe.

Le tableau suivant résume les contributions des différentes sources d'erreur. Il a été obtenu en supposant les erreurs de base de la connaissance des paramètres de largage suivantes :

Paramètre d'erreur	Nom	Valeur à 1 σ
Erreur position axe X	ΔX_o	10 m
Erreur position axe Y	ΔY_o	10 m
Erreur position altitude	ΔZ_o	10 m
Erreur de vitesse	ΔV_o	0.1 m/s
Erreur de visée en cap	$\Delta\psi_o$	0.05 °
Erreur angle de largage	$\Delta\gamma_o$	0.05 °
Erreur harmonisation tangage	$\Delta\theta_o$	0.5 °
Erreur harmonisation en cap	$\Delta\psi_1$	0.5 °
Erreur sur valeur gravité	Δg_z	$2\ 10^{-4}$ m/s^2
Erreur instant de largage	ΔT_l	0.01 s

Avec les valeurs décrites dans le tableau précédent et pour les trois cas de largage évoqués au §6.6, nous obtenons, pour les erreurs uniquement dues aux défauts de largage, les résultats suivants en effectuant une simulation de type Monte-Carlo sur 100 tirages :

Cas n° 1

Origine de l'erreur	ΔX (m) (1 σ)	ΔY (m) (1 σ)	CEP (m)
Position avion	14	10	
Vitesse avion	5	0	
Erreur de visée	0	13	
Harmonisation	8	14	
Connaissance de g	0.2	0	
Instant de largage	7	0	
Toutes erreurs	17	22	24

Cas n° 2

Origine de l'erreur	ΔX (m) (1 σ)	ΔY (m) (1 σ)	CEP (m)
Position avion	12	10	
Vitesse avion	5	0	
Erreur de visée	0	11	
Harmonisation	0	13	
Connaissance de g	0.2	0	
Instant de largage	1	0	
Toutes erreurs	12	19	19

Cas n° 3

Origine de l'erreur	ΔX (m) (1 σ)	ΔY (m) (1 σ)	CEP (m)
Position avion	12	10	
Vitesse avion	4	0	
Erreur de visée	0	15	
Harmonisation	13	17	
Connaissance de g	0.1	0	
Instant de largage	3	0	
Toutes erreurs	19	25	27

A titre d'exemple, la figure n°8 montre 100 points d'impact obtenus avec un tirage de Monte-Carlo sur l'ensemble des erreurs de la conduite de tir et l'installation de la bombe.

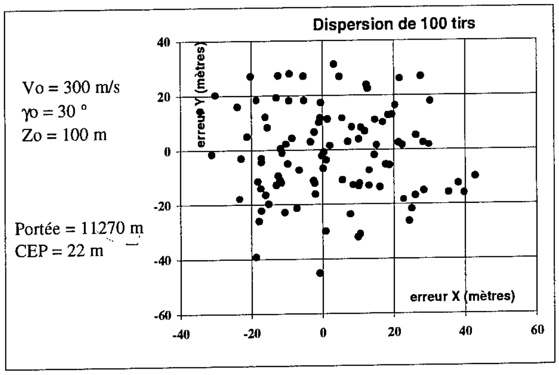

FIGURE 8

8. SYNTHESE DES RESULTATS GLOBAUX

Afin de pouvoir comparer le gain sur la portée et la précision d'une bombe propulsée guidée par rapport à une bombe lisse classique, nous avons effectué les calculs relatifs à la précision globale de chacune des armes. Pour la bombe lisse, les seules erreurs proviennent de la conduite de tir et de la dispersion des caractéristiques aérodynamiques. Les erreurs de base de la conduite de tir sont les mêmes que pour la bombe propulsée guidée, auxquelles il faut cependant ajouter la dispersion des conditions d'éjection.

Les résultats suivants prennent donc en compte pour la bombe guidée **les erreurs d'algorithme de guidage et les erreurs de la conduite de tir et des conditions de largage**. Ils prennent donc en compte les résultats du § 6.6 et ceux du § 7.2.

Cas n°	Paramètre	Bombe lisse	Bombe guidée
1	Portée (m)	5980	11260
	Précision (CEP) (m)	63	38
2	Portée	4900	9160
	Précision (CEP) (m)	47	34
3	Portée	9200	12500
	Précision (CEP) (m)	60	35

Il est clair que, dans tous les cas simulés, **les portées sont très nettement augmentées** (de 2.3 à 5.2 kilomètres supplémentaires) **et la précision est aussi améliorée** (dans un rapport de 30 à 40 %) .

9. CONCLUSIONS

L'étude de ce procédé de guidage d'une bombe propulsée et guidée a montré que l'on peut obtenir des portées supérieures à 10 kilomètres avec une précision globale très satisfaisante.

Les principaux résultats acquis pour une telle bombe sont :

- comparée à une bombe lisse classique, la bombe propulsée guidée augmente la portée d'environ 50% et a une meilleure précision,
- l'installation mécanique de la bombe avec les types de fixations utilisées actuellement,

- l'installation électrique de la bombe est compatible des conduites de tir actuelles,
- les modifications logicielles de la conduite de tir ne posent pas de problème de réalisation,
- cette modification est transparente pour le pilote qui opère comme avec une conduite de tir de bombe lisse en Calcul Continu de Point de Largage (CCPL),
- un propulseur rustique d'une durée de propulsion relativement courte (20 secondes environ) et donc d'un coût faible est compatible du besoin,
- des moyens de pilotage simples permettant un guidage jusqu'à l'impact sont suffisants pour assurer la réussite de la mission et un coût faible de l'arme,
- les caractéristiques d'une centrale inertielle de performances moyennes et de coût faible pour la bombe sont compatibles des précisions de guidage nécessaires.

Cependant, ce procédé a ses limites et il ne permet pas en particulier d'augmenter la portée d'une bombe guidée au delà d'une douzaine de kilomètres tout en maintenant une précision d'impact acceptable. Même si, théoriquement, il est possible d'avoir un vecteur additionnel de module beaucoup plus grand, la précision se dégrade rapidement lorsque la portée dépasse une douzaine de kilomètres. Cela est principalement dû au fait qu'un certain nombre d'erreurs sont proportionnelles au module de ce vecteur additionnel. Lorsqu'il représente une proportion trop importante de la portée, les erreurs d'impact deviennent trop grandes pour conserver une efficacité opérationnelle à l'arme.

Ce procédé présente comme intérêt principal qu'il permet aux avions de génération précédente d'être dotés de bombes plus sophistiquées sans nécessiter de modifications très importantes et onéreuses.

10. REMERCIEMENTS

SFIM Industries tient à remercier la D.R.E.T (Direction des Recherches et Etudes Techniques) qui a participé au financement de cette étude.

Nous remercions aussi le L.R.B.A (Laboratoire de Recherches Balistiques et Aérodynamiques) et, en particulier, MM. BERARD et ARMAL qui ont contribué par leurs conseils et analyses à l'amélioration de nos algorithmes.

Analysis of Differential Global Positioning System (DGPS) Techniques and GPS Jamming on Precision Guided Munition (PGM) Performance

Dr. Sultan Mahmood, Mr. Joseph Solomon,
Mr. Rick James, and Mr. Danny Lawrence

Sverdrup Technology, Inc., TEAS Group
308 West D Avenue, Suite 1
Eglin AFB, FL 32542

1. SUMMARY

The Joint Direct Attack Munition (JDAM) program office at Eglin AFB, Florida is engaged in the JDAM Product Improvement Program (PIP) under which Differential GPS (DGPS), adaptive filtering, and Anti-Jam (A/J) techniques are being evaluated to enhance the accuracy of the weapon in adverse weather as well as reduce its susceptibility to Electronic Countermeasures (ECM). Sverdrup Technology is providing technical study and analysis support for this program.

This paper provides a comparison of two candidate DGPS techniques and their associated error budgets. A candidate adaptive filtering scheme in which the tropospheric (tropo) error is estimated in real-time is postulated. Its performance potential is assessed through a Monte Carlo analysis based on a JDAM type PGM configuration using the GPS JPO proposed Wide Area GPS Enhancements (WAGE). In addition to accuracy, another key issue with the use of GPS signals is the ability to acquire satellite signals and continue to track them in the presence of jamming or interference. A parametric analysis of jamming susceptibility, effects on receiver operation, and potential mitigation techniques are presented based on recent advancements in A/J and Fast Acquisition (FA) technologies.

2. INTRODUCTION

PGMs are essential in the neutralization of high value fixed targets while minimizing collateral damage. In the past, the majority of these weapons were based on electro-optical and infra-red terminal seekers depending on man-in-the-loop terminal guidance. However, these weapons have limited capability when deployed against time critical targets in adverse weather. An adverse weather PGM capability will be provided by using GPS signals to aid the Inertial Measurement Unit (IMU). The current development of GPS aided PGMs is based on 5 channel, P(Y) code, FA GPS receivers, coupled with a weapon grade IMU and a navigation Kalman filter to attain target impact accuracy on the order of 13 meters, Circular Error Probability (CEP). This accuracy assumes that GPS signals are available and the Target Location Error (TLE) can be limited to 7 meters CEP.

In addition to this capability, a need exists for a PGM accurate to 3 meters CEP in adverse weather. Possible solutions entail the use of DGPS, anti-jam, and adaptive Kalman filter techniques in PGM guidance, possibly coupled to terminal radar seekers. This paper quantifies the potential PGM performance gains. A typical scenario is presented in Figure 1.

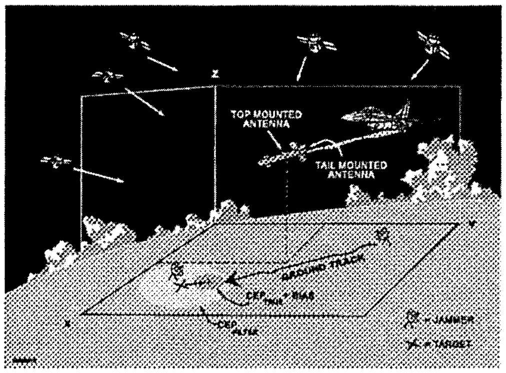

Figure 1. The PGM Scenario

Figure 1 depicts a conceptual scenario in which a PGM is deployed from a F-16 host aircraft at an altitude of 10,000 meters at a target 22 km down range. The ECM threat is represented by a jammer at the PGM release point and another jammer at the target. Before release from the host aircraft the PGM is initialized with GPS satellite ephemeris data and wide area differential pseudorange corrections. After release the PGM uses anti-jam and FA techniques to acquire the GPS P(Y) code signals from 5 satellites in under 15 seconds. This allows the PGM to use DGPS pseudorange and delta range measurements at a 1 Hz rate for the remainder of the 100 second trajectory to the target. If a TLE of 2 meters CEP is provided, the following discussion will establish that a target impact accuracy of 3 meters is possible using DGPS/INS guidance.

3. COMPARISON OF DGPS IMPLEMENTATION CONCEPTS

Differential GPS techniques rely upon the removal of a combination of common errors between the mobile receiver and a Reference Receiver (RR). The product of this technique is a differential correction that is applied at the mobile receiver to its pseudorange measurements. For military receivers the ionospheric error (iono) is determined

Paper presented at the AGARD MSP Symposium on "Technologies for Precision Air Strike Operations in Rapid-Reaction and Localised-Conflict Scenarios", held in Seville, Spain, from 16-19 October 1995, and published in CP-576.

by the two-frequency approach and the tropo error is estimated using a deterministic model. The only significant remaining errors include Satellite Vehicle (SV) clock and ephemeris errors. The Exploitation of DGPS for Guidance Enhancement (EDGE) concept [1] has convincingly demonstrated that this component of the error can be reduced to less than 0.4m in real-time by deploying a network of widely separated (~1600 km) high quality reference receivers. Table 1 provides the error budget for the Range Application Joint Program Office (RAJPO) High Dynamic Instrumentation Set (HDIS) in the standard Precise Positioning Service (PPS) GPS mode. The extensive flight test results for HDIS [2] have demonstrated accuracy levels that are equivalent to a 4.8 m CEP as opposed to the 7.3 m CEP specified in this table. Therefore, the iono, tropo and tracking/multipath errors of the HDIS may be considered achievable goals for a PGM type of receiver. In order to explore navigation accuracy improvement methods two schemes are proposed in table 1. The first exploits the EDGE concept that has reduced the ephemeris/clock error to about 0.5 m (including latency) and the other exploits the recently proposed WAGE concept [3]. Two ephemeris/clock improvement levels for WAGE are shown. (It is the understanding of the authors at this writing that the WAGE concept is still evolving, with potential for further improvement in accuracy).

Table 1. GPS Error Budget Comparison (RMS)

Error Source	HDIS	EDGE*	WAGE*	
Clock and Ephemeris [m]	4.2	0.3	1-1.6 Apr 95	0.5-0.8 Nov 95
Ionospheric [m]	0.2	0.2	0.2	0.2
Tropospheric [m]	0.5	0.5	0.5	0.5
Tracking and Multipath [m]	1.0	1.0	1.0	1.0
Latency [m]	n/a	0.4	0.4	0.4
User Equivalent Range Error (UERE) [m]	4.4	1.2	1.6-1.9	1.3-1.4
CEP [m] [HDOP=1.5, VDOP=2.5, Impact=60°]	7.3	2.0	2.6-3.1	2.2-2.3

* Assumes enhanced GPS receiver with performance equal to HDIS receiver. EDGE and WAGE schemes only affect the clock and ephemeris errors.

WAGE is explored in this paper due to its potential operational advantages in terms of cost and logistics since it will embed the corrections in the GPS navigation message and thus provide global coverage without a separate data link [3]. The increased WAGE (April 95) clock and ephemeris errors compared to the EDGE performance of about 0.5m increases the overall CEP navigation error to 2.6 m from a value of 2.0 m. This small increase in CEP should be traded against the expense of an extensive RR network and the risk with a data link. The error budget for WAGE assumes a uniformly distributed (0 to 1 day) correction upload scheme resulting in a 2.2 hour average age for the corrections. It is expected that the upload scheme will be optimized for specific theaters, thereby further reducing the difference in accuracy.

The exploitation of WAGE corrections for a PGM is depicted conceptually in Figure 2. The proposed scheme [3] is to incorporate the corrections to the satellite clock and ephemeris in the spare words of subframe 4 of page 13 of the GPS navigation message, requiring a maximum of 12.5 minutes of access time. The demodulation of these corrections by the PGM receiver after release will not occur in time to make them useful. A feasible solution to this problem is to transmit the corrections at weapon initialization across the aircraft interface with the weapon. These initialization messages from the aircraft currently include GPS time and ephemeris information. The other possibility is for the aircraft to transmit WAGE corrected clock and ephemeris data, in which case the JDAM receiver will not require any modifications. The use of WAGE corrections reduces the space segment component of the UERE to around 1 m. The receiver tracking and multipath errors, as well as iono errors, may be reduced by carrier-smoothing types of algorithms. A combination of these error reduction methodologies is expected to allow the tropo error to become observable. This idea, as recommended in [4], is discussed in the next section with the incorporation of a fifth SV measurement in Monte Carlo simulations of a PGM configuration.

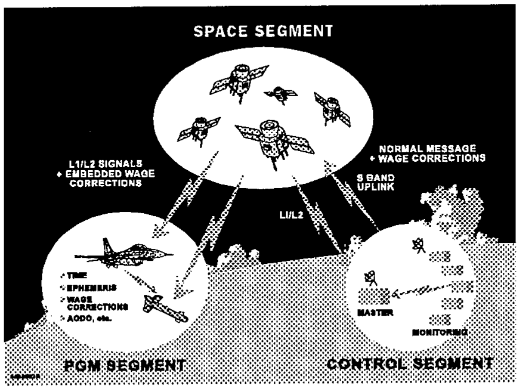

Figure 2. PGM Concept for Exploiting WAGE

4. STOCHASTIC ESTIMATION OF TROPOSPHERIC ERROR

Background. The tropospheric sector of the atmosphere is defined as the region from the surface of the earth to an altitude of 80 km. GPS Radio Frequency (RF) waves transversing this region of space experience refraction independent of frequency. In contrast to the ionospheric effect, this phenomena is not dispersive, resulting in an equivalent group and phase delay. Tropospheric refraction has two distinct components: the "dry" segment, which is a strong function of the atmospheric pressure, accounts for 90% of the error with the remaining 10% of the error attributed to the "wet" segment, which is a function of the atmospheric water vapor pressure and temperature. Both components are a function of user altitude (h) and the elevation of the satellite (θ). GPS receivers estimate and remove this error from the pseudorange measurement with corrections based on various deterministic algorithms [5].

A high fidelity tropospheric pseudorange correction for users of ground based GPS receivers can be obtained using the Chao compensation model [6]. This compensation is applied by post processing the pseudorange measurements with good knowledge of the atmospheric conditions (pressure, temperature, and water vapor pressure). These equations are defined as:

$$\textbf{\textit{Tropospheric Delay}} = (\mathrm{DOF} \cdot \mathrm{DTC}) + (\mathrm{WOF} \cdot \mathrm{WTC}) \qquad (1)$$

$$\mathrm{DTC} = \text{Dry Tropospheric Correction} = 2.276 \cdot 10^{-3} \cdot P_o \qquad (2)$$

$$\mathrm{WTC} = \text{Wet Tropospheric Correction} = 10230 \cdot \frac{e_o^{1.46}}{T_o^3} \qquad (3)$$

$$\mathrm{DOF} = \text{Dry Obliquity Factor} = \frac{1}{sin(\theta) + \dfrac{0.00143}{tan(\theta) + 0.0455}} \qquad (4)$$

$$\mathrm{WOF} = \text{Wet Obliquity Factor} = \frac{1}{sin(\theta) + \dfrac{0.00035}{tan(\theta) + 0.017}} \qquad (5)$$

where:

eo = Vapor Pressure = RHo · 10 7.617-2285/To
Po = Atmospheric Pressure (mbars)
To = Atmospheric Temperature (Kelvin)
RHo = Relative Humidity
θ = Satellite Elevation

For airborne receivers, the user's altitude must be taken into consideration. The majority of military GPS receivers correct the "dry" component of the troposphere and disregard the "wet" component as negligible. A representative set of tropospheric compensation equations are published by the Navstar GPS technical support group. These equations are based on three spherically stratified atmospheric layers where the error varies linearly with altitude under 1 km and exponentially with altitude at 1 km and above. These equations are defined as follows [7]:

$$R(h,\theta) = f(\theta) \cdot DR(h) \qquad (6)$$

where:

$R(h,\theta)$ = Total range error.
DR (h) = Zenith range error as a function of altitude.
h = Altitude above mean sea level in km.
θ = Elevation angle defined with respect to the horizon.
f (θ) = Mapping equation as a function of elevation angle.

$$f(\theta) = \frac{1}{sin(\theta) + \dfrac{0.00143}{tan(\theta) + 0.0455}} \qquad (7)$$

for: $0 \text{ km} \leq h_u < 1 \text{ km}$:

$$\Delta R(h) = \left(\left[N_S \bullet h + 0.5 \bullet \Delta N \bullet h^2 \right]_{h_u}^{1} + 1430 + 732 \right) \bullet 10^{-3} \text{ meters} \qquad (8)$$

$$\Delta N = -7.32 \cdot \exp(0.005577 \cdot N_s) \qquad (9)$$

for: $1 \text{ km} \leq h_u < 9 \text{ km}$:

$$\Delta R(h) = \left(\left[\frac{-8 \bullet N_1}{\ln\left[\dfrac{N_1}{105}\right]} \bullet \exp\left[0.125 \bullet (1-h) \bullet \ln\left[\frac{N_1}{105}\right]\right] \right]_{h_u}^{9} + 732 \right) \bullet 10^{-3} \text{ meters} \qquad (10)$$

for: $9 \text{ km} \leq h_u$:

$$\Delta R(h) = \left(\left[\frac{-105}{0.1424} \bullet \exp\left[-0.1424 \bullet (h-9)\right] \right]_{h_u}^{20186.8} \right) \bullet 10^{-3} \text{ meters} \qquad (11)$$

The parameters N_s and N_1 represent values for the refractivity index at sea level and at an altitude of 1 km, respectively. After the application of tropospheric compensation based on equation (6), the remaining error in the pseudorange measurement is described statistically as zero mean with a standard deviation on the order of 0.5 meters. To put this error in perspective, it must be examined as part of the overall PGM GPS error budget. Table 1 illustrates a typical error budget for a PGM receiver utilizing differential techniques.

For this analysis the WAGE error budget is chosen (Nov 95). Table 1 depicts the contribution of the tropospheric error on an overall User Equivalent Range Error (UERE) of 1.3 m with a target impact CEP of 2.2 m. In the differential error budget all the errors are on the same order of magnitude. Elimination of the tropospheric error would result in an approximate final impact CEP reduction of only 10%.

It is clear from the discussion above that the quality of the airborne PGM tropospheric compensation could be improved by estimating, in real-time, the "wet" component and refractivity indices (N_s and N_1). The cost and complexity of computing these parameters on a PGM is not viable at this time. However, with the introduction of 5 channel PGM GPS receivers it may be possible to stochastically estimate the gross tropospheric error by augmenting states to the navigation Kalman filter [4]. The discussion that follows describes an effort to simulate this concept using Monte Carlo techniques.

Truth Model. The truth model for this analysis is based on a nominal JDAM mission and configuration. The mission chosen for this analysis represents the launch of a glide bomb from an altitude of 10,000 m at a horizontal target 17 km downrange with an impact angle of 60°; total mission time is on the order of 100 seconds (see Figure 1). The aerodynamic parameters for a GBU-15 glide bomb are used to generate a 6 Degree-Of-Freedom (DOF) trajectory for this profile. A set of 5 satellites is chosen to maintain a Position Dilution of Precision (PDOP) of approximately 2.5 for the entire mission. The ephemeris data for these satellites is generated using the standard GPS satellite orbit equations from a set of nominal GPS satellite constellation almanac data.

Stochastic models are used to simulate the expected errors in the Inertial Measurement Unit (IMU) position/velocity estimates and the GPS receiver pseudorange/delta range measurements. The error budget for the GPS measurements is presented in Table 1 (WAGE) and is used to generate the Line-of-Sight (LOS) errors for each of the 5 satellites. The IMU error budget is based on typical weapon grade IMU sensors: gyros with a drift of 1°/hr and a scale factor error of 150 parts per million (ppm), accelerometers with a bias of 1 milli g and a scale factor error of 300 ppm. The final configuration of the truth model is depicted in Figure 3. The overall truth model is represented by stochastic differential equations consisting of a total of 45 states. There are 21 states assigned to IMU model and 24 states for the GPS measurements (2 states for the user clock error, 2 states for the tropospheric error, and 4 states per satellite for the remaining LOS errors).

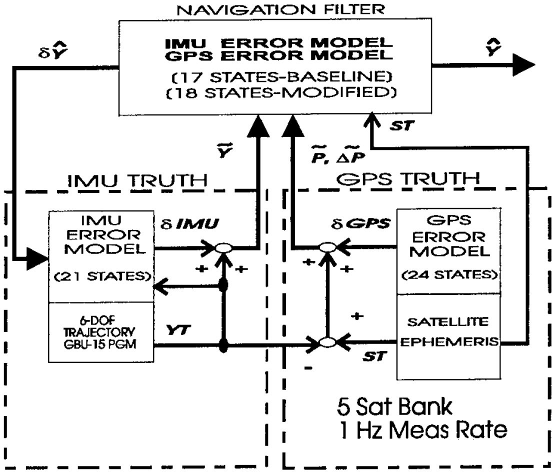

Figure 3. Truth Model and Simulation Configuration

The error of interest for this analysis is the tropospheric error. The detailed structure of the stochastic shaping filter used to generate this error is presented in Figure 4.

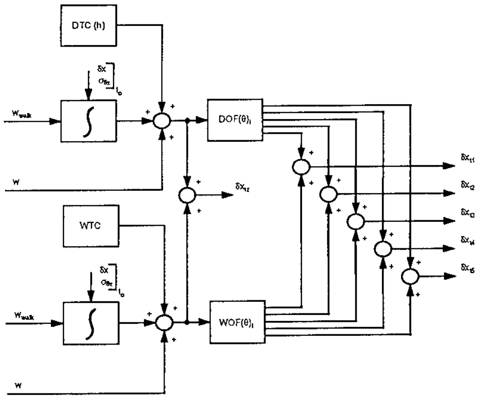

Figure 4. Stochastic Shaping Filter for Tropospheric Error

Equations 3, 4, and 5 are used to compute the WTC, DOF, and WOF parameters, respectively. The DTC parameter is computed as a function of altitude using equations 8 through 11. The stochastic uncertainty defined in Table 1, WAGE is injected by using a random walk shaping filter plus a white noise on both the "dry" and "wet" components. The error statistics ($\bar{e}$:mean, σ_{TRUE} : standard deviation) for the underlying zenith error (δx_{tz}) from a 50 sample Monte Carlo analysis are presented in Figure 5. In addition, a single sample of each of the 5 LOS satellite errors (δx_{t1}, δx_{t2}, δx_{t3}, δx_{t4}, and δx_{t5}), for a typical Monte Carlo run, are presented in Figure 5.

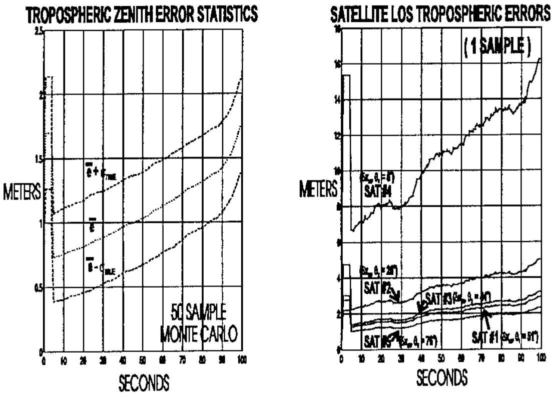

Figure 5. Truth Model Generated Tropospheric Error

Figure 5 clearly indicates that the temporal and spatial characteristics of the tropospheric error have been captured in the truth model.

Filter Model. The ***baseline*** navigation Kalman filter consists of 17 error states: 3 position, 3 velocity, 3 tilt, 3 gyro drift, 3 accelerometer bias, and 2 GPS user clock. It utilizes pseudorange and delta range measurements at a 1 Hz rate. The tropospheric error is removed by applying a deterministic correction to each satellite's pseudorange measurement before processing by the navigation Kalman filter; this correction is based on equation (6).

The modified Kalman filter has 18 states. A 1 state, random walk shaping filter is augmented to the baseline navigation filter to estimate the zenith tropospheric error (δx_{tz}). The baseline filter's deterministic correction is disabled and the observation equation for the filter's estimate of the pseudorange measurement for the *ith* satellite is modified as follows:

$$\hat{z}_{pi} = \hat{\rho}\,(\hat{P}_{IMU},\ P_{SATi}) + \delta\hat{x}_b + \frac{1}{sin(\theta)_i}\delta\hat{x}_{tz} \qquad (12)$$

Where $\hat{\rho}$ is the nonlinear computation of the pseudorange based on the satellite position (P_{SATi}) and the filter corrected IMU position estimate ($\hat{P}_{IMU}$; $\delta\hat{x}_b$ is the filter's estimate of user clock bias; sin(θ)i is the sine of the elevation angle to the *ith* satellite; and finally (the added term), $\delta\hat{x}_{tz}$ is the filter's estimate of the zenith tropospheric error. The performance of the baseline and modified versions of the navigation filter are characterized in the next section.

Results of Monte Carlo Simulations. To obtain statistical validity a set of 50 samples were generated for each of the performance plots presented below. The IMU truth model is initialized based on the results of a nominal in-flight transfer alignment from the host aircraft and a fast acquisition receiver begins to generate the GPS measurements after 5 seconds of uncompensated IMU error growth. The performance parameter of interest for this analysis is the CEP. Performance plots will consist of 3 curves: the filter predicted CEP, the true CEP, and the true CEP shifted by any true bias. These performance indicators were illustrated in Figure 1. The baseline navigation filter is investigated first. After a series of Monte Carlo runs to tune the navigation filter, a final filter parameter set was determined. The final CEP performance is presented in Figure 6.

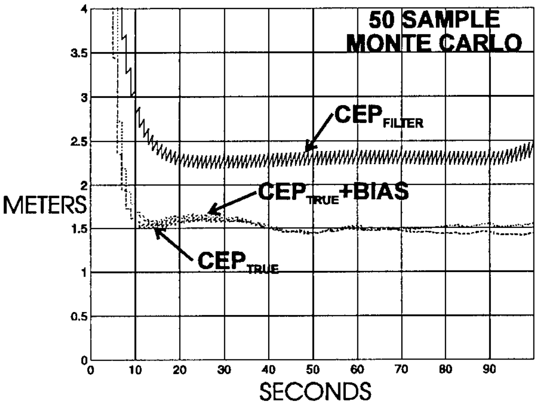

Figure 6. Baseline Navigation Filter Performance

The filter is conservatively tuned with a filter predicted uncertainty of 2.3 meters versus a true uncertainty of 1.5 meters. The true bias in this case is negligible.

The modified navigation filter is applied to the pseudorange measurements with *uncompensated* tropospheric error. An initial set of runs were made to tune the process noise value on the tropospheric error shaping filter. The resulting performance after tuning is presented in Figure 7.

In this configuration the 18 state filter generates an uncertainty CEP of 2.6 meters with a true CEP of 1.3 meters with negligible bias. The filter uncertainty has increased from 2.3 to 2.6 meters, but the magnitude of the true CEP has decreased from 1.5 to 1.3 meters. This indicates that with further tuning the overall performance of the modified filter could surpass the baseline. In order to further quantify the performance of the modified filter, the filter's tropospheric zenith error state is differenced with the truth model over the 50 sample Monte Carlo analysis. The ensemble statistics for the zenith tropospheric error difference and the characteristics of a single sample are presented in Figure 8.

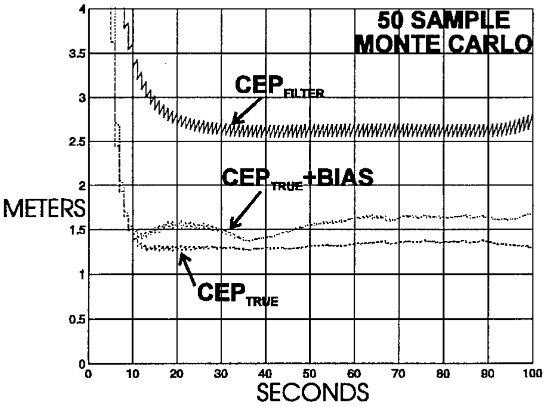

Figure 7. Modified Navigation Filter Performance

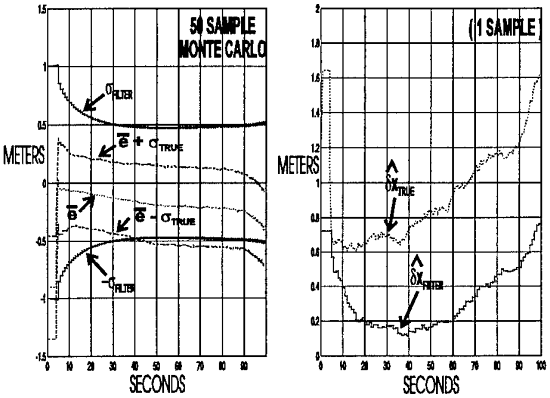

Figure 8. Filter's Tropospheric Zenith Error Performance

The ensemble statistics consist of the true *mean* of the difference or error ($\bar{e}$) and the true uncertainty bounds ($\bar{e} \pm \sigma_{TRUE}$). These true statistics are plotted with the filter's predicted uncertainty ($\pm\sigma_{FILTER}$) to facilitate comparisons. The collapsing filter uncertainty ($\pm\sigma_{FILTER}$) indicates that the tropospheric zenith error *is observable* and that the filter is aggressively tuned to just encompass the bounded true error statistics. However, it is clear that a bias remains indicating the filter model does not exactly model the temporal and spatial characteristics of the error. To confirm that 5 satellites are required for observability, the analysis was repeated with measurements from only 4 satellites, while keeping the PDOP unchanged. The resulting performance of the filter's tropospheric error state is presented in Figure 9.

In this case the filter's predicted uncertainty ($\pm\sigma_{FILTER}$) is divergent after the initial measurement updates, indicating the error state is *not observable* to the filter. This confirms the hypothesis that 5 satellites are required to guarantee observability.

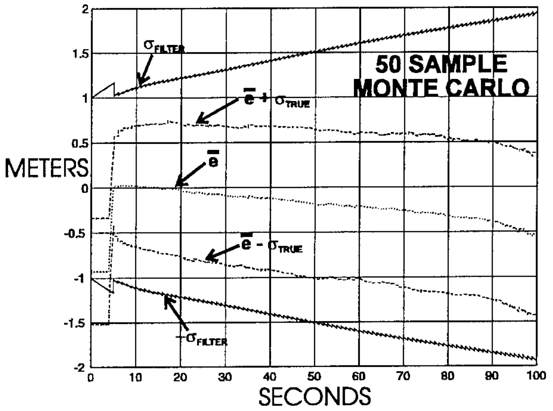

Figure 9. Filter's Tropospheric Zenith Error Performance [4 Satellites]

Conclusions. The initial hypothesis postulated that the tropospheric zenith error could be estimated using a properly structured shaping filter and observation equation in conjunction with the measurements from 5 satellites. This theory has been demonstrated with a detailed Monte Carlo analysis.

A comparison of the baseline navigation performance (Figure 6) with the modified navigation performance (Figure 7) indicates a negligible increase in accuracy. However, in the modified filter the tropospheric zenith error is being estimated in real-time based on the content of the GPS measurements. This allows the navigation filter to better adjust to the unknown conditions of the troposphere at PGM launch at a cost of one additional Kalman filter state. Figure 8 does indicate a higher order model is required to fully capture the remaining tropospheric bias.

5. GPS JAMMING-TO-SIGNAL RATIO ANALYSIS

A GPS equipped PGM relies on sufficient C/No values in order to acquire satellite signals after launch and maintain track in the presence of jammers. This critical parameter is controlled by the effective jamming-to-signal ratio (J/S). This ratio is directly affected by the PGM's attitude which determines the jamming power at the weapon, the antenna gain towards the jammer, and the antenna gain towards the SV. A closed form solution to the GPS performance equation subject to jamming is not possible due to the number of variables such as the flight trajectory, antenna placement, and location of actual or expected threats. The significance of the problem and some mitigation techniques are discussed in this section using simplified simulations. A simulation has been developed to generate J/S plots which may be used to specify an additional A/J antenna subsystem that will suppress the potential ECM threat to a weapon guided by a GPS/inertial navigation system. Two configurations of GPS patch antenna are considered here for analysis, one top mounted and another tail mounted. A cardioid is a convenient analytical model for the gain pattern of such an antenna. The pitch cut pattern for such an antenna in both the configurations is shown in Figure 10. The J/S ratios are computed for a typical PGM trajectory with pitch dynamics as depicted in Figure 11. As an example, we will consider one watt jammers placed at the target and directly underneath the PGM launch point (see Figure 1). The simulation can be easily modified and scaled to accommodate any power level jammer and actual threat scenarios. The classified reference [8] contains the analysis of several scenarios that were generated as an interpretation of the latest GPS threats established by the Defense Intelligence Agency.

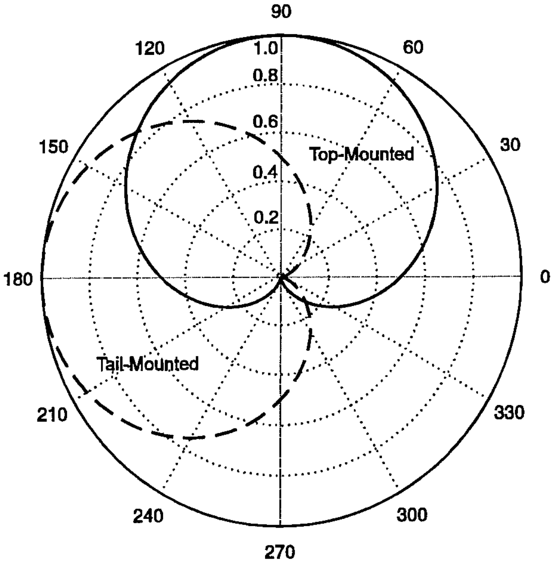

Figure 10. Top and Tail Mounted Antenna Patterns

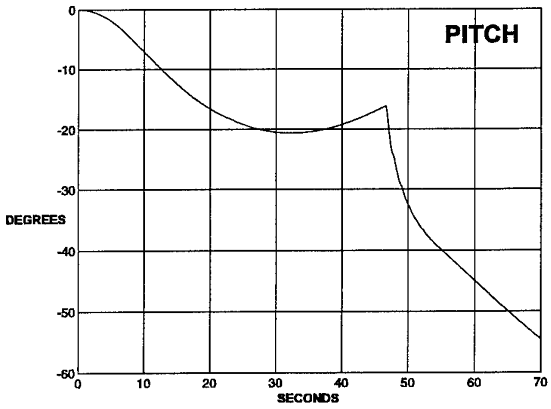

Figure 11. Pitch Dynamics of the PGM Trajectory

The geometry of the weapon and each jammer, defined in a North-East-Down (NED) frame, is used to compute a pointing vector defined in a Local Tangent Plane (LTP) frame. The LTP frame is aligned with the NED frame, but with its origin at the weapon Center-of-Gravity (CG). Hence, if $\vec{R}_j$ and $\vec{R}_m$ are the weapon and jammer position vectors, the pointing vector is given by

$$\vec{R}_{mj} = \vec{R}_j - \vec{R}_m \qquad (13)$$

The orientation of the missile body frame (X_b, Y_b, Z_b) with respect to the LTP frame (X_l, Y_l, Z_l) is obtained from the 6-DOF simulation in terms of the roll, pitch and yaw angles (ϕ, θ, ψ). These angles are used to rotate the LTP pointing vector into the weapon body frame through the direction matrix C_l^b, i.e.,

$$\vec{r}_{mj} = C_l^b \vec{R}_{mj} \tag{14}$$

where, $\vec{r}_{mj}$ is the jammer to weapon pointing vector in the body frame. Next, this vector is converted to a unit vector as

$$\vec{U} = \frac{\vec{r}_{mj}}{\left|\vec{r}_{mj}\right|} = \left[e_1 \quad e_2 \quad e_3\right]^T \tag{15}$$

The body referenced azimuth A and elevation E of the pointing vector is determined from the components of this unit vector for each point on the trajectory. This technique allows the antenna pattern to be fixed in the body frame and can be replaced by an actual pattern in terms of its appropriate A and E angles. When retrieving the gains the (A, E) pair for each trajectory point is determined from the unit vector.

Once the antenna gain, G, is determined the jammer power at the weapon is calculated as

$$J_i = 10\,log(GP_i) - 20\,log\left(\frac{4\pi R_{mji}}{\lambda}\right) \tag{16}$$

where,

G = antenna gain toward the jammer

P_i = radiated power from the *ith* jammer in watts

R_{mji} = slant range to the *ith* jammer

λ = GPS L_1 carrier wavelength

The total jamming power due to 'N' jammers is given by

$$J = \Sigma_1^N 10^{J_i/10} \tag{17}$$

Finally, the J/S ratio for the L_1 P-code is given by

$$J/S\ (dB) = 10 \log\left[\Sigma_1^N 10^{J_i/10}\right] + 163 \tag{18}$$

This equation is computed and plotted as a function of time for three different cases of one watt jammers in Figure 12, Figure 13, and Figure 14, respectively. The J/S plots for the L_1 C/A code can be obtained from these curves by subtracting 3 dB since this code is 3 dB stronger than the P(Y) code.

It can be seen from Figure 12, for the target located jammer, that the tail-mounted antenna produces a lower J/S ratio for the entire duration of the flight as compared to the top mounted antenna. On the other hand the top mounted antenna is preferable for the launch point jammer, as shown in Figure 13. For the two jammer case of Figure 14, an antenna switching methodology may be required; with the top antenna used for the first 48 seconds and the tail antenna for the remainder of the flight. In this case of antenna switching a very important consideration is the Dilution Of Precision (DOP) available from the satellites visible to either of the antennas; since it determines the accuracy achievable with their measurements. For some trajectories a mode may be required where satellites from both the antennas will have to be mixed for an optimum solution. Plots of J/S such as these can be used in assessing the Time To First Fix (TTFF) and tracking

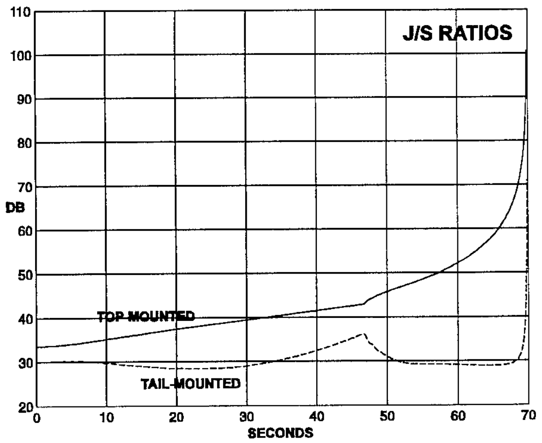

Figure 12. Case 1, J/S for Jammer at Target

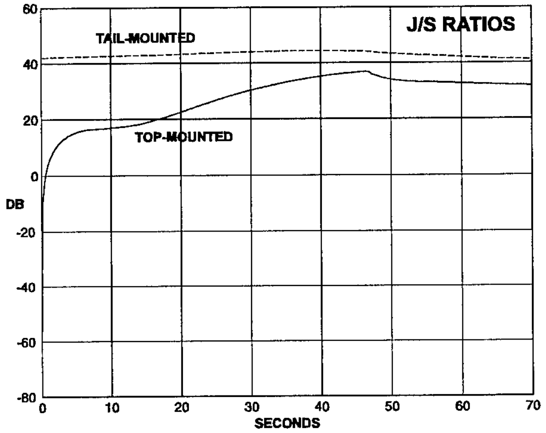

Figure 13. Case 2, J/S for Jammer at Launch Origin

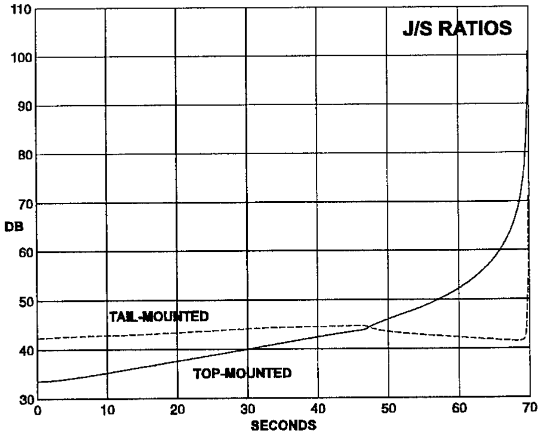

Figure 14. Case 3, J/S for Jammers at Target and Launch Origin

performance of an integrated GPS/inertial navigation system.

The key states of a GPS receiver along with the threshold C/No values are shown in Table 2. Both P(Y) and C/A codes are considered in the presence of a 20 MHz Broad Band (BB) jammer and a Continuous Wave (CW) jammer. The corresponding J/S thresholds for these representative C/No thresholds [9] as shown in this table, are calculated from the relationship

$$C/N_0 = \frac{S}{N_{sys} + (J/G_pB)} \qquad (19)$$

where

S = Signal Power

N_{sys} = System noise density

J = Jammer power

G_pB = Gain-Bandwidth product for the code under consideration

Table 2. J/S Thresholds for a Conventional GPS Receiver

State	C/No [dB-Hz]	P-Code J/S Thresholds BB	CW	C/A-Code J/S Thresholds BB	CW
1	34	37.8	34.5	35.4	25.4
3	15	58.4	55.1	55.1	45.1
5 (unaided)	26	47.2	43.9	44.0	34.0
5 (aided)	16	57.4	54.1	54.1	44.1

The J/S plots for a one watt jammer and the threshold J/S values for the critical receiver states can be used to determine the jamming margin or the maximum jammer power that can be withstood by a conventional receiver. The jamming margins P_J can be calculated from the following relationship

$$J/S_{th} = J/S_1 + 10 \log P_J \qquad (20)$$

J/S_1 is taken from Figures 12, 13, and 14 at 15 seconds for the acquisition mode and at 50 seconds for the track mode. J/S_{th} was selected from Table 2 for the P-code receiver, broad band jamming, with State 1 for acquisition mode and State 5 (aided) for track mode. It can be seen from Table 3 that the track mode is relatively more resistant to jamming and that the acquisition mode sets the limit on the maximum jamming that can be tolerated by the weapon receiver (this result is denoted by the X in the Limiter column). This also means that if the receiver were to be in the track mode during the captive portion of flight then the track mode sets the limit to a tolerable jamming level.

However, for a sufficiently large jammer power level GPS acquisition may be completely denied. In these cases it is necessary to implement additional A/J capability in the front-end of the receiver. The Tactical High Anti- Jam GPS Guidance (THAGG) technology program [10] has developed a tightly coupled GPS/INS/AJ system that allows fast (15 seconds) acquisition in environments up to a 75 dB J/S and tracking in environments up to a 120 dB J/S. The THAGG unit is currently undergoing detailed characterization tests. Table 4 shows the jamming margins for the three jamming cases. The improvement when compared to the conventional receiver is quite impressive.

Table 3. Jamming Margin for a Conventional GPS Receiver

Case	Mode	Antenna Type Tail [W]	Top [W]	Limiter
1	Acquisition	7.6	1.4	X
	Track	437	14.8	
2	Acquisition	0.3	79.4	X
	Track	26	224	
3	Acquisition	0.3	1.4	X
	Track	25	14	

Table 4. Jamming Margin for the THAGG Type of Receiver

Case	Mode	Antenna Type Tail [W]	Top [W]	Limiter
1	Acquisition	40,000	7,400	X
	Track	1,000,000,000	31,600,000	
2	Acquisition	1,700	420,000	X
	Track	63,000,000	316,000,000	
3	Acquisition	1,600	7,400	X
	Track	50,000,000	25,000,000	

6. ANALYSIS OF FAST ACQUISITION UNDER JAMMING

The use of GPS in military applications such as the PGMs places stringent requirements on P(Y) code acquisition times. This is true for both direct P(Y) code acquisition and for P(Y) code acquisition by first acquiring the C/A code. The problem is made more severe when short acquisition times are required under significant jamming. The THAGG technology may be used to counter jamming, to the extent shown in Table 4. In addition, the actual acquisition time depends upon several other parameters such as position, time, velocity and frequency uncertainties. The use of a parallel bank of 1024 correlators for speeding up C/A code acquisition in the presence of timing errors, and the extension of this scheme for fast P(Y) code acquisition within a few seconds has been successfully demonstrated [11,[12]. A general parametric study of this problem was performed in [13] with respect to a two-dimensional signal search receiver architecture. These results are extended here to establish guidelines for selecting receiver architectures to meet the acquisition requirements under significant jamming. Both BB and CW interference is considered.

The parameter of primary interest is the TTFF which is defined as the maximum (3σ) amount of time required from the instant that signal is first available (from the antenna) to the instant the system provides a valid navigation solution (position, velocity, etc.). In general, the TTFF can be represented as the sum of three time segments associated with three distinct receiver processes as follows

$$\mathrm{TTFF} = T_{acq1} + T_{acq2} + T_{KF} \qquad (21)$$

where,

T_{acq1} = Time to acquire the first SV

T_{acq2} = Time to acquire and track the remaining SVs

T_{KF} = Time for the Kalman filter to settle to required solution accuracy

T_{acq2} and T_{KF} together are on the order of a few seconds, the exact value varying from manufacturer to manufacturer depending upon a number of proprietary hardware and software design features. The most critical time segment is T_{acq1} which could be prohibitively large for conventional receivers in a PGM scenario. These receivers use a sequential search scheme, stepping through half code chips and single Doppler cells, and have first SV acquisition time given by

$$T_{acqs} = M \bullet N \bullet N_{nc} \bullet T_c \qquad (22)$$

where,

N = No. of half code chips to be searched

$$= 2\left[\sqrt{(3\sigma_p)^2 + (3\sigma_t)^2}\right]/(15) \text{ for P-code} \qquad (23)$$

$$= 1024 \text{ for C/A code with } \sigma_t \geq 1 \text{ ms} \qquad (24)$$

M = No. of frequency cells of width ΔF to be searched

$$= 2\left[\sqrt{(3\sigma_v)^2 + (3\sigma_f)^2}\right]/\Delta F \text{ for both P(Y) and C/A codes} \qquad (25)$$

In these equations the variables are defined as:

σ_p = Position uncertainty

σ_t = Time uncertainty

σ_v = Velocity uncertainty

σ_f = Frequency uncertainty

N_{nc} = Number of noncoherent correlations

T_c = Correlator coherent dwell time

ΔF = Frequency bin width (442 Hz)

When the P(Y) code is acquired through the C/A code and the time ambiguity is a multiple of one millisecond, an additional 6 seconds are required to demodulate the Handover Word from the 50 Hz GPS message. The T_{acqs} plots for C/A code and direct P(Y) code acquisition as a function of J/S ratios are shown with the oscillator error as a parameter in Figure 15 for a BB jammer and in Figure 16 for a CW jammer.

It can be seen from these plots that acquisition within a reasonable amount of time is achieved for a PGM application only when jamming is extremely low, C/A code is available, and the oscillator is of high quality. For small values of T_{acq1} under reasonably high jamming the receiver will have to employ some form of parallel search circuitry.

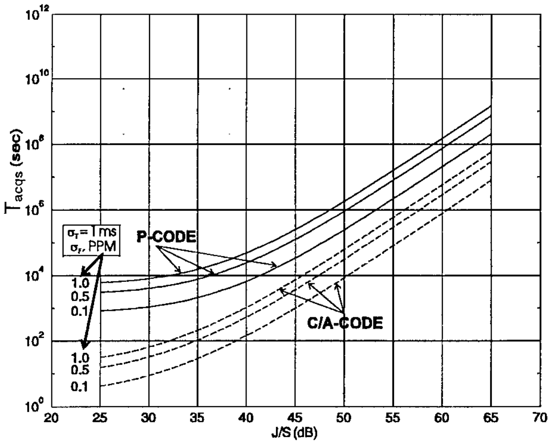

Figure 15. Serial Search Code Acquisition Time versus J/S (20 MHz BB jammer)

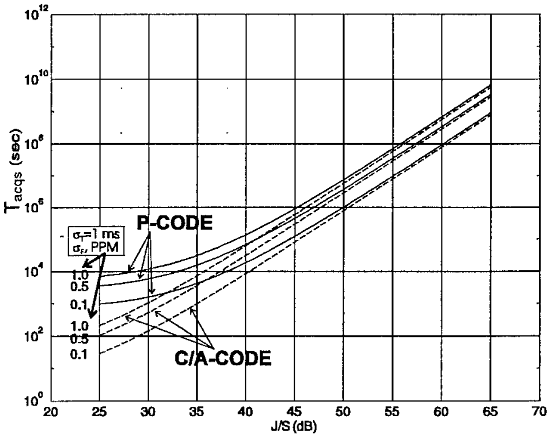

Figure 16. Serial Search Code Acquisition Time versus J/S (CW jammer)

The equations and strategy has been outlined in [12]. It can be employed here as follows. Assume that the required value for T_{acq1} is T_{acqr} for a PGM application under a given J/S and oscillator error. Then a factor β can be obtained as

$$\frac{T_{acqs}}{T_{acqr}} = \beta = \frac{MNN_{nc}T_c}{M_r N_r N_{nc} T_c} \qquad (26)$$

where

M_r = No. of frequency blocks with β_f parallel frequency cells

N_r = No. of code blocks of β_c parallel half chip code cells

and

$$\beta = \beta_c \, \beta_f \qquad (27)$$

Thus, the receiver can be mechanized with β_c parallel correlators and β_f parallel frequency cells. The M_r frequency blocks and N_r code blocks, however, are searched sequentially. As an example if direct P(Y) code acquisition is required in 10 seconds when the initial time uncertainty is 1 millisecond, a J/S ration of 40 dB (20 MHz BB) and oscillator error of 1 ppm, the value of β can determined with the help of figure 15 as

$$\beta = T_{acq}/10 = 8000 \qquad (28)$$

Using equation 25 to determine the number of frequency cells and equation 27 for the number of code correlators, this receiver can be implemented with 22 frequency cells and 364 code correlators per block.

7. CONCLUSIONS

This paper has illustrated the potential of DGPS corrections and receiver enhancements in providing a 2 meter CEP navigation (excluding TLE) capability for a PGM. The DGPS techniques of interest for PGM applications are the WAGE and EDGE concepts. Error budgets presented quantified the potential performance gains. Receiver enhancements considered were adaptive filtering, A/J, and FA techniques.

The adaptive filtering methodology chosen as an example in this analysis was the stochastic estimation of the tropo error. However, adaptive filtering covers the broad range of deterministic and stochastic techniques that can be used to increase the accuracy in GPS measurement error estimation and removal (i.e., oscillator uncertainty, multipath, tropo, iono, etc.). The Monte Carlo simulations used in this analysis demonstrated the feasibility of stochastically estimating the tropo error in real-time using a fifth satellite measurement.

The availability of GPS itself (in terms of acquiring and tracking satellites) under jamming was parametrically analyzed, and guidelines provided for specifying a receiver architecture (number of correlators, etc.). A procedure was developed for generating J/S ratios and determining jamming margins for conventional and A/J GPS receivers using unclassified scenarios.

8. REFERENCES

[1] Blackwell, Earl G., "Differential GPS Solution to Achieve a Low-Cost, Adverse Weather, Precision Strike JDAM," Joint GPS Working Group Meeting, USAF Academy, Colorado Springs, CO, 8 Dec 1993

[2] Burkett, Samuel, et al., "GPS Based TSPI for DOD Ranges - RAJPO HDIS Test Results," Proceedings of ION-GPS '94, Salt Lake City, UT, 20-23 Sep 1994, pp. 765-772.

[3] Butts, Jim, Capt. C. Shank, "Navigation Message Correction Tables: A Proposal," Proceedings ION National Technical Meeting, Anaheim, CA, 1995.

[4] Butts, Jim, BD Systems, Torrance, CA, Private Communication.

[5] Wells, David, "Guide to GPS Positioning," Canadian GPS Associates, 1987.

[6] Mahmood, Sultan, "Enhanced GPS for Combat Applications," Final Technical Report, 1992.

[7] Navtech Seminars & Navtech Book and Software Store, Inc., "Technical Characteristics of the Navstar GPS," Arlington, VA, Jun 1991.

[8] Gibbs, G.E., "Generation of Jamming Scenarios and Jamming-to-Signal Ratios for the Anti-Jam GPS Technology Flight Test (AGTFT) (S)," Proceedings of the 17th Biennial Guidance Symposium, 2-4 May 1995, CIGTF, Holoman AFB, NM.

[9] "Introduction to NAVSTAR GPS User Equipment, Annex A: Jamming," NATO Team, NATO Document Number ANP2, For Official Use Only, Jun 1987.

[10] Gibbs, G.E., et al., "Tactical High Anti-Jam GPS Guidance," Proceedings of the 16th Biennial Guidance Symposium, Oct 1993, CIGTF, Holoman AFB, NM.

[11] Kohli, Sanjai, "Application of Massively Parallel Signal Processing Architecture to GPS/Inertial Systems," IEEE PLANS '92 Symposium, Monterey, CA.

[12] Kohli, Sanjai, "High Performance GPS Receiver for Air Launched Munitions," IEEE PLANS, 1994.

[13] Mahmood, Sultan, et al., "An Analytical Study of Fast Acquisition Issues in GPS Exploitation for Electronic Combat," Proceedings of the ION-GPS '94, 7th International Symposium, 20-23 Sep 1994, Salt Lake City, UT.

Neural Network Techniques for Missile Guidance and Control

U.K. Krogmann
Bodenseewerk Gerätetechnik GmbH
Postfach 10 11 55
D-88641 Überlingen
Germany

SUMMARY

The present paper deals with the application of artificial Neural Networks for flight guidance and control. After an introduction to the problem, the structure and functioning of feedforward Neural Networks, the transient response and the learning mechanism for these networks will be examined. This will be followed by the development of the structure of the flight guidance and control loop with Neural Networks. The neuronal flight controller is not programmed but first learns the knowledge needed for stable flight guidance and control in a separate training and learning phase and then continues learning in the actual utilisation phase. For a typical missile as a concrete example, the neural controller is trained and tested in a simulated utilisation phase. On the whole, a good to very good control behavior is achieved with the time-variant, nonlinear control plant. This paper shows a new way of implementing reliable, nonlinear, learning autopilots which can be realized in hardware as parallel signal processing modules.

1 INTRODUCTION

Neural Networks consist of a number of simple processor elements which - arranged in specific structures - process information in parallel. They are not programmed but develop autonomously the solution to a problem on the basis of examples by means of learning. Their structure loosely resembles biological information processing where strategies for solving problems are also learnt by examples. Man is, for example, able to control and coordinate movements without any problems although he has no mathematical idea of the control plants involved. On the level of sensomotor control, man learns to take the actions required in a particular situation by testing. The application of at least parts of these human abilities to technical systems is a great challenge. In this paper a step shall be performed towards Neural Network application in missile guidance and control.

Paper presented at the AGARD MSP Symposium on "Technologies for Precision Air Strike Operations in Rapid-Reaction and Localised-Conflict Scenarios", held in Seville, Spain, from 16-19 October 1995, and published in CP-576.

The basic elements of a guided missile system are represented in Fig. 1. This figure shows the major elements of a missile guidance and control loop in a very general form valid for a variety of missile systems.

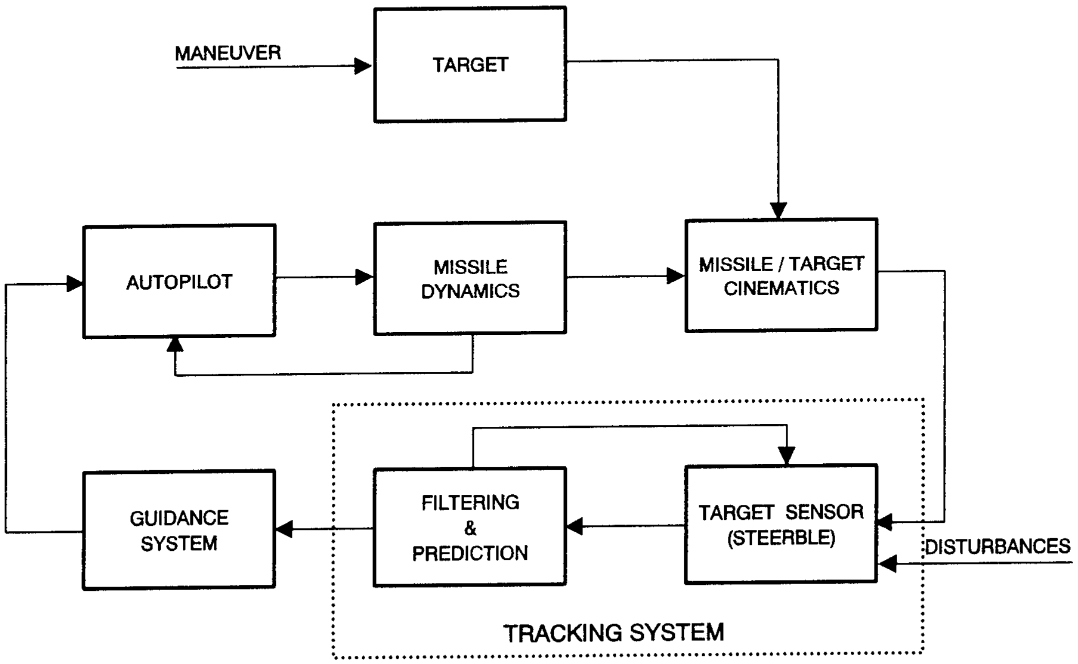

Figure 1: Elements of a missile guidance and control system

The task of missile guidance can be imagined as a control loop where it is tried to offset the external disturbances caused by launch errors and target maneuvers by an appropriate missile control. For this purpose, the relative geometry between the missile and the target is measured by a target sensor. A large number of disturbances, which can be caused by both the sensor physics and countermeasures, have an effect on the target sensor signals. The actual target sensor is part of the target tracking system in which the target signals are processed by a filter and prediction algorithm to obtain optimum signals for sensor tracking and missile guidance.

The tracking system signals are subsequently converted by the guidance unit into commands to the missile´s autopilot. These can, for instance, be acceleration commands. The missile autopilot can then finally be regarded as "acting instrument" for observing the commanded state of flight variables. The autopilot and the tracking system are underlying control systems in the missile guidance and control loop. In the following, the possibility of utilizing a Neural Network as autopilot for a tail-controlled missile is to be examined.

Neural Networks [1] have so far been used above all in pattern recognition, as classifiers for speech recognition, for machine vision and in robotics. In [2], a self-regenerative quadruplex sensor unit for fault-tolerant , high-reliability measurement of the inertial state of motion of an aircraft is described. In this connection, Neural Networks are used for the first time for detecting and localizing errors. The application of neuronal approaches in the control of nonlinear plants with unknown mathematical model is dealt with in [3]. This real-time implementation of a learning controller is described using a Neural Network designed as associative memory. The work described in [4] deals with neuronal control with the so-called *reinforcement* learning method. A survey of the application of Neural Networks with the backpropagation learning algorithm also used in this paper is given in [5]. Basic observations about the implementation of learning controllers with such networks are made in [6]. Finally, different structures of neuronal control loops are examined in [7] whereas [8] contains some remarks on the application of Neural Networks in flight control.

2 THE MISSILE AUTOPILOT CONTROL LOOP

The function of the missile autopilot control loop is to quickly and accurately generate the acceleration demands for the missile as commanded by the guidance system. For this purpose the autopilot must

- yield well behaved stability characteristics of the airframe over the entire flight envelope
- provide fast and adequate air frame response to the command signals from the guidance system
- offer robustness with respect to changing parameters and attenuate the sensitivity to disturbances

Due to their symmetrical form and roll stabilisation, the flight controllers for lateral and vertical movements of such missiles are identical. The example of application concerns a flight controller for the lateral movement of an aerodynamically controlled missile with tail control, which can be represented by means of a 3-DOF model with the state variables of velocity in longitudinal (u) and lateral direction (v) as well as the angular rate (r) about the yaw axis. Fig. 2 shows a simplified block diagram of the flight control loop with a commanded lateral acceleration a_{yc} as reference variable, rudder deflection ζ as control quantity, the missile as control plant and the current lateral acceleration a_y of the missile as output variable (controlled variable).

With the thrust and gravitational forces (x, y, z: airframe longitudinal, lateral, vertical axes) acting on the missile

$$\underline{F} = [F_x, F_y, F_z]^T \tag{1}$$

and the aerodynamic and thrust moments acting about the center of gravity

$$\underline{M} = [L, M, N]^T \tag{2}$$

the following equations of motion (translatory and rotatory) apply for the missile

$$\frac{1}{m}\sum \underline{F} = \frac{d\underline{V}}{dt} + \underline{\omega} \times \underline{V} \tag{3}$$

$$\sum \underline{M} = \frac{d\underline{D}}{dt} + \underline{\omega} \times \underline{D} \tag{4}$$

where

$$\underline{V} = [u, v, w]^T, \text{ missile velocity vector} \tag{5}$$

$\underline{\omega} = [p, q, r]^T$, angular rate vector (6)

$\underline{D} = [D_x, D_y, D_z)^T$, angular momentum vector (7)

The forces and moments mentioned above cause a nonlinear dynamics of the missile as control plant with considerable changes in missile mass, moments of inertia, dynamic pressure and nonlinear aerodynamics over time.

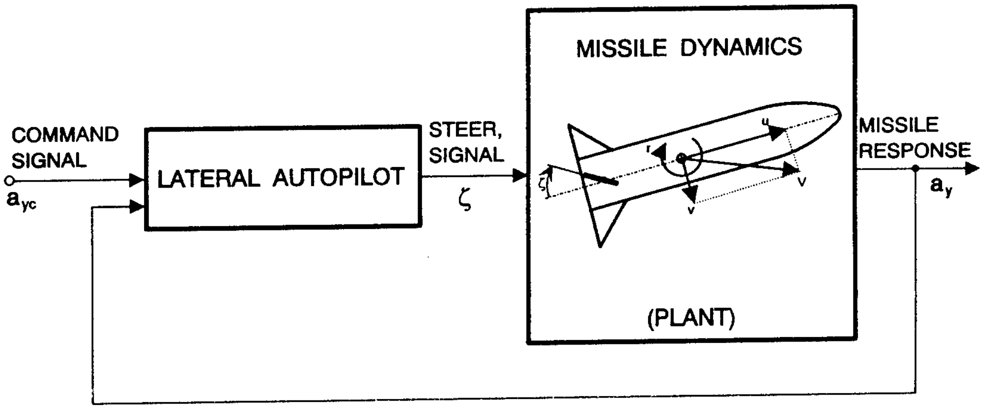

Figure 2: Simplified lateral autopilot control loop

Nowadays, such nonlinear systems are usually treated such that simplifications of the state and measurement equation are introduced on the basis of the knowledge about the system, the operational conditions and disturbances. Systematic steps of simplification are, for instance, shown in [9]. The limits of simplification are attained in case of complete linearisation, assumption of time-invariant parameters and when taking into account the disturbances by time-invariant, stochastic Gauss processes. On this basis, PID or state controllers can be designed methodically. This method of controller design is characterized by the fact that models are developed for the system to be controlled and the disturbances which can be treated mathematically for the design of a controller.

For nonlinear control plants with time-varying parameters, a linear controller firmly adjusted can yield satisfactory results only in a limited area around a set point. Therefore, robust controllers which are insensitive to changes of the plant parameters are designed as well. Robustness frequently leads to slow controllers. This disadvantage is ruled out in the case of adaptive controllers whose parameters and sometimes also structure can be adapted depending on the current set point. This is why velocity (V^2) and Mach (Ma) number adaptations have very long been used in flight control due to the large dynamic pressure range (gain scheduling).

Nonlinear controllers become necessary when in extreme flight situations (large angles of incidence, high angular rates) sufficient stability and satisfactory control behavior is to be achieved [10]. To manage this situation, flight control also uses the inverse characteristics of the control plant [11]. Due to the "non-phase minimum characteristic" of tail-controlled missiles, the inverse of the control plant cannot be used in the present case.

Information processing with Neural Networks is rapidly progressing. For the autopilot problems examined here, artificial Neural Networks have the following important features. They

- are not programmed but learn the mathematical correlations between input and output quantities,
- even learn from noisy measurement data,
- can learn nonlinear static and dynamic mappings between their multi-variable input and output quantities and thus map them without the aid of a mathematical model,
- allow very rapid signal processing due to their parallel structure with simple processor elements,
- have an inherent redundancy and thus fault tolerance through their parallel structure,
- offer robust operation through generalizing behavior, i.e. have the capability to react appropriately within certain limits even in the case of nonlearnt patterns,
- offer the possibility of simple implementation in hardware; adaptation to different tasks is achieved through learnability and not by reprogramming.

These features and characteristics of Neural Networks are complementary to the problems, conditions and requirements of flight control as stated above. Artificial Neural Networks are thus a challenge for the design of a neuronal autopilot. The present paper is meant to be a general contribution to this. The following is a short description of Neural Networks with representation of their capability to model static and dynamic systems.

3 ARTIFICIAL NEURAL NETWORKS

3.1 Structure

Artificial Neural Networks are parallel information processing structures consisting of simple processor elements (PE) and interconnected via unidirectional connections as shown in Fig. 3. Each processor element (Fig. 4) has a local memory for the weighting factors of its input connections which can be changed during the learning phase of the network. The processor element processes only locally available information in the form of the signals just applied to its input connections which are multiplied by the locally stored weighting factor of the input connection concerned. The processor element only calculates *one* output signal which is transmitted to other PE of the network as input signal according to the network structure. The PE are arranged in so-called layers. The PE of a layer of the network shown in Fig. 3 are not connected among each other or backward but only with the PE of the following layer via appropriate connecting weights. Here such multi-layer structures with exclusive feedforward connections are to be used, the so-called feedforward networks or multi-layer perceptrons (MLP).

The PE in a network all have the same simple basic function. According to Fig. 4, the activity z_i of the i-th PE is equivalent to the sum of all weighted input signals with a so-called bias value (threshold) with the signal level 1 and the weighting factor w_{io} being taken into account. Hence,

$$z_i = \sum_{j=1}^{n} w_{ij} x_j + w_{io} \tag{8}$$

The output signal x_i of the i-th PE is a nonlinear function of its activity, i.e.

$$x_i = f(z_i) \tag{9}$$

Sigmoid functions (Fig. 4) are used as nonlinear output function. On the one hand, they limit the output signal of a PE. On the other, they enable the learning of nonlinear mappings between input and output patterns of a network.

The *knowledge* of the Neural Network is stored in the connecting weights by which the PE are weighted in summation. The connecting weights are adjusted during a learning phase of the network and are acomodated in the weight matrices W(i) with i = 1, ...(K-1) and k = 1, ... K as number of the layer. Thus, the feedforward signal processing of the network shown in Fig. 3 is described by the following equations:

$$\begin{aligned} \underline{x}(1) &= G \cdot \underline{u} \\ \underline{z}(k+1) &= W(k) \cdot \underline{x}(k) \\ \underline{x}(k+1) &= \underline{f}(\, W(k) \cdot \underline{x}(k) \,) \\ \underline{y} &= M \cdot \underline{x}(K) \end{aligned} \tag{10}$$

with $\underline{u}$: input vector, G: input matrix, $\underline{y}$: output vector, M: output matrix.

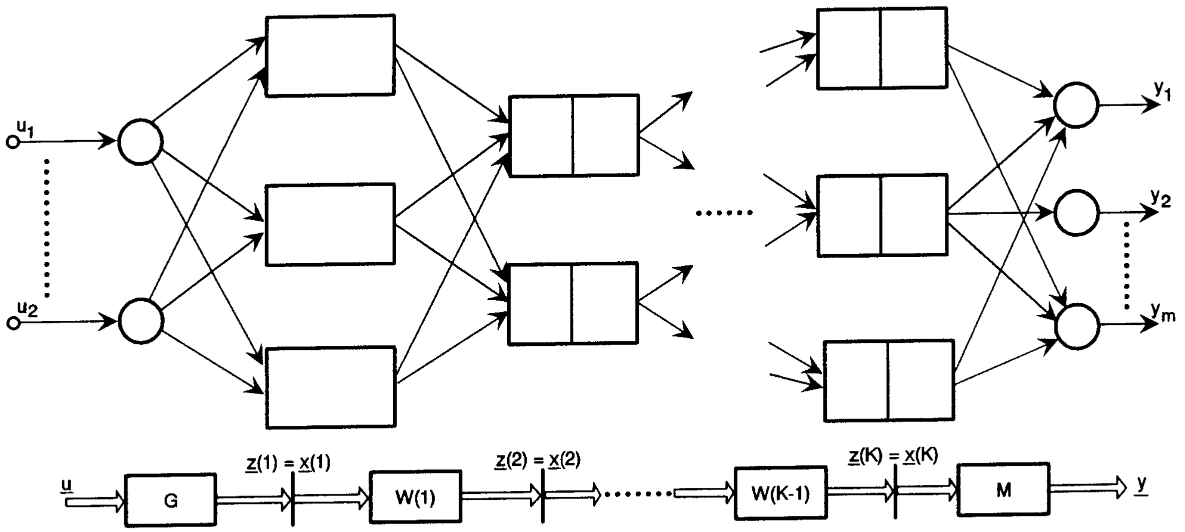
u_1
u_2
y_1
y_2
y_m
$\underline{u}$
G
$\underline{z}(1) = \underline{x}(1)$
W(1)
$\underline{z}(2) = \underline{x}(2)$
W(K-1)
$\underline{z}(K) = \underline{x}(K)$
M
$\underline{y}$

Figure 3: Feedforward Neural Network

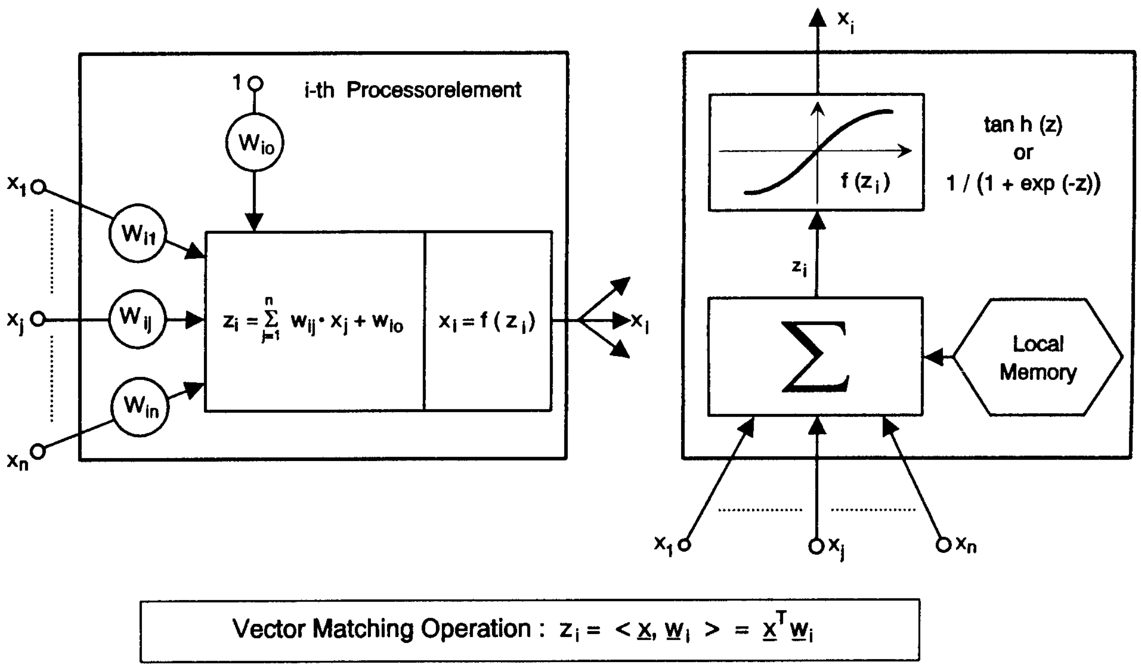
i-th Processorelement
1
W_{io}
x_1
x_j
x_n
W_{i1}
W_{ij}
W_{in}
$z_i = \sum_{j=1}^{n} w_{ij} \cdot x_j + w_{io}$
$x_i = f(z_i)$
x_i
x_i
$f(z_i)$
tan h (z)
or
1 / (1 + exp (-z))
z_i
$\sum$
Local Memory
x_1
x_j
x_n
Vector Matching Operation : $z_i = \langle \underline{x}, \underline{w}_i \rangle = \underline{x}^T \underline{w}_i$

Figure 4: Processorelement

3.2 Learning static mappings

During the learning process, the network learns the mathematical relation

$$f_N: \{U\} \varepsilon R^n \rightarrow \{Y\} \varepsilon R^m \tag{11}$$

between vectors $\underline{u}_p$ of the input set {U} in the n-dimensional Euclidian vector space R^n and vectors $\underline{y}_p$ of the output set {Y} of the m-dimensional space R^m with

$$\underline{y}_p = f_N(\underline{u}_p) \tag{12}$$

The mapping or function f_N is learnt during the training phase by processing training vectors in pairs $(\underline{u}_1, \underline{y}_1^*) \ldots (\underline{u}_p, \underline{y}_p^*) \ldots (\underline{u}_P, \underline{y}_P^*)$. As an example of learnability, Fig. 5 shows the approximation of the function $y = \cos(x_1^2 + x_2^2)$ with a three- and four-layer network (networks III and IV). When the learning rate (μ) is lower and the initial values for the weights (σ) are small, a four-layer network is necessary for acceptable approximation.

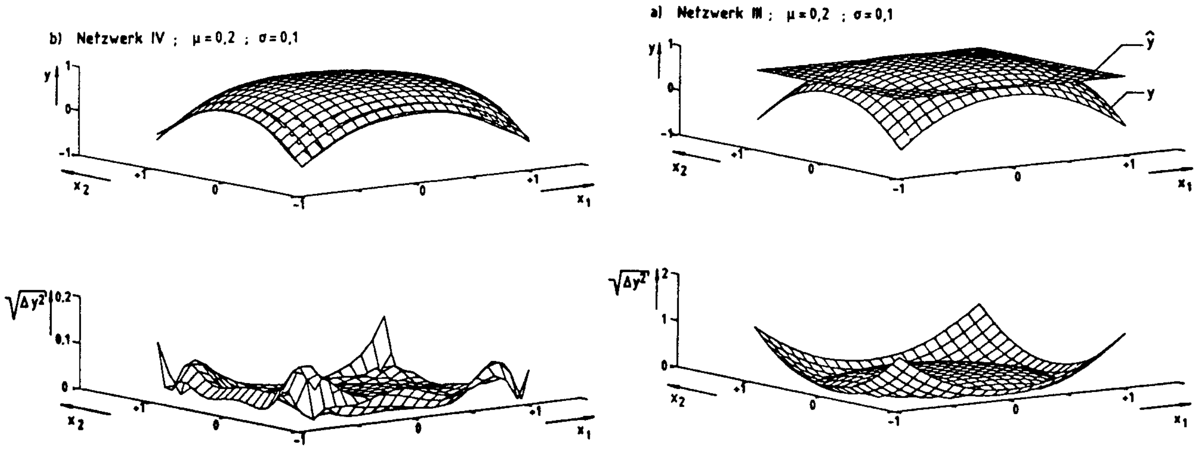

Figure 5: Approximation of a static function

3.3 Learning dynamic mappings

To describe the input-output relationship of a dynamic system, the state vector and its time dependence must be taken into account. The mapping of a dynamic system can be learnt by a Neural Network in the same manner as mentioned for a static system, provided delayed inputs are utilized and a short-term memory capability is incorporated for the network by additionally implementing external feedbacks of delayed outputs. This is represented in Fig. 6. Taking the dynamic system shown as an example, the good tracking of the system output (y) by the network output (y) is demonstrated after learning the system response to positive and negative inputs.

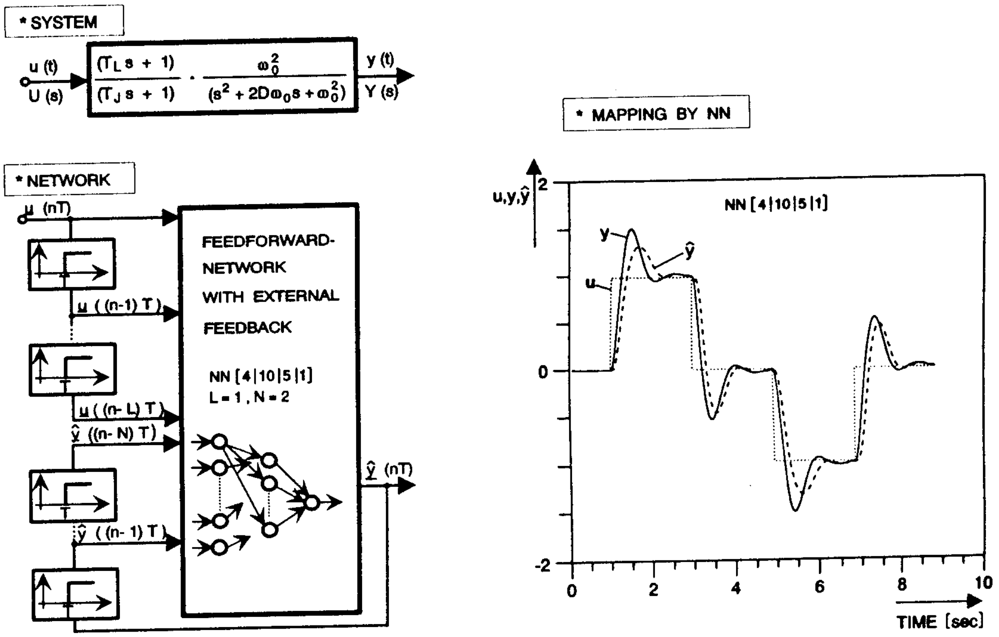
* SYSTEM
u (t)
U (s)
$\frac{(T_L s + 1)}{(T_J s + 1)} \cdot \frac{\omega_0^2}{(s^2 + 2D\omega_0 s + \omega_0^2)}$
y (t)
Y (s)
* NETWORK
u (nT)
u ((n-1) T)
u ((n- L) T)
ŷ ((n- N) T)
ŷ ((n- 1) T)
FEEDFORWARD-NETWORK WITH EXTERNAL FEEDBACK
NN [4|10|5|1]
L = 1 , N = 2
ŷ (nT)
* MAPPING BY NN
u,y,ŷ
2
0
-2
NN [4|10|5|1]
y
ŷ
u
0
2
4
6
8
10
TIME [sec]

Figure 6: Dynamical System identification by a Neural Network

4 GENERALIZED STRUCTURE OF THE LEARNING AUTOPILOT CONTROL LOOP

Based on the subjects and results as dealt with so far, a generic learning control system can be structured which embodies the autopilot control loop and which is depicted in Fig. 7.

Within this context a learning control system is one that has the ability to improve its performance at present and in the future based on experimental information it has gained in the past. This is accomplished through closed-loop interaction of the controller elements with the plant and the environment. Learning control requires the implementation of both a learning function and a performance feedback. As shown in Fig. 7, a control loop structure thus follows which contains a performance feedback besides the control feedback for continuous adaptation of the connecting weights of the controller network. This performance feedback branch results from the comparison of the measurable output quantity of the control plant with a nominal value to be calculated by means of the performance function from the reference variables of the control loop.

To obtain adequate performance, preknowledge necessary to provide stable control behavior is injected into the control network (neural autopilot) during an off-line training period. This knowledge is taken from a classical controller design (PID or state feedback controller). To cope with nonlinear, time-varying effects of the missile (plant) this preknowledge is autonomously adapted during a simulation and experimental phase as well as while the neural controller is operating on-line.

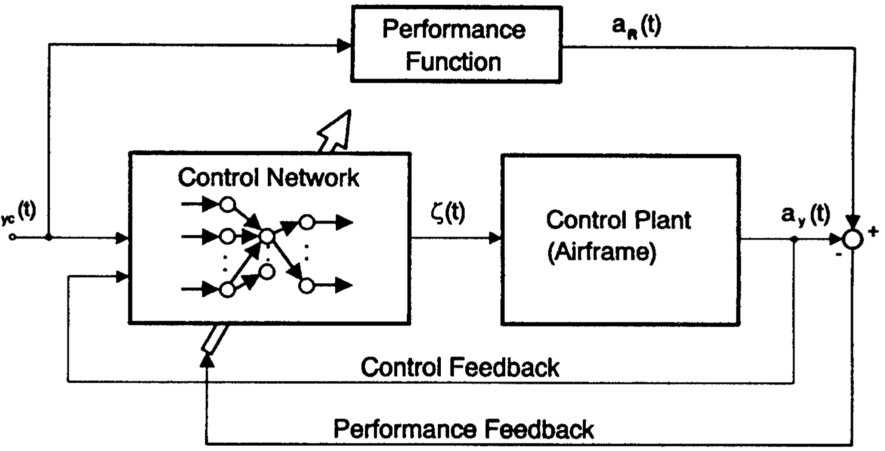

Figure 7: Learning autopilot control loop

5 PERFORMANCE RESULTS

With a suitable neural controller as represented by feedforward networks with appropriate topology and parameters, the lateral autopilot performance was investigated by simulation. For this purpose the full nonlinear, time-varying dynamic model of an existing missile airframe was utilized.

A typical sample performance result is represented in Fig. 8 together with the time histories of missile mass (m) and velocity (Mach number, Ma). Curves ① are plots of the commanded and the actual lateral missile acceleration a_{yc} and a_y as a function of time, after the neural controller has gained its experience during the training phase by processing step- and ramp-type input signals. It is important to note that the performance feedback was not closed in this case.

With activated performance feedback, i. e. continued on-line learning, curves ② reveal the improvement of the input signal tracking performance. This is obtained after only two learning steps have been processed in order to modify the neural controller´s weighting factors accordingly.

These results are very promising and should attract attention within the missile guidance and control community.

6 CONCLUSION

The work results summarized in the present paper show that Neural Networks can be used as nonlinear autopilots for missile guidance and control. Further detailed investigations will show in how far they are superior to conventional autopilots without/with gain scheduling. In this connection, network paradigms other than the feedforward network used here will have to be investigated.

When judging the possible application of Neural Networks as autopilots, it is to be especially taken into account that until now there is no method for systematically checking the stability of neural control loops.

Owing to their simple structure, Neural Networks can be implemented as chip/ASIC with a certain fault tolerance being guaranteed by the parallel structure of information processing.

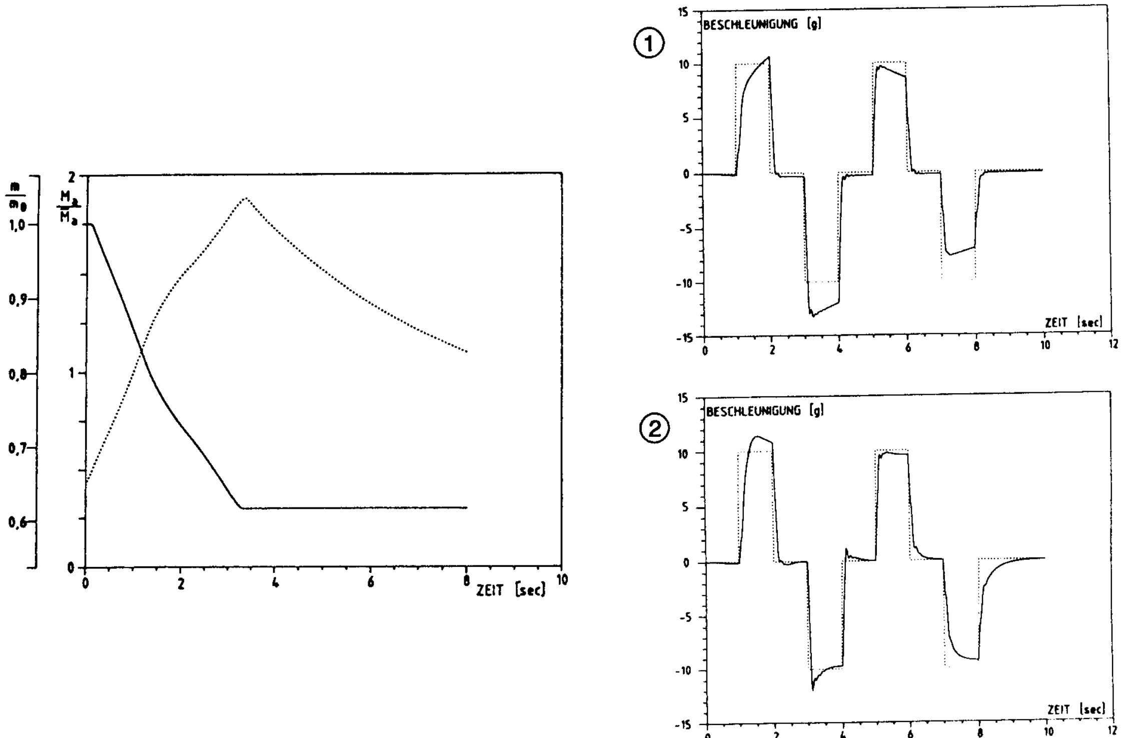

Figure 8: Performance results

7 LITERATURE

[1] U. Krogmann
Introduction to Neural Computing and Categories of Neural Network Applications to Guidance, Navigation and Control
AGARD LS 179, Monterey, USA, October 1991

[2] U. Krogmann
Neue Verfahren der Informationsverarbeitung: Neuronale Netze
Bodenseewerk-Bericht, Überlingen, FRG, Dezember 1992

[3] E. Ersü, J. Militzer
Real-time implementation of an associative memory-based learning control scheme
Symp. Application of multi-variable system techniques, Plymouth, UK, October 1984

[4] A. G. Barto, R. S. Sutton, C. W. Anderson
Neuronlike Adaptive Elements that can solve difficult Learning Control Problems
IEEE Transaction on Systems, Man and Cybernetics, 13(5), 1983

[5] P. J. Werbos
Backpropagation and Neurocontrol: A Review and Prospectus
February 1988, source unknown

[6] D. Psaltis, A. Sideris, A. Yamamura
A Multilayered Neural Network Controller
IEEE Conf. Neural Networks, San Diego, USA, June 1987

[7] M. Adams
Application of Neural Networks for Guidance, Navigation and Control
AGARD-WG Knowledge-Based-Systems, Edinbourgh, UK, October 1992

[8] R. Stengel
Toward Intelligent Flight Control
Workshop Stability in Aerospace Systems, Toulouse, France, June 1992

[8] U. Krogmann
Fault-Tolerant, Spatio-Temporal, Redundant Flight Control and Navigation Reference System
IFAC-Symposium SAFEPROCESS '91, Baden-Baden, FRG, September 1991

[9] P. Eykhoff
System Identification
John Wiley & Sons, Boston, USA, 1974

[10] D. Linse, R. Stengel
A System Identification Model for Adaptive Nonlinear Control
Proc. American Control Conf., Boston, USA, 1991

[11] S. H. Lane, R. Stengel
Flight Control Design using Non-Linear Inverse Dynamics
Proc. American Control Conf., Seattle, USA, 1986

DIRCM: An Effective Technology for Aircraft Self Protection against Optronic Missile Seekers

M. NOLL

B. WARM

P. KASSENS

Optoelectronics Division

Diehl GmbH & Co

Fischbachstraße 16

90549 Röthenbach/Peg.

Germany

1. SUMMARY

This report relates to a self-protection concept for softkill measures based on DIRCM (Directed Infrared Countermeasures) technologies for air transport units, fighter aircraft and helicopters defeating sensor systems, e.g. optronic reconnaissance equipment, as well as missile seekers of a hostile air threat.

First, the main characteristics of such a complete DIRCM system will be discussed, highlighting the system-inherent benefits. To define such a self-protection system for fighter aircraft and helicopters as well as for transportation aircraft it is necessary to consider operational and tactical requirements as well as missile seeker characteristics.

The fundamentals for the effective use of DIRCM systems will be described.

The resulting concepts for the different methods of engagement (jamming, blinding, or sensor kill) and the resulting inputs for the definition of the system key components are described concerning both their technical implementation and their overall effectiveness when engaging different types of seekers.

For a better evaluation of the technical efforts and understanding of the complete system the key components i.e. missile warning system (MAWS,MLDS), laser source and high speed tracking system will be discussed.

Because the missile warning system is very important for the system performance, a definition of the basic requirements for using the system within the scope of DIRCM, evaluating the influence of its performance on the operational parameters (engagement distance and acquisition time), will be provided.

The report will dicuss the influence of the parameters of a laser system (wave-length, repetition rate and output power) and the requirements to a suitable tracking system including possible ways of implementing tracking system hardware and concepts for controller loop design. for a specific engagement situation.

Based upon a scenario involving surface-to-air-missiles with optronic seekers, the possibility of integration of key components with technology available today and usability of the system by the Rapid Reaction Forces will be shown.

The last section of the report will describe an example for an DIRCM system for transport aircraft.

2. INTRODUCTION

In addition to ensuring the traditional - and still valid - function of territorial defence, the NATO will have to grow into their new role as a mobile reaction force securing peace and humanitarian operations in regions of conflict.

To accomplish such out-of-area missions and provide adequate self-protection for our own troops during transport or military missions to "hot spots", a new, task-related equipment is needed but it is not yet available to the necessary extent.

The requirements imposed on weapon systems for this purpose were substantially revised. The weapons needed for "out-of-area" missions in support of human rights or in an anti-terrorist role are required to provide optimal protection of own troops and reliable neutralization of hostile elements without creating undue hazard to civil persons.

The partial destruction of sensors of weapons systems relying on optronic guidance or command and the interruption of pilot or gunner line-of-sight by loss of visual or optical transmission will lead to enemy mission abort without usually entailing total aircraft loss.

Those non-lethal weapons will become ever more important for such out-of-area missions in the future.

The use of compact, air-transportable DIRCM systems against optical equipment, fire control systems of aircraft or helicopters and seekers of air-to-ground and air-to-air missiles is a most suitable means providing such non-lethal defence capability.

Judging from recent out of area experience the logistic units like undefended aerotransport for humanitary missions or air combat units during fighting missions are particularly vulnerable to guided missiles attacking with optronic seekers, because advances in detector and seeker technology cause the available countermeasures to become increasingly ineffective.

The DIRCM (Directed Infrared Countermeasures) technology allows to close this gap in the field of softkill measures by applying highly dynamic low energy laser systems with suitable wavelength bandwidth in combination with high precision tracking techniques and target acquisition.

The objective of such defence is always the jamming, dazzling or destruction of the sensor systems which are indispensable for the attacking weapon.

Paper presented at the AGARD MSP Symposium on "Technologies for Precision Air Strike Operations in Rapid-Reaction and Localised-Conflict Scenarios", held in Seville, Spain, from 16-19 October 1995, and published in CP-576.

Accordingly, the hostile air threat will be neutralized by "mission abort" or "target miss".

2.1 System Features of a DIRCM Systems

As described in [1], the benefits of a DIRCM system as a low energy laser weapon, when compared to a traditional weapon system can be summarized as follows:

* energy delivery at the speed of light

* fast reaction

* simple fire control system (no lead computation)

* high hit accuracy through optical tracking

* high firing rate

In this context, the effectiveness of a DIRCM System is conditional on a number of parameters, such as:

- Environmental Factors

* weapon to target distance

* atmospheric transmission properties

* atmospheric turbulences

- Target Characteristics

* optical bandwidth of seeker

* target movement

* target geometry (size, dimensions, vulnerability)

- DIRCM System Characteristics

* light source (arc lamp, laser) performance

* wavelength

* operating mode (pulsed or cw operation)

* light source properties like pulse duration, power and wavelength

* range, resolution and acquisition time of the target acquisition system

* accuracy and velocity of the beam director unit

* beam forming features (optional)

The problems associated with a laser based DIRCM system are essentially related to limitation in volume and weight and therefore of available energy.

2.2 Weapon System Performance Requirements

In order to fully profit from the benefits of a DIRCM system as described at Chapter 2.1 and to optimize its effectiveness the respective requirements must be specified such as to reduce the stated drawbacks while maintaining all characteristic benefits. Accordingly, the following general requirements are retained defining the defence system:

* high resolution long-range target acquisition with detection of the aimpoint to be defeated. (e.g. sensor, optical window, seeker)

* highly precise target tracking

* maximum power concentration on the hit point

* kill assessment for determination of duration and success of engagement

* short engagement time

These requirements summarize the basic specification for air defence missions involving sensor and seeker defeat. A laser light source also enables other engagement modes in the face of optronic sensor systems which may result in different weighting of the individual requirements.

3. EFFECTS OF INFRARED COUNTERMEASURES AGAINST OPTRONIC MISSILE SEEKERS

For the disturbance or incapacitation of the hostile optronic sensor systems the DIRCM system relies on intensive light beams, genenerated by arc lamps or by lasers.

Very intensive laser beams are capable of destroying the sensor in a thermo-mechanical process. The spectral bandwidth of the hostile optics is of no importance. Therefore, this engagement mode is often referred to as "out-of-band" engagement. It allows even the neutralization of non-optical sensor systems such as radar or radiometers, provided the terminal energy available on the target is sufficient to ensure appropriate thermal or mechanical damage to the radom material.

In the event of merely defensive missions and the engagement of purely optronic systems the so-called "in-band" engagement provides substantial benefits in terms of light energy required and, hence, small-size design features of the DIRCM System.

However, this engagement mode is conditional on the laser beam wave length falling within the spectral bandwidth of the sensor to be defeated. In this context, it is quite helpful to consider that, within its operational bandwidth, the optical system will focus its entire radiation power on the detector. It is, of course, understood, that laser irradiation will take place within the sensor system's field of view which is usually the case in a self-defence scenario.

3.1 Mission Spectrum of the DIRCM System

As mentioned at Chapter 2, the DIRCM System will be used to ensure mission abort on the side of the aggressor. Accordingly, all weapons suffering operating problems or even functional loss and, hence, mission abort, are within the DIRCM System's target spectrum.

The following listing describes some of the major targets and the implications of their incapacitation or destruction:

Target	**Effect of IR countermeasures**
Reconnaissance electronics	target acquisition loss
Aiming device/ sight	no target engagement
Seeker	target loss
Fire control sensor system	no target assignment

The DIRCM system for use against the target spectrum listed allows an effective protection of aircraft, ships, vehicles etc. against attacking missiles with optronic seekers.

Typical mission examples include:

* Anti-missile frontal defence for ships or aircraft (protection against missiles with optronic seekers)

* Protection of armored units against helicopter or fixed-wing aircraft attacking with guided munitions

* Defeat of reconnaissance drones

Fig. 3-1 shows a typical scenario of DIRCM versus SAM engagement.

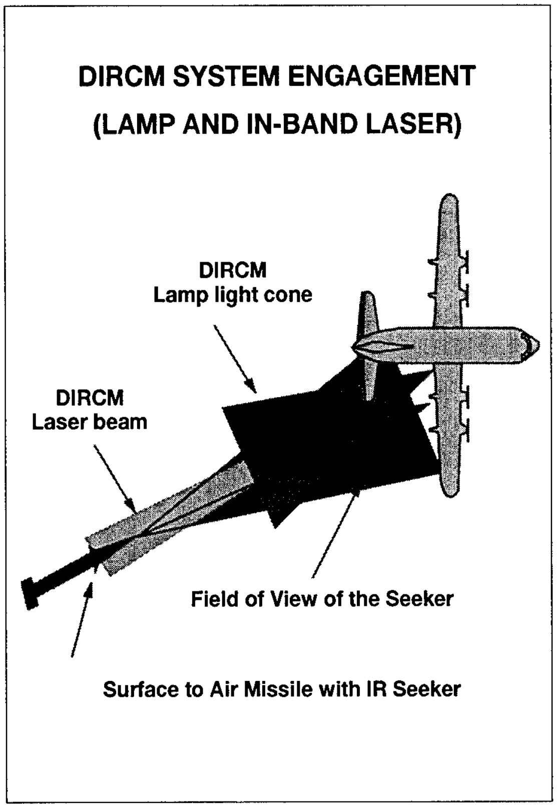
DIRCM SYSTEM ENGAGEMENT
(LAMP AND IN-BAND LASER)
DIRCM
Lamp light cone
DIRCM
Laser beam
Field of View of the Seeker
Surface to Air Missile with IR Seeker

Fig. 3-1: Example: "SAM versus DIRCM" engagement scenario

3.2 Classification of Missile Seekers

Optronic seekers of anti-aircraft missiles work in the visible and infrared spectral ranges from 0.3 µm to 5 µm, depending on missile type.

Optronic missile seekers operate on a lot of different principles. The principles can roughly be classed in four groups (Fig. 3-2):

1. spinning reticles (fig. 3-3)
2. static reticles
3. moving detectors
4. image processing

Illumination of these seekers with infrared radiation can result in the following effects:

Illumination with amplitude modulated radiation of relative low intensity can disturb the electronics of the seeker (Fig. 3-3). The modulated radiation interferes with the modulation generated by the reticle, yielding wrong control signals. To get this effect, the infrared radiation of the DIRCM-system still must be a factor of 10 to 100 higher than the thermal radiation, which the seeker is receiving from his target. This effect is possible for the above mentioned working principles 1 and 2. The necessary modulation frequencies depend on the internal frequencies of the seeker and vary between different seeker types. Repeated short infrared light pulses have a lot of harmonics and can disturb at several frequencies.

With higher light intensities, the detectors of infrared seekers can be saturated, such that the electronics of the seeker cannot generate a valid guidance signal. This can be done with all types of seekers, but some seekers are protected against saturation effects, and some will be destroyed before saturated.

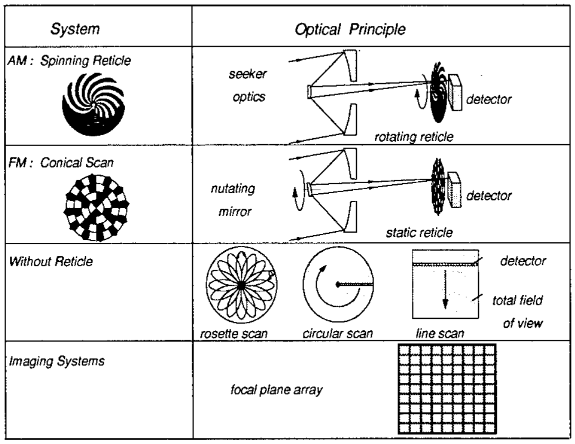
System
Optical Principle
AM : Spinning Reticle
seeker
optics
detector
rotating reticle
FM : Conical Scan
nutating
mirror
detector
static reticle
Without Reticle
detector
total field
of view
rosette scan
circular scan
line scan
Imaging Systems
focal plane array

Fig. 3-2: Surface-Air-Missile Seeker Types

With even higher intensities, usually generated by lasers, parts of the seeker (reticle, detector) can be damaged or destroyed. The radiation must be in the spectral range of the seeker to be transmitted and focused by the optics of the seeker (inband effects).

Very intensive laserbeams are able to damage the dome and lenses of a seeker, even if outside the spectral range of the seeker (outband effects). For these effects intensities are necessary, which are a factor of 10^4 to 10^6 higher than for inband effects. These lasers are too large for compact DIRCM systems, accordingly the following considerations neclect outband effects.

Inband and outband damage can be done to all types of sensors. Fig. 3-4 displays a summary of the required light fluence levels.

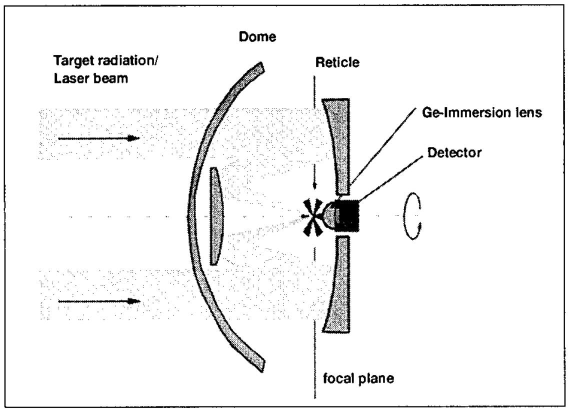
Dome
Target radiation/
Laser beam
Reticle
Ge-Immersion lens
Detector
focal plane

Fig. 3-3: Missile seeker with rotating reticle

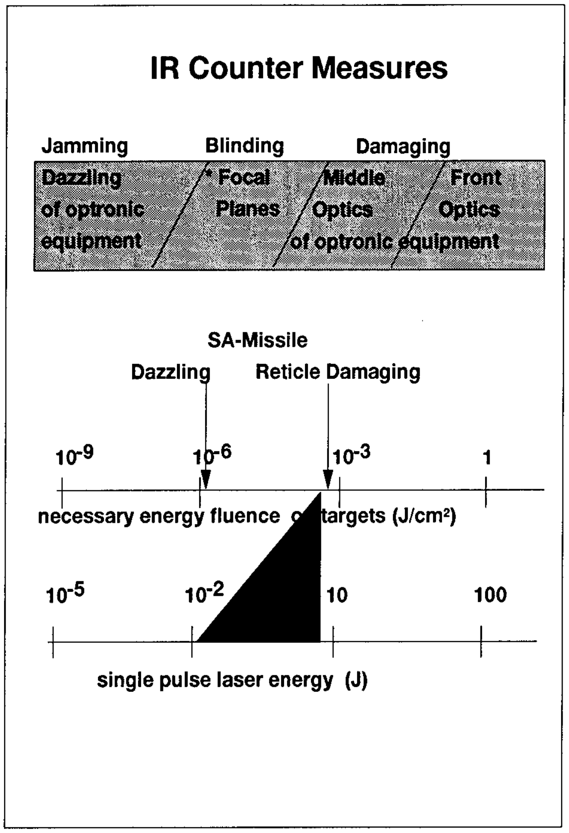

Fig. 3-4: Required Light Fluence Levels

4. USE OF DIRCM SYSTEMS AGAINST SEEKERS

A DIRCM system for use against sensors and seekers will be a meaningful addition to existing weapon systems.

Examples are:

- Ship-board laser systems can blind approaching missiles with IR-Seekers and defeat this threat at extremely low cost, when compared to air-defence missiles. The laser system is not saturable.
- A battle tank with a laser system can prevent a hostile battle tank from firing, if it puts the enemies total sensor system out of operation. In a duel situation he will outgun the opponent.
- An air defence system can protect itself against attacks by helicopter and aircraft, if it dazzles the sensors of approaching missiles.

4.1 Parameters Affecting DIRCM System Effectiveness

The effectiveness of a DIRCM system is determined by a multitude of parameters described in chapter 2.1.

At inband operation the optical system of the seeker is permeable to the laser wavelength and it focuses the laser beam on the detectors. Damaging of optronic sensors requires very low laser intensities, if the laser beam is focused on the detector. Trials have shown that ccd-arrays of cameras may be destroyed by energies of a few ten mikrojoules, not only incapacitating a few pixels but the total array. Also, several pixels of infrared sensors were destroyed by such low energies. Some of the specific problems of an in-band DIRCM system are as follows:

1. Because the laser beam has to be focused onto the detector, its sensor optics has to look in the direction of the DIRCM system. That is, the DIRCM system has to be in the field of view of the sensor. Accordingly, the DIRCM System can be used only for self-protection, not for point defence.

2. Protection by attachment of optical filters is possible against a DIRCM System with a fixed wavelength. It is, however, not possible to protect the whole spectral range, because then the sensor would receive no light at all. A DIRCM System must therefore possess various laser wavelengths, to be effective in the whole spectral range of the sensor optics.

3. Another possibility for defence is provided by optical elements with an intensity dependent transmission, which now are under development. If the light intensity on these elements exceeds a certain threshold, these elements become opaque. This is a protection for the sensors, but they will be inoperative at least for the duration of the laser illumination. For missiles this generally means missing the target; for weapon platforms it causes a mission break.

4. In the case of missiles the sensor breakdown must occur at a sufficient stand-off distance in order to prevent the missile from scoring a hit by use of a inertial navigation guidance system or by chance.

Typical wavelength ranges of optronic sensors are displayed in figure 4-1.

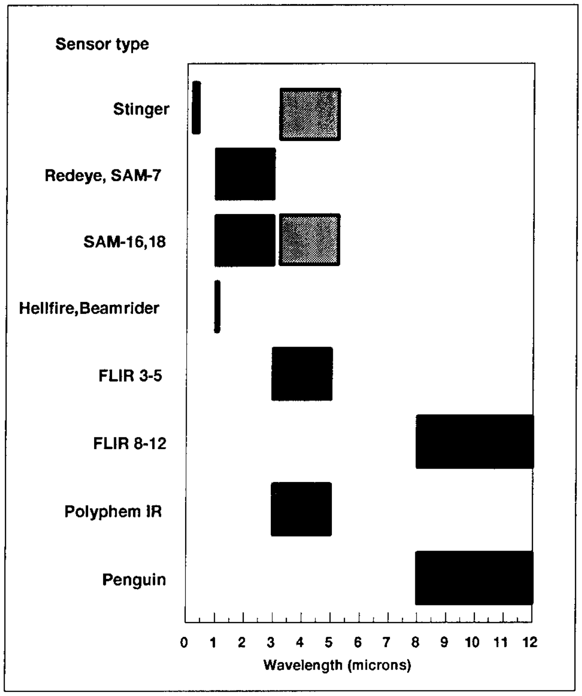

Fig. 4-1.: Wavelength Ranges of Optronic Sensors

5. KEY COMPONENTS OF THE DIRCM SYSTEM

The key components of a DIRCM System system are:

* the laser source (lamp) including power supply

* a target acquisition system

* the beam guidance system, possibly with beam conditioning components

5.1 Light Source

For the selection of a light source for a weapon system a multitude of parameters is to be considered:

- availability of the lamps/lasers
- scalability
- wavelength
- required laser power or energy
- pulse duration
- volume
- power efficiency
- power supply
- atmospheric transmission

Arc lamps can be used for the generation of light bursts in the spectral region from the visible to the 5 micron region. The spectrum of an arc lamp consists of the continuum radiation of a black body, overlapped with line components. The maximum output energy is technically limited by flashtube explosions and lamp envelope melting. With lenses or mirrors of about 10 cm in diameter the light can can be concentrated into a cone with a divergence of about five to ten degrees.

Therefore, the light power received by an IR seeker from an arc lamp beam can be much larger than the light power from the helicopter engine and hull, on which the lamp is mounted. Helicopters and propeller-driven aircraft can be protected by arc lamps systems with modulated IR radiation.

But the light power of the lamp cannot be larger than the light power from a jet exhaust, that means, a jet aircraft cannot be protected by a DIRCM system working with arc lamps.

Arc lamps jam the seekers of approaching missiles. It is not possible to damage seekers with the light of an arc lamp. High power lasers are needed.

Available lasers of high performance are for example:

- CO_2-lasers, frequency doubled
- HF/DF-lasers
- COIL-lasers (Chemical Oxygen Iodine Lasers)
- Solid state lasers (e.g. Nd:YAG, Ho:YAG)
- Solid state lasers with optical parametric oscillators (OPOs)

For in-band operation you need not only a high laser power, but lasers with a broad tuning range are necessary. Several technical solutions exist to achieve broad tuning ranges for a laser.

- many lasers have by nature more or less tunable frequencies
- frequency multiplying can be used for the generation of other wavelengths
- with OPOs (optical parametric oscillators) laserlight can be generated within almost the whole visible and infrared spectral range. Key components of OPOs are nonlinear optical crystals. The output power of OPOs is currently limited to about 10 Watt; the limits are dependent on crystal technology.

Figure 5-1 displays the tuning ranges of several laser types. In this illustration the wavelengths of pulse lasers are displayed. Systems for in-band damaging must have laser energies in the region of some joules with repetition rates of some 10 Hertz; systems intended for jamming need millijoules pulses with repetition rates of some kilohertz.

For the distinction of in-band/out-of-band operation the size and complexity of the laser system together with the power supply is of special interest. Assuming linear scalability, a system with 3 lasers, each with a power of about 100 watt, has a volume of only three hundredth of the volume of a laser of about 100 kW; frequency shifting elements add some additional volume. In all, laser source and power supply of an in-band system will need only a small portion of the volume of a so-called "laser weapon" for out-band damaging.

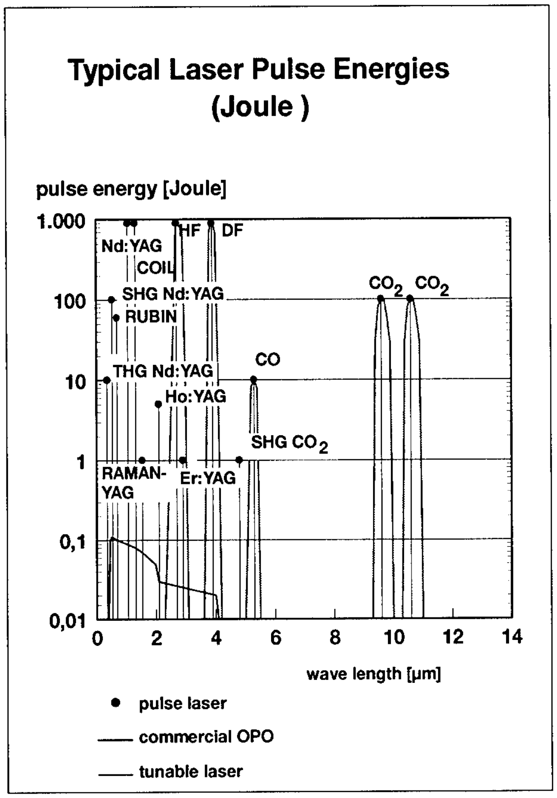

Fig. 5-1: Wavelengths and Energies of Weapon Lasers

5.2 Target Acquisition

An acquisition system for DIRCM systems is faced with the problems of an early target acquisition to fight incoming missiles, e.g. approaching missiles must be detected at distances of several kilometers. This gives rise to new requirements for detection sensors regarding range, as well as spatial and time resolution. For detection, the total electromagnetic spectral range can be used, from the microwave range and the infrared and visible spectrum to the ultraviolett light.

For optical detection of missiles, two spectral ranges are especially interesting:

- In the ultraviolett range below 300 nm rocket motors display intensive radiation. The ozone layer absorbs the ultraviolett light of the sun, whilst the lower atmosphere transmits ultraviolett light. So, there are hardly any light sources in this spectral range except for rocket motors.

- In the infrared band at 4,2 µm the CO_2 exhaust fumes of the plume show intensive radiation. Therefore, the motor plumes can be recognized in pictures of spectral-resolving infrared cameras against clutter. But an automatic picture evaluation needs very high computer capacities.

Today, a lot of missile warning systems (MWS) are available. Some of them are able to detect approaching missiles (MAWS: Missile Approach Warning Systems), some detect the launch of the missiles (MLWS: Missile Launch Warning Systems).

5.3 Beam Guidance and Forming

The term "beam guidance" designates the components which serve to hit the target with the laser beam. The laser beam conditioning subsystem also includes the components which serve to maximize the intensity on the target. Accordingly, beam guidance is necessary for every DIRCM System. Whether beam conditioning components are to be added, depends on the required intensities and ranges. If a sensor must be damaged at very long ranges to score a hardkill, then a beam conditioning system is a prerequisite. Major components of a beam guidance system are:

* the beam transmitting telescope

* mirrors and other optical components

* motors for the telescope movement

* cameras for target recognition, aim point selection, as well as for the analyzing of effects.

* computer with tracking electronics and control electronics

* possibly fast tilt mirrors and a focus correcting mirror with sensors for fine tracking

Components of a beam conditioning system are:

* deformable mirrors

* wave front sensors

* computer for the adaptive optics control

Figure 5-2 shows the key components of a DIRCM system in a diagrammatic illustration.

The subsystems are described in Chapters 6 and 7 in more detail.

6. TRACKING CONCEPT FOR A DIRCM SYSTEM

The tracking system has to accomplish the following two tasks:

- switch as fast as possible to the position of the approaching missile, detected by the missile warning system
- follow the missile with angular deviations not larger than some ten microradians. The smaller the deviation, the smaller the light beam can be made, the better the effect on the missile seeker.

The optical components of the tracking system are shown in figure 6-1, in a simplified fashion.

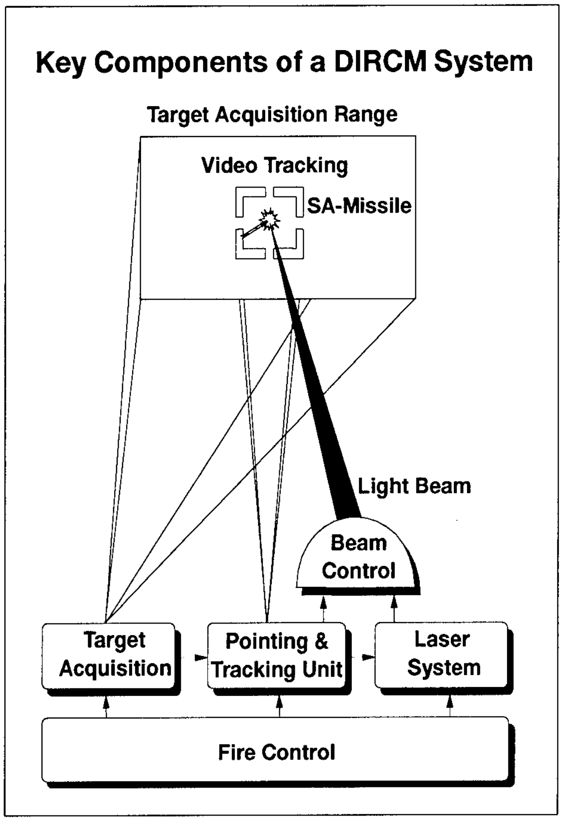
Key Components of a DIRCM System
Target Acquisition Range
Video Tracking
SA-Missile
Light Beam
Beam Control
Target Acquisition
Pointing & Tracking Unit
Laser System
Fire Control

Fig. 5-2: Key Components of a DIRCM System

The control loops for the tracking system as well as the characteristics of its components are described below.

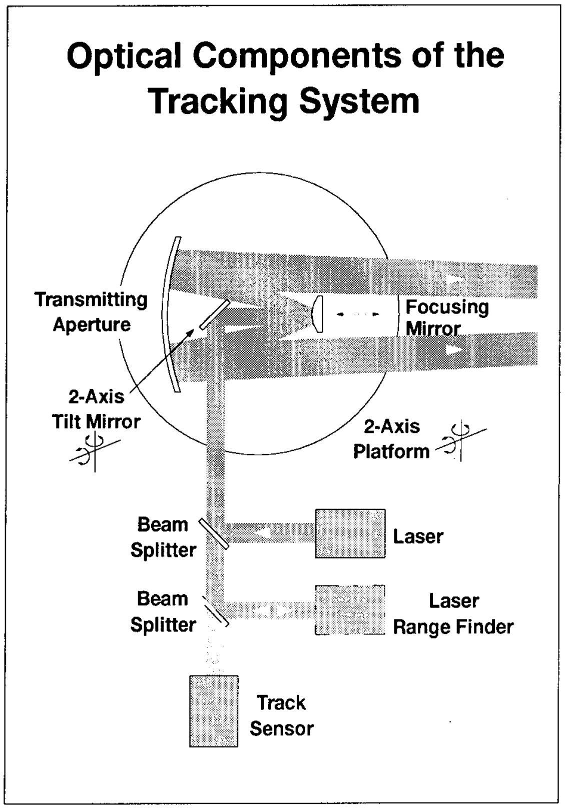
Optical Components of the Tracking System
Transmitting Aperture
Focusing Mirror
2-Axis Tilt Mirror
2-Axis Platform
Beam Splitter
Laser
Beam Splitter
Laser Range Finder
Track Sensor

Fig. 6-1: Optical Components of the Tracking System

6.1 Tracking

The tracking system takes over the coordinates of the detected target from the external acquisition system to track the assigned target with a high accuracy to allow stabilization of the line of sight as a prerequisite for hit point selection.

The tracking system consists of a closed control loop with track sensor, tracker electronics, 2-axis stabilized platform and a control loop with laser range finder and focusing mirror. A data processing unit executes the computations of control algorithms and controls the data link between the elements of the loops.

Figure 6-2 shows a block diagram and the data flow between the elements of the tracking system.

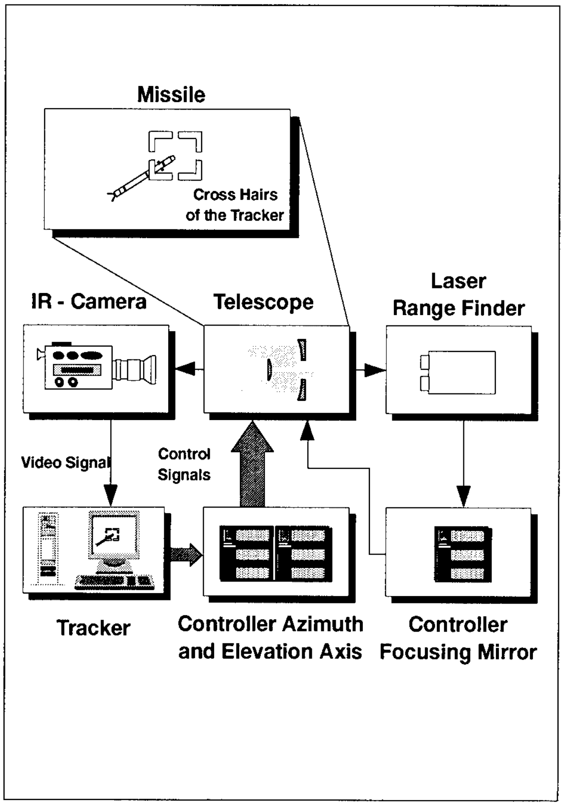
Missile
Cross Hairs of the Tracker
IR - Camera
Telescope
Laser Range Finder
Video Signal
Control Signals
Tracker
Controller Azimuth and Elevation Axis
Controller Focusing Mirror

Fig. 6-2: Block Diagram of a Tracking System

6.1.1 Track Sensor

Among the various methods for target tracking, the video tracking seemed to be the most suitable, since the state of the art in image processing and computer technology enables optimal and most reliable tracking results.

The track sensor detects and generates the image information of the target. The requirements can be defined as follows:

1. Independence of daylight
2. High transmission through atmosphere
3. High area resolution
4. Adequate field of view
5. Frame rate much greater than 50 Hz

The selection of the spectral range is influenced by the above requirements like high independence of daylight and high atmospheric transmission.

As with missile warning systems, the preferred spectral ranges for track sensors are the ultraviolett "solar blind region" and the infrared range from 3 to 5 µm. If UV sensors work well for missile warning, they will work for tracking too. But they will track the missile plume, not the head with the seeker. For this reason, an IR track sensor is preferred.

The cooling system for the detector is generally a Stirling cooler, because it only requires electrical power and no liquid nitrogen.

IR cameras used as tracking sensors with staring arrays in PtSi or InSb technology (up to 640 x 480 pixels) and < 0,2 K temperature resolution are available today.

To achieve high local resolution the field of view is in the range of 2 degrees with a large aperture ensuring sufficient speed and optical resolution. In order to track targets in different distances a zoom function should be available. The required distance data are generated by a laser range finder.

The performance of the tracking loop also depends on the update rate of the target image. The tracking loop for very fast targets, like missiles and aircraft, needs a high capability of response and therefore high rates of input data (target images). Unfortunately, nearly all video trackers available operate on the TV standard CCIR, which means a frame rate fixed at 50 Hz. This is enough for lamps as light sources.

An optimal track result for lasers as light sources can only be achieved, if the frame rate of a video tracker is increased in accordance with the target dynamics. A frame rate of about 500 Hz will be adequate.

If all elements (including control techniques) are matched perfectly, a tracking system accuracy better than ±50 micro-radians can be achieved.

This allows to use a laser beam with the same dimensions, maximizing the radiation intensity at the missile.

To improve the signal to noise ratio of the missile picture, it is possible to use backscattered laser radiation. Because the seeker of the approaching missile is staring at the DIRCM system, a large portion of laser light, which is aimed at the seeker, will be backscattered by the seeker (cat's eye effect).

6.1.2 Laser Range Finder

The target distance information is required for important functions:

- focus control of transmitting optics (telescope)
- control of the focal length of the track sensor
- exact determination of the three-dimensional coordinates of the target, which are necessary for improvements of the control loops

The target distance can be measured by a laser range finder, which is to be mounted on the platform. The maximum operational range must be in accordance with the other components of the DIRCM system. If the jam laser works in a pulse mode, then this laser and an additional receiver will form an adequate pulse echo range finder.

6.2 Tracker Electronics

The tracker electronics is the key element in the tracking loop. In the case of video tracking, the tracker electronics consists of a digital image processing system, which analyses the incoming video signal from the track sensor. At the beginning of the process, the tracker stores a reference signal of the target, which can be selected with the help of a window, cross hair or automatically from the sensor signal. After the initial phase, this stored reference is compared with every incoming sensor image. When the reference has been detected in the actual image, then the tracker generates an error vector, which describes the position between the actual and initial phases.

In consideration of signature change of the target during the tracking process, the reference signal is updated from time to time. In the closed loop, the generated error signals, normally separated in azimuth and elevation signals, are used for driving the 2-axis platform.

The quality of the tracker in detecting and measuring the target position is dependent mainly on the tracker algorithm used and consequently on the available processing performance.

A very simple, but sufficient method for many applications is the so-called contrast tracking. The algorithm has only to decide whether or not the intensity is greater than a commanded threshold. If the target is a hot spot, it is very easy to detect such a target by using this method.

But the above-described method will fail, if the targets have a much more complex signature. In this case, a correlation track algorithm is the better solution: The tracker takes a complete signature as its reference and compares the actual image to it. By using correlation methods, it is now possible to find the target position which best matches the reference.

Correlation trackers are more flexible than contrast trackers, but they need more computer capacity and are therefore limited in their update rate.

The intelligence of such tracker algorithm has increased in connection with the increasing of computer capacity in the last years. For this reason, the target detection and tracking provides excellent quality, even when the target must be detected in difficult background (clutter etc.).

6.3 Platform

The error signals, generated by the tracker, are used in the closed loop to drive the sensor and transmitter platform. The mechanical design of the beam director has an important influence on the tracking result determined by dynamic properties like acceleration and static properties like position resolution.

6.4 Tracking Performance Enhancements

Normally, in case of a DIRCM system equipped with arc lamps or jam lasers, the accuracy of the beam direction is sufficient to hit the target. But if long ranges for sensor destruction are required, additional fine tracking elements are necessary, because the tracking system may cause tilt errors for short times, which cannot be compensated for by the platform mirror. They can consist of a fast 2-axis tilt mirror, a zoom optic for the laserbeam and additional beam position sensors. Eventually an adaptive optics system will be necessary [2].

6.5 Control Methods

The quality of the closed loop and its behaviour in relation to targets with different dynamic profiles is finally dependent on the control concept. For that reason, the work carried out in the field of control engineering to develop controller layout for tracking missions is finally the most important and most difficult task for satisfactory tracking results.

The methods used for designing the appropriate controller layout and the corresponding controller coefficients are most varied.

The tracking system described in the preceding chapter consists of the following control loops:

loop	sensor	positioning element
1.	track sensor	2-axis platform
2.	track sensor	tilt mirror
3.	laser range finder	focusing mirror

Due to the limited local and time resolution of the track sensor and the tracker electronics the control of the platform is the most important objective for the application of modern control methods.

The deviation relating to hit point and beam axis depends on:

1. area resolution of the track sensor
2. frame rate of the track sensor
3. atmospheric disturbances
4. computing time of the tracker
5. position resolution of the platform drive
6. dynamic properties of the platform drive
7. axis controller

The following sections describe different methods for the control of the platform and include simulation results for comparison purposes.

6.5.1 Conventional Controller

Classic methods, like the root locus method or the Nyquist criterium in connection with PI or PID controller provide good results, but adaptive controllers allow better results.

6.5.2 Use of Kalman Filter Technology

The biggest disadvantage of those conventional control loops is the limitation in terms of tracking target movements with satisfactory results. Although, it is possible to use adaptive controller functions (the controller coefficents are changed depending on the track process) to improve this feature. State-of-the-art controller with estimate and predictor functions are more flexible in managing different movement profiles of targets with invariably excellent results. But the requirements for their implementation are sufficient computing capacity and a good knowledge of the modelling and dynamic simulation of the respective target movement spectrum.

Figure 6-3 shows an example of a such control loop using Kalman filter techniques. In order to achieve the high precision tracker results required in DIRCM System application, digital controllers with complex filter techniques are necessary.

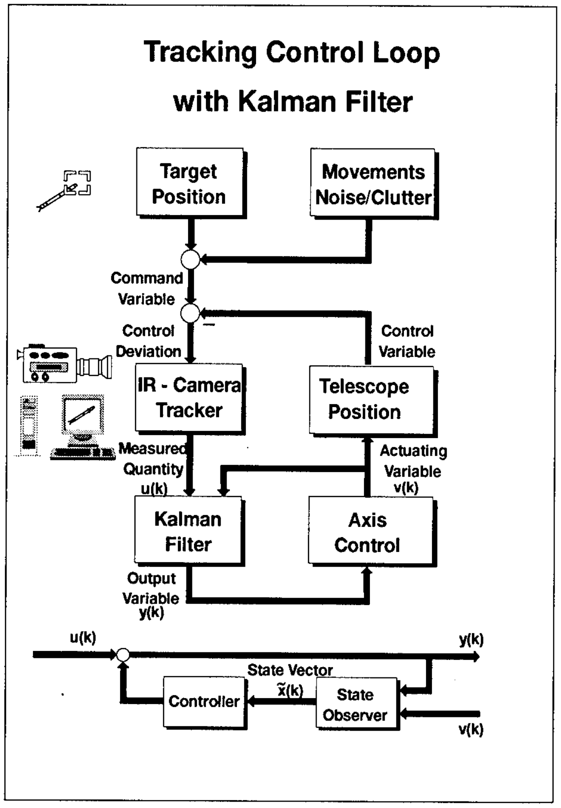
Tracking Control Loop
with Kalman Filter
Target Position
Movements Noise/Clutter
Command Variable
Control Deviation
Control Variable
IR - Camera Tracker
Telescope Position
Measured Quantity u(k)
Actuating Variable v(k)
Kalman Filter
Axis Control
Output Variable y(k)
u(k)
y(k)
State Vector $\tilde{x}(k)$
Controller
State Observer
v(k)

Fig. 6-3: Tracking Control Loop with Kalman Filter

6.5.3 Simulation Results for Different Control Methods

The following parameters are used for a simulation of missile jamming:

track sensor			
	area resolution	50	µrad
	frame rate	50	Hz (standard tracker)
		500	Hz (high speed tracker)
tracking electronics			
	calculating time	20	ms (standard tracker)
		2	ms (high speed tracker)
platform drive			
	position resolution	50	µrad
	cut-off frequency	40	Hz
	max. acceleration	50	rad/s²
	damping	0,7	
target			
	velocity	500	m/s total
	up to	100	m/s lateral

Figure 6-4 shows the simulated scenario.

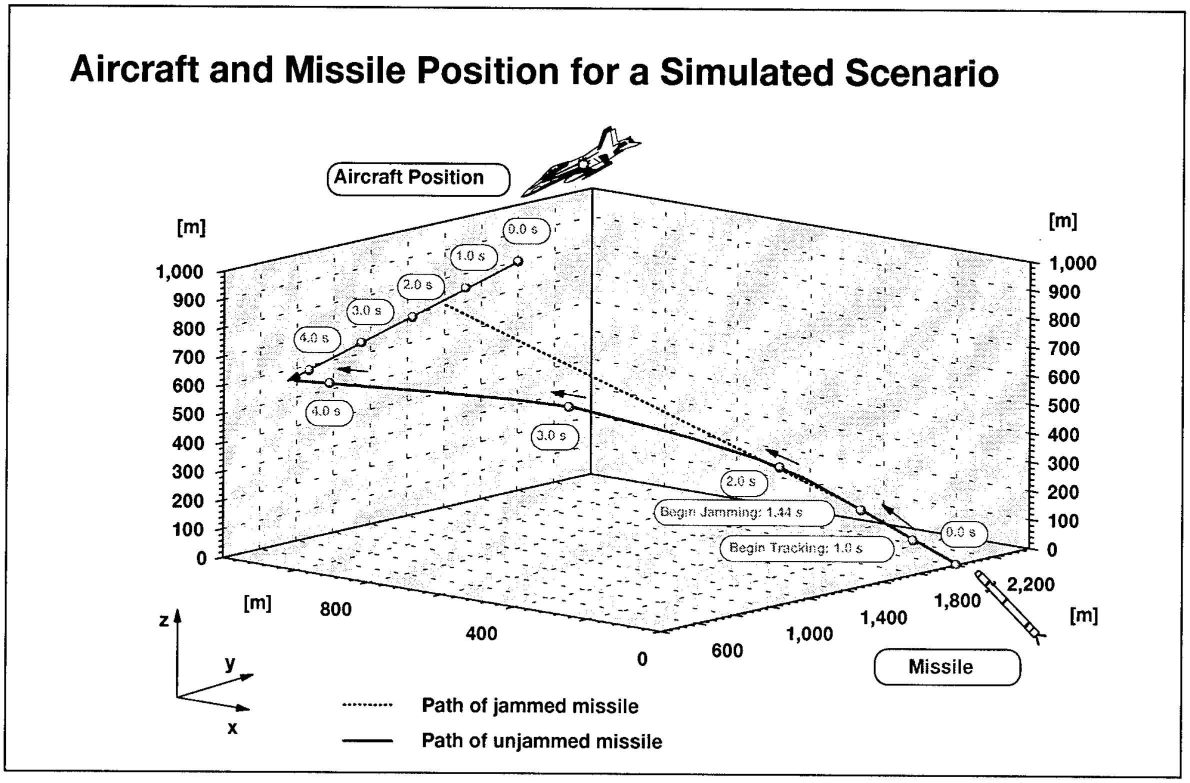

Fig. 6-4: Example for a Simulated Scenario

The engagement sequence contains three characteristic phases:

t = 0,0 s	begin of simulation; start of missile
t = 1,2 s	target acquisition; the platform controller gets the command variables from an external acquisition system
t = 1,44 s	tracking and jamming

The simulation results are shown in figure 6-5.

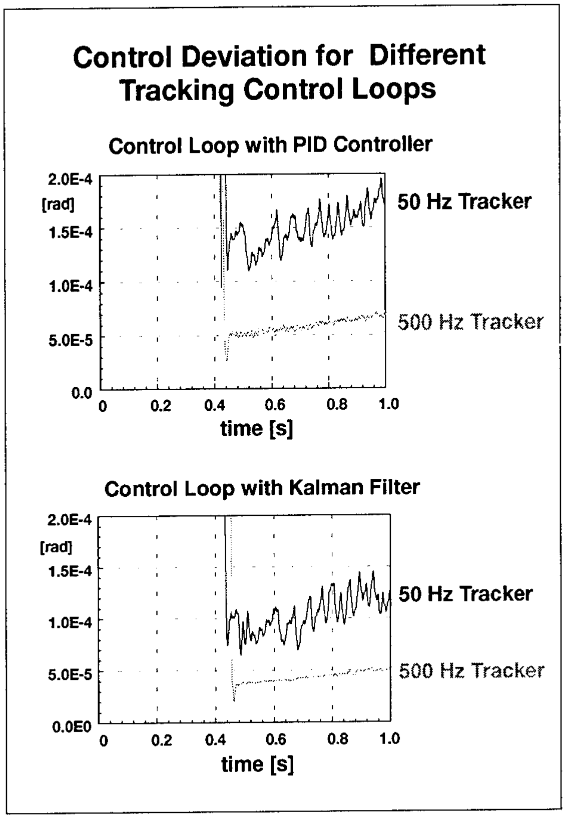

Fig. 6-5: Simulation Results for Different Track Sensors and Control Methods

7. ENGAGEMENT SEQUENCE

The different phases of a typical engagement mission to defeat optronic sensor systems and sights may be subdivided into phases as follows:

1. Target acquisition and assignment by passive (IR or UV surveillance systems) or active (radar) warning sensors.
2. Target tracking
3. Laser engagement (target irradiation)
4. Kill assessment phase
5. End (or engagement of next target)

As explained in Chapter 3, a typical "in-band" engagement mode requires only a small amount of energy to jam or to destroy the detectors of seekers or other optronic reconnaissance systems.

This fact generally simplifies also the overall engagement sequence because sufficient laser energy is available to dispense with additional laser beam corrections by means of adaptive optics. Also, laser beam widening up to a few mrad will enable to dispense with any sophisticated hit point selections such that a high-resolution target assignment by the acquisition system and subsequent target tracking during the engagement process will usually be sufficient for successful "in-band" engagement, in the majority of cases. In this connection, the accuracy of the tracking system will be a function of laser beam divergence (Fig. 7-1).

Kill assessment is a special problem, because it is not clear, how the trajectory of a missile with a jammed or damaged seeker will evolve. Future missiles will follow a straight trajectory (their last command), because they "know", that they are jammed. Therefore, the missile has to be tracked and illuminated, until it is certain, that it will miss the target.

If extreme ranges are necessary and if it is required to have a maximum amount of energy available at the target, successful target destruction is only possible if accurate hit point selection is ensured and if an adaptive optics system is used for fine-tracking and final effectiveness optimization.

Due to the very small target cross-sections (for the target spectrum considered here) the expenditure involved in hit point selection is extremely high.

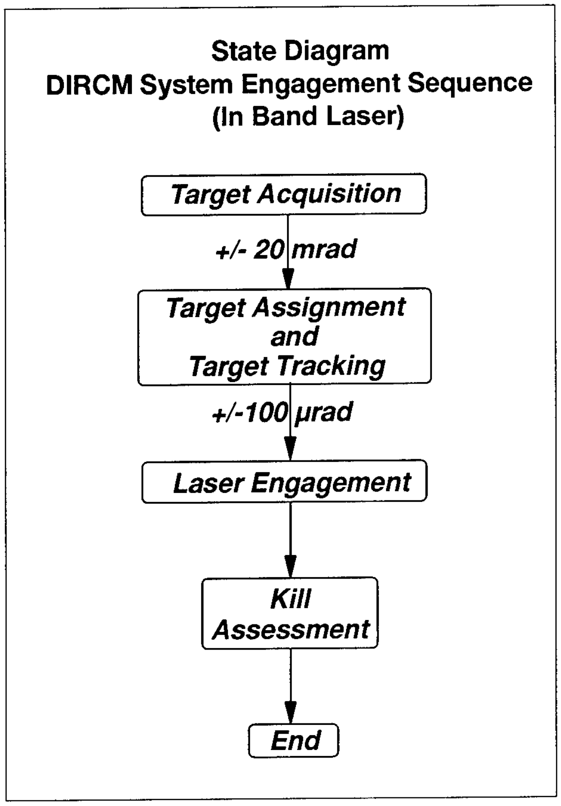

Fig. 7-1: "In-band" engagement sequence

The target assignment function and the subsequent tracking sequence for line-of-sight stabilization will be required to ensure hit point selection with a high-resolution imaging optical system within the tracking sensor system's field of view.

The transmitting telescope of the laser may be used for this job, so that a highly accurate positioning of the laser spot on the aimpoint can be achieved by means of a high-resolution picture of the aimpoint and its surroundings. After switching on the adaptive optics and the laser the hostile sensor can thus be destroyed within the space of less than one second.

8. EXAMPLE: CONCEPTION OF A DIRCM SYSTEM FOR AIRCRAFT PROTECTION

The following example relates to a large aircraft defence DIRCM system. Similar systems can be used for air defence systems for helicopter.

It is expected, that the aircraft can be threatened at take-offs and landings by terrorists with manportable SAMs. Surface-air-missiles (SAM) are fired at the aircraft from a distance of about 500 meters to some kilometers. Typical SA Missiles are:

SAM-7,-14, 16, 18

Redeye

Stinger

Today aircraft equipped with the following defence equipment:

- chaff and flares
- jammers etc.

This equipment allows an effective defence against approaching SAMs of older technology. But newer missiles are able to make a distinction between aircraft and flares, and modern imaging seekers are difficult to jam. That means, an aircraft is not protected against modern surface air missiles.

A DIRCM system for aircraft defence must be able to put the sensors of older and newer missiles out of action at a distance of about 1000 m, to be sure, that the ballistically flying missile will not hit the aircraft.

Therefore the DIRCM system must be able to destroy the seeker of the approaching missile, or if this is not possible, it has to illuminate the sensor with light intensities several orders of magnitude above the IR-radiation of the aircraft, until it is sure that the missile will miss the aircraft.

The thermal radiation in the 3-5 µm spectral range from the aircraft, received by the missile seeker (typically 25 mm aperture radius) will be in the order of 100..1000 nWatt. (for comparison: If the seeker looks at the sun, it will receive a power of about 20 mWatt in this spectral range). A laser beam with a power of 10 Watt with a diameter of 0,5 m will illuminate the missile seeker with about 100 mWatt, $10^5..10^6$ times more than the thermal radiation. This will be sufficient to irritate the seeker. If the laser power has the form of short pulses, it will damage the seeker.

An appropriate DIRCM system with a 3 laser system (for different seekers) weighs about hundred kilogramms, and can be mounted as a separate pod or integrated in the aircraft. Its targets are exclusively missiles with infrared seeker. Against these missiles the laser system can score a softkill by blinding the sensor at a distance of more than 1000 meters.

This capability makes the in-band DIRCM System systems an effective supplement to flares and chaff.

Typical design data for an in-band laser system (fig. 8-1) are:

- Three lasers with several wavelengths
- 2 Joule pulse energy
- 25 Hertz repetition rate
- ca. 100-150 kg weight
- beam guidance system with 50 µradians accuracy
- transmitter aperture with a diameter of 10 cm
- range of about 1 km for sensor destruction, several km for jamming

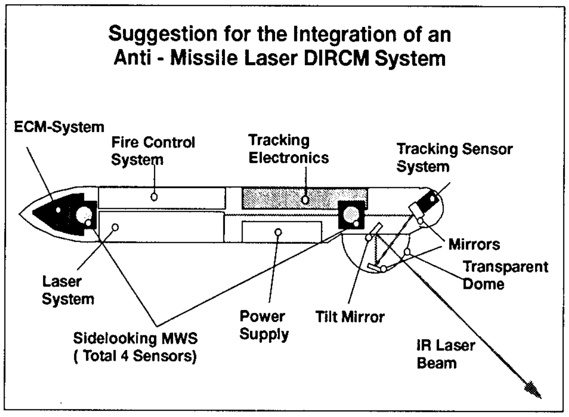

Fig. 8-1: DIRCM laser system, integrated in a pod

9. CONCLUSION

The control and tracking concept for an anti-sensor DIRCM System as described herein clearly shows that it is feasible based on the technology available today.

The implementation of a compact and airtransportable weapon system for defence and self-defence missions against air and ground targets will provide an ideal complement or replacement to traditional defence systems offering capabilities not otherwise obtainable.

With a view to "out-of-area missions" of the Rapid Reaction Forces such systems offering non-lethal characteristics through pin-point engagement and enforcement of enemy mission abort will gain ever more significance in the light of future weapon trends.

10. REFERENCES

[1] M.Noll, B.Warm: "Pointing and Tracking Concept for a High Energy Weapon Application"

57th AGARD Symposium Seattle USA 1993

[2] M.Noll, B.Warm, P.Kassens: "Control and Tracking Concept for an Air Defence Weapon against Optronic Seekers an Sensors"

AGARD Conference Proceedings 555

REPORT DOCUMENTATION PAGE

1. Recipient's Reference	**2. Originator's Reference**	**3. Further Reference**	**4. Security Classification of Document**
	AGARD-CP-576	ISBN 92-836-0028-2	NATO/ UNCLASSIFIED

5. Originator

Advisory Group for Aerospace Research and Development
North Atlantic Treaty Organization
7 rue Ancelle, 92200 Neuilly-sur-Seine, France

6. Title

Technologies for Precision Air Strike Operations in Rapid-Reaction and Localised-Conflict Scenarios

7. Presented at/sponsored by

The Mission Systems Panel 4th Symposium held in Seville, Spain from 16-19 October 1995.

8. Author(s)/Editor(s)	**9. Date**
Multiple	June 1996
10. Author's/Editor's Address	**11. Pages**
Multiple	180

12. Distribution Statement

There are no restrictions on the distribution of this document. Information about the availability of this and other AGARD unclassified publications is given on the back cover.

13. Keywords/Descriptors

NATO forces
Scenarios
Airborne operations
Technology
Aerial warfare
Weapon systems
Deployment
Military planning
Joint operations
Interoperability
Industries
Weapon delivery
Reconnaissance
Air navigation
Target acquisition

14. Abstract

This volume contains the Technical Evaluation Report and the 16 unclassified papers presented at the Mission Systems Panel Symposium held in Seville, Spain from 16-19 October 1995.

Papers were presented covering the following headings:

- Operational Aspects;
- Mission Planning/Mission Management;
- Navigation;
- Reconnaissance and Target Identification;
- Targeting and Weapon Delivery Guidance.

AGARD

NATO OTAN

7 RUE ANCELLE • 92200 NEUILLY-SUR-SEINE

FRANCE

Télécopie (1)47.38.57.99 • Télex 610 176

DIFFUSION DES PUBLICATIONS
AGARD NON CLASSIFIEES

Aucun stock de publications n'a existé à AGARD. A partir de 1993, AGARD détiendra un stock limité des publications associées aux cycles de conférences et cours spéciaux ainsi que les AGARDographies et les rapports des groupes de travail, organisés et publiés à partir de 1993 inclus. Les demandes de renseignements doivent être adressées à AGARD par lettre ou par fax à l'adresse indiquée ci-dessus. *Veuillez ne pas téléphoner*. La diffusion initiale de toutes les publications de l'AGARD est effectuée auprès des pays membres de l'OTAN par l'intermédiaire des centres de distribution nationaux indiqués ci-dessous. Des exemplaires supplémentaires peuvent parfois être obtenus auprès de ces centres (à l'exception des Etats-Unis). Si vous souhaitez recevoir toutes les publications de l'AGARD, ou simplement celles qui concernent certains Panels, vous pouvez demander à être inclu sur la liste d'envoi de l'un de ces centres. Les publications de l'AGARD sont en vente auprès des agences indiquées ci-dessous, sous forme de photocopie ou de microfiche.

CENTRES DE DIFFUSION NATIONAUX

ALLEMAGNE
Fachinformationszentrum Karlsruhe
D-76344 Eggenstein-Leopoldshafen 2

BELGIQUE
Coordonnateur AGARD-VSL
Etat-major de la Force aérienne
Quartier Reine Elisabeth
Rue d'Evere, 1140 Bruxelles

CANADA
Directeur, Services d'information scientifique
Ministère de la Défense nationale
Ottawa, Ontario K1A 0K2

DANEMARK
Danish Defence Research Establishment
Ryvangs Allé 1
P.O. Box 2715
DK-2100 Copenhagen Ø

ESPAGNE
INTA (AGARD Publications)
Carretera de Torrejón a Ajalvir, Pk.4
28850 Torrejón de Ardoz - Madrid

ETATS-UNIS
NASA Headquarters
Code JOB-1
Washington, D.C. 20546

FRANCE
O.N.E.R.A. (Direction)
29, Avenue de la Division Leclerc
92322 Châtillon Cedex

GRECE
Hellenic Air Force
Air War College
Scientific and Technical Library
Dekelia Air Force Base
Dekelia, Athens TGA 1010

ISLANDE
Director of Aviation
c/o Flugrad
Reykjavik

ITALIE
Aeronautica Militare
Ufficio del Delegato Nazionale all'AGARD
Aeroporto Pratica di Mare
00040 Pomezia (Roma)

LUXEMBOURG
Voir Belgique

NORVEGE
Norwegian Defence Research Establishment
Attn: Biblioteket
P.O. Box 25
N-2007 Kjeller

PAYS-BAS
Netherlands Delegation to AGARD
National Aerospace Laboratory NLR
P.O. Box 90502
1006 BM Amsterdam

PORTUGAL
Estado Maior da Força Aérea
SDFA - Centro de Documentação
Alfragide
2700 Amadora

ROYAUME-UNI
Defence Research Information Centre
Kentigern House
65 Brown Street
Glasgow G2 8EX

TURQUIE
Millî Savunma Başkanliği (MSB)
ARGE Dairesi Başkanliği (MSB)
06650 Bakanliklar-Ankara

Le centre de distribution national des Etats-Unis ne détient PAS de stocks des publications de l'AGARD.

D'éventuelles demandes de photocopies doivent être formulées directement auprès du NASA Center for AeroSpace Information (CASI) à l'adresse ci-dessous. Toute notification de changement d'adresse doit être fait également auprès de CASI.

AGENCES DE VENTE

NASA Center for
AeroSpace Information (CASI)
800 Elkridge Landing Road
Linthicum Heights, MD 21090-2934
Etats-Unis

ESA/Information Retrieval Service
European Space Agency
10, rue Mario Nikis
75015 Paris
France

The British Library
Document Supply Division
Boston Spa, Wetherby
West Yorkshire LS23 7BQ
Royaume-Uni

Les demandes de microfiches ou de photocopies de documents AGARD (y compris les demandes faites auprès du CASI) doivent comporter la dénomination AGARD, ainsi que le numéro de série d'AGARD (par exemple AGARD-AG-315). Des informations analogues, telles que le titre et la date de publication sont souhaitables. Veuiller noter qu'il y a lieu de spécifier AGARD-R-nnn et AGARD-AR-nnn lors de la commande des rapports AGARD et des rapports consultatifs AGARD respectivement. Des références bibliographiques complètes ainsi que des résumés des publications AGARD figurent dans les journaux suivants:

Scientific and Technical Aerospace Reports (STAR)
publié par la NASA Scientific and Technical
Information Division
NASA Headquarters (JTT)
Washington D.C. 20546
Etats-Unis

Government Reports Announcements and Index (GRA&I)
publié par le National Technical Information Service
Springfield
Virginia 22161
Etats-Unis
(accessible également en mode interactif dans la base de données bibliographiques en ligne du NTIS, et sur CD-ROM)

Imprimé par le Groupe Communication Canada
45, boul. Sacré-Cœur, Hull (Québec), Canada K1A 0S7

AGARD
NATO - OTAN
7 RUE ANCELLE • 92200 NEUILLY-SUR-SEINE
FRANCE
Telefax (1)47.38.57.99 • Telex 610 176

DISTRIBUTION OF UNCLASSIFIED AGARD PUBLICATIONS

AGARD holds limited quantities of the publications that accompanied Lecture Series and Special Courses held in 1993 or later, and of AGARDographs and Working Group reports published from 1993 onward. For details, write or send a telefax to the address given above. *Please do not telephone.*
AGARD does not hold stocks of publications that accompanied earlier Lecture Series or Courses or of any other publications. Initial distribution of all AGARD publications is made to NATO nations through the National Distribution Centres listed below. Further copies are sometimes available from these centres (except in the United States). If you have a need to receive all AGARD publications, or just those relating to one or more specific AGARD Panels, they may be willing to include you (or your organisation) on their distribution list. AGARD publications may be purchased from the Sales Agencies listed below, in photocopy or microfiche form.

NATIONAL DISTRIBUTION CENTRES

BELGIUM
Coordonnateur AGARD — VSL
Etat-major de la Force aérienne
Quartier Reine Elisabeth
Rue d'Evere, 1140 Bruxelles

CANADA
Director Scientific Information Services
Dept of National Defence
Ottawa, Ontario K1A 0K2

DENMARK
Danish Defence Research Establishment
Ryvangs Allé 1
P.O. Box 2715
DK-2100 Copenhagen Ø

FRANCE
O.N.E.R.A. (Direction)
29 Avenue de la Division Leclerc
92322 Châtillon Cedex

GERMANY
Fachinformationszentrum Karlsruhe
D-76344 Eggenstein-Leopoldshafen 2

GREECE
Hellenic Air Force
Air War College
Scientific and Technical Library
Dekelia Air Force Base
Dekelia, Athens TGA 1010

ICELAND
Director of Aviation
c/o Flugrad
Reykjavik

ITALY
Aeronautica Militare
Ufficio del Delegato Nazionale all'AGARD
Aeroporto Pratica di Mare
00040 Pomezia (Roma)

LUXEMBOURG
See Belgium

NETHERLANDS
Netherlands Delegation to AGARD
National Aerospace Laboratory, NLR
P.O. Box 90502
1006 BM Amsterdam

NORWAY
Norwegian Defence Research Establishment
Attn: Biblioteket
P.O. Box 25
N-2007 Kjeller

PORTUGAL
Estado Maior da Força Aérea
SDFA - Centro de Documentação
Alfragide
2700 Amadora

SPAIN
INTA (AGARD Publications)
Carretera de Torrejón a Ajalvir, Pk.4
28850 Torrejón de Ardoz - Madrid

TURKEY
Millî Savunma Başkanliği (MSB)
ARGE Dairesi Başkanliği (MSB)
06650 Bakanliklar-Ankara

UNITED KINGDOM
Defence Research Information Centre
Kentigern House
65 Brown Street
Glasgow G2 8EX

UNITED STATES
NASA Headquarters
Code JOB-1
Washington, D.C. 20546

The United States National Distribution Centre does NOT hold stocks of AGARD publications.
Applications for copies should be made direct to the NASA Center for AeroSpace Information (CASI) at the address below.
Change of address requests should also go to CASI.

SALES AGENCIES

NASA Center for
AeroSpace Information (CASI)
800 Elkridge Landing Road
Linthicum Heights, MD 21090-2934
United States

ESA/Information Retrieval Service
European Space Agency
10, rue Mario Nikis
75015 Paris
France

The British Library
Document Supply Centre
Boston Spa, Wetherby
West Yorkshire LS23 7BQ
United Kingdom

Requests for microfiches or photocopies of AGARD documents (including requests to CASI) should include the word 'AGARD' and the AGARD serial number (for example AGARD-AG-315). Collateral information such as title and publication date is desirable. Note that AGARD Reports and Advisory Reports should be specified as AGARD-R-nnn and AGARD-AR-nnn, respectively. Full bibliographical references and abstracts of AGARD publications are given in the following journals:

Scientific and Technical Aerospace Reports (STAR)
published by NASA Scientific and Technical
Information Division
NASA Headquarters (JTT)
Washington D.C. 20546
United States

Government Reports Announcements and Index (GRA&I)
published by the National Technical Information Service
Springfield
Virginia 22161
United States
(also available online in the NTIS Bibliographic
Database or on CD-ROM)

Printed by Canada Communication Group
45 Sacré-Cœur Blvd., Hull (Québec), Canada K1A 0S7

ISBN 92-836-0028-2